



Spinal Implants:

ARE WE EVALUATING THEM
APPROPRIATELY?

STP1431

Mark N. Melkerson,
John S. Kirkpatrick
and Steven L. Griffith



STP 1431

***Spinal Implants:
Are We Evaluating Them
Appropriately?***

*M. N. Melkerson, M. S.; S. L. Griffith, Ph.D.;
and J. S. Kirkpatrick, M.D., editors*

ASTM Stock Number: STP1431



ASTM International
100 Barr Harbor Drive
PO Box C700
West Conshohocken, PA 19428-2959

Printed in the U.S.A.

Foreword

The Symposium on *Spinal Implants: Are We Evaluating Them Appropriately?* was held in Dallas, Texas on 6–7 November 2001. ASTM International Committee F04 on Medical and Surgical Materials and Devices was its sponsor. Symposium chairmen and co-editors of this publication were Mark N. Melkerson, M.S.; John S. Kirkpatrick, M.D.; and Steven L. Griffith, Ph.D.

Library of Congress Cataloging-in-Publication Data

Symposium on Spinal Implants, Are We Evaluating Them Appropriately? (2001 : Dallas, Tex.)

Spinal implants : are we evaluating them appropriately? / M.N. Melkerson, S.L. Griffith, and J.S. Kirkpatrick, editors.

p. ; cm. — (STP ; 1431)

Symposium on Spinal Implants, Are We Evaluating Them Appropriately? was held in Dallas, Texas on 6-7 November 2001.

Includes bibliographical references and index.

ISBN 0-8031-3463-0

Spinal Implants: Are We Evaluating Them Appropriately?

"ASTM Stock Number: STP1431."

1. Spinal implants—Testing—Congresses. I. Melkerson, M. N. (Mark N.) 1961-II. Griffith, Steven L., 1960-III. Kirkpatrick, J.S. (John S.) 1958-IV. Title. V. ASTM special technical publication ; 1431.

[DNLM: 1. Spine—surgery—Congresses. 2. Device Approval—Congresses. 3. Implants. Experimental—Congresses. 4. Prosthesis Design—Congresses. WE 725 S9869s 2003]

RD768.S847 2003

617.5'6059—dc21

2003049605

Copyright © 2003 ASTM International, West Conshohocken, PA. All rights reserved. This material may not be reproduced or copied, in whole or in part, in any printed, mechanical, electronic, film, or other distribution and storage media, without the written consent of the publisher.

Photocopy Rights

Authorization to photocopy items for internal, personal, or educational classroom use, or the internal, personal, or educational classroom use of specific clients, is granted by ASTM International (ASTM) provided that the appropriate fee is paid to the Copyright Clearance Center, 222 Rosewood Drive, Danvers, MA 01923; Tel: 978-750-8400; online: <http://www.copyright.com/>.

Peer Review Policy

Each paper published in this volume was evaluated by two peer reviewers and at least one editor. The authors addressed all of the reviewers' comments to the satisfaction of both the technical editor(s) and the ASTM International Committee on Publications.

To make technical information available as quickly as possible, the peer-reviewed papers in this publication were prepared "camera-ready" as submitted by the authors.

The quality of the papers in this publication reflects not only the obvious efforts of the authors and the technical editor(s), but also the work of the peer reviewers. In keeping with long-standing publication practices, ASTM International maintains the anonymity of the peer reviewers. The ASTM International Committee on Publications acknowledges with appreciation their dedication and contribution of time and effort on behalf of ASTM International.

Contents

FOREWORD	iii
OVERVIEW	vii
SESSION I: SPINAL CONSTRUCTS	
History of Isola-VSP Fatigue Testing Results with Correlation to Clinical Implant Failures—W. L. CARSON, M. ASHER, O. BOACHIE-ADJEI, B. AKBARNIA, R. DZIOBA, AND N. LEBWOHL	3
Gauge Length and Mobility of Test Blocks Strongly Affect the Strength and Stiffness of Posterior Occipito-Cervico-Thoracic Corpectomy Constructs—M. SLIVKA, H. SERHAN, D. SELVITELLI, AND K. TORRES	17
Relative 3 Dimensional Motions Between End Vertebrae in a Bi-level Construct, The Effect of Fixture Constraints on Test Results—W. L. CARSON	24
Spinal Implant Transverse Rod Connectors: A Delicate Balance Between Stability and Fatigue Performance—H. SERHAN AND M. A. SLIVKA	34
Corrosion on Spinal Implant Constructs: Should Standards be Revised?—J. S. KIRKPATRICK, R. VENUGOLOPALAN, M. BIBBS, J. E. LEMONS, AND P. BECK	40
SESSION II: SPINAL DEVICE COMPONENTS, SUBASSEMBLIES, AND INTERCONNECTIONS	
Effect of Transverse Connector Design on Development of Late Operative Site Pain: Preliminary Clinical Findings—S. M. COOK, M. ASHER, W. L. CARSON, AND S. M. LAI	47
Interconnection Strength Testing and its Value in Evaluating Clinical Performance—L. M. JENSEN, S. SPRINGER, S. CAMPBELL, AND E. GRAY	55
Protection of the Longitudinal Member Interconnection by ASTM F1798-97 Interconnection Mechanism and Subassemblies Standard Guide—W. L. CARSON	63
Clinical Relevance of Pull-out Strength Testing of Pedicle Screws—J. M. DAWSON, P. BOSCHERT, M. MACENSKI, AND N. RAND	68

SESSION III: CAGES AND INTERBODY FUSION DEVICES

Extrusion of Interbody Fusion Devices—Clinical Examples—S. M. THEISS 81

Is Push-out Testing of Cage Devices Worthwhile in Evaluating Clinical Performance?—S. SPRINGER, S. CAMPBELL, R. HOUFBURG, A. SHINBROT, AND J. PAVLOVIC 86

A Comparison of Two Strength-Testing Methodologies for Interbody Structural Allografts for Spinal Fusion—J. M. DAWSON, AND S. L. GRIFFITH 92

SESSION IV: FUNCTIONAL SPINAL DEVICES AND/OR ARTIFICIAL DISKS

The Influence of *In Vitro* Testing Method on Measured Intervertebral Disc Characteristics—G. HUBER, B. LINKE, M. M. MORLOCK, AND K. ITO 101

Testing of Human Cadaveric Functional Spinal Units to the ASTM Draft Standard, “Standard Test Methods for Static and Dynamic Characterization of Spinal Artificial Discs”—D. B. SPENCINER, J. PAIRA, AND J. J. CRISCO 114

Durability Test Method for a Prosthetic Nucleus (PN)—R. G. HUDGINS AND Q. B. BAO 127

SESSION V: SUGGESTED TEST METHODS, MODELS, FIXTURES, OR NEEDED IMPROVEMENTS

Mechanical Analogue Model of the Human Lumbar Spine: Development and Initial Evaluation—E. A. FRIIS, C. D. PENCE, C. D. GRABER, AND J. A. MONTOYA 143

An Improved Biomechanical Testing Protocol for Evaluating Multilevel Cervical Instrumentation in a Human Cadaveric Corpectomy Model—D. J. DIANGELO AND K. T. FOLEY 155

Influence of Preload in Flexibility Testing of Native and Instrumented Lumbar Spine Specimens—B. LINKE, G. MEYER, S. KNÖLLER, AND E. SCHNEIDER 173

Transverse Connectors: Clinical Objectives, Biomechanical Parameters Involved in Their Achievement, and Summary of Current and Needed *In Vitro* Tests—W. L. CARSON, M. ASHER, O. BOACHIE-ADJEI, AND B. AKBARNIA 191

An Evaluation of the Influence of UHMWPE Test Block Design on the Mechanical Performance of Bilateral Lumbar Corpectomy Constructs—W. L. DUNBAR, D. CESARONE, AND H. SERHAN 209

Vertebral Bone Density—A Critical Element in the Performance of Spinal Implants—J. S. TAN, B. K. KWON, D. SAMARASEKERA, M. F. DVORAK, AND C. G. FISHER, AND T. R. OXLAND 217

Index 231

Overview*

The field of spinal implants continues to be a dynamic one. New designs of modular constructs and components used in spinal fusions and the development of spinal implants intended to allow or maintain motion are major areas of change. Current implants allow the surgeon to tailor the spinal device used to impact the patho-anatomy confronted on the operating table. The multiple implant options also present some interesting problems to the designing engineers, surgeons, researchers, and regulatory entities in testing and evaluating the appropriateness of the devices' designs and/or materials in a given patient or population of patients. In May 1989, ASTM Committee F04, Medical and Surgical Devices and Materials, conducted a workshop on the subject of Spinal Implant testing and initiated standards development for spinal implants with the establishment of Subcommittee F04.25.

Members of this subcommittee (F04.25 of the ASTM Committee F04), that include industry, academic, and private concerns, have continued to collaborate on the development of standardized test methods evaluating numerous mechanical characteristics of components, subassemblies, and constructs of spinal systems. Existing ASTM standards published at the time of the symposium included: F1717-96, "Standard Test Methods for Static and Fatigue for Spinal Implant Constructs in a Corpectomy Model"; F1798-97 "Standard Guide for Evaluating the Static and Fatigue Properties of Interconnection Mechanisms and Subassemblies Used in Spinal Arthrodesis Implants"; F1582-98 "Standard Terminology Relating to Spinal Implants"; and F2077-00 "Static and Dynamic Test Methods for Intervertebral Body Fusion Devices." Standards under development included Static and Dynamic Test Methods for Spinal Disc Replacement Devices.

These published and draft standards are intended to be applied to constructs, assemblies, and subassemblies of posterior hook, wire, and pedicle screw spinal systems, anterior spinal systems, intervertebral body cages, total and partial spinal disc replacements, and vertebral body replacements for the cervical, thoracic, and lumbar levels. After several years of clinical experience and standards utilization, the subcommittee deemed it prudent to compare clinical results from these various devices with the results from standardized mechanical testing, failure analyses, and device retrieval analyses. This would help to determine whether current standards and drafts are relevant. Correlation of bench and clinical results would determine whether standards are adequately addressing each of the real or perceived potential failure modes seen clinically. Results from these analyses could then be used to improve existing standards or suggest new ones. Other goals included determining the critical clinical loading parameters and determining the most relevant mechanical testing performance characteristics.

In November 2001, ASTM Committee F04 on Medical and Surgical Materials and Devices and the AAOS (American Academy of Orthopaedic Surgeons) Committee on Biomedical Engineering sponsored a symposium on the subject of "Spinal Implants: Are We Evaluating Them Appropriately?" The objectives of the symposium were to assess our knowledge base at that time for testing of spinal implants, improve the published standards and draft standards under development,

* This overview represents the professional opinion of the authors and is not an official document, guidance or policy of the U.S. Government, the Department of Health and Human Services, or the Food and Drug Administration, nor should any official endorsement be inferred.

identify, and encourage new standards activities, and determine whether the standards were adequately predicting clinical experience. The symposium also continued the global harmonization efforts of the F04.25 Spinal Implant Subcommittee by seeking out participation of international presenters, researchers, and manufacturers. The symposium papers published here evaluate the experience available at that time for testing spinal constructs, spinal device components, subassemblies and interconnections; cages and interbody fusion devices; and functional spinal devices and/or artificial discs. Also considered in this symposium were suggestions for future directions for test methods, models, fixtures, or needed improvements. All presenters were encouraged to submit their work for inclusion in this publication. The editors applied strict peer review criteria utilizing independent qualified reviewers, but in order to facilitate prompt dissemination of the material, the editorial requirements were very liberal. This publication presents those topics whose authors met the peer review and editorial requirements of the editors.

Spinal Constructs

The intent of this section was to present developments and results associated the application of ASTM F1717-96 test methods. Papers described the clinical results from spinal constructs having marketing clearance or approval using these test methods, addressed device failure modes, and examined corrosion seen with explanted devices. Other papers evaluated impact on results due to gauge length used in tests, mobility or constraint of the test blocks, and use of transverse rod connection. These issues continue to be of particular interest in the improving of the existing spinal construct test methods.

Spinal Device Components, Subassemblies, and Interconnections

The developments of a new component or modifications to existing components of a construct do not necessarily require retesting of the entire construct. Instead, only the component or sub-assembly needs to be tested. ASTM F1798-97, the test methods and draft test methods for components, provided the background for this section. Papers describing the impact from application of different transverse connector designs on clinical outcomes are included. Other papers evaluated impact on bench testing results due to protection of the longitudinal member, to the anchoring materials, gauge length used in tests, mobility or constraint of the test blocks, and use of transverse rod connection. The issues identified during this session of the symposium related to the spinal components, subassemblies, and interconnections standards and are likely to be considered in future review and revision of these test methods.

Interbody Spacers and Intervertebral Body Fusion Devices

Standards efforts have not only focused on spinal fusion constructs attaching to the anterior and posterior spine, but have also included interbody spacers and other devices. The intent of this section was to present developments and results associated the application of ASTM F2077-00 test methods for intervertebral body fusion devices (spacers and fusion cages). One paper described the clinical results from lumbar interbody fusion devices and examined the causes of some of these devices that extruded. The remaining papers compared strength testing methodologies and evaluated the usefulness of pull-out or push-out testing for spinal cages. The issues discussed in this session of the symposium have led to the proposed revision of F2077-00 to exclude push-out testing and continue to be of particular interest in the improvement of the existing intervertebral body fusion device test methods.

Functional Spinal Devices and/or Artificial Discs

Recent standards development efforts have also been initiated for those devices that are not necessarily intended to fuse the spine. The intent of this section was to present developments associated with the application of draft ASTM test methods for disc replacement prostheses. The remaining presentations in this session of the symposium examined comparative cadaveric testing, durability testing, and alternative test methods for spinal constructs intended for posterior stabilization without fusion. The issues identified in this session of the symposium provide the basis of further development and refinement of draft standards for functional and motion preserving spinal devices.

Suggested Test Methods, Models, Fixtures, or Needed Improvements

Addressing today's limitations and tomorrow's concerns in spinal implants standards was the intent of this section. Papers describing the results from alternative models for fusion, non-fusion, or functional spinal implants are discussed in this section. The remaining presentations in this session of the symposium examined the impact on testing due to preload, block design, and material properties. The issues identified in this session of the symposium provide the basis of future development and refinement of existing, draft, and yet to be developed standards for spinal implants. The subcommittee plans to further investigate these issues.

Significance and Future Work

The symposium presentations and publications demonstrated the appropriateness and limitations of the existing and draft standards for spinal implants and identified many potential improvements. While the magnitude of some of these issues raised, like corrosion, remains unquantified, they may, at a later date, present a reason to alter the scientific wisdom expressed here. While changes to improve existing and draft standards have been initiated or are justified, none of the changes appear to be extreme. Future areas to be considered by Subcommittee F 04.25 should include determining the critical clinical loading parameters thus determining the most relevant mechanical testing performance characteristics, and examining the mechanistic interaction of these implants with anatomy and physiology.

Mark N. Melkerson, M.S.

Symposium chairman and co-editor;
Food Drug Administration
Center for Devices and Radiological Health
Office of Device Evaluation
9200 Corporate Boulevard
Rockville, MD 20850

John S. Kirkpatrick, M.D.

Symposium co-chairman and co-editor;
University of Alabama, Birmingham and
Birmingham Veterans Administration Medical Center
940 Faculty Office Tower
510 20th Street South
Birmingham, Alabama 35294

Steven Griffith, Ph.D.

Symposium co-chairman and co-editor;
Centerpulse Spine-Tech Division
7375 Bush Lake Road
Minneapolis, MN 55439

Session I: Spinal Constructs

William L. Carson,¹ Marc A. Asher,² Oheneba Boachie-Adjei,³ Behrooz Akbarnia,⁴ Robert Dzioba,⁵ and Nathan H. Lebowhl⁶

History of Isola-VSP Fatigue Testing Results with Correlation to Clinical Implant Failures

Reference: Carson, W. L., Asher, M., Boachie-Adjei, O., Akbarnia, B., Dzioba, R., and Lebowhl, N. H., “History of Isola-VSP Fatigue Testing Results with Correlation to Clinical Implant Failures,” *Spinal Implants: Are We Evaluating Them Appropriately, ASTM STP 1431*, M. N. Melkerson, S. L. Griffith, and J. S. Kirkpatrick, Eds., ASTM International, West Conshohocken, PA, 2003.

Abstract: The objective was to compare the history of Isola-VSP in vitro fatigue testing results with clinical implant failures from a five-center retrospective survey of 2499 cases to determine if the appropriate types of tests had been performed. To determine the effect of bending iron marks, bends, and connectors on ¼” rod fatigue, 4-point bend fatigue tests were conducted. To characterize bone anchor-connector-rod assemblies, unilateral construct flexion fatigue tests were conducted. Clinically 111 components failed: 41 screws, 57 rods, nine transverse connectors, two interbody graft/cages, one extended slotted connector, and one at unreported location. The screw, rod, and connector clinical data correlate to the lower to higher relative fatigue strength respectively of original integral nut screws; rods at bending iron marks, connectors and lordotic bends; original slotted connector, current slotted connector, and straight rods with unblemished surface. In vitro and clinical failure locations also correlated. The transverse connector cross member failed near the longitudinal rod in 8/9 instances. This implies a lateral bending profile similar to that produced by the H construct used to test them in reversed lateral bending. Recommendations relative to ASTM standards/guides include: incorporation of an H construct to test transverse connectors in lateral bending, replacement of fixed-fixed end with fixed-free end assembly in F 1798-97, and replacement of constrained

¹ Ph.D., Professor Emeritus Mechanical and Aerospace Engineering, University of Missouri-Columbia, 2111 Fairmont, Columbia, Missouri, USA.

² M.D., Dept. of Surgery Orthopedic Section, The University of Kansas Medical Center, 3901 Rainbow Blvd., Kansas City, Kansas, USA.

³ M.D., The Hospital for Special Surgery, 523 East 72nd Street, New York, New York, USA.

⁴ M.D., San Diego Center for Spinal Disorders, 4130 La Jolla Village Drive, Suite 300, La Jolla, California, USA.

⁵ M.D., Dept. Orthopaedic Surgery, The University of Arizona Health Sciences Center, PO box 245064, Tucson, Arizona, USA.

⁶ M.D., Department of Orthopaedics and Rehabilitation, University of Miami, Miami, Florida, USA.

4 SPINAL IMPLANTS

fixtures in F 1717-01 with unconstrained.

Keywords: Retrospective clinical survey, implant failure, in vitro test history, relative fatigue strength, bent/straight rod, bending iron marks, rod, connector, pedicle screw

Objective

The objective of this paper is to compare in vitro biomechanical fatigue testing results performed by Carson over the history of Isola-VSP hardware to clinical implant failures from a multi-center retrospective survey of cases to determine if the appropriate types of in vitro tests had been performed.

History of Fatigue Testing Results

To determine the effect of bending iron marks, bends, and connectors on rod fatigue, 4-point bend fatigue tests (Fig. 1) were conducted on four types of SS and Ti ¼" rod specimens: straight (Fig. 4a), 10° central kyphotic bend with 137 mm (5.4 inch) radius of curvature (Fig. 2), 45° central kyphotic bend with 22.5° adjacent outer lordotic bends both with 31.75 mm (1.25 inch) radius of curvature (Fig. 3); and on straight rods with Isola TRC, MCC, and Isola VHG body connectors attached (Fig. 4). All of these tests were conducted in an environmental chamber (Fig. 1b) filled with lactated Ringer's solution that was recirculated and aerated by a flow through heater that maintained it at 37° C. The solution was maintained at $6 < \text{pH} < 7$ by adding diluted hydrochloric acid. The results are summarized in (Table 1a–b), and graphically compared in Figs. 6 and 7.

To biomechanically characterize bone anchor-connector-rod assemblies, a series of axially loaded unilateral construct flexion fatigue tests were conducted with straight and bent rods. These tests were also conducted in a lactated Ringer's solution environment. A representative sample of these tests is presented in this paper. Isola PMA tests were conducted with only the tips of 45 mm long original integral nut VSP screws inserted into nylon mounting blocks to simulate the "worst case" of no bony support to the cancellous threads (Fig. 5a). This was done to identify the component or interconnection that would be most vulnerable to fatigue failure. The original Isola slotted connectors were tested with 7 mm iliac screws to eliminate screw fatigue, and thus be able to evaluate the fatigue properties of the slotted connector and its interconnections to the rod and screw (Fig. 5b). To test hooks, the blade of each hook was placed over the pin of the corresponding yoke fixture (Fig. 5c). The yoke pin diameter was equal to or slightly larger than the hook throat to maintain a constant AP distance between point of load application and the longitudinal rod axis. Table 2 contains results from these representative tests, which are graphically compared along with 4-point bend test results in Fig. 7.

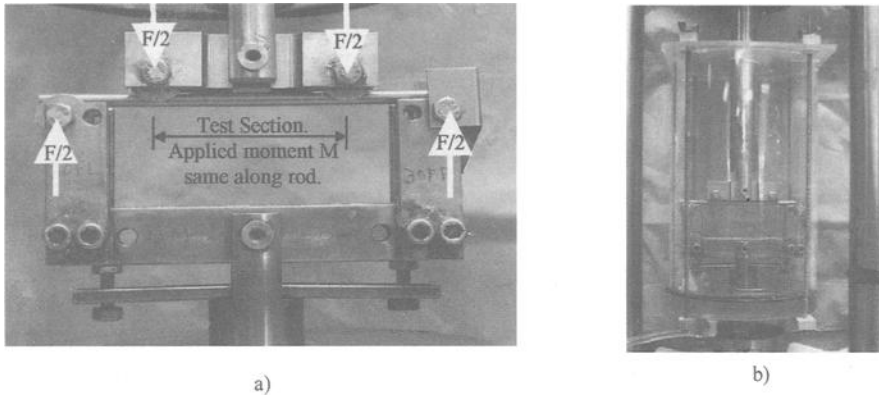


Figure 1 - 4-point bend test: a) fixture, and b) Ringer's solution environmental chamber.

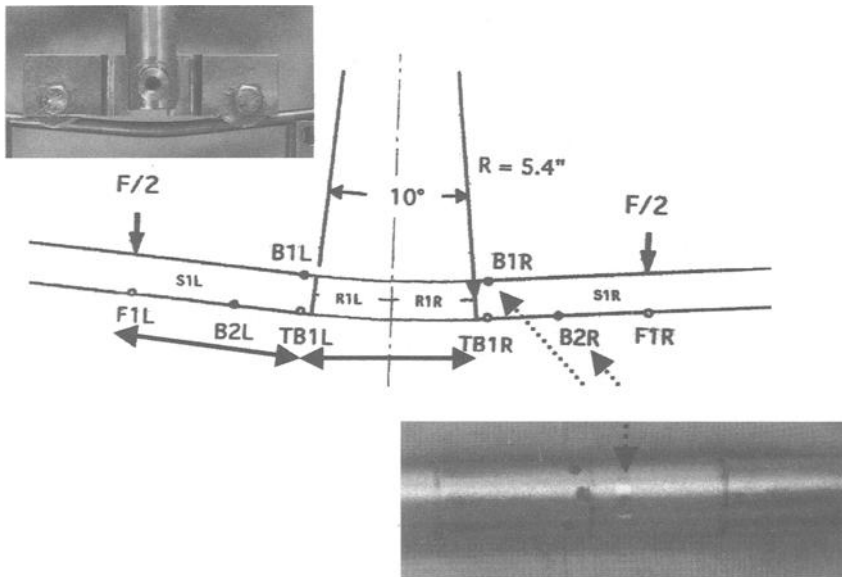


Figure 2 - 10° central kyphotic bend with 137 mm radius of curvature rod specimen.
 Nomenclature: B1R Bending iron mark #1, Right side.
 F1R Point on opposite side of rod to force application #1, Right side.
 R1R Radiused section of rod #1, Right side.
 S1R Straight section of rod #1, Right side.
 TB1R Tensile side of rod opposite to bending iron mark #1, Right side.

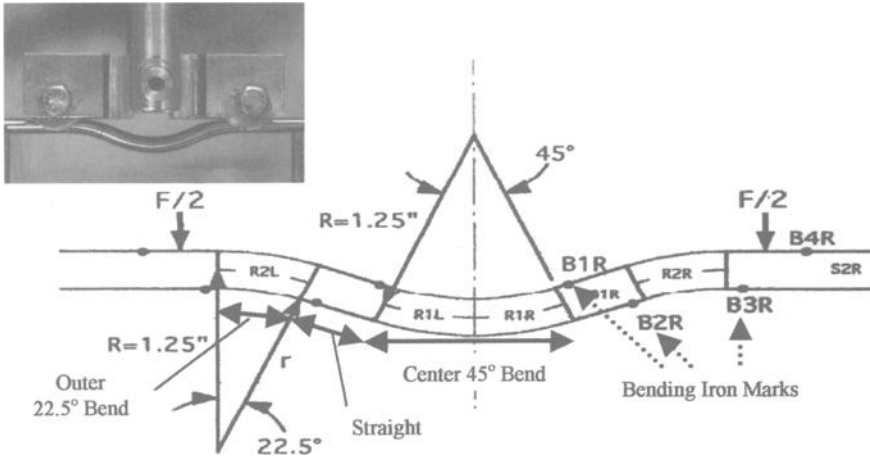
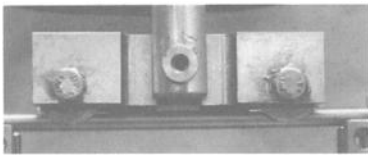
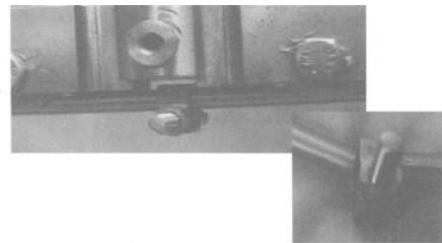


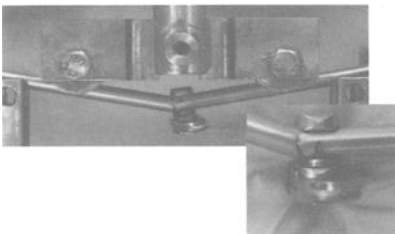
Figure 3 - 45° central bend, 22.5° outer bend with 31.75 mm radii of curvature rod specimen. Nomenclature listed in Figure 2.



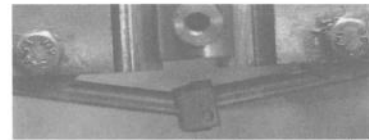
a) Straight plain rod (control)



b) Isola TRC (Transverse Rod Connector)



c) MCC (cross-link)



d) VHG body (with hook blade removed)
Edge of set screw imprint

Figure 4 - Specimens used to test the effect of connectors on rod fatigue life, and typical location of failure adjacent to connector.

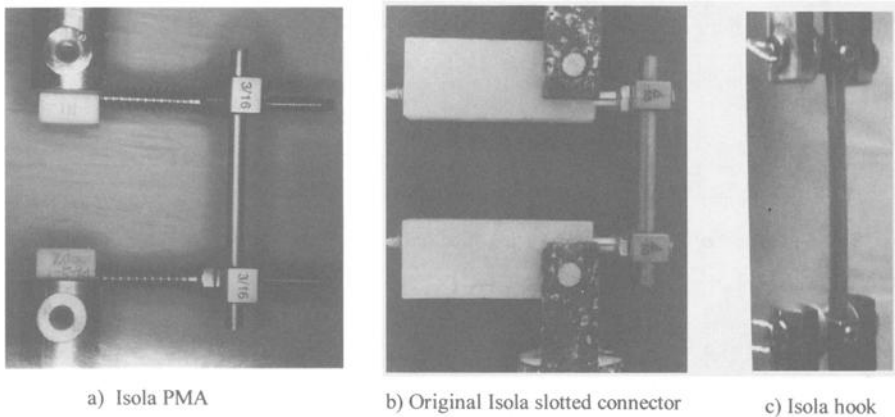


Figure 5 - Representative unilateral construct tests:

- a) *Isola PMA: SS, 7 mm original integral nut VSP screw design, 1/4" & 3/16" rod & slotted connectors.*
- b) *Original Isola slotted connector: SS, 7 mm iliac screw, 1/4" rod & slotted connectors.*
- c) *Hook: Ti, 1/4" rod shown.*

Five Center Survey of Cases for Clinical Implant Failures

The five spine surgeons listed as co-authors surveyed their cases for implant failures. A total of 2499 mixed gender cases were reviewed. As summarized in table 3a these cases: spanned an age range from 2 to 87 years; were instrumented for a multitude of indications; and resulted in 143 cases with 111 implant component failures, bone-implant interconnection failures, or complications possibly related to an implant. Instrumentation was primarily posterior and stainless steel, some being Titanium. Table 3b contains a summary of bone-implant failures and/or complications possibly related to the existence of an implant as reported by two surgeons. Table 3b was included in this paper to indicate the types of complications that can occur clinically other than implant component failure, which in itself does not always result in a clinical failure. Table 3c contains the number of failed components listed by type of component. The number of failed components include each failed component within a case involving multiple component failures. Rods not identified by size were included in the 1/4" diameter count. The authors realize that some differences exist among the centers with respect to how cases were reported, and do not claim 100% accuracy. The clinical survey in its present form does however produce a good initial indication with respect to answering the in vitro testing question, "Are We Evaluating Them Appropriately?"

8 SPINAL IMPLANTS

Table 1a - The effect of connectors on fatigue life of straight rod, 4-point bend tests.

	Plain rod - fine texture	TRC (rod fail edge of TRC)	MCC (rod fail edge of set screw)	VHG Hook./Slotted connector (rod fail edge of set screw)
Cycles to fatigue fracture at 23.7 Nm flexion bending load				
SS	1,000,000 +/- 0 (n = 6)	275,932 +/- 170,094 (n = 3)	108,689 +/- 24,336 (n = 3)	151,069 +/- 29,079 (n = 2) / 244,453 +/- 163,155 (n = 3)
Ti	2,000,000 +/- 0 (n = 3)	182,267 +/- 106,951 (n = 3)	70,500 +/- 7,281 (n = 3)	--

Table 1b - The effect of bending iron marks and bends on rod fatigue, 4-point bend tests.

Mo- ment (Nm)	Mat- erial	10° central bend, 137 mm radius		45° central, 22.5° adjacent bend, 31.75 mm radius	
		Cycles to failure	Location of failure	Cycles to failure	Location of failure
23.7	SS	138,872 +/- 14,771	Bending iron mark (n = 3)	37,897 +/- 1,089	Outer 22.5° bend (n = 3)
	Ti	73,139 +/- 8,397	Bending iron mark (n = 3)	11,760 +/- 681	Bending iron mark (n = 2) Outer 22.5° bend (n = 1)
21.3	SS	944,825 +/- 262,466	Bending iron mark (n = 1) Central section (n = 1) Straight section (n = 1)	41,874 +/- 2,133	Outer 22.5° bend (n = 2)
	Ti	88,958 +/- 0 2,000,000 +/- 0	Bending iron mark (n = 1) Run Out (n = 2)	15,176 +/- 641	Bending iron mark (n = 2)

Table 2 - Summary of results for selected unilateral construct flexion fatigue tests with straight and bent rods.

Unilateral construct (straight rod)	Endurance limit estimated from Figure 7 (Nm)	Failure location
Screw-Connector-Rod constructs:		
SS: Isola PMA testing: original integral nut 7mm VSP 3 thread tapered root screw design unprotected by 18mm long nylon loading block at tip of screw, 1/4" straight rod & slotted connectors.	6	Root of 3 rd +/- 1 cancellous thread from integral nut.
SS: Original Isola slotted connector (SCM1), 7 mm iliac screw, 1/4" straight rod.	11	Transition between VHG body and slot.
SS: Current slotted connector (SCM10): 7mm 2 nd generation VSP screws protected by nylon loading block over length of cancellous thread, 1/4" straight rod.	14	Slotted section, screw located middle of slot.
Ti: Prototype slotted connector and pedicle screw, 1/4" straight rod.	For rod only, less than 17.5	Rod fatigue failure at edge of set screw, average life from 240,000 to 560,000 cycles.
Hook-Rod constructs:		
Ti: Isola 6.5 mm throat solid VHG body hooks, 1/4" straight Isola rod.	Greater than 9.75 (1068 N applied force)	Run out > 5,000,000 cycles. (n = 2)
SS: Isola 6.5 mm throat or greater open and solid body hooks, 1/4" and 3/16" straight Isola rod.	Greater than 7.3 (800 N applied force)	Run out > 5,000,000 cycles. (n = 18)
SS: Harrington, 1/4" straight Harrington rod with ratchets.	Less than 7.3 (800 N applied force)	Rod at small diameter of ratchet. 1,224,642 +/- 477,560 cycles (n = 3)
Unilateral construct (bent and straight rod)	Moment at rod (Nm)	Location of and cycles to failure
SS: Prototype connector and pedicle screw: • 1/4" rod bent in lordosis with 35.9° radius of curvature.	15.6	161,075 +/- 12,306 (n = 3) Greater than 3 mm from connector.
	12.5	308,709 +/- 70,153 (n = 2) Greater than 3 mm from connector. 1,178,983 +/- 380,394 (n = 2) At edge of connector.
• 1/4" straight rod (same lot as bent rod).	15.6	2,220,150 (n = 1) Run out
	12.5	2,030,259 (n = 1) Run out

Table 3a - Five center retrospective survey of clinical cases: number of cases reviewed, indications, number of cases with implant failure, and center clarification footnotes.

Center-Surgeon	1	2	3	4 Degen. : Other	5	Total
Cases reviewed, # of:	600	771	269	105 : 632	122	2499
Reviewed case patient age:	Range (yrs)	- 3 - 87	18 - 79	20-80 : 2-77	-	
	Mean, +/- st. dev. (yrs)	- 44, ?	45, 9	59, 12 : 18, ?	-	
Reviewed case indication, # of:	Deformity	- 167	124	505	-	
	Degenerative	- 294	111	105	-	
	Trauma-Tumor	- 141	32	78	-	
	Spondylolisthesis	- 109	2	40	-	
	Other	- 60	0	9	-	
Cases reported with:	Implant component failure only,	18	10	5	-	5
	+ bone-implant interconnection failure, or complications possibly related to implant.	-	-	-	28 : 77	-
Failed components within cases reported, # of. (See table 3c for listing by type of component.)						143
Footnotes relative to each center:						111
<ol style="list-style-type: none"> 1. Includes hardware from previous surgeries in addition to Isola and VSP. 2. Includes Isola, VSP and Pediatric. No broken screws identified after 1991. Does not include implant connection or screw pullout problems. 3. Only Isola hardware cases reported. Screw fracture all in S1 and bilateral. Does not include bone failure around intact hardware. Does include hardware failure as result of osteoporosis or pseudarthrosis. All five implant failure cases proven pseudo. 4. Broke out cases by degenerative and all others as reported herein. Not all implant failure cases required re-operation. Approximately 80% of degenerative group had prior surgery, average 2.4 per patient. 5. Bone lucency around distal screws not tracked, thus not included. 						

Table 3b - Five center retrospective survey of clinical cases: bone-implant failures, complications possibly related to implant.

Center-Surgeon	1	2	3	4 Degen. : Other	5	Total
Bone-Implant Failures, Complications Possibly Related to Implant						
Bone-implant failure:	Hallo: Around screw			5 : 2		7
	Vertebra fracture (end instrumented): Proximal			1 : 0		1
	Distal			2 : 0		2
	Hook: Migration and other			7		7
	Wire/cable: Cut out			-		-
Prominence of hardware:	Wire			2		2
Skin break down over implant.				0 : 3		3
Late operative site pain at:	Isola TRC - fretting corrosion	1?		2 : 10		13
	Isola open drop entry transverse connector	-		1 : 0		1
	Ilium - loose screw in bone/post	1		3 : 2		6
	Rod fracture - fretting corrosion	1		-		1
	Undetermined component	-		1 : 5		6
Infection:	Late	1		1 : 9		11
	Acute	-		5 : 6		11
Adjacent segment degeneration:	New			14 : 5		19
	Pre-existing			5 : 1		6
Neurological complication (usually associated with reduction)				4 : 5		9

Table 3c - Five center retrospective survey of clinical cases: type and number of failed implant components.

Center-Surgeon	1	2	3	4	5	Total
				Degen. : Other		
Number of Failed Implant Components						
Screw : All tyoes: Cancellous thread 3rd ± 1 from integral nut	4	5	4	6 : 11	4	34
<u>VSP:</u> Nut back off post	1	-	-	-	-	1
Pre-integral nut, 10-32 below anterior nut	-	-	-	0 : 2	-	2
Post fracture	-	-	-	-	-	-
<u>Isola open:</u> Cap disengage	-	-	-	0 : 1	-	1
<u>Iliac:</u> Cancellous thread at shank	-	-	-	0 : 2	-	2
<u>Location not reported.</u>	1	-	-	-	-	1
Screw total						41
Rod (1/4" ; 3/16"): <u>Adjacent to:</u> Isola TRC	-	-	-	8 : 6	-	14
MCC	-	-	-	none used	-	-
Slotted connector	1	-	2 : 1	4 : 2	-	10
Fixed closed/open screw	-	-	-	-	-	-
Hook/claw	-	-	-	-	-	-
Growth, tandem connector	2	-	-	-	-	2
<u>Open section:</u> Straight	-	-	-	-	-	-
Lordotic bend	-	-	-	2 : 3	-	5
Kyphotic bend	-	-	-	1	-	1
Type not reported	6	-	-	0 : 5	-	11
<u>Galvaston/sacral bend up to 90° :</u>	2	-	-	2 : 1	-	5
<u>Location not reported.</u>	4	3 ; 2	-	-	-	9
Rod total						57
Connector: <u>Slotted:</u> Original, standard, mini-offset	0	0	0	0 : 0	0	0
Extended	1	-	-	-	-	1
<u>Split:</u> As part of TRC	0	0	0	0 : 0	0	0
As rod to VSP screw connector	0	0	0	0 : 0	0	0
Slotted/split connector total						1
Hook/claw: (does not include pull out/migration)	0	0	0	0 : 0	0	0
Hook/claw "hardware" total						0
Wire/Cable: (does not include cut out/migration)	0	-	-	-	0	0
Wire/cable "hardware" total						0
Transverse connector: X-member fracture near connector	2	-	-	4 : 2	1	8
Disconnect from longitudinal rod	1	-	-	-	-	1
Transverse connector total						9
Interbody graft/cage: Expelled	-	-	-	-	-	-
Lose position	-	-	-	-	-	-
Subside, migrate through end plate	-	-	-	-	1	1
Resorb, collapse	-	-	-	0 - 1 allograft	-	1
Interbody graft/cage total						2
Implant failure location not reported.	1	-	-	-	-	1
Pseudo/lack ant. col. support at level of implant failure.	10	3	5	5 : 10	4	37

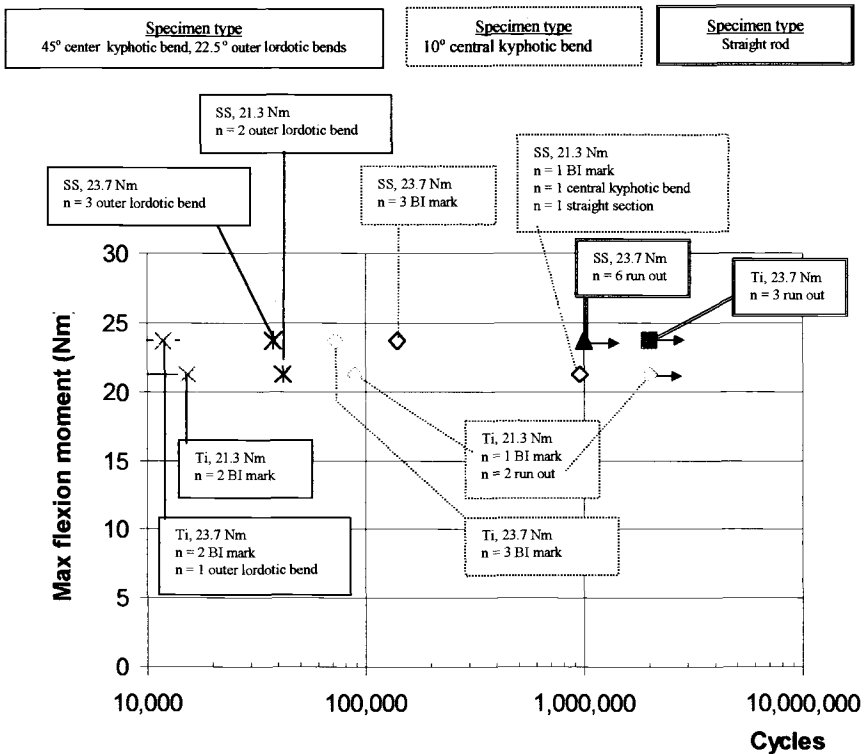


Figure 6 - Mn flexion bending moment diagram, the effect of rod bending and bending iron marks on rod fatigue life.

Observations, and Correlations of In Vitro Tests to Clinical Results

The following are observations, and correlations of in vitro test results to clinical results.

1. 111 component failures were observed in the 143 (5.7%) out of 2499 cases that were reported with some type of implant component failure, bone-implant interconnection failure, or complications possibly related to an implant (Table 3a).
2. Implant failure was frequently associated with a pseudoarthrosis (37 being at a confirmed pseudo) and thus inadequate load sharing by the anterior column. This correlates to the in vitro practice of conducting tests with a comminuted construct.

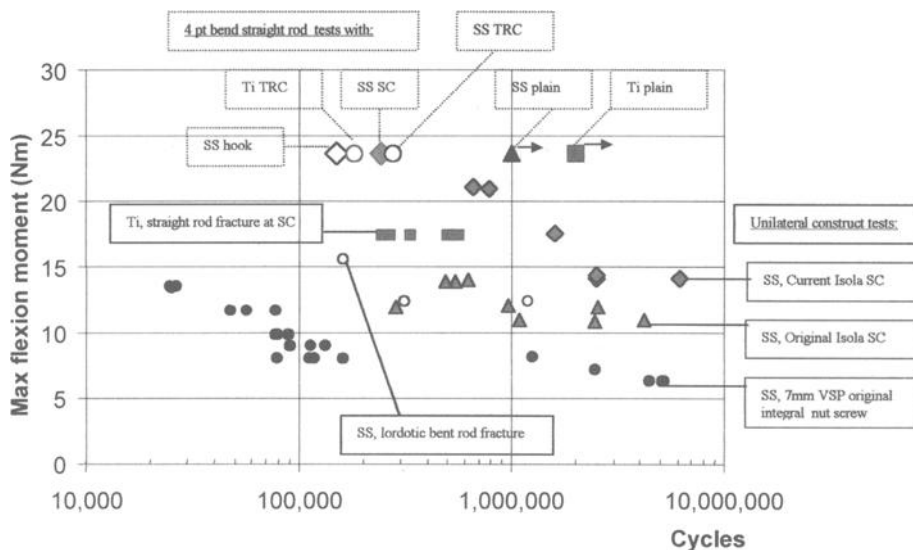


Figure 7 - Mn flexion bending moment diagram, comparison of unilateral construct fatigue life and 4 point bend straight rod without and with connectors.

3. Screw (41 or 36.9%) and Rod (57 or 51.4%) failures were the most numerous of the 111 reported clinical component failures. Their location corresponds to those observed during unilateral construct testing, at posterior locations which are subject to higher flexion bending moments coupled with higher stress within the component due to location of a stress concentration and/or surface alteration of the rod. For example:

a. Screw fracture at third +/-1 cancellous thread from integral nut (34) out of the 40 clinical screw failures with reported location correlates to the location observed during in vitro tests as illustrated in Figure 8.

b. Rod fracture adjacent to a connector (26) is more likely than in an open thoracolumbar straight or bent section (17) according to the clinical data where location has been identified. This correlates to the lowering of rod fatigue life by connectors observed during in vitro tests (Figure 7), and also to their adjacent location shown in Figure 4.

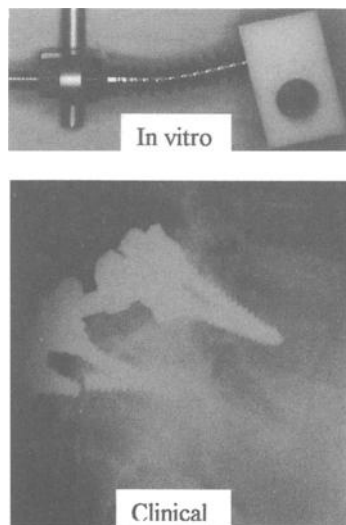


Figure 8 - Typical screw failure in third +/-1cancellous thread from integral nut.

c. Rod fracture in open thoracolumbar expanses according to the in vitro data in Figures 6 and 7 is more likely to occur at either bending iron marks, or in a lordotically bent rod. The 6 clinical open section rod failures identified by type of thoracolumbar bend produced 5 fractures in lordotic bends compared to 1 in a kyphotic bend. This correlates to the lower fatigue life of lordotically bent rods compared to that of straight rods used in unilateral construct tests (Table 2 and Figure 7). Clinical data to identify whether rod failure in open sections occurred at bending iron marks was not available for comparison to their observed in vitro effect of lowering rod fatigue life.

d. Rod fracture in Galveston/sacral bends of up to 90° occurred in 5 instances. An in vitro test fixture for sacral/ilic foundations that would test these types of bends with clinically relevant loading is proposed in reference [1].

4. No original, standard or mini-offset slotted connector failures were reported clinically. This correlates with the relative strength of components observed during in vitro tests as displayed in Figure 7, and their corresponding endurance limits reported in Table 2:
 - a. The original Isola slotted connector had greater fatigue strength (endurance limit = 11 Nm) compared to the original integral nut VSP screws used at that time (endurance limit = 6 Nm).
 - b. The standard Isola slotted connector that replaced the original has greater fatigue strength (endurance limit = 14 Nm) than does rod at connectors, bent in lordosis, or with known surface blemish.
 - c. Clinically rod failures appear to be more prevalent between or adjacent to end foundations, and in long constructs. Hypothetically, the flexion bending moment within the foundations are distributed to multiple anchors thus reducing the likelihood of screw, slotted connector and rod failure within the foundation.
5. One extended slotted connector failure was reported clinically, which occurred at its connection to a pelvic bolt. This corresponds to in vitro tests in which shorter fatigue life occurred for longer slots and when the screw was located at far end of slot opposite to the body of slotted connectors.
6. No hook/claw hardware failure was reported. One co-author reported 7 incidences of hook migration or disengagement from bone. Others did not specifically look for or count bone-implant interconnection problems.
 - a. Absence of hook/claw implant failure corresponds to Carson's in vitro testing reported in table 2 in which hook-rod and corresponding interconnections went to 5,000,000 cycle run out with axial loads of 800 N for ¼" and 3/16" rod SS hooks, and 1068 N for Ti ¼" hooks. Harrington hook-rod unilateral constructs that were similarly tested at 800 N failed in the small diameter ratchets of the rod at 1,224,642 +/- 477,260 cycles. This location of Harrington rod failure has been observed clinically.
 - b. Hook/claw disengagement from or migration through bone is a clinical mode of failure as evidenced by the 7 incidences reported by the one surgeon who looked for this mode of failure. There is no current ASTM in vitro test standard for this mode of failure.

7. Transverse connector failure (9 or 8.1%) ranked 3rd in number of clinical component failures:

a. Eight out of the 9 were fracture of the cross member adjacent to the longitudinal rod connector, an example of which is shown in Figure 8.

b. These occurred in Galveston foundations apparently due to the lateral bending moment within the transverse connector as a result of the “piston effect” between longitudinal members during ambulation.

c. This mode of failure was observed by Carson when testing transverse connectors with an H construct that produced reversed direction of lateral bending moment in the transverse member [1].

d. Flexion bending load on transfixed bilateral constructs in ASTM Standard Test

Methods for Spinal Implant Constructs in a Vertebrectomy Model (F 1717-01) does not create this type of loading, thus there is no current ASTM standard creating this mode of failure.

8. Wire or cable fracture, or cut out through bone did not surface as a mode of failure during the survey. However, some co-authors have indicated that these modes of failure have clinically occurred.

9. Twenty seven cases of Late Operative Site Pain (LOSP) were clinically reported. Fretting-corrosion was reported to exist in 14 of these incidences.

a. Having conducted most all fatigue tests in a Ringer’s solution environment (Figure 1b), Carson observed greater tendency for fretting-corrosion within interconnections having lower axial-torsional gripping strength when testing transverse connectors in reverse lateral bending load with an H construct, as well as when testing interconnections in flexion bending with unilateral constructs.

b. Cook et al [2] reported that stronger cross-link interconnections appear to correlate with a decreased incidence of LOSP in their biomechanical and clinical study.

10. In addition to LOSP, one co-author reported 17 bone-implant failures and complications possibly related to an implant: prominence of hardware (2 wire), skin breakdown over implant (3), infection (21), adjacent segment degeneration (25), and neurological complication usually associated with reduction (9).

a. Other than the possible correlation between LOSP and fretting corrosion [2], there is no direct evidence of correlation to past in vitro test results and these bone-implant failures and/or complications.

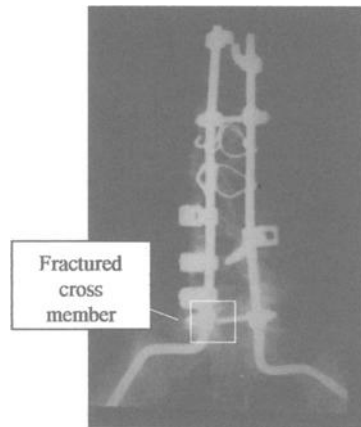


Figure 8 - Galveston foundation with typical fracture location of cross member due to lateral bending within it caused by the construct piston effect.

Conclusions, Discussion, and Recommendations

The following are general conclusions based on the in vitro and clinical results presented in this paper, and associated recommendations with discussion.

1. Flexion tests on comminuted unilateral constructs with cancellous threads unprotected, unilateral hook constructs, and four point bend tests on straight/bent longitudinal members with/without connectors have produced implant failure modes and relative fatigue strength of bone anchors, longitudinal members, and their connectors that correspond in location and relative fatigue strength to those observed clinically.
 - a. Based in part on the correlation of unilateral construct test results to clinical results, in a companion paper [3] a recommendation is made to eliminate the protection of the longitudinal member by the fixed-fixed end assembly used in ASTM Guide for Evaluating the Static and Fatigue Properties of Interconnection Mechanisms and Subassemblies Used in Spinal Arthrodesis Implants (F 1798-97).
 - b. The flexion test protocol on bilateral vertebrectomy constructs in F 1717-01 has produced rod failure at transverse connectors, and screw failure within the cancellous thread and interconnections similar to those produced by unilateral construct tests. However the true magnitude of internal load at the failure site is in question due in part to 3 of the 6 degrees of freedom being constrained by the pinned fixtures and the existence of bilateral hardware, each side of which does not necessarily resist the load equally. The degree of screw cancellous thread protection is also in question with the F 1717-01 protocol. Unconstrained fixtures to test bilateral construct stability, strength and fatigue properties in axial-flexion and torsional loading is proposed as a modification to F 1717-01 in a companion paper [4]. Unconstrained fixtures might or might not produce equal load in each side of a bilateral construct that is symmetrical about a mid-sagittal plane. Regardless, constructs in general will not be or will not remain symmetrical about a mid plane, both geometrically and in biomechanical characteristics of their components and interconnections. Thus to assure that loads on individual components and interconnections are known, unilateral constructs or the proposed equivalent fixed-free end assembly test proposed for F 1798-97 should be used to characterize the fatigue properties of rods, screws, and their connectors and interconnections.
2. Reverse direction loading of H constructs has produced the clinically observe lateral bending mode of transverse connector failure.
 - a. A modified H construct test for transverse connectors is recommended [1] as part of an ASTM standard/guide.
3. Fretting corrosion does occur clinically and is hypothesized to be one cause of late operative site pain [2]. There appears to be a correlation between stronger cross-link interconnections and the associated lower propensity for fretting corrosion observed during in vitro tests, and the clinical absence of late operative site pain at transverse connectors having stronger interconnections.
 - a. In vitro fatigue testing of interconnections in a saline environment should be either required or more strongly encouraged in ASTM standards/guides to be able to evaluate the relative propensity of fretting corrosion.

References

- [1] Carson, W.L., Asher, M., Boachie-Adjei, O., Akbarnia, B., "Transverse Connectors: Clinical Objectives, Biomechanical Parameters Involved in Their Achievement, and Summary of Current and Needed In Vitro Tests," *Symposium on Spinal Implants: Are We Evaluating Them Appropriately, ASTM STP 1431*, M. N. Melkerson, S. L. Griffith, and J. S. Kirkpatrick, Eds., ASTM International, West Conshohocken, PA, 2002.
- [2] Cook, S., Asher, M., Lai, S. M., Carson, W. L., "Effect of Transverse Connector Design on Development of Late Operative Site Pain: A Biomechanical and Clinical Study," *Symposium on Spinal Implants: Are We Evaluating Them Appropriately, ASTM STP 1431*, M. N. Melkerson, S. L. Griffith, and J. S. Kirkpatrick, Eds., ASTM International, West Conshohocken, PA, 2002.
- [3] Carson, W. L., "Protection of the Longitudinal Member Interconnection by ASTM F 1798-97 Interconnection Mechanism and Subassemblies Standard Guide," *Symposium on Spinal Implants: Are We Evaluating Them Appropriately, ASTM STP 1431*, M. N. Melkerson, S. L. Griffith, and J. S. Kirkpatrick, Eds., ASTM International, West Conshohocken, PA, 2002.
- [4] Carson, W. L., "Relative 3 Dimensional Motions between End Vertebrae in a Bilevel Construct, the Effect of Fixture Constraints on Test Results," *Symposium on Spinal Implants: Are We Evaluating Them Appropriately, ASTM STP 1431*, M. N. Melkerson, S. L. Griffith, and J. S. Kirkpatrick, Eds., ASTM International, West Conshohocken, PA, 2002.

Michael A. Slivka,¹ Hassan Serhan,² David M. Selvitelli³ and Katherine Torres¹

Gauge Length and Mobility of Test Blocks Strongly Affect the Strength and Stiffness of Posterior Occipito-Cervico-Thoracic Corpectomy Constructs

Reference: Slivka, M. A., Serhan, H., Selvitelli, D. M., and Torres, K., “Gauge Length and Mobility of Test Blocks Strongly Affect the Strength and Stiffness of Posterior Occipito-Cervico-Thoracic Corpectomy Constructs,” *Spinal Implants: Are We Evaluating Them Appropriately? ASTM STP 1431*, M. N. Melkerson, S. L. Griffith, and J. S. Kirkpatrick, Eds., ASTM International, West Conshohocken, PA, 2003.

Abstract: This study was conducted to investigate the effect of test block mobility and gauge length on the strength and stiffness of rod-based posterior occipito-cervico-thoracic corpectomy constructs. The influence of inferior test block mobility was studied by evaluating both pivoting and clamped boundary conditions. Gauge length was varied from 55 mm, the shortest possible length, to 196 mm, simulating the connection of the occipital plate down to T3. Static compression bending and torsion tests were performed in general accordance with ASTM Test Methods for Static and Fatigue for Spinal Implant Constructs in a Corpectomy Model (F 1717-96) to determine the strength and stiffness of the various configurations. Additionally, dynamic compression bending tests were performed to determine the fatigue strength of two types of constructs: 1) 76 mm gauge length with pivoting inferior (and superior) blocks, and 2) longest 196 mm gauge length with clamped inferior block (superior block pivoting). As expected, the stiffness and 2% offset yield load of the constructs in static compression bending decreased with increasing gauge length and clamping the inferior test block caused a dramatic increase in both. The torsional stiffness increased when the gauge length was increased from 55 mm to 116 mm due to the addition of cross-connectors, but then decreased with gauge lengths higher than 116 mm despite adding more cross-connectors. Without adding cross-connectors, the stiffness decreased with increasing gauge length. In dynamic compression bending, the endurance limit nearly doubled for the construct with almost three times longer gauge length simply due to clamping the inferior test block.

Keywords: corpectomy, posterior cervical, biomechanical testing model, fatigue

¹ Research Engineer, DePuy AcroMed, 325 Paramount Dr., Raynham, MA 02767.

² Manager of Research and Technology, DePuy AcroMed, 325 Paramount Dr., Raynham, MA 02767.

³ Product Development Engineer, Mitek Products, 249 Vanderbilt Ave, Norwood, MA 02062.

Introduction

Testing standards have been established for evaluating posterior and anterior cervical and lumbar spinal systems (F 1717). However, these methods do not adequately address testing systems involving posterior fixation from the occiput to the cervical and upper thoracic spine. For example, in order to test the performance of a system that connects from the occiput to the upper thoracic spine in a corpectomy model, a gauge length longer than the recommendations in F 1717 is needed for anatomical accuracy. Furthermore, since the flexion-extension range of motion in the thoracic spine is much less than in the cervical and lumbar regions [1], the use of a clamped test block will likely mimic the *in vivo* loading more accurately than a freely pivoting test block as recommended in F 1717. The objective of this study was to investigate the effect of gauge length and mobility of the inferior test block on the strength and stiffness of rod-based posterior occipito-cervical-thoracic corpectomy constructs.

Materials and Methods

Corpectomy constructs consisted of occipital plates, pre-bent 3/4/3 mm transition rods, spinal screws and cross-connectors, all made from Ti-6Al-4V alloy (DePuy AcroMed, Raynham, MA). All constructs were assembled using UHMWPE (meeting specifications called out in F 1717) test blocks designed to simulate the occiput and lower vertebral body (Fig. 1). Constructs were built with the following gauge lengths: 55, 76, 116, 156 and 196 mm. The shortest length that could be achieved was 55 mm. The 76 mm length accommodated one cross-connector in the construct. The latter gauge lengths of 116, 156 and 196 mm represent the approximate distance from the midline keel of the occiput to T1, T2 and T3, respectively [2,3]. No cross-connectors were used for the shortest gauge length and one additional cross-connector was added for each gauge length increment. The superior cross-connector was always placed just below the transition in the rod and additional cross-connectors were placed equidistant between the superior cross-connector and the inferior screws.

Static and dynamic compression bending and static torsion testing were performed following F 1717 on bilateral corpectomy constructs. Static compression bending was performed using an Instron electromechanical test frame with a crosshead speed of 25 mm/min and force versus displacement were recorded at a rate of 5 Hz. Static torsion was performed using a biaxial MTS servohydraulic test frame. The actuator was moved at an angular displacement rate of 1 deg/sec and torque versus angular displacement data were recorded at a rate of 5 Hz. One construct per gauge length was tested with the pin joints mounted at both test blocks. Additionally, the 55, 116, and 196 mm gauge length constructs were tested in static compression bending by clamping the inferior block to the test fixture using a C-clamp, preventing rotation, while the superior test block was attached using the pin joint. Static torsion was also performed on the 116 and

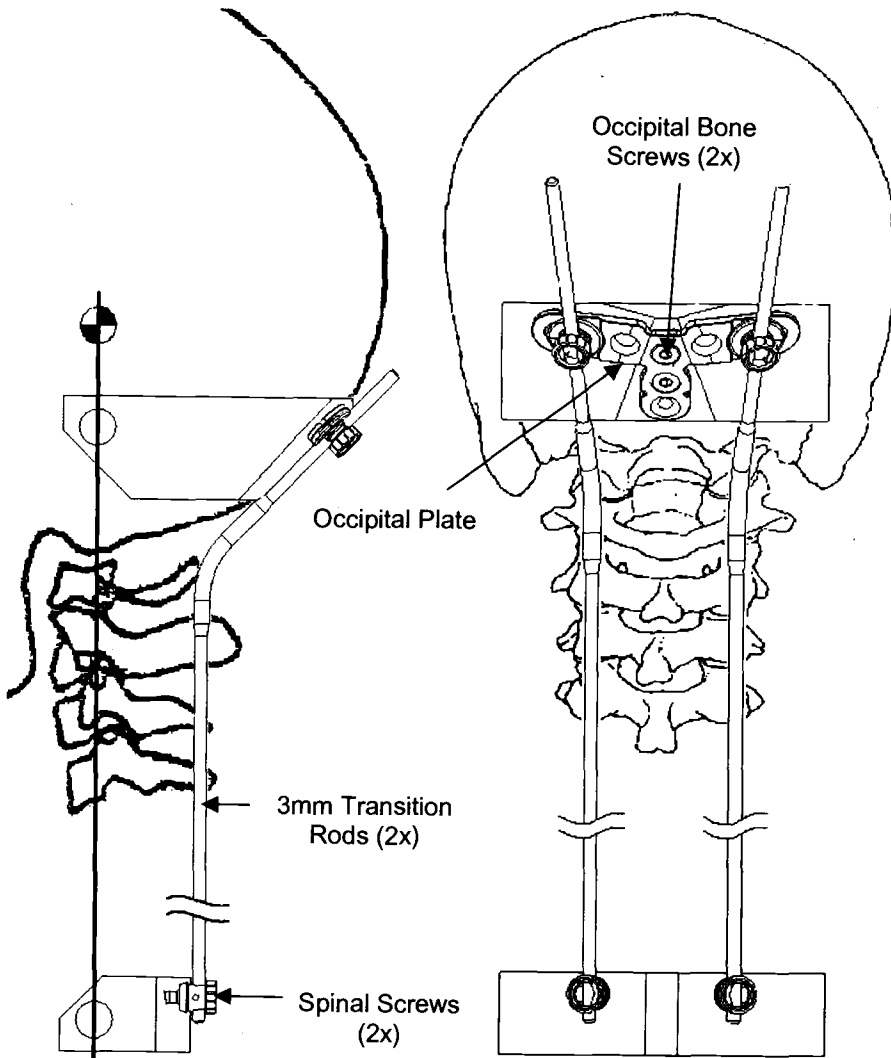


Figure 1—Test block configuration for posterior occipito-cervico-thoracic corpectomy constructs.

196 mm gauge length constructs with no cross-connectors. Stiffnesses in both test modes were calculated using the methods described in F 1717. The fatigue performance in compression bending of the longest (196 mm) construct with clamped inferior block was compared to the 76 mm gauge length construct with pivoting blocks. Dynamic compression bending was performed using an MTS servohydraulic test frame applying a sinusoidal force wave at a frequency of 5 Hz using a maximum/minimum ratio of 10. Testing was stopped upon displacement of the construct 3 mm beyond the initial peak compressive displacement during dynamic loading or when 5,000,000 cycles had been reached. The fatigue life curve fit and its 95% confidence intervals were generated using a commercially available software package (Table Curve 2D, Jandel Scientific).

Results and Discussion

As expected, the stiffness and 2% offset yield load of the constructs in static compression bending decreased with increasing gauge length and clamping the inferior test block caused a dramatic increase in both (Figs. 2 and 3). With the inferior test block fixed, the compression bending stiffness increased as much as four times for the longest construct and yield load increased up to two times. The stiffness of the 196 mm gauge length construct with clamped inferior block was comparable to the 76 mm gauge length construct with pivoting inferior block and had a slightly higher yield load.

Static torsion testing results indicated that the stiffness increased initially with increasing gauge length and number of cross-connectors (Fig. 4). This is understandable since it has been shown that for posterior lumbar spinal fixation systems, the addition of one or two cross-connectors significantly increases the torsional stiffness in axial rotation [4]. After the gauge length was increased beyond 116 mm, the stiffness decreased dramatically despite the addition of cross-connectors. Without cross-connectors, the stiffness decreased with increasing gauge length. Although the sample size was small (n = 1) for both static compression and torsion testing, the trends shown are clear and logical.

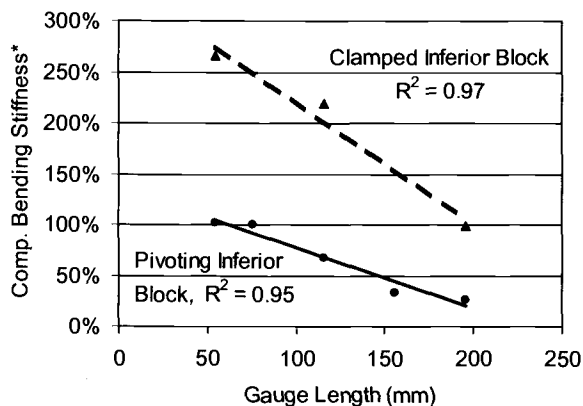


Figure 2—Compression bending stiffness of posterior occipito-cervico-thoracic.

constructs with varying gauge length and inferior test block mobility (n=1) (*relative to the 76 mm gauge length construct with pivoting blocks).

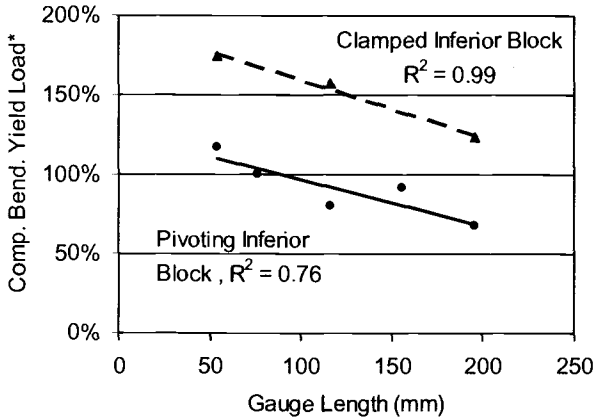


Figure 3—Compression bending 2% offset yield load of posterior occipito-cervico-thoracic constructs with varying gauge length and inferior test block mobility (n=1) (*relative to the 76 mm gauge length construct with pivoting blocks).

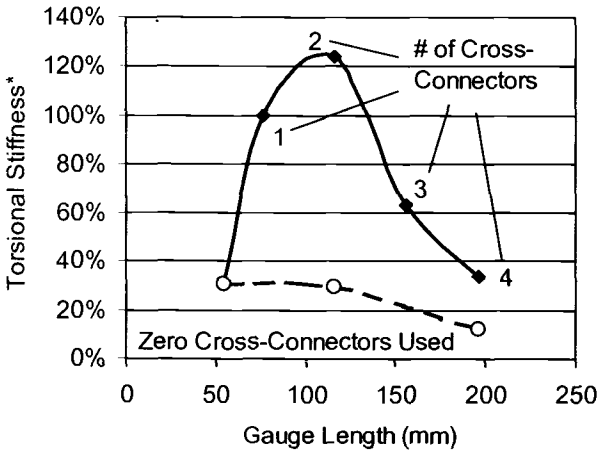


Figure 4—Torsional stiffness of posterior occipito-cervico-thoracic constructs with varying gauge length and addition of cross-connectors (n = 1) (*relative to the 76 mm gauge length construct with pivoting blocks).

In dynamic compression bending, all of the constructs failed due to fracture of the rod, most of these fractures occurring at the lower screws. The 5 million cycle endurance limit of the 76 mm gauge length construct with pivoting blocks was only 54% of that found with the 196 mm gauge length construct with clamped inferior block

(Fig. 5). Thus, the endurance limit nearly doubled for the construct with almost three times longer gauge length simply due to clamping the inferior test block. One reason for these results is that by clamping the inferior block, much of the bending moment is transferred to the lower fixture. In the case of the pivoting blocks, the implants must resist all of the bending moment. Thus, the local tensile stresses in the rod where the fatigue cracks begin are expected to be much higher in constructs with pivoting blocks given equivalent gauge lengths. Since the fractures rarely occurred at the cross-connectors, they probably had negligible effects on the results of the fatigue testing.

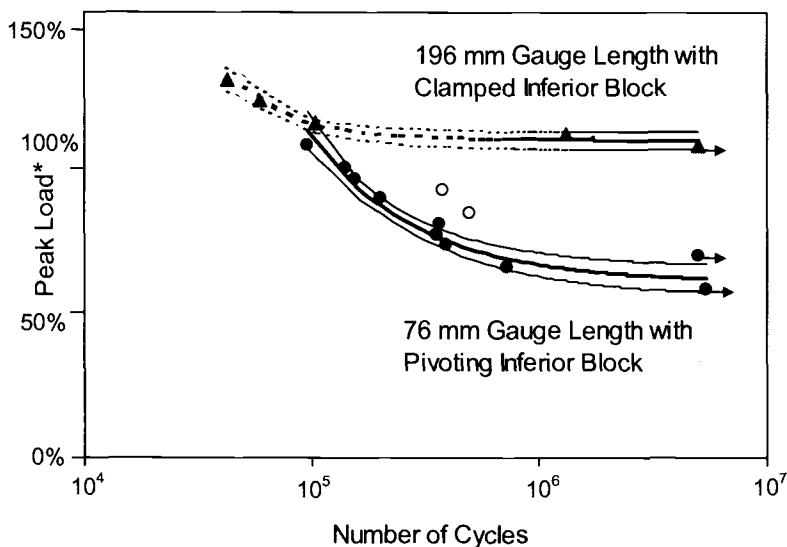


Figure 5—Fatigue strength of posterior occipito-cervico-thoracic constructs, showing curve fits and 95% confidence limits (*relative to the 2% offset yield load of the 76 mm gauge length construct with pivoting blocks).

Conclusions

Although the effect of gauge length and test block mobility on the mechanical properties of rod-based posterior occipito-cervico-thoracic constructs was predictable, the magnitude of these differences was surprising. When choosing a test protocol for evaluating implant devices, it is important to mimic both the *in vivo* loading conditions and the worst-case normal daily living activities. With more understanding of how different factors affect spine implant construct performance, a more effective model can be chosen that mimics the *in vivo* situation.

References

- [1] White A. A. and Panjabi M. M., *Clinical Biomechanics of the Spine*, 2nd ed., J. B. Lippincott Co., Philadelphia, 1990, p. 107.

- [2] Shin E. K., Panjabi M. M., Chen N. C. and Wang J. L., "The Anatomic Variability of Human Cervical Pedicles: Considerations for Transpedicular Screw Fixation in the Middle and Lower Cervical Spine," *European Spine Journal*, 2000, No. 9, pp. 61–66.
- [3] White A. A. and Panjabi M. M., *Clinical Biomechanics of the Spine*, 2nd ed., J. B. Lippincott Co., Philadelphia, 1990, p. 29.
- [4] Lim T. H., Eck J. C., An H. S., Hong J. H., Ahn J. Y., and You J. W., "Biomechanics of Transfixation in Pedicle Screw Instrumentation," *Spine*, 1996, No. 21, pp. 2224–2229.

William L. Carson¹

Relative 3 Dimensional Motions between End Vertebrae in a Bi-level Construct, the Effect of Fixture Constraints on Test Results

Reference: Carson, W. L., “Relative 3 Dimensional Motions between End Vertebrae in a Bilevel Construct, The Effect of Fixture Constraints on Test Results,” *Spinal Implants: Are We Evaluating Them Appropriately*, ASTM STP 1431, M. N. Melkerson, S. L. Griffith, and J. S. Kirkpatrick, Eds., ASTM International, West Conshohocken, PA, 2003.

Abstract: Bilevel spinal implant constructs are 3 dimensional with 6 degrees-of-freedom of superior relative to inferior vertebra motion. ASTM F 1717-01 pinned fixtures constrain 3 degrees-of-freedom, which for posterior constructs are: lateral translation, PA axis rotation, and axial rotation to be about axis through the center of each vertebral body mounting pin. Also, F 1717-01 only illustrates testing of rectangular constructs that are symmetrical about a mid plane. Clinical examples, unconstrained finite element models, and hand held-loaded models are used to illustrate that in general some of the primary components of construct displacement and modes of failure are those constrained by the fixtures in F 1717-01; with one exception being the axial loading of rectangular constructs that remain symmetrical in geometry and biomechanical characteristics of components and interconnections. This raises two questions: the possibility of some clinical modes of failure being obscured by F 1717-01, and the clinical relevance of some numerical test results. Gimbal-gimbal or pushrod-gimbal fixtures for unconstrained axial and torsional load, static and fatigue testing, unsymmetrical as well as symmetrical constructs is proposed as a replacement for the current pinned fixtures.

Keywords: Construct, constrained, unconstrained, axial, torsion, F 1717-01

¹ Professor Emeritus Mechanical and Aerospace Engineering, University of Missouri-Columbia, 2111 Fairmont, Columbia, Missouri, USA.

Introduction

Bilevel spinal implant constructs are 3 dimensional with 6 degrees-of-freedom of superior relative to inferior vertebral body motion. ASTM Test Methods for Spinal Implant Constructs in a Vertebrectomy Model (F 1717-01) constrains three degrees-of-freedom, which for a posterior construct are: lateral translation, lateral rotation about the (AP) X axis, and axial rotation to be about an axis, which passes through the center of each vertebral body's mounting pin (the center line of the test cell's ram and load cell). Also, F 1717-01 only illustrates testing of rectangular configuration constructs that are symmetrical about a mid plane (sagittal for example). Clinical constructs would rarely be perfect symmetrical rectangles (geometric and in biomechanical characteristics of components) due to lateral variation in vertebra dimensions, the correction clinically achievable, construct assembly tolerances, variation in component-interconnection characteristics, and/or by design of the implant itself (for example the unequal length of longitudinal members of some anterior systems). The first objective of this paper is to present examples of potential modes of construct failure and biomechanical characteristics (relative motion, internal loading of components, and stiffness) that would be obscured by F 1717-01 fixture constraints and rectangular configurations. The second objective is to propose alternative unconstrained axial-torsional loading fixtures that would be applicable to static and fatigue testing unsymmetrical as well as symmetrical constructs.

Examples of Potential Modes of Construct Failure and Biomechanical Characteristics That Would Be Obscured by ASTM F 1717-01

The following clinical examples and unconstrained construct models illustrate that some primary components of displacement (superior relative to inferior vertebra) are those constrained by the fixtures of F 1717-01, which would thus obscure potential modes of construct failure and also produce questionable construct biomechanical test results.

(Figure 1a) is a PA X-ray of an unstable rod-pedicle screw construct that collapsed laterally and axially until load sharing by the anterior column resisted further displacement. A hand held model (Figure 1b) was made of the construct to study the effect of negligible torsional grip of screw interconnections to the longitudinal rods, which was the clinical situation in (Figure 1a) due to the threaded longitudinal rod with no locking device on the connectors. This construct was found to have little to no resistance to torsional load when two or more of the interconnections lost their torsional grip on the longitudinal rod, even though the model's pedicle angle was 40°. The pedicle screws were left free to rotate within the model blocks (vertebrae) in this example, since clinically the magnitude of screw torque within bone cannot be relied upon and decreases with time. When resistance to rotation of the pedicle screws within the blocks was increased by tightening the set screws, the model with longitudinal rods free to rotate was able to resist torsional loading. However, this did not prevent the type of construct collapse shown in (Figure 1b) when the constructs limited resistance to applied torque was exceeded and screw rotation within the blocks commenced. Simultaneous lateral translation, lateral (AP X axis) rotation, axial translation, and axial rotation of the

superior relative to the inferior vertebra can be observed in (Figure 1), the first two of which would be constrained by F 1717-01. Thus torsional testing using the fixtures in F 1717-01 would prevent the mode of failure shown in (Figure 1) from being observed, and would alter the internal loads within the construct and its torsional stiffness (based upon the known general affect of constraints on internal loads and stiffness in structural mechanics [1]).

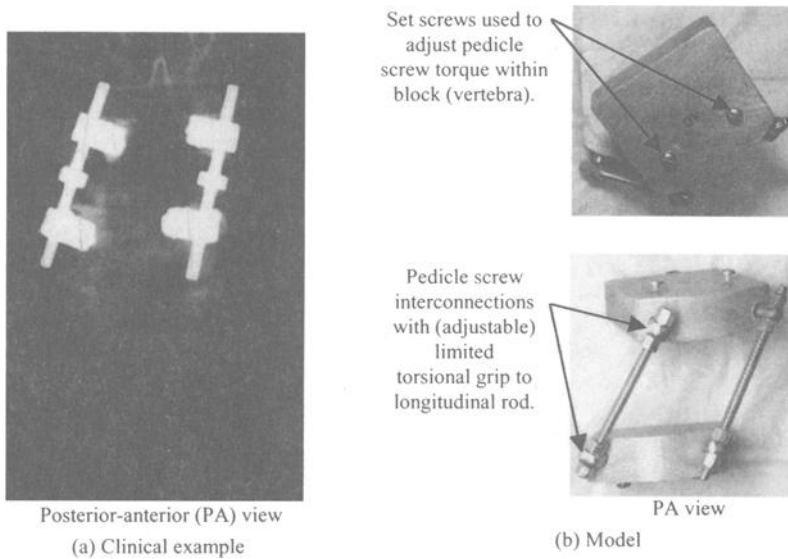


Figure 1 - *Clinical example and model illustrating the 3 dimensional 6 degree-of-freedom superior vertebra displacement in a construct having limited torsional load resistance due to low torsional grip within the screw-longitudinal member interconnections.*

Figure 2 is a PA X-ray of an unstable plate-screw construct that collapsed laterally and axially into a parallelogram configuration until load sharing by the anterior column resisted further displacement. The plates prevented rotation of the pedicle screws about the longitudinal members in contrast to the construct in (Figure 1). To study the biomechanical characteristics of this construct and the mode of failure shown in (Figure 1), Carson et al [2] used unconstrained strain gauged models and finite element models of rectangular configurations having pedicle angle ranging from 0° to 60° . Chen [3] extended the finite element model work to constructs with initial lateral offset of superior vertebra to investigate parallelogram configurations, and to constructs with different size superior vertebra to investigate trapezoidal configurations. Hand held-loaded models were also used to verify the stability of and relative displacements within these constructs, (Figure 3) being an example of a trapezoidal configuration model. Untransfixed constructs with smaller pedicle angle were observed to be less resistant (stable) to some

components of applied load, with 0° pedicle angle resulting in no resistance to some components of loading. The rectangular configuration if laterally displaced slightly into or if assembled in a parallelogram configuration would not resist an axial component in addition to a lateral component of applied force, and would continue to simultaneously displace laterally and axially until load sharing stopped the motion, similar to the clinical example in (Figure 2). The superior vertebra of trapezoidal configurations was observed to also simultaneously rotate about an (AP) X axis in addition to lateral and axial translational displacement (Figure 3). The trapezoidal construct also lacked resistance to lateral bending in addition to axial and lateral load. This was observed to be true in general of any construct that had one or more unequal length of the opposite sides. These examples illustrate that there will be a tendency for simultaneous lateral translation, lateral (AP X axis) rotation, axial translation, and flexion rotation of bilevel constructs (unless they are perfect rectangles) when axially loaded; the first two of which would be constrained by F 1717-01. Thus axial testing using the fixtures in F 1717-01 would prevent the mode of failure shown in (Figures 2, 3) from being observed, and would alter the internal loads within the construct and its axial stiffness unless the construct is initially and remains to be perfectly symmetrical (geometrically and in component-interconnection characteristics) during axial loading.

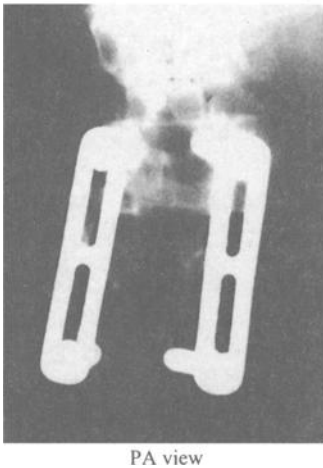


Figure 2 - Clinical example illustrating the coronal plane axial and lateral displacement of the superior vertebra in a parallelogram construct due to pedicle screws being nearly parallel to each other and having a low torsional resistance within bone.

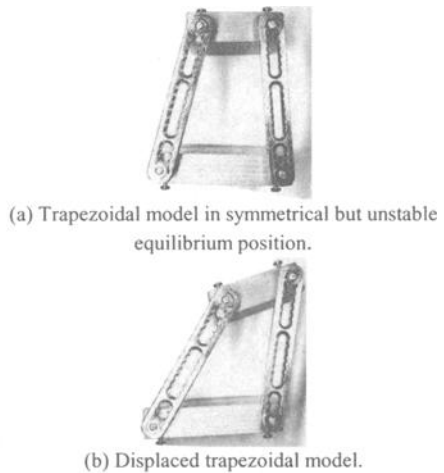


Figure 3 - Model of trapezoidal construct illustrating coronal plane axial and lateral displacement, and lateral rotation of superior vertebra due to pedicle screws being parallel to each other and having low torsional resistance within the vertebral blocks.

Elastic deflections of a finite element model are shown in (Figure 4) of a construct that before loading was in a perfect rectangular configuration, and was also symmetrical about a mid saggital plane with respect to all characteristics of its components [4]. When an axial load of 445 N (100 lbf) was applied to the center of the unconstrained superior vertebra (Figure 4a), its motion was parallel to the sagittal plane with simultaneous axial translation, PA translation, and flexion rotation; due primarily to the symmetrical flexion bending of the longitudinal members. This illustrates that F 1717-01 would appropriately test under axial load conditions a perfectly rectangular-symmetrical construct. When a pure torque of 11.3 Nm (100 in-lbf) was applied to the center of the unconstrained superior vertebra (Figure 4b), its motion was 3 dimensional with simultaneous lateral translation, lateral (AP X axis) rotation, and axial rotation; due primarily to flexion bending of the right longitudinal member and extension bending of the left. Axial rotation appears to be about an axis parallel to and centered between the longitudinal members as judged by the rotation of the centrally located transverse connector. This illustrates that even with a perfectly rectangular-symmetrical construct, the torsional loading protocol of F 1717-01 would produce questionable results due to its constraints on the primary components of motion: lateral translation, lateral (AP X axis) rotation, and axial rotation to be about an axis through the center of the vertebral bodies.

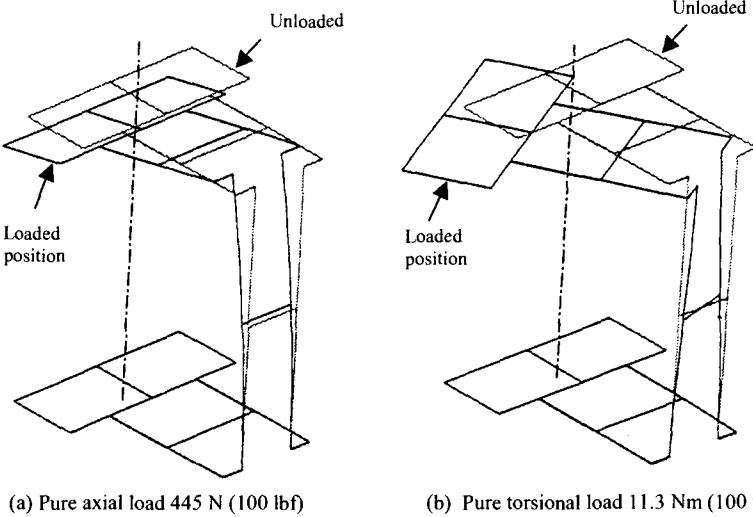


Figure 4 - Finite Element Model [2] predicted displacement of superior vertebra and implant relative to inferior vertebra for a 4.76 mm (3/16") diameter rod Isola slotted connector bilevel comminuted construct with one transverse connector centrally located.

F 1717-01 states that "it allows comparison of spinal implant constructs with

different intended spinal locations and methods of application to the spine.” This implies relevance of implant comparisons for tests conducted under similar in vitro conditions, but does not address relevance to clinical locations and methods of application. For example, using F 1717-01 to test anterior constructs would result in the hinge pins being oriented in a PA direction, which would thus constrain PA translation, flexion-extension rotation, and axial rotation to be about an axis through the center of each vertebral body. Flexion-extension rotation and PA translation are two primary degrees-of-freedom that clinically must be resisted by an anterior construct, and thus should not be constrained during in vitro testing.

These examples illustrate that to assure biomechanical characteristics indicative of clinical conditions and to not obscure some possible modes of clinical failure, in vitro testing of constructs should be 3 dimensional and allow all 6 degrees-of-freedom of superior relative to inferior vertebra. The examples also illustrate: a) that the major components of motion that occur do not solely correspond to the direction of or in the plane of the applied load, and b) that the unconstrained motions which occur depend upon the construct’s geometric configuration and the relative strength and/or flexibility of its interconnections and components.

Comparison of Torsional Test Methods and Results Reported in the Literature

Dick et al [5] and Lynn et al [6] both performed in vitro torsion tests to determine the torsional stiffness characteristics of bilevel pedicle screw constructs with no, one and two cross-links. Both apparently constrained flexion-extension rotation in addition to the constraints imposed by F 1717-01. Dick et al “locked the platforms in the sagittal plane to prevent buckling” during torsional tests on comminuted constructs assembled from five different implant systems (TSRH, PWB, CD, Isola, Rogozinski) on polyurethane models of L3 and L4. Lynn et al used embalmed T12-L2 segments having L1 osteotomy instrumented with AO hardware, whose end vertebrae were secured to circumferential jigs “mounted in an Instron Testing Machine.”

Representative torsional stiffness results from these constrained in vitro tests compared to Sharma’s unconstrained FEM results are presented in table 1 to see if obvious differences in trends could be detected due to differences in constraints.

Table 1 - Comparison of Torsional Stiffness Results

Number of cross-links	Bilevel construct torsional stiffness (N-m/deg)		
	<i>Constrained in vitro tests</i>		<i>Unconstrained FEM</i>
	Dick et al [5] Isola medial ¼” rods 5 Nm torque, 50 N axial load	Lynn et al [6] AO medial rods 2.5° rotation, 356 N pre-axial load	Sharma [4] Isola medial ¼” rods 30° pedicle angle, 11.3 Nm torque, 0 N axial load
0	1.87	1.89	...
1 center	2.93	2.53	4.83
2 (1 each end)	3.80	3.01	5.23

Increased stiffness with addition of cross connectors was observed by all three, regardless of constraint conditions. Based on classical mechanics [1], one would expect to observe greater stiffness for the constrained constructs compared to the unconstrained, which was not the case for the data in table 1. There are several possible factors that would explain the apparent discrepancy: lower in vitro results due to inclusion of the torsional flexibility of the vertebra-fixture mounting assemblies; differences in human vertebra [6], polyurethane vertebra [5], and nylon vertebra model [4] elastic properties; and differences in construct dimensions and component properties. Unfortunately, Chen [3] did not model a construct with the constraints imposed by F 1717-01 which would have provided direct comparison of results: construct displacements, stiffness and internal loads. Lynn et al reported frequent sliding of the cross-link along the threaded rod during torsional testing. Carson has observed this same phenomenon with a finger tightened Isola TRC cross-link placed on the unconstrained model shown in (Figure 1b) when it was manually loaded in torsion [7]. Based on this limited sample of results reported in the literature and personal experience with hand held physical models, constrained torsional tests compared to unconstrained have produced some similar trends and observations. However, additional testing with identical constructs in a constrained and unconstrained condition would be needed to make definitive conclusions about the effect of F 1717-01 fixture constraints on the relative magnitude of numerical test results. This exercise along with continued use of the fixtures in F1717-01 is not an effective means of dealing with the 3D 6 degree-of-freedom reality of clinical constructs, since each new type of construct would have to be tested unconstrained as well as constrained to establish the true relative effect on its characteristics. Even then, there would continue to be some question as to the true clinical applicability of the constrained construct test results.

Proposed Unconstrained Fixture for Bi-level Construct Axial and Torsional Testing

The rationale for the pinned fixtures in F 1717-01 was to accomplish the following design objectives: a) to be able to perform torsional as well as axial testing with the same fixtures, b) to minimize the change in AP moment arm as construct flexion occurred by keeping the axis of the pins close to the transverse plane of the pedicle screws, and c) to be able to apply axial loading in both directions to flex as well as extend the construct. The simple ball joint fixture arrangement used by Cunningham et al. [8] produced an axial unconstrained two force body loading of the construct. This ball joint fixture concept was rejected since none of the three design objectives were satisfied.

Figure 5 and 6 illustrate two alternative types of fixtures: that will allow all 6 relative degrees-of-freedom between the end vertebrae of a construct, that can be used to apply axial as well as torsional load, and that applies the resultant load at a selected point within the vertebral body (center of the vertebral body or in the transverse plane of the pedicle screws for example). The common center of the gimbal hemispheres can be located anywhere within the vertebral body (within reason). They are shown in the plane of the two screws at each level. This reduces change in moment arm from longitudinal rod to the line of applied force, compared to when the pins are above or below the screws as is the case in F 1717-01. The proposed fixtures (as shown) will not allow axial loading in tension, however F 1717-01 specifies that an $R \geq 10$ is to be used, which does not

produce reversed direction compression-tension loading. Testing that I am aware of has been done with compression only loading, with one possible exception being cervical construct testing.

For axial load testing with the gimbal-gimbal fixture, the superior gimbal's inner component is replaced with one that does not have tangs. This releases the superior vertebra's axial rotation degree-of-freedom, and makes the construct itself a two-force member. Thus the applied axial force acts at the center of each gimbal, and remains coincident with the test machine's axis. For torsional testing, the applied axial bias force acts identical to that during axial testing, since the gimbals cannot transmit moments about any axis in their transverse plane. The applied torque is about an axis through the center of the two gimbals, which remains coincident with the axis of the test machine.

For axial load testing with the pushrod-gimbal fixture, the gimbal's inner component is replaced with one that does not have tangs. This releases the superior vertebra's axial rotation degree-of-freedom, and makes the pushrod a two-force member. Thus the applied force acts at the center of the gimbal and remains parallel to the pushrod axis. A 38.1 cm (15") or longer pushrod is shown to reduce the pushrod's angulation from vertical as the superior vertebra displaces in the transverse plane. For torsional testing, the applied axial bias force acts identical to that during axial testing, since the universal joint and gimbal cannot transmit moments about any axis in their transverse plane. The applied torque is about the pushrod's axis.

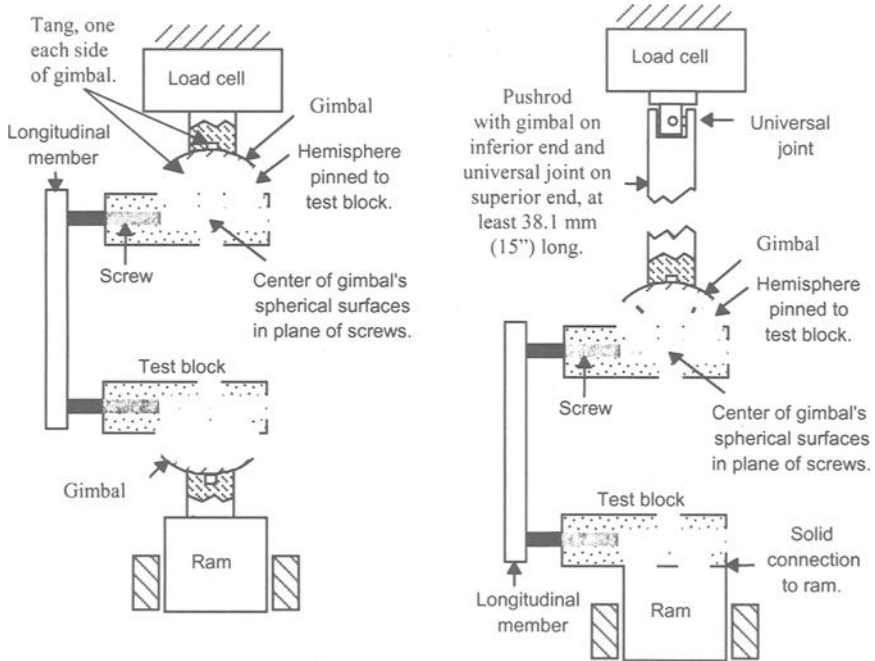


Figure 5—*Proposed gimbal-gimbal type fixture.*

Figure 6—*Proposed pushrod with gimbal and universal joint type fixture.*

Recommendation

To reduce the questions related to the possibility of obscuring modes of clinical failure and clinical relevance of numerical results, I recommend dropping the pinned fixtures out of F 1717-01 and replacing them with one of the proposed fixtures in figures 5 and 6. The pushrod-gimbal fixture in Figure 6 would be preferred based on: a) the superior vertebra's motion relative to the inferior vertebra being easier to visualize since the inferior "reference" vertebra does not rotate relative to an individual watching the test, and b) the pushrod with gimbal and universal joint system is identical to the one used in the recently adopted ASTM Test Methods For Intervertebral Body Fusion Devices (F 2077-01).

References

- [1] Avallone, E. A., Baumeister III, T., (eds.), *Marks' Standard Handbook for Mechanical Engineers*, 9th ed., McGraw-Hill, 1987, p. 5–28.
- [2] Carson, W. L., Duffield, R. C., Arendt, M., Ridgely, B. J., Gaines, R. W., "Internal Forces and Moments in Transpedicular Spine Instrumentation, The Effect of Pedicle Screw Angle and Transfixation—The 4R-4Bar Linkage Concept," *Spine*, September 1990, Vol. 15, No. 9, pp. 893–901.
- [3] Chen, Liu-Yuan, "Finite Element Analysis of Internal Forces and Moments in Bilevel and Trilevel Spine Instrumentation—The Effects of Pedicle Angle, Transfixation, Vertebra Offset and Variations in Vertebra Size," M. S. thesis, University of Missouri-Columbia, Dec. 1992.
- [4] Sharma, M. S., "The Effect of Transverse Connector Articulation on Bilevel Spinal Implant Construct's Stability, and Internal Forces and Moments," M.S. thesis, University of Missouri-Columbia, May 1994.
- [5] Dick, J. C., Zdeblick, T. A., Bartel, B. D., Kunz, D. N., "Mechanical Evaluation of Cross-Link Designs in Rigid Pedicle Screw Systems," *Spine*, March 15, 2000, Vol. 25, No. 6S, pp. 13S–18S.
- [6] Lynn, G., Mukherjee, D. P., Kruse, R. N., Sadasivan, K. K., Albright, J. A., "Mechanical Stability of Thoracolumbar Pedicle Screw Fixation," *Spine*, March 15, 2000, Vol. 25, No. 6S, pp. 31S–35S.
- [7] Carson, W.L., Asher, M., Boachie-Adjei, O., Akbarnia, B., "Transverse Connectors: Clinical Objectives, Biomechanical Parameters Involved in Their Achievement, and Summary of Current and Needed In Vitro Tests," *Spinal Implants: Are We Evaluating Them Appropriately, ASTM STP 1431*, ASTM International, West Coshohocken, PA, 2002.

- [8] Cunningham, B. W., Seftor, J. C., Shono, Y., McAfee, P. C., "Static and Cyclical Biomechanical Analysis of Pedicle Screw Spinal Constructs," *Spine*, March 15, 2000, Vol. 25, No. 6S, pp. 1S–12S.

Spinal Implant Transverse Rod Connectors: A Delicate Balance Between Stability and Fatigue Performance

Reference: Serhan, H. and Slivka, M., “**Spinal Implant Transverse Rod Connectors: A Delicate Balance Between Stability and Fatigue Performance.**” *Spinal Implants: Are We Evaluating Them Appropriately? ASTM STP 1431*, M. N. Melkerson, S. L. Griffith, and J. S. Kirkpatrick, Eds., ASTM International, West Conshohocken, PA, 2003.

Abstract: Transverse rod connectors have been shown to significantly increase the torsional stability of rod-based posterior spinal implant systems, which may improve clinical fusion outcomes. This study was conducted to determine the effect of number and positioning of transverse rod connectors on the torsional stiffness and compression bending fatigue strength of ISOLA spinal corpectomy test constructs. Results from static torsion testing indicated that the addition of one and two transverse rod connectors between the pedicle screws greatly increased the torsional stiffness of the constructs (45% and 63%, respectively). When placed above and below the pedicle screws, the increase was less pronounced. Placement of one or two transverse rod connectors between the pedicle screws decreased the fatigue life of constructs in dynamic compression bending. Placement of two rod connectors above and below the upper and lower pedicle screws, respectively, did not reduce the fatigue performance of the constructs. Therefore, there is a delicate balance between torsional stiffness and fatigue performance of spinal constructs when transverse rod connectors are used.

Keywords: spinal corpectomy, transverse rod connectors, torsional stiffness, fatigue performance

Introduction

Since their introduction and subsequent improvements, posterior implants have become clinically established and are being increasingly used in interbody and posterior fusion procedures, with a rate of growth of approximately 15% in recent years. The use

¹ Manager of Research and Technology, DePuy AcroMed, 325 Paramount Dr., Raynham, MA 02767.

² Research Engineer, DePuy AcroMed, 325 Paramount Dr., Raynham, MA 02767.

of posterior spinal implants in conjunction with anterior column support is thought to be the best method for achieving a strong mechanical construct and a high fusion rate. Posterior spinal implants have been successfully used by spine surgeons to provide stability of the spine, allowing for speedy fusion and short postoperative immobilization. Many surgeons have incorporated the use of transverse rod connectors (TRCs) to increase the axial and torsional stability of the instrumented spine.

Previous researchers have identified and experimentally evaluated an increase in torsional stability of spinal implants when used with transverse rod connectors [1-6]. In a recent biomechanical study of a rod-based spinal system, rod fractures near the transverse rod connectors were the common fatigue failure sites [7]. These findings prompted us to investigate the effects of the transverse rod connectors on the torsional stiffness and fatigue performance of spinal implants. In this study, we examined the delicate balance between the number of transverse rod connectors used and their location in a bilateral corpectomy model with respect to the torsional stiffness and the fatigue performance in dynamic compression bending of the construct.

Materials and Methods

Ultra high molecular weight polyethylene (UHMWPE) blocks were used to simulate the lumbar vertebral bodies in a corpectomy model as per the ASTM Test Methods for Static and Fatigue for Spinal Implant Constructs in a Corpectomy Model (F1717-96). These blocks have a 15° medial angulation from the point of screw entry to simulate lumbar pedicle angulation and a 40 mm distance between screw insertion points to simulate the interpedicular distance. The stainless steel ISOLA Spinal System (DePuy AcroMed, Raynham, MA) was used for this study. Each construct consisted of: (4) 7 mm pedicle screws, (4) slotted connectors and (2) 6.35 mm rods spanning a 78 mm gap between the upper and lower screws in the corpectomy model. The pedicle screws were first inserted into the UHMWPE blocks, then the slotted connectors were assembled to the pedicle screws over the machine post and tightened with a nut. Rods were assembled to the slotted connectors using a set screw. Since all constructs were assembled with a 78 mm distance versus the recommended 76 mm distance, the comparisons were valid. ISOLA TRC™ transverse rod connectors were used to investigate torsional stiffness and fatigue performance. These connectors attach to the rod by tightening two “C”-shaped halves in a clamping configuration around the rod.

The torsional stability of the spinal constructs in a corpectomy model following ASTM F1717-96 was evaluated in six configurations: 1) no cross connector, 2) one TRC mid-way between the upper and lower screws, 3) two TRCs equally spaced between each other and the upper and lower screws, 4) one TRC placed 3 mm below the lower screws, 5) one TRC placed 3 mm above the upper screws, and 6) two TRCs placed 3 mm above and below the upper and lower screws, respectively (Fig. 1). One sample was tested per condition. Torsional testing was performed on a MTS (Eden Prairie, MN) 858 Mini-Bionix biaxial, servohydraulic machine using an angular displacement rate of 30°/minute and a constant axial pre-load of 200 N. This compressive preload was used because the spine is in a state of compression even while lying supine [8]. The torque and angular displacement were recorded at a rate of 2 Hz.

Torsional stiffness was calculated from the initial linear region of the torque-angular displacement curve.

The fatigue performance was evaluated in four separate configurations, one sample per condition: 1) no TRC, 2) one TRC midway between the upper and lower screws, 3) two TRCs equally spaced between each other and the upper and lower screws and 4) two TRCs placed 3 mm above and below the upper and lower screws, respectively. Axial compressive bending loading was used to evaluate the fatigue performance using MTS 858 Mini-Bionix servohydraulic machines. Peak compressive bending load levels of 500 N, 750 N, and 1,000 N with $R = 10$ were used in this study. In a previous study [9], statistical analysis of fatigue test data showed no difference in the compressive bending fatigue performance of the stainless steel ISOLA system at 4 and 16 Hz test frequency when using MTS servohydraulic test machines. Therefore, all fatigue testing was performed at 16 Hz. Failure was defined as fracture or permanent deformation as determined by setting displacement limits at ± 3 mm beyond the initial peak/valley displacements. Tests were run until failure or achieving one million cycles. Because the purpose of this part of the study was to evaluate differences in fatigue performance rather than determine the endurance limit of the constructs, one million cycles was used instead of the ASTM recommended 5 million cycles.

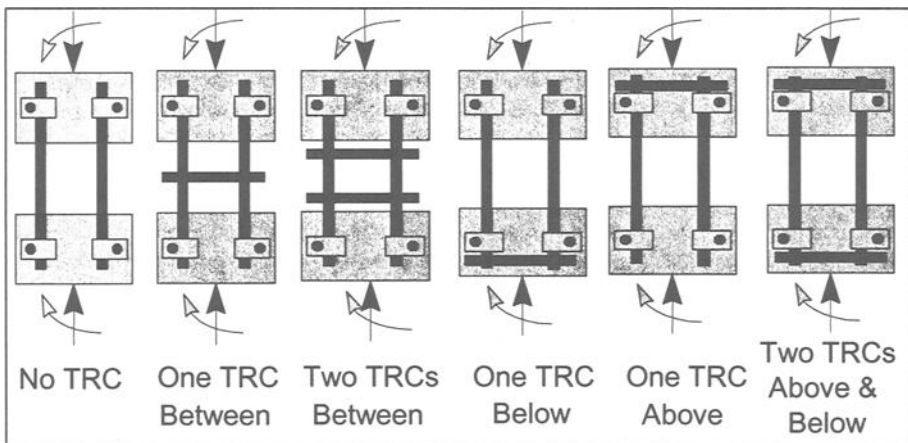


Figure 1-Torsional test configurations.

Results

The torsional stiffness and the percent of increase in the torsional stiffness are shown in Table 1. With the addition of one or two TRCs between the pedicle screws, the torsional stiffness was increased by 45% and 63%, respectively. Test results also showed that the torsional stiffness of constructs with one TRC between the screws (9.48 N·m/degrees) was higher than constructs with two TRCs mounted above and below the

pedicle screws (9.13 N· m/degrees).

Table 1-Results from static torsion testing of spinal constructs (n=1).

Transverse Rod Connector	Torsional Stiffness (N· m/degrees)	Increase from No TRC
No TRC	6.52	0.0 %
One TRC Between	9.48	45.4 %
Two TRCs Between	10.6	63.0 %
One TRC Above	8.33	27.8 %
One TRC below	8.01	22.8 %
Two TRCs Below & Above	9.13	40.1 %

Figure 2 summarizes the fatigue test results of the four different construct configurations. Without transverse rod connectors, the constructs reached one million cycles at compressive bending peak loads of 500 and 750 N. At 1000 N, the number of cycles to failure dropped by two thirds, establishing the endurance limit between 750 and 1000 N for the construct without TRCs. Constructs with one or two cross connectors between the pedicle screws reached one million cycles at 500 N, but the number of cycles to failure dropped dramatically when the compressive bending peak load was increased to 750 N, thus establishing the endurance limit between 500 and 750 N. Placement of two TRCs above and below the upper and lower pedicle screws, respectively, did not reduce the fatigue performance of the constructs.

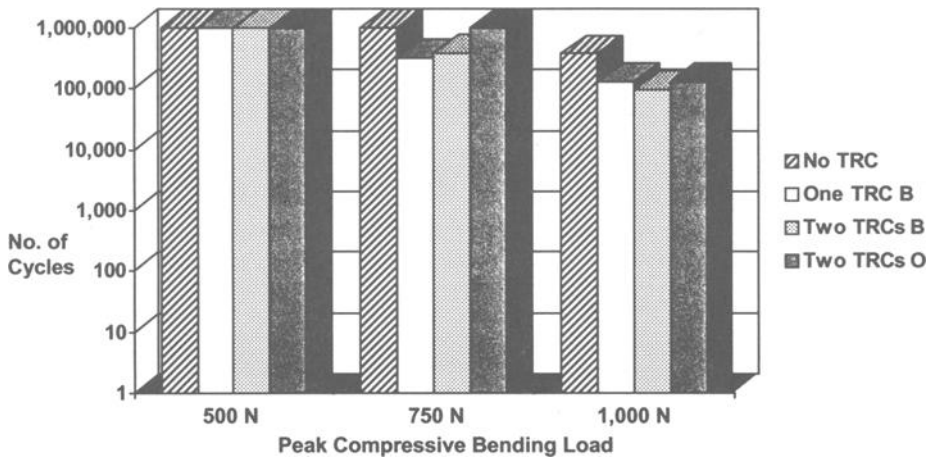


Figure 2-Results of fatigue testing in axial compressive bending (peak loads shown) of spinal constructs with transverse rod connectors (TRC) between (B) or above and below (outside, O) the pedicle screws.

Discussion

It has become widely accepted that transverse rod connectors increase the stiffness and can improve the stability of posterior rod-based screw and hook constructs [1-6]. This increase in stiffness is thought to correlate with higher fusion rates. This study, although limited by a low sample size ($n=1$), shows a number of important trends seen with the use of TRCs. We found that the addition of TRCs on the rods was directly correlated to the torsional stiffness of the constructs. Further, placing the TRCs between the upper and lower pedicle screws had a more pronounced effect on torsional stiffness than placement above and/or below.

However, TRCs reduced the fatigue performance of rod-based pedicle screw constructs when placed on the rods between the upper and lower pedicle screws in the spinal corpectomy model. This reduction in fatigue strength was likely caused by stress risers imposed by the TRCs on the rods. These results were found for ISOLA spinal constructs, and the design of the TRC should impact the magnitude of fatigue strength reduction. The addition of TRCs outside the bending loading area at the 500 N and 750 N peak compressive bending loads did not reduce the fatigue performance simply because the rod at these locations is not subjected to any axial bending loading. The difference seen at the 1000 N load may not be significant.

Conclusions

The use of transverse rod connectors in spinal fusion increases torsional stiffness of pedicle screw and hook constructs, and is thought to improve fusion rates. This study showed that the number of TRCs and their location affect both the torsional stiffness and the fatigue performance of rod-based posterior spinal constructs. Therefore, there is a delicate balance between torsional stiffness and fatigue performance of spinal constructs when transverse rod connectors are used.

References

- [1] Rahmatalla A. T., Hastings G. W., Dove J., and Crawshaw A. H., "A Pedicle Screw Bridging Device for Posterior Segmental Fixation of the Spine: Preliminary Mechanical Testing Results," *Journal of Biomedical Engineering*, 1991, Vol. 13, pp. 97-102.
- [2] Lim T. H., Eck J. C., An H. S., Hong J. H., Ahn J. Y., and You J. W., "Biomechanics of Transfixation in Pedicle Screw Instrumentation," *Spine*, 1996, Vol. 21, pp. 2224-2229.
- [3] Dick J. C., Zdeblick T. A., Bartel B. D., and Kunz D. N., "Mechanical Evaluation of Cross-link Designs in Rigid Pedicle Screw Systems," *Spine*, 1997, Vol. 22, pp. 370-375.
- [4] Asher M., Carson W. L., Heinig C., Strippgen W., Arendt M., Lark R., and Hartley M., "A Modular Spinal Rod Linkage System to Provide Rotational Stability,"

Spine, 1988, Vol. 13, pp. 272–277.

- [5] Pintar F. A., Maiman D. J., Yoganandan N., Droese K. W., Hollowell J. P., and Woodard E., “Rotational Stability of a Spinal Pedicle Screw/Rod System”, *Journal of Spinal Disorders*, 1995, Vol. 8, pp. 49–55.
- [6] Carson W. L., Duffield R. C., Arendt M., Ridgely B. J., and Gaines R. W., “Internal Forces and Moments in Transpedicular Spine Instrumentation. The Effect of Pedicle Screw Angle and Transfixation--the 4R-4bar Linkage Concept,” *Spine*, 1990, Vol. 15, pp. 893–901.
- [7] Stambough J. L., Sabri E. H., Huston R. L., Genaidy A. M., El-Khatib F., and Serhan H. A., “Effects of Cross-linkage on Fatigue Life and Failure Modes of Stainless Steel Posterior Spinal Constructs,” *Journal of Spinal Disorders*, 1998, Vol. 11, pp. 221–226.
- [8] White A. A. and Panjabi M. M., *Clinical Biomechanics of the Spine*, 2nd Ed., Philadelphia, J. B. Lippincott, 1990, p. 461.
- [9] Stambough J. L., Genaidy A. M., Huston R. L., Serhan H., El-Khatib F. and Sabri E. H., “Biomechanical Assessment of Titanium and Stainless Steel Posterior Spinal Constructs: Effects of Absolute/Relative Loading and Frequency on Fatigue Life and Determination of Failure Modes,” *Journal of Spinal Disorders*, 1997, Vol. 10, pp. 473–81.

John S. Kirkpatrick,¹ Ramakrishna Venugolopalan,² Monique Bibbs,³ Jack E. Lemons,⁴ Preston Beck⁵

Corrosion on Spinal Implant Constructs: Should Standards Be Revised?

Reference: Kirkpatrick, J.S., Venugolopalan, R., Bibbs, M., Lemons, J. E., and Beck, P., “**Corrosion on Spinal Implant Constructs: Should Standards be Revised?**,” *Spineal Implants: Are We Evaluating Them Appropriately*, ASTM STP 1431, M. N. Melkerson, S. L. Griffith, and J. S. Kirkpatrick, Eds., ASTM International, West Conshohocken, PA, 2003.

Abstract: Corrosion is known to occur on modular spinal implants but design features such as material, surface finish, and interconnection characteristics have not been related to corrosion. Literature review was combined with retrieval analysis of thirty-three constructs to identify which design features were associated with corrosion. Corrosion was found consistently on implants where stainless steel components with differing surface finishes (Matte and polished) were designed with rigid interconnections. No clear direction for new standards activity was identified.

Keywords: Spinal fixation, spinal fusion construct, crevice corrosion, stainless steel, titanium.

¹Associate Professor, Division of Orthopaedic Surgery, University of Alabama at Birmingham, 1813 Sixth Avenue South #601, Birmingham, Alabama 35294.

²Research Assistant Professor, Department of Biomedical Engineering, University of Alabama at Birmingham, Hoen 340, Birmingham, Alabama 35294.

³Student Assistant, DNMH 101, University of Alabama at Birmingham, Birmingham, Alabama 35294.

⁴Professor, School of Dentistry (Biomaterials) and Division of Orthopaedic Surgery, SDB 615, University of Alabama at Birmingham, Birmingham, Alabama 35294.

⁵Research Assistant, School of Dentistry (Biomaterials) and Division of Orthopaedic Surgery, SDB 615, University of Alabama at Birmingham, Birmingham, Alabama 35294.

Modular spine implants are frequently used as an aid to obtaining fusion. More than 100,000 fusion procedures are done annually with an implant market exceeding \$100 million, leading to significance among individual patients and society as a whole. These devices are available in a variety of surface finishes, materials and designs. Corrosion is known to occur between modular components of different materials and different surface finishes when in a biologic environment. Recent studies have been performed to assess corrosion in spine constructs of a variety of materials and surface finishes. These studies are reviewed in the context of standardized testing of spinal implants.

Corrosion has been reported on retrieved spinal implants for a number of years. Early reports of failures raised concern that corrosion and fatigue combined to lead to rod failure in Harrington and Luque constructs [1]. These implants utilized semirigid connectors but failures were not routinely noted at the connector sites. Later studies of more rigid connectors with a threaded mechanism found extensive corrosion at the area of the clamps in Fixateur Interne [2]. These findings helped to raise concern about the relevance of corrosion to the use of implants in the spine.

An animal study was developed to evaluate the amount of debris associated with spinal fusion. They determined that fretting corrosion was the most likely source of particulate debris found associated with instrumented spinal fusion [3]. They also noted an inverse correlation between stiffness of the fusion construct, bone formation and log particle number. They hypothesized that the absence of a joint capsule retaining the particulate debris may allow migration of the particles away from the fusion mass, somewhat protecting the fusion mass from resorption. A clinical study of soft tissue surrounding retrieved implants noted a high concentration of fretting debris in patients with pseudarthrosis[4]. Low amounts of debris were noted in patients with solid fusion. They hypothesized that the debris had a potential deleterious effect on the fusion mass, spinal tissues, and/or neural elements. Moody et al have described the soft tissue histology surrounding spine implants made of stainless steel[5]. They noted a fibrous tissue matrix of variable extent, with epithelial layers in about 1/3 of patients and metallic debris in about ¼ of cases. They could not relate these findings to implant design or length of time implanted.

The clinical significance of corrosion remains controversial. Some associations of Late Operative Site Pain (LOSP) and late appearing drainage with corrosion debris have been suggested. Dubosset et al suggested a possible association of corrosion with infection [6]. Later studies found late appearing drainage was associated with infection [7]. Recent studies on LOSP have suggested corrosion contributed to this problem [8]. Others, however, have suggested again that chronic deep infections are present in these cases [9]. The presence of inflammatory response in some but not all patients with LOSP further confuses the issue [8]. Some have suggested that LOSP may be related to metal allergy [8], but others have noted LOSP in patients with negative antigen testing [9].

The authors have examined corrosion on retrieved implants from 33 patients with preliminary results presented here. These implants were of various designs and materials from several different manufacturers. The devices were examined for mechanical damage and corrosion using stereomicroscopy with some specific regions subjected to scanning electron microscopy. Stainless steel implants (n = 18) were found to have polished-finished rods and fixation components (n = 7) or matte-finished rods with polished components (n = 11). The polished-finished implants commonly exhibited fretting damage and corrosion in the interconnecting interfaces. The matte-finished components had corrosion at more interconnections and was more extensive compared to the polished-finish implants. Corrosion damage was consistent with those commonly observed in mechanically-assisted crevice corrosion phenomena. Ti64 implants (n = 14) had little corrosion evident. As corrosion was noted on all stainless implants regardless of indication for removal, an association with LOSP is questioned.

It is not clear whether corrosion testing should be a part of consensus standards for spinal implants. Corrosion has long been reported on stainless steel implants, and more articles in recent years may mean a higher incidence with newer designs. In our study, corrosion was found to be most significant in those patients with rigid constructs made of stainless steel. Little corrosion was found on titanium components. These findings seem to suggest testing in a physiologic solution should be done for stainless steel constructs. The selection of a physiologic solution is a challenging process. While electrolyte solutions represent ionic content, they eliminate the protein content of the *in vivo* situation and cannot begin to simulate regional differences in pH and oxygen tension, which may also be a part of the *in vivo* corrosion process. The fact that in neither material was corrosion found to be associated with mechanical failure leads to the question of relevance to the clinical situation. As such, no clear recommendation for testing in "physiologic" solution can be made at this time.

The potential for fretting corrosion and subsequent debris also raises the question of whether the microscopic particulates should be considered for standards related to spinal implants. This may be more relevant as the introduction of dynamic constructs and prosthetic discs occur with some degree of wear debris expected. While we may learn much from the total joint literature on this topic, there may be physiologic local and regional differences when such particulates are in the area of the spine. With current standards concentrating on implants for fusion, no revision or new standards for debris seems appropriate. This should be reconsidered as standards for dynamic implants are developed.

Mechanically assisted crevice corrosion and fretting corrosion clearly occur with spinal implants. The association of this corrosion to clinical failures of LOSP, pseudarthrosis, and implant breakage has been suggested but not clearly defined. As we gain further understanding of these problems related to spinal implants, future standards activity related to these forms of corrosion should be considered.

References

- [1] Prikryl, M., Srivastava, S. C., Viviani, G. R., Ives, M. B., Purdy, G. R., "Role of corrosion in Harrington and Luque rods failure," *Biomaterials*, Vol. 10, 1989, pp. 109–117.
- [2] Sim, E., Stergar, P. M., "The Fixateur Interne for stabilising fractures of the thoracolumbar and lumbar spine," *International Orthopaedics*, Vol. 16, 1992, pp. 322–329.
- [3] Mochida, Y., Bauer, T. W., Nitti, H., Kambic, H. E., Muschler, G. F., "Influence of Stability and Mechanical Properties of a Spinal Fixation device on Production of Wear Debris Particles In Vivo," *Journal of Biomedical Materials Research* Vol. 53, No. 3, 2000, pp. 193–198.
- [4] Wang, J., Yu, W.D., Sandhu, H. S., Betts F., Bhutta S., Delamarter, R. B., "Metal Debris from Titanium Spinal Implants," *Spine*, Vol. 24, No. 9, 1999, pp. 899–903.
- [5] Moody, D. R., Esses, S. I., Heggeness, M. H., "A Histologic Study of Soft-Tissue reactions to Spinal Implants," *Spine*, Vol. 19, 1994, pp.1153–1156.
- [6] Dubousset, J., Shufflebarger, H. L., Wenger, D., "Late "infection" with CD instrumentation." *Orthopaedic Transactions* (abstract), Vol. 18, 1994, p. 121.
- [7] Clark, C. E., Shufflebarger, H. L., "Late-Developing Infection in Instrumented Idiopathic Scoliosis," *Spine*, Vol. 24, 1999, pp. 1909–1912.
- [8] Cook, S., Asher, M., Lai, S., Shobe, J., "Reoperation After Primary Posterior Instrumentation and Fusion for Idiopathic Scoliosis. Toward Defining Late Operative Site pain of Unknown Cause," *Spine*, Vol. 25, 2000, pp.463–468.
- [9] Gaine, W.J., Andrew, S.M., Chadwick, P., Cooke, E., and Williamson, J.B., "Late Operative Site Pain with Isola Posterior Instrumentation Requiring Implant Removal. Infection or Metal Reaction?" *Spine*, Vol. 26, No.5, 2001, pp.583–587.

Session II: Spinal Device Components, Subassemblies, and Interconnections

Scott Cook,¹ Marc A. Asher,¹ William L. Carson,² Sue Min Lai¹

Effect of Transverse Connector Design on Development of Late Operative Site Pain: Preliminary Clinical Findings

Reference: Cook, S., Asher, M. A., Carson, W. L., and Lai, S. M., “Effect of Transverse Connector Design on Development of Late Operative Site Pain: A Biomechanical and Clinical Study,” *Spinal Implants: Are We Evaluating Them Appropriately? ASTM STP 1431*, M. N. Melkerson, S. L. Griffith, and J. S. Kirkpatrick, Eds., ASTM International, West Conshohocken, PA, 2003.

Abstract: A leading cause for reoperation in patients with idiopathic scoliosis receiving posterior instrumentation and arthrodesis is Late Operative Site Pain (LOSP), with corrosion at the transverse connection site being a common observation. Clinically, a consecutive series of 55 adolescent idiopathic scoliosis patients with Isola Drop Entry Transverse Rod Connector’s (DETCs) was compared with an earlier consecutive series of 97 having Isola Threaded Transverse Rod Connectors (TRCs). Both groups were less than 21 years of age, with TRC average follow-up 87 months and DETC 32 months. Kaplan-Meier survivorship analysis, utilizing implant removal for LOSP, was performed on both groups. Biomechanically, axial and torsional gripping capacity tests were performed on the DETC and TRC interconnections to the longitudinal rod. The axial gripping capacity was 1164 and 1191 N for the two DETC connector components versus 363 N for the TRC connector component. Correspondingly the torsional gripping capacity was 4.1 and 4.7 Nm compared to 1.3 Nm. The Kaplan-Meier probability of reoperation for LOSP by 60 months was 4.7% in the TRC group compared to 0% for DETC ($p = 0.3993$). Seven TRC patients underwent removal for LOSP versus zero for DETC ($p = 0.0504$). The stronger DETC interconnections possibly correlate with a decreased incidence of LOSP.

Keywords: scoliosis, late operative site pain (LOSP), transverse connector, corrosion

Introduction

Commonly recognized indications for reoperation after posterior instrumentation for idiopathic scoliosis include neurologic complications, infection, pseudarthrosis, alignment, implant dislodgment, prominence, breakage, and adjacent motion segment degeneration [1–8]. The authors have reported in a previous publication that late operative site pain (LOSP) was the most common indication for reoperation in a

¹University of Kansas Medical Center, 3901 Rainbow Boulevard, Kansas City, KS 66160-7387

²Professor Emeritus, University of Missouri-Columbia, 2111 Fairmont Rd., Columbia, MO 65212

consecutive series of patients with adolescent scoliosis implanted with the C-D or ISOLA spinal fixation system [9] and second only to pseudarthrosis in patients with Harrington instrumentation. At the time of reoperation, the most common finding was corrosion or corrosion and bursa formation. This was most frequently located at the CD or Isola upper transverse connector site or at the Harrington upper hook site. Electron micrographs of samples taken at the time of implant removal showed intracellular metallic debris in the surrounding soft tissue.

In an attempt to address this issue, a new, stronger transverse connector was designed. The purpose of this study is to compare strengths of the transverse connectors through *in vitro* testing and to review clinical experience with LOSP using the two different connectors.

Materials and Methods

The original threaded transverse rod connector (TRC) and the new drop entry transverse rod connector (DETC) transverse connector are shown in Fig. 1. Their axial and torsional gripping capacities to the longitudinal rod were determined using procedures similar to those in ASTM Standard Guide for Evaluating the Static and Fatigue Properties of Interconnection Mechanisms and Subassemblies Used in Spinal Arthrodesis Implants (F 1798-97) [10]. Torsional gripping capacity was taken as the maximum applied torque to the connector within a 1° offset displacement to the initial linear segment of the torsional load-displacement trace. Axial gripping capacity was taken as the maximum axial force applied to the longitudinal member within a 0.25 mm offset displacement relative to the initial linear segment of the load-displacement trace.

Ninety-seven consecutive patients (17 male, 80 female) with adolescent idiopathic scoliosis were included in the treaded transverse connector (TRC) group. All procedures used the ISOLA implant system and were performed between February 11, 1989, and September 1, 1995, by the senior author (MAA). The index case was included. The average follow-up was 87 months (range, 20 months to 143 months). A minimum follow-up period of 12 months was attained for all patients. None of the included patients were older than 21 years at the time of their primary instrumentation and fusion (range, 10 years 6 months to 20 years 11 months).

The drop entry transverse connector (DETC) group consisted of 55 consecutive patients (6 male, 49 female) with adolescent idiopathic scoliosis. The senior author performed all procedures utilizing the ISOLA implant system between October 2, 1995, and December 28, 1998. The index case was included for review. Average follow-up was 32 months (range, 12 months to 62 months). One patient was excluded from the study secondary to insufficient follow-up. None of the patients were older than 21 years at the time of their primary surgery (range, 10 years 0 months to 20 years 8 months).

Follow-up was obtained through clinic chart review or telephone interview when necessary. The date of reoperation was recorded as well as tabulation of the indications for all pertinent patients.

Fisher's exact probability test was used to directly compare the two groups. Kaplan-Meier analysis [11] was used to determine the risk of reoperation while accounting for differences in available follow-up. Removal secondary to LOSP was used as the end-point.

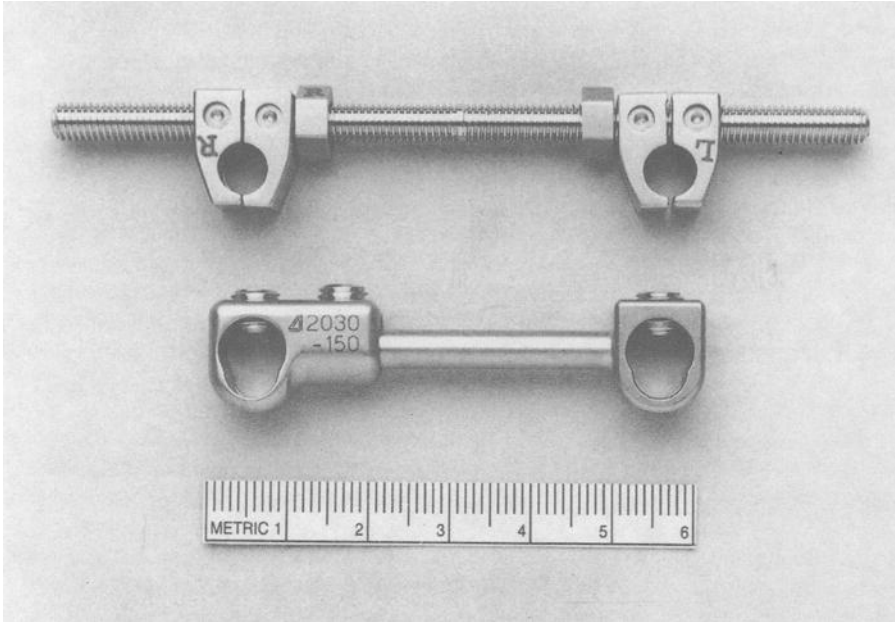


FIG. 1 — Threaded transverse rod connector TRC (top) and drop entry transverse rod connector DETC (bottom).

As previously described [9] LOSP was characterized by midline or parascapular pain that was made worse with direct palpation of the incision. There usually, but not always, was a pain-free interval between the primary surgery and the onset of LOSP. To a large extent, LOSP is a rule-out diagnosis that cannot be confirmed until surgery, when other potential pain generators can be excluded with certainty. In order to qualify for implant removal for the presumed diagnosis of LOSP, the patient's pain must be severe enough that he or she wants some action performed if at all possible. All patients who had their implants removed for LOSP were later questioned as to whether or not the surgery was successful in relieving their pain.

Results

The axial gripping capacity of the stainless steel (SS) DETC was 1164 N for the connector with transverse connector body and 1191 N for connector with integral rod, compared to 363 N for the SS TRC [10]. The corresponding torsional gripping capacity for the DETC was 4.1 and 4.7 Nm compared to 1.3 Nm for the TRC.

There were 11 reoperations (11%) in the TRC group; 7 for LOSP, 2 for pseudarthrosis, and 2 for delayed deep wound infection. Reoperations were performed at 12 and 44 months in the two patients with delayed deep wound infection. The earliest reoperation for LOSP occurred at 22 months following the primary surgery whereas the

latest occurred 135 months. The average time interval to reoperation for LOSP was 67 months.

There have been no reoperations for the indication of LOSP in the DETC group up to this point. The only reoperation in this subset of patients was for the indication of pseudarthrosis and occurred at 23 months after the primary surgery.

The rate of reoperation for LOSP in the groups was compared with the use of a Fisher's exact probability test and found to be marginally significant ($p = 0.0504$). This obviously does not take into account the differences in available follow-up between the two groups and therefore the probability of reoperation for LOSP was studied utilizing Kaplan-Meier survivorship studies (Fig. 2).

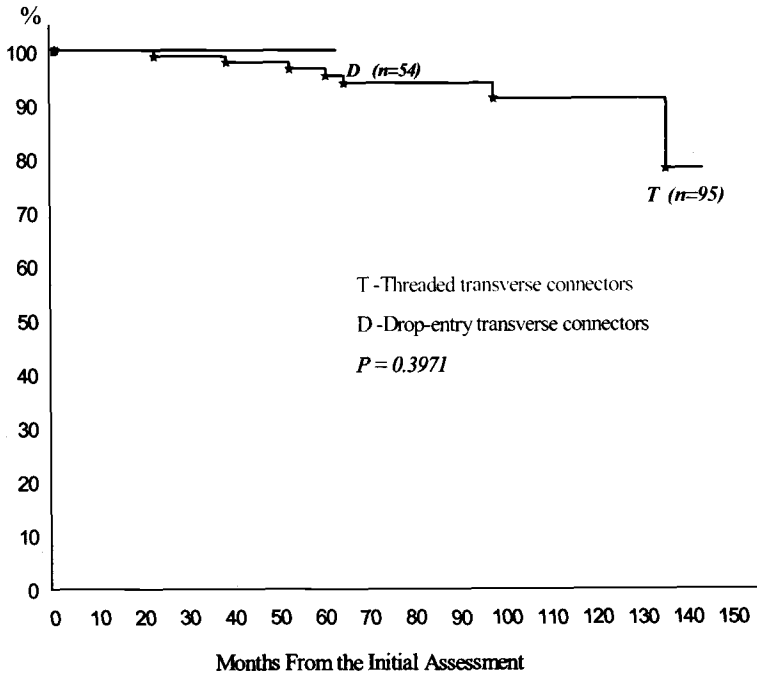


FIG. 2—Kaplan-Meier Estimates- Free from Reoperation for Late Operative Site pain.

These results showed that the probability of reoperation for LOSP at 5 years was 4.7% in the TRC group versus 0% in the DETC group. Probability of reoperation for LOSP at 10 years was 8.9% (TRC) versus 0% (DETC) $p = 0.3993$ (non-significant).

Charts and operative reports were carefully reviewed of the 7 patients who were reoperated for LOSP. None of these patients had positive cultures at the time of reoperation except for one patient who had one culture grow one colony of coagulase-negative staphylococci, interpreted by a microbiologist to be a contaminant. No evidence of glycocalyx was found at the time of reoperation. All fusions were explored at the time

of surgery and there was no evidence of an occult pseudarthrosis in any patient. Six patients had 75 to 100% relief of their symptoms, one did not.

Electron microscopy was available for the soft tissues adjacent to areas of corrosion in two patients. These showed multiple electron dense wear particles that have been ingested by histiocytes indicative of a fibrohistiocytic foreign body reaction associated with metallic wear particles.

Discussion

The aim of this study was to specifically determine whether a newly designed transverse connector would decrease the frequency of LOSP requiring reoperation. In a previous study at this institution [9], LOSP was determined to be the most frequent indication for reoperation in patients with adolescent idiopathic scoliosis who underwent primary fusion and instrumentation with either C-D or ISOLA instrumentation and second only to pseudarthrosis in these patients with Harrington instrumentation. At the time of that study, several possible etiologies for LOSP were proposed, including delayed occult infection, implant prominence, and occult pseudarthrosis. The authors, however, report that the most probable etiology is inflammation secondary to fretting corrosion at the implant connections.

The results and conclusions of the above-mentioned study are in line with a recently published report by Vieweg et al. [12]. The authors prospectively examine 13 spinal fixators for evidence of corrosion after a mean implant time of 10 months. At reoperation, tissue discoloration was found in 4 cases. Histologic evaluation was also performed showing extensive fibrosis, foreign body reaction and inflammation associated with a small number of metal particles, indicating metallosis in five cases. Vieweg et al. conclude that new spinal implants should not only be tested *in vitro* but also *in vivo* to determine whether or not corrosion and adjacent tissue reaction occur.

Wang et al. [13] also demonstrated metal particles in the soft tissues surrounding spinal implants. The authors of this study looked at tissue samples in nine patients with titanium instrumentation from a previous lumbar decompression and fusion procedure. They report that the particles appear to be phagocytized by histiocytes and may incite an inflammatory response similar to that caused by metal particles deposited in soft tissues by loose joint prostheses. Tissue concentrations of titanium particles were highest in patients with a pseudarthrosis. Thus, it is intuitive that stronger spinal implants with motion-resistant connections would produce less wear debris.

All of these studies agree with recent reports looking at the soft tissue and systemic effects of metal particles produced by joint replacement implants. Hallab et al. [14], in a recent current concepts review, state that corroding metals produce ions, which form complexes with native proteins capable of eliciting an immune response. Archibeck et al. [15] have also published a recent review specifically focusing on studies in the joint arthroplasty literature, which report on the biologic effects of various types of particulate debris including metal. These studies are mainly concerned with the events leading to osteolysis; however, a complex immunogenic cytokine cascade consisting of many mediators including macrophages, fibroblasts, osteoblasts, and osteoclasts is outlined in this comprehensive review. Many questions arise when attempting to correlate the arthroplasty results with those associated with spinal implants; nevertheless, these studies

concerning the effects of particulate debris can certainly be utilized with caution in the attempt to study peri-instrumentation pain encountered in spinal surgery.

Further follow-up will be necessary to confirm or refute our preliminary observations. Future work by us and others could help determine whether or not axial and torsional gripping strength of other transverse connector designs correlate with the incidence of LOSP.

Conclusions

In vitro biomechanical testing shows that the newly designed drop entry transverse connector is stronger than threaded transverse connectors with regard to both axial and torsional gripping strengths. In short term follow-up, this appears to correlate with a decreased incidence of LOSP.

References

- [1] Connolly, P. J., Von Schroeder, H. P., Johnson, G. E., and Kostuik, J. P. "Adolescent Idiopathic Scoliosis: Long-Term Effect of Instrumentation Extending to the Lumbar Spine," *Journal of Bone and Joint Surgery [Am]* 1995, Vol. 77, pp.1210–1216.
- [2] Dickson, J. H., Mirkovic, S., Noble, P. C., Nalty, T., and Erwin, W. D. "Results of Operative Treatment of Idiopathic Scoliosis in Adults," *Journal of Bone Joint and Surgery [Am]* 1995, Vol. 77, pp. 513–523.
- [3] Harrington, P. R., "Treatment of scoliosis: Correction and internal fixation by spine instrumentation," *Journal of Bone and Joint Surgery [Am]* 1962, 44, pp. 591–611.
- [4] Harrington, P. R., Dickson, J. H., "An Eleven-Year Clinical Investigation of Harrington Instrumentation: A Preliminary Report on 578 Cases," *Clinical Orthopaedics and Related Research*, 1973, Vol. 93, pp. 113–130.
- [5] McAfee, P. C., Weiland, D. J., Carlow, J. J., "Survivorship Analysis of Pedicle Spinal Instrumentation," *Spine*, 1991, Vol. 16, (Suppl), pp. S422–427.
- [6] Ponder, R. C., Dickson, J. H., Harrington, P. R., Erwin, W. D., "Results of Harrington Instrumentation and Fusion in the Adult Idiopathic Scoliosis Patient," *Journal of Bone and Joint Surgery [Am]*, 1975, Vol. 57, pp. 797–801.
- [7] Richard, B. S., Herring, J. A., Johnston, C. E., Birch, J. G., Roach, J. W., "Treatment of Adolescent Idiopathic Scoliosis Using Texas Scottish Rite Hospital Instrumentation," *Spine*, 1994, Vol. 19, pp. 1598–1605.
- [8] Tambornino, J. M., Ambrust, E. N., Moe, J. H., "Harrington Instrumentation in Correction of Scoliosis: A Comparison with Cast Correction," *Journal of Bone and Joint Surgery [Am]* 1964, Vol. 46, pp. 313–323.
- [9] Cook, S., Asher, M., Lai, S., Shobe, J., "Reoperation After Primary Posterior Instrumentation and Fusion for Idiopathic Scoliosis: Toward Defining Late Operative Site Pain of Unknown Cause," *Spine*, 2000, Vol. 25, pp. 463–468.
- [10] Carson, W. L., Elphinston, J., "In Vitro Static and Fatigue Testing of SS and Ti Closed (Drop Entry) Threadless TRC, SS Open (Drop Entry) Threadless TRC, and SS Threaded TRC for ¼" Dia. Rod," Confidential report submitted to AcroMed Corp., May 15, 1997.
- [11] Kaplan, E. L., "Nonparametric Estimation from Incomplete Observations," *American Statistical Association Journal*, 1958, Vol. 53, pp. 459–481.

- [12] Vieweg, U., Roost, D., Wolf, H. K., Schyma, C. A., and Schramm, J., "Corrosion on an Internal Spinal Fixator System," *Spine*, 1999, Vol. 24, pp. 946–951.
- [13] Wang, J. C., Yu, W. D., Sandhu, H. S., Betts, F., Bhuta, S., and Delamarter, R. B., "Metal Debris from Titanium Spinal Implants," *Spine*, 1999, 24, pp. 899-903.
- [14] Hallab, N., Merritt, K., Jacobs, J. J., "Current Concepts Review: Metal Sensitivity in Patients with Orthopaedic Implants," *Journal of Bone and Joint Surgery [Am]* 2001, Vol. 83, pp. 428–436.
- [15] Archibeck, M. J., Jacobs, J. J., Roebuck, K. A., Glant, T. T., "The Basic Science of Periprosthetic Osteolysis," *Journal of Bone and Joint Surgery [Am]* 2000, Vol. 82, pp. 1478–1489.

Laura M. Jensen,¹ MS, Shannon S. Springer,¹ BME, Sean F. Campbell,¹ and Eric Gray¹

Interconnection Strength Testing and its Value in Evaluating Clinical Performance

Reference: Jensen, L. M., Springer, S. S., Campbell, S. F., and Gray, E., “**Interconnection Strength Testing and Its Value in Evaluating Clinical Performance,**” *Spinal Implants: Are We Evaluating Them Appropriately*, ASTM STP 1431, M. N. Melkerson, S. L. Griffith, and J. S. Kirkpatrick, Eds., ASTM International, West Conshohocken, PA, 2003.

Abstract: ASTM standard F1798-97 provides guidelines for evaluating the strength of interconnection mechanisms used in pedicle screws and hooks. A literature search indicates the following as common significant clinical complications: fractured pedicle screws; fractured rods; disconnection between the rods, bolts, nuts and screws; screw loosening; loss of correction; inaccurate screw placement; broken pedicles; dural leaks; infection; transient and permanent neural injury. The tests outlined in ASTM standard F1798-97 may correspond to disconnection between the rods and screws or loss of correction. The standard does not correspond to any other known causes of the common complications. Therefore, interconnection strength tests may not have any bearing on the clinical outcomes of patients since there is no direct evidence that they sufficiently test for relevant device failures.

Keywords: pedicle screws, interconnection, spine, spinal implants, clinical data.

Introduction

Pedicle screw fixation systems are widely used to stabilize spinal motion segments to facilitate fusion of the vertebral bodies. In certain systems, stabilization is provided by the locking mechanism present between the rods and screws. The strength of this interconnection is measured by following the guidelines of ASTM F1798-97, “Standard Guide for Evaluating the Static and Fatigue Properties of Interconnection Mechanisms and Subassemblies Used in Spinal Arthrodesis Implants.”

The tests prescribed in ASTM F1798-97 are often used for developmental and quality purposes. The standard is used with the assumption that the modes of failure seen during any of its tests correlate with the causes of failure in a clinical situation. If this is a valid assumption, then there should be evidence in the literature to indicate failures or complications in spinal surgery due, potentially, to interconnection strength failures in

¹ Associate Research Engineer, Research Engineer, Co-Op Research Engineer, Silhouette Product Manager, respectively, at Centerpulse Spine-Tech, 7375 Bush Lake Road, Minneapolis MN 55439.

pedicle screw fixation systems.

The purpose of this paper is to examine the types of failures tested with ASTM F1798-97 guidelines and compare them to clinical complications mentioned in the literature.

Methods

The Interconnection Tests

The guidelines in ASTM F1798-97 describe six specific different uniaxial tests that can measure either static or fatigue strength. Each test is designed to test a subassembly interconnection strength in a specific major direction of loading as follows:

1. Anterior-posterior test—measures the screw or hook's ability to resist a separating force along the screw axis and perpendicular to the rod.
2. Transverse test—similar to the anterior-posterior test, measures the transverse component's ability to stay perpendicularly attached to the rod.
3. Flexion-extension moment test—measures the screw or hook's capacity to resist changing angular orientation with respect to the rod. The screw or hook is attached perpendicularly to the longitudinal element (the rod). Then a force is applied parallel to the rod but applied to the screw at a distance 25 mm away from the center of the rod. This force produces a bending moment where the screw assembly and the rod connect.
4. Transverse moment test—similar to the flexion-extension moment test, measures the transverse component's capacity to resist changing angular orientation with respect to the rod.
5. Axial gripping capacity—measures the component's capacity to resist sliding with respect to the rod. A collar applies an evenly distributed force around the interconnection. The force causes the interconnection to slip along the axis of the rod.
6. Axial torque gripping capacity—measures the component's capacity to resist twisting or rotating about the rod axis.

In our laboratory, the authors examined data from static flexion-extension moment interconnection strength tests performed over the period of about one year. In the flexion-extension moment test, a force is applied to displace the end of the screw a certain distance at the point of force application. To pass the test, each subassembly must provide a minimum resistive load to the displacement force. In addition, the average strength of all samples from a group must also be above a higher minimum. The minimum strengths were chosen to match demonstrated strengths of pedicle screws currently on the market. There were well over 100 tests performed; each test included a number of samples from 3–9 with most groups having about 6 samples each.

Clinical Performance

Literature data bases including Medline, Biological Abstracts, Engineering Index, Embase, Federal Research in Progress, and Inspec were searched to find information including pedicle screw failures, complications associated with pedicle screws, or studies examining clinical results of various pedicle screw surgeries. The articles were examined to find clinical complications that surgeons and authors felt were important enough to

mention.

Results

The Interconnection Tests

All samples in 91% of the groups possessed adequate individual minimum strengths within the tested displacement range. The average strength of each group was also above the minimum criteria for 87% of the groups. However, those results meant that about 10% of the groups in our quality assurance tests failed our internal criteria (the end of the screw could deflect under too small a load) and were refused for distribution. There was no evidence of screw or rod fracture/bending from any of the tests.

Clinical Performance

In examining the literature, there are several complications that are mentioned frequently including: screw fractures; rod fractures; and disconnection between rod, bolt, nut and screw. The incidences of each type of failure are listed in Table 1 below.

Table 1— *Frequency of screw or rod fractures and construct disconnections by study.*

Author	# patients (specimen)	# screw fractures	# rod fractures	# disconnection between rod, bolt, nut and screw	Comments ^a
Blumenthal <i>et al.</i> , 1993	470	8 (4 patients)	4	4	1
Esses <i>et al.</i> , 1993	617	18 (2.9%)	...	5	1,3
Faraj <i>et al.</i> , 1997	91	0	3	1	2
Lonstein <i>et al.</i> , 1999	875 (4790)	25 screws (20 patients)	
Masferrer <i>et al.</i> , 1998	95 (434)	0	...	1	1
Ohlin <i>et al.</i> , 1994	193	10 (8 cases)	3 or 4	3 or 5	1
Okuyama <i>et al.</i> , 1999	148	1	...	2	1
van Royen <i>et al.</i> , 1998	21	...	7	5	1

a: 1 = retrospective study, 2 = prospective study, 3 = data provided by voluntary questionnaires to surgeons.

Note that some of the 4 rod-fractures discovered in the Blumenthal *et al.* [1] study (Table 1) were only noticed incidentally during hardware removal. The authors attributed the disconnection in the Faraj *et al.* [3] study to a technical error rather than implant failure. The disconnection in the Masferrer *et al.* [5] study appeared after 8 months but had no accompanying symptoms and had a radiographically solid fusion.

Other complications include screw loosening from the bone, loss of correction, inaccurate screw placements, and pedicle fracture as screws were inserted or manipulated. Those complication rates were comparable to the complication incidences of Table 1. Screw loosening, if it was mentioned, was seen between 0.6% and 2.7% with one large

rate of 17.6%. [1-3, 6, 7] Ohlin *et al.* [6] attribute their large incidence rate of 17.6% to their strict definition of loosening and they suggest that many of the instances they describe as failures were clinically insignificant.

Three authors mentioned loss of correction as a complication. Ohlin *et al.* [6] mention that 6.7% of their cases experienced loss of correction, but they did not characterize how extensive the loss was. Okuyama *et al.* [7] state that 1 of their 148 patients had loss of correction, but again there was no quantification. Van Royen *et al.* [8] gave an overall mean loss of correction of 10.7 degrees with a range of 0 to 36 degrees in their 21 patients. Initial correction in the same study ranged from 0 to 52 degrees with an average correction of 25.6 degrees.

Inaccurate screw placements occurred between 4.1% and 8.8 % of the time if they were detected and reported. [2-4, 6-7] There was also a complication with the pedicle itself fracturing. Van Royan *et al.* [8] report the pedicle fracturing during tightening of the instrumentation in 33% of their cases. The authors claim that this relatively large number of fractures is due to the complexity of the surgeries they performed. Most instances of pedicle fracture occurred during placement of the screw and usually occurred less than 1 percent of the time [1, 4-6] with only one higher instance at 4.2% [2].

Other complications that were mentioned include dural leaks (0.4% to 4.2%) [2, 4-7], infection (1.0% to 4.2%) [1, 2, 5-7], transient neural injury (0.2% to 8%) [1, 2, 7], and more permanent neural injury with rates between 0.2% and 2.3% [1, 2, 4, 5].

Discussion

A significant clinical complication included fractured screws. Screw fracture resistance can be measured with strength and fatigue tests. However, interconnection strength testing is probably not the most appropriate way to test the screw's strength; when the interconnection strength is weaker than the strength of the screw itself, then the interconnection fails before the strength of the screw is even tested.

Most of the studies did not indicate the location of the fracture. However, many screws have been known to fracture mid-shaft as shown in the x-ray of figure 1. Figure 1 of the article by Okuyama *et al.* [7] also shows a good image of this type of fracture.



Figure 1— *A typical case of a broken pedicle screw. Notice that the fracture is in the middle of the shaft rather than towards the head of the screw. The fracture is near the anterior portion of the vertebral pedicle.*

The flexion-extension moment test is the one most likely to create screw fractures, if any of the interconnection strength tests create fractures. However, the screw would only break if the interconnection strength were stronger than the screw. Breakage would

occur where the moment arm is the greatest—near the head of the screw closer to the rod for most screw designs. This theoretical test mode of fracture is not consistent with the mid-shaft failures seen *in vivo*.

Rods do not break as a direct result of interconnection strength mechanisms. Therefore, ASTM standard F1798-97 is not an appropriate mechanism to test rod breakage failures. (Indirectly, loose interconnections could lead to fretting corrosion, which could contribute to rod fractures. A fatigue test from standard F1798-97 might indicate if fretting corrosion could be a problem, but it would still not directly test rod breakages.) ASTM standard F1717-96 Standard Test Methods for Static and Fatigue for Spinal Implant Constructs in a Corpectomy Model may be a more appropriate means to test rod failures.

Disconnection between the rod, bolt, nut, or screw would seem to be a failure of the interconnection mechanisms. However, these failures can also be caused by improper installation of the spinal assemblies themselves. Faraj *et al.* [3] allude to these problems when they point out that their one instance of disconnection is due to technical error rather than failure of the implant components. Figure 2, below, shows a rare problem but is another disconnection example. The rod has slipped out of both screws presumably because the locking nuts of the assembly were not properly tightened.

ASTM F1798-97 does not test for improper installation of the device. However, since it cannot be determined retrospectively if correct surgical technique was followed during installation, the interconnection strength tests do at least give reasonable assurance

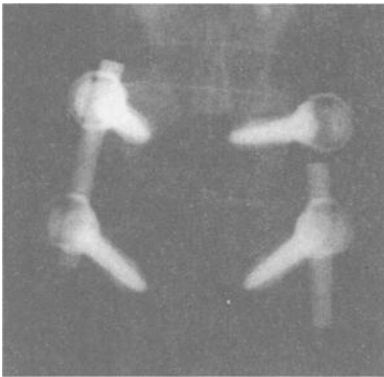


Figure 2— *There is an obvious disconnection between the rod and the pedicle screws. The disconnection is attributed to insufficient tightening of the lock nut and not due to any inherent interconnection failure of the implant.*

that, if installed properly, these kinds of disconnections will not happen.

Screw loosening from the bone is a more complex mechanism that may or may not be related to the screw itself but cannot be evaluated with interconnection strength testing.

Loss of correction is a complex phenomenon and its causes are not well understood. Is it indicative of an interconnection strength failure? We are not aware of any study that correlates loss of correction to an interconnection deficiency. Loss of correction *in vivo* is extremely difficult to measure accurately, and in many cases the loss may not even be a problem. Only 3 authors even mentioned it [6-8] and of those, only van Royen *et al.* [8] tried to quantify it. Presumably it was not noticeable or noteworthy for any of the other cases.

Neural injury, infection, dural leaks, broken pedicles, and inaccurate screw placements cannot be addressed with any ASTM test standards. They are all highly dependent on the surgeon and each individual case rather than the implant itself. Still, comparing their incidence rates to those that might be considered more related to the implant itself can be informative and keep things in perspective by noting the small number of occurrences.

Examining the issue from another angle, if an implant's interconnection mechanism were to fail, could it even be detected or measured? Given the complex nature of measuring objects in 3 dimensions, it seems unlikely that one could detect a moderate change, especially one *in vivo*, corresponding to a failure mode in one of the interconnection strength tests. If the problem cannot be detected *in vivo*, and it does not seem to be contributing to any complications seen in the clinic, is it worth devoting resources to test?

In a world of limited resources, it is an important question to ask. On the other hand, lack of evidence does not necessarily mean that no problem exists or that it should be ignored. For example, intuition suggests that some interconnection strength is required to avoid loss of correction. If the interconnection strength were zero, the system would not be able maintain a surgical correction. The optimal required interconnection strength is unknown, and a wide range of system stiffnesses have been found to be successful. [9, 10] The minimum required strength is unknown, and recent studies indicate that stiffer constructs are not necessarily more effective, and may even be less effective, than more flexible systems. [11,12] Fortunately, ASTM F1798-97 can be used to compare new systems to other systems that have been shown through clinical trials to have adequate strength.

The clinical performance data have not shown direct evidence of an interconnection mechanism failure. Even if such a failure were to be detected, it would still need to be determined if the failure were the cause of, the result of, or incidental to a symptomatic problem.

Several authors cited examples where broken implants were discovered but the patient did not have any associated symptoms. For example, Boos *et al.* [13] mention that 12 patients had bent, broken, or loose pedicle screws. However, all 12 were asymptomatic and their fusions appeared solid. Ohlin *et al.* [6] state that their failure criteria were high, and therefore many of the complications that they termed as failures were not clinically significant. Are asymptomatic failures a problem?

One limitation of this study is that the literature examines cases where patients have had their implants for several years. Therefore, complications from newer technologies such as polyaxial screws are not as well documented.

The scope of this paper was limited to examining evidence of clinical relevance for ASTM standard 1798-97. Clinical relevance is extremely important because pedicle screws must ultimately succeed within the patient to improve their quality of life. Therefore, it is an important consideration to keep in the overall picture (e.g. when prioritizing resources to provide the most effective device for the patient) even though clinical relevance is beyond the stated scope of the standard itself. This is not to say that the standard does not have merit as a development tool because, as stated earlier, the standard can be useful to compare new systems to other systems that have been shown

through clinical trials to have adequate strength. However, “adequate strength” is such a nebulous and unknown quantity that more research needs to be done to define its optimal parameters. Currently, there is still not enough evidence in the literature to show that interconnection strength (related to construct stiffness) has a direct correlation in clinical success.

Conclusion

The tests outlined in ASTM F1798-97 do not adequately test for noteworthy failures seen in clinical practice as documented in the literature. In fact, their results may not have any bearing on the clinical outcomes of patients who use the spinal devices. The only evidence of possible interconnection failures in vivo have been cases where the rods disconnect from the pedicle screws, and these cases seem likely to be caused by complications seen only in the surgical environment and not in the lab. The failures do not seem to be inherent device failures that the current interconnection strength tests as written would detect.

Broken screws do seem to be a problem in vivo and should be addressed. More study into these occurrences could be beneficial. However, the interconnection strength guidelines of ASTM F1798-97 are not appropriate tests for these particular failures.

There is still a question as to whether interconnection strengths might contribute to loss of correction. However, the causes, possible correlations, and optimal strengths are unknown. More studies need to be done to understand the mechanisms for loss of correction or screw breakage more specifically. These studies should also suggest better test methods that correlate more directly to clinical problems.

Otherwise there has not been any other documented direct evidence of an interconnection failure in vivo. Even if one were to be detected, it should be determined that the interconnection failure is not just incidental to or the result of a symptomatic clinical problem.

References

- [1] Blumenthal, S. and Gill, K., “Complications of the Wiltse Pedicle Screw Fixation System,” *Spine*, Vol. 18, No. 13, 1993, pp. 1867–1871.
- [2] Esses, S. I., Sachs, B.L., Dreyzin, V., “Complications Associated with the Technique of Pedicle Screw Fixation: A Selected Survey of ABS Members,” *Spine*, Vol. 18, No. 15, 1993, pp. 2231–2239.
- [3] Faraj, A. A., Webb, J.K., “Early Complications of Spinal Pedicle Screw,” *European Spine Journal*, Vol. 6, 1997, pp. 324–326.
- [4] Lonstein, J.E., Denis, F., Perra, J.H., Pinto, M.R., Smith, M.D., Winter, R.B., “Complications Associated with Pedicle Screws,” *The Journal of Bone and Joint Surgery*, Vol. 81-A, No. 11, November 1999, pp. 1519-1528.
- [5] Masferrer, R., Gomez, C.H., Karahalios, D.G., Sonntag, V.K.H., “Efficacy of Pedicle Screw Fixation in the Treatment of Spinal Instability and Failed Back Surgery: a 5-Year Review.” *Journal of Neurosurgery*, Vol. 89, 1998, pp.371–

377.

- [6] Ohlin, A., Karlsson, M., D ppe, H., Hasseri s, R., Redlund-Johnell, I., "Complications After Transpedicular Stabilization of the Spine: A Survivorship Analysis of 163 Cases," *Spine*, Vol. 19, No. 24, 1994, pp. 2774-2779.
- [7] Okuyama, K., Abe, E., Suzuki, T., Tamura, Y., Chiba, M., Sato, K., "Posterior Lumbar Interbody Fusion: A Retrospective Study of Complications after Facet Joint Excision and Pedicle Screw Fixation in 148 Cases," *Acta Orthopaedica Scandinavica*, Vol. 70, No. 4, 1999, pp. 329-334.
- [8] van Royen, B.J., de Kleuver, M., Slot, G.H., "Polysegmental Lumbar Posterior Wedge Osteotomy for Correction of Kyphosis in Ankylosing Spondylitis," *European Spine Journal*, Vol. 7, 1998, pp. 104-110.
- [9] Gurr, K. R., McAfee, P. C., Shih, C. M., "Biomechanical Analysis of Anterior and Posterior Instrumentation Systems After Corpectomy. A Calf-Spine Model," *Journal of Bone and Joint Surgery American*, Vol. 70, No. 8, 1988, pp. 1182-1191.
- [10] Mardjetko, S. M., Connolly, P.J., Shott, S., "Degenerative Lumbar Spondylolisthesis. A meta-Analysis of Literature 1970-1993." *Spine*, Vol. 19, No. 20, Supplemental, 1994, pp. 2256S-2265S.
- [11] Pfeiffer, M., Deike, B., Clausen, J. D., Wilke, A., Griss, P., "A New Semirigid Implant for Instrumentation of Scoliosis: Preliminary Report," *European Spine Journal*, Vol. 10, No. 5, 2001, pp. 427-436.
- [12] Foster, M. R., Allen, M. J., Schoonmaker, J.E., Yuan, H. A., Kanazawa, A., Park, S.-A., Baowei, L., "Characterization of a Developing Lumbar Arthrodesis in a Sheep Model with Quantitative Instability," *The Spine Journal*, Vol. 2, 2002, pp. 244-250.
- [13] Boos, N., Marchesi, D., Aebi, M., "Survivorship Analysis of Pedicular Fixation Systems in the Treatment of Degenerative Disorders of the Lumbar Spine: A Comparison of Cotrel-Dubousset Instrumentation and the AO Internal Fixator," *Journal of Spinal Disorders*, Vol. 5, No. 4, 1992, pp. 403-409.

Carson, W. L.¹

Protection of the Longitudinal Member Interconnection by ASTM F 1798-97 Interconnection Mechanism and Subassemblies Standard Guide

REFERENCE: Carson, W. L., "Protection of the Longitudinal Member Interconnection by ASTM F 1798-97 Interconnection Mechanism and Subassemblies Standard Guide," *Spinal Implants: Are We Evaluating Them Appropriately*, ASTM STP 1431, M. N. Melkerson, S. L. Griffith, and J. S. Kirkpatrick, Eds., ASTM International, West Conshohocken, PA, 2003.

ABSTRACT: The same screw-rod interconnection was tested at two labs. One used the fixed-fixed end straight rod assembly in ASTM F 1798-97. The other used a fixed-free end equivalent assembly unilateral construct. The fixed-fixed assembly consistently produced higher fatigue strength, and a different failure mode with only one exception. Freebody diagram analysis of the fixed-fixed end rod-connector assembly revealed that the superior and inferior ends of the rod shared in resisting the applied load, which resulted in lower internal forces and moments than in the inferior rod end of the fixed-free assembly. Lordotically contoured rods had lower flexion fatigue life than straight rods due to the residual tensile stress from contouring. Changing ASTM F 1798-97 to fixed-free end assembly testing is recommended since the interconnection loading conditions created are "worst case" and are more clinically relevant (particularly at ends of constructs), and tests can be performed with bent or straight rods.

KEYWORDS: ASTM 1798-97, interconnection, flexion, fatigue, contoured

Introduction

The same spinal instrumentation screw-rod interconnection was tested in flexion bending in two different labs. The DePuy AcroMed lab [1] followed the interconnection flexion fatigue test procedure in ASTM Standard Guide for Evaluating the Static and Fatigue Properties of Interconnection Mechanisms and Subassemblies Used in Spinal Arthrodesis Implants (F 1798-97), which specifies the use of the fixed-fixed end straight rod assembly shown in Fig. 1. Carson [2] performed interconnection flexion fatigue tests with both straight and lordotically contoured rods using the unilateral construct shown in Fig. 2. Each end of the unilateral construct is equivalent to a single fixed-free end assembly since the construct is symmetrical about a mid transverse plane. Bent rods were used to determine their effect if any on the spinal instrumentation interconnection.

¹ Professor Emeritus, University of Missouri-Columbia, 2111 Fairmont Rd., Columbia, MO. 65203.

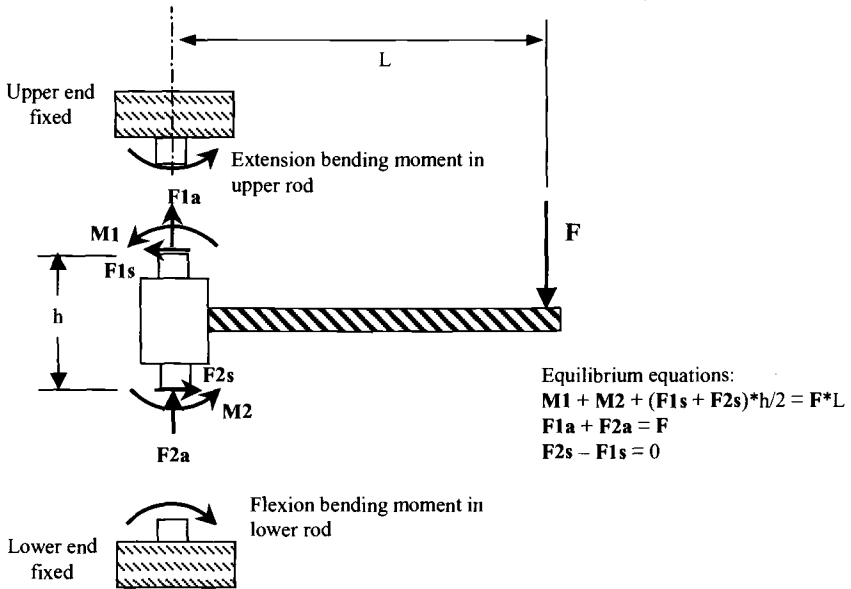


FIG. 1 – ASTM F 1798-97 fixed-fixed end assembly for flexion testing, and freebody diagram of the connector assembly.

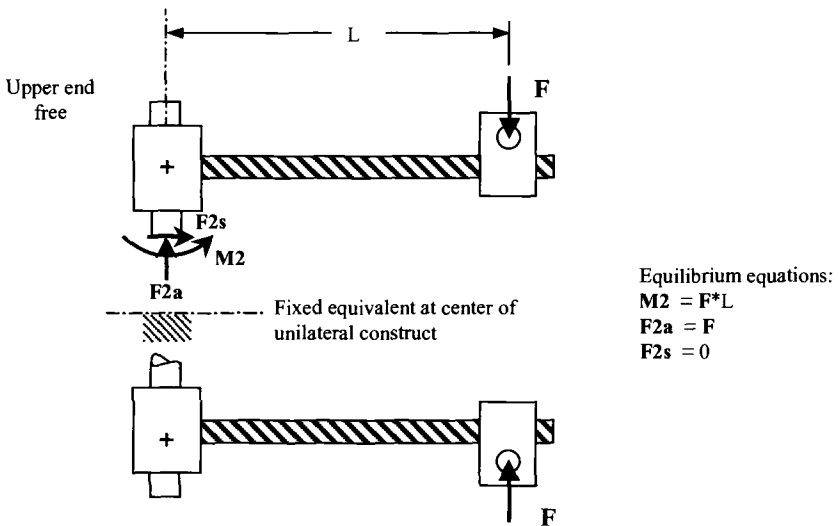


FIG. 2–Unilateral construct Carson used for flexion testing (each end being equivalent to a fixed-free end assembly), and freebody diagram of the upper connector assembly.

Another observation is that lordotically contoured rods consistently had shorter fatigue life away from, as well as at the connector compared to when straight rods were used. The apparent explanation for this is the residual tensile stress in the outer yielded layer on the concave (posterior) side of the rod as a result of contouring. This residual tensile stress adds to the tensile stress created by the flexion moment M_2 acting on the rod, thus creating a greater total tensile stress with correspondingly shorter fatigue life of the rod. The residual stress on the posterior side of a kyphotically contoured rod is compressive and is thus negative. When the compressive residual stress is added to the tensile stress created by flexion bending moment M_2 acting on the rod, the sum is a tensile stress lower in magnitude compared to that in a virgin straight rod. This analysis implies that a kyphotically contoured rod would have greater flexion fatigue strength than either a straight or lordotically contoured rod.

Discussion

The reason stated for using a fixed-fixed rod end assembly during ASTM F 1798-97 development was to be able to test the strength and stiffness of the interconnection itself, and thus to minimize rod compliance and chance of the rod failing in fatigue. Both test methods apply the same internal loads and stresses to the screw and its interconnection to the connector. However, the internal loads and resulting stresses within the rod adjacent to and within the rod-connector interconnection are significantly different. Fixed-free end assembly (unilateral construct) tests produce greater moment and stress within the end of the rod that resists the applied load, and within the adjacent side of the rod-connector interconnection. This internal loading of the spinal instrumentation hardware is typical of in vivo conditions (particularly at the end of constructs), which correlates to clinical rod failures frequently occurring adjacent to or within the connector [3]. In vitro interconnection and subassembly tests should have internal loading and stress conditions similar to worst-case clinical conditions to more accurately predict their in vivo fatigue characteristics.

Recommend Changes to ASTM F 1798-97

The following are recommended changes to ASTM F 1798-97:

1. Replace the fixed-fixed end rod assembly with a fixed-free end rod assembly having a reduced length of exposed rod between the fixed constraint and the axis of the screw (12.5 instead of 25 mm for example) to reduce the influence of rod stiffness on assembly stiffness, and to reduce screw displacement at the point of load application.
2. Calculate flexion bending stiffness of the exposed longitudinal member (which can be done easily for the rod and most other longitudinal members), and substitute it and the experimental assembly stiffness into the springs-in-series equation to determine the stiffness of the rod connector interconnection and the rest of the connector-screw assembly.
3. If the connector is likely to be clinically used on a contoured rod, conduct interconnection flexion tests on straight as well as rod contoured to a clinically representative maximum bend (minimum radius of curvature).

References

- [1] Slivka, M., “*Mechanical Testing Report...*,” Internal DePuy AcroMed Confidential Report on a Prototype Connector, November 15, 2000.
- [2] Carson, W. L., “*Research Summary, Review, and Reports*,” Confidential Report to DePuy AcroMed on a Prototype Connector, February 26, 2001.
- [3] Carson, W. L., Asher, M., Boachie-Adjei, O., Lebowhl, N., Dzioba, R., Akbarnia, B., “History of Isola-VSP Fatigue Testing Results with Correlation to Clinical Implant Failures,” *Spinal Implants: Are We Evaluating Them Appropriately? ASTM STP 1431*, M. N. Melkerson, S. L. Griffith, and J. S. Kirkpatrick, Eds., ASTM International, West Conshohocken, PA, 2002.

John M. Dawson,¹ Paul Boschert,¹ M. Mason Macenski,¹ and Nahshon Rand²

Clinical Relevance of Pull-out Strength Testing of Pedicle Screws

Reference: Dawson, J. M., Boschert, P., Macenski, M. M., and Rand, N., “**Clinical Relevance of Pull-out Strength Testing of Pedicle Screws,**” *Spinal Implants: Are We Evaluating Them Appropriately, ASTM STP 1431*, M. N. Melkerson, S. L. Griffith, and J. S. Kirkpatrick, Eds., ASTM International, West Conshohocken, PA, 2003.

Abstract: Pull-out strength testing is described in many published manuscripts and is specially treated in ASTM F1692-96, “Standard Test Method for Determining Axial Pull-Out Strength of Medical Bone Screws.” Extensive biomechanics are reported on the importance of variables like hole preparation and cement augmentation. In this study, the pull-out strengths of variously-shaped, titanium pedicle screws were tested and the literature was searched for cited incidences of pull-out. The screws were extracted from polyurethane foam that modeled weak, moderate, and strong cancellous bone. Testing revealed significantly different pull-out strengths depending upon screw design and substrate strength. However, the literature search yielded few citations of screw pull-out. Screw loosening and hardware failure are sometimes mentioned in clinical reports but rarely is pull-out documented as a failure mechanism. Standardized testing is useful in comparing various designs but may have little relationship to *in vivo* performance.

Keywords: spine, orthopaedic medical devices, bone screws, pedicle screws, pull-out strength, fixation strength.

Background

Pedicle screws are available in a variety of designs. For instance, the threads may be vee, square, or buttress shaped and the major and minor diameters may be straight or tapered. These features affect the strength, the stiffness, and the holding power of a screw. It is assumed that a well-fixed screw will help maintain a surgical reduction until fusion occurs. A loose screw may lead to construct or hardware failure, including screw breakage, loosening, and pull-out, that will preclude fusion. Pull-out strength is defined as the maximum axial load sustained by the screw. A method for measuring pull-out load is defined in the ASTM Test Method for Determining Axial Pull-Out Strength of Medical bone Screws (F1692-96). The intent of the standard is “to provide a uniform test

¹ Director of Spine Biomechanics Research, Centerpulse SpineTech Inc., 7375 Bush Lake Road, Minneapolis, MN 55439.

² Senior orthopedic surgeon, Israel Spine Center, Assuta Hospital, 62 Jabotinsky st. Tel-Aviv 62748, ISRAEL, Adjunct Professor, Dept. of Orthopaedics and Rehabilitation, Vanderbilt University, Nashville TN.

procedure for measuring the axial pull-out strength of bone screws in a uniform medium.” A further intent of the standard is to address “an immediate need in the industry for a standard testing procedure for measuring the pull-out strength of bone screws.”

A variety of values for pull-out loads has been reported by a number of investigators (Table 1) [1-9]. In addition, extensive biomechanics are reported on the importance of hole preparation [10-13] and cement augmentation [14-18]. Some techniques more effectively enhance pull-out strength than others. For instance, drilled holes yield pull-out strengths no greater than probed holes [10] but cement augmentation increases pull-out strength by 70% [14]. Clearly, pull-out is perceived as major mode of screw failure and prevention of pull-out is an important design objective. Is this perception valid in terms of the clinical experience? This study quantified the effects of various screw design parameters on pull-out strength. These data are contrasted with incidences of pull-out cited in the literature.

Table 1— *Reported values for pull-out strength*

Screw (Diameter x Length), mm	Screw Style, Major/Minor	Thread Shape	Investigator	Substrate	Pull-out Strength (Mean ± 1 SD), N
6.5 x 40	Straight/ Taper	Vee	Daftari [10]	Calf	1488 ± 378
6 or 7 x 40	Straight/ Straight	Vee	Saiyro [6]	Calf	934 ± 276
6.25 x 40	Straight/ Straight	Buttress	Wittenberg [17]	Human & Calf	300 ± 200
6.5	Taper/ Taper	Vee	Pfeiffer [5]	Human	800 ± 400
6.5 x 40	Straight/ Taper	Vee	Daftari [10]	Foam	1134 ± 112
6.5 x 50	Straight/ Straight	Vee	Thompson [7]	Foam	1264 ± 158

Methods

Pull-out Testing

Various pedicle screws were fabricated of titanium (Table 2). All possessed a 6.5 mm major diameter, a 3.8 mm minor diameter, 40 mm length and 2 mm pitch. These dimensions were chosen because this screw size was easily fabricated by the study sponsor and because similarly-sized screws have been studied by others (Table 1). The heads of all screws were cylindrical with a transverse hole to accommodate a fixture pin.

The screws were extracted from rigid polyurethane foam (Last-a-Foam™, General Plastics Manufacturing Company, Tacoma, WA), which is an accepted material for implant testing (ASTM F1839-97, “Standard Specification for Rigid Polyurethane Foam for Use as a Standard Material for Testing Orthopaedic Devices and Instruments”). Three

densities of foam (10, 12, and 15 lb/ft³) were tested to model weak, moderate, and strong cancellous bone [19-22]. Because of its cellular structure, rigid foam mimics some of the biomechanical properties of cancellous bone: its compressive modulus and compressive strength depend upon its density. (Table 3) [2,7,10]. To facilitate insertion, pilot holes were drilled; the pilot holes were 4mm in diameter, which was the appropriate size for the screws. The pilot holes were untapped because specially made taps would have been required for each thread form and these were not available. Testing was accomplished under displacement control at a rate of 5mm/min. Each screw design was tested in all three foams 6 times each. The load vector was co-aligned at the start of the test with the long axis of the screw. Force (N) was recorded and plotted against displacement (mm).

Table 2 — *Pedicle screw design variables.*

Group Number	Major Diameter (Shape along length)	Minor Diameter (Shape along length)	Thread Form
1	Straight	Taper	Square
2	Straight	Taper	Buttress
3	Straight	Taper	Vee
4	Straight	Straight	Square
5	Straight	Straight	Buttress
6	Straight	Straight	Vee
7	Taper	Taper	Square
8	Taper	Taper	Buttress
9	Taper	Taper	Vee

Table 3 — *Mechanical Properties of Cancellous Bone and Structural Foam.*

Investigator	Material	Compressive Strength (Mean ± 1 SD), MPa	Compressive Modulus (Mean ± 1 SD), MPa
Carter [20]	Cancellous Bone	5.90 ± 0.72	54 ± 68
Lindah [21]	Cancellous Bone	4.60 ± 0.37	56 ± 7
Rohl [22]	Cancellous Bone	2.22 ± 0.64	489 ± 68
Rohlman [23]	Cancellous Bone	7.36 ± 0.54	389 ± 69
GMP*	Foam (0.160 g/cm ³ , 10 lb/ft ³)	1.67	43.8
GMP	Foam (0.192 g/cm ³ , 12 lb/ft ³)	2.51	65.2
GMP	Foam (0.240 g/cm ³ , 15 lb/ft ³)	3.39	102

*General Plastics Manufacturing Co., PO Box 9097, Tacoma, WA 98409

Statistical Analysis

The pull-out strength was determined for each screw design in all three substrates. Data were analyzed using an analysis of variance to establish differences between the several screw types. To isolate these differences between screw types, multiple comparison tests were made (Student-Newman-Keuls).

Literature Search

Cited incidences of pedicle screw pull-out in English-language journals were of interest. The National Library of Medicine was searched from 1980 to the present via MEDLINE. Search terms such as "pedicle screw loosening," "pedicle screw pull-out," and "pedicle screw failure," "screw breakage" were used. The MEDLINE database includes articles from over 4,000 biomedical journals for the biomedical sciences. The search was first conducted by the primary author (JMD) and then by an information retrieval service (NERAC, Inc. One Technology Drive, Tolland, CT).

Results

Pull-out Testing

Pull-out loads were greatest from the densest foam and for screws with vee-shaped threads (Figure). Screws with tapered major diameters exhibited lower pull-out loads compared to straight designs. The figure presents the pull-out loads (mean + 1 SD) of the various screw designs. Most differences were statistically significant (Table 4).

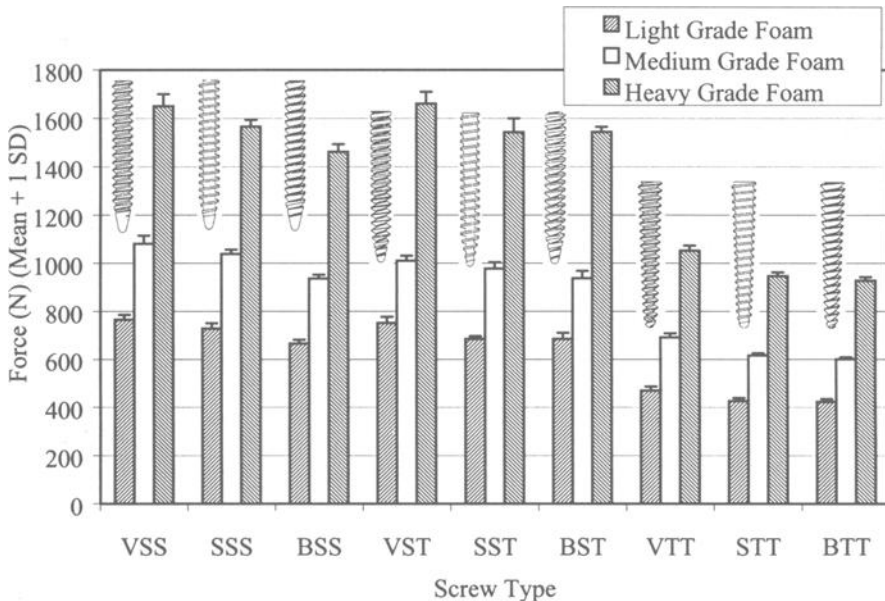


Figure. Loads required to pull-out different screw designs. VSS = Vee Straight Straight; SSS = Square Straight Straight; BSS = Buttress Straight Straight; VST = Vee Straight Taper; SST = Square Straight Taper; BST = Buttress Straight Taper; VTT = Vee Taper Taper; STT = Square Taper Taper; BTT = Buttress Taper Taper

Literature Search

The literature of the past twenty years yielded fifteen citations of screw loosening [23–37], sixteen citations of screw breakage [26-28, 31, 35, 36, 38–47], seven citations of hardware failure [27, 29, 38, 39, 49–50], and one citation of screw pull-out [48].

TABLE 4 — Statistically Insignificant (NS) Differences ($p > 0.05$)

Heavy Grade Foam (15 lb/cu. ft.):								
	BTT	STT	VTT	BST	SST	VST	BSS	SSS
VSS						NS		
SSS				NS	NS			
BSS								
VST								
SST				NS				
BST								
VTT								
STT	NS							
Medium Grade Foam (12 lb/cu. ft.):								
	BTT	STT	VTT	BST	SST	VST	BSS	SSS
VSS								
SSS								
BSS				NS				
VST								
SST								
BST								
VTT								
STT	NS							
Light Grade Foam (10 lb/cu. ft.):								
	BTT	STT	VTT	BST	SST	VST	BSS	SSS
VSS						NS		
SSS								
BSS				NS	NS			
VST								
SST				NS				
BST								
VTT								
STT	NS							
VSS = Vee Straight Straight; SSS = Square Straight Straight; BSS = Buttress Straight Straight; VST = Vee Straight Taper; SST = Square Straight Taper; BST = Buttress Straight Taper; VTT = Vee Taper Taper; STT = Square Taper Taper; BTT = Buttress Taper Taper								

Discussion

The pull-out loads measured in this study ranged from 1661N (vee-straight-taper, heavy grade foam) to 423N (buttress-taper-taper, light grade foam). These loads are comparable to those reported by others for foam. For instance, Thompson and Daftari reported average pull-out loads from foam of 1264N and 1134N, respectively [7,10]. These findings suggest that the test methodology is repeatable. Further, the pull-out loads measured in this study are also comparable to those reported by Berlemann, Wittenberg and Pfeiffer from human bone (1650N, 800N and 300N, respectively) [16, 17, 51]. Thus, the testing methodology, in particular the utilization of a foam substrate in lieu of human bone, yields realistic estimates of strengths for pull-out from cadaveric bone.

Within each grade of foam, the results for the taper/taper screws were always less than the results for straight/straight and straight/taper screws. Taper/taper screws did not engage the foam along their entire length. It may be surmised that the lower pull-out strengths for taper/taper screws reflect this fact. For taper/taper screws, however, the differences between thread form and the differences between foams were consistent with those observed for straight/straight and straight/taper screws. Specially-made drills matching the taper/taper geometry would overcome this limitation of the study, but these were not available.

Pull-out strength testing has been the subject of many published manuscripts and is specially treated in an ASTM standard. This study demonstrated that pull-out testing discriminates among designs. Extensive biomechanical testing is reported on the importance of variables such as hole preparation and bone cement augmentation. Screw loosening, screw breakage, and hardware failure are sometimes mentioned in clinical reports. Pull-out is but rarely documented as a failure mechanism. Unless pull-out is substantially under reported as a failure mechanism, *in vivo* pull-out failures seldom occur. The ASTM testing guideline for pull-out of pedicle screws is useful in comparing various designs but may have little relationship to *in vivo* performance. Clearly, the important mode of failure is loosening. The cited evidence suggests that pull-out is not the mechanism by which this failure occurs. Little effort has been devoted to investigating alternative testing methods, such as caudo-cephalad loading [52], that may have more clinical relevance.

Conclusions

The testing guideline for pull-out of pedicle screws is easily implemented and useful for comparing the strength of various designs. However, clinical reports that cite screw loosening rarely document pull-out as the failure mechanism. The testing guideline should not be considered a predictor of clinical performance.

References

- [1] Barber, J. W., Boden, S. D., Ganey, T., and Hutton, W. C., "Biomechanical study of lumbar pedicle screws: does convergence affect axial pullout strength?" *Journal of Spinal Disorders*, Vol. 11, No. 3, 1998, pp. 215–20.
- [2] Berzins, A., Shah, B., Weinans, H., and Sumner, D. R., "Nondestructive measurements of implant-bone interface shear modulus and effects of implant geometry in pull-out tests," *Journal of Biomedical Materials Research*, Vol. 34, No. 3, 1997, pp. 337–40.
- [3] Chapman, J. R., Harrington, R. M., Lee, K. M., Anderson, P. A., Tencer, A. F., and Kowalski, D., "Factors affecting the pullout strength of cancellous bone screws," *Journal of Biomechanical Engineering*, Vol. 118, No. 3, 1996, pp. 391–8.
- [4] McLain, R. F., Fry M. F., Moseley T. A., and Sharkey N. A., "Lumbar pedicle screw salvage: pullout testing of three different pedicle screw designs," *Journal of Spinal Disorders*, Vol. 8, No. 1, 1995, pp. 62–8.
- [5] Pfeiffer, M., Gilbertson, L. G., Goel, V. K., Griss, P., Keller, J. C., Ryken, T. C., and Hoffman, H. E., "Effect of specimen fixation method on pullout tests of pedicle screws," *Spine*, Vol. 21, No. 9, 1996, pp. 1037–44.
- [6] Sairyo, K., Scifert, J., Goel, V. K., Grosland, N., Grobler, L. J., "Neurocentral synchondrosis fracture in immature spines associated with pedicle screw type fixation devices," *Journal of Spinal Disorders*, Vol. 11, No. 2, 1998, pp. 142–5.
- [7] Thompson, J. D., Benjamin, J. B., and Szivek, J. A., "Pullout strengths of cannulated and noncannulated cancellous bone screws," *Clinical Orthopaedics and Related Research*, No. 341, 1997, pp. 241–9.
- [8] Tomkvist, H., Hearn, T. C., and Schatzker, J., "The strength of plate fixation in relation to the number and spacing of bone screws," *Journal of Orthopaedic Trauma*, Vol. 10, No. 3, 1996, pp. 204–8.
- [9] Zdeblick, T. A., Kunz, D. N., Cooke, M. E., and McCabe, R., "Pedicle screw pullout strength. Correlation with insertional torque," *Spine*, Vol. 18, No. 12, 1993, pp. 1673–6.
- [10] Daftari, T. K., Horton, W. C., and Hutton, W. C., "Correlations between screw hole preparation, torque of insertion, and pullout strength for spinal screws," *Journal of Spinal Disorders*, Vol. 7, No. 2, 1994, pp. 139–45.
- [11] George, D. C., Krag, M. H., Johnson, C. C., Van Hal, M. E., Haugh, L. D., and Grobler, L. J., "Hole preparation techniques for transpedicle screws. Effect on pull-out strength from human cadaveric vertebrae," *Spine*, Vol. 16, No. 2, 1991, pp. 181–4.
- [12] Oktenoglu B. T., Ferrara L. A., Andalkar N., Ozer A. F., Sarioglu A. C., and Benzel E. C., "Effects of hole preparation on screw pullout resistance and insertional torque: a biomechanical study," *Journal of Neurosurgery*, Vol. 94, No. 1 Suppl, 2001, pp. 91-6.
- [13] Ronderos, J. F., Jacobowitz, R., Sonntag, V. K., Crawford, N. R., and Dickman, C. A., "Comparative pull-out strength of tapped and untapped pilot holes for

- bicortical anterior cervical screws," *Spine*, Vol. 22, No. 2, 1997, pp. 167-70.
- [14] Lotz, J. C., Hu, S. S., Chiu, D. F., Yu, M., Colliou, O., and Poser, R. D., "Carbonated apatite cement augmentation of pedicle screw fixation in the lumbar spine," *Spine*, Vol. 22, No. 23, 1997, pp. 2716-23.
- [15] Moore, D. C., Maitra, R. S., Farjo, L. A., Graziano, G. P., and Goldstein, S. A., "Restoration of pedicle screw fixation with an in situ setting calcium phosphate cement," *Spine*, Vol. 22, No. 15, 1997, pp. 1696-705.
- [16] Pfeifer, B. A., Krag, M. H., and Johnson, C., "Repair of failed transpedicle screw fixation. A biomechanical study comparing polymethylmethacrylate, milled bone, and matchstick bone reconstruction," *Spine*, Vol. 19, No. 3, 1994, pp. 350-3.
- [17] Wittenberg, R. H., Lee, K. S., Shea, M., White, A. A. 3d, and Hayes, W. C., "Effect of screw diameter, insertion technique, and bone cement augmentation of pedicular screw fixation strength," *Clinical Orthopaedics and Related Research*, No. 296, 1993, pp. 278-87.
- [18] Yerby, S. A., Toh, E., and McLain, R. F., "Revision of failed pedicle screws using hydroxyapatite cement. A biomechanical analysis," *Spine*, Vol. 23, No. 15, 1998, pp. 1657-61.
- [19] Carter, D. R., and Hayes, W. C., "The compressive behavior of bone as a two-phase porous structure," *Journal of Bone and Joint Surgery [Am]*, Vol. 59, No. 7, 1977, pp. 954-62.
- [20] Lindahl, O., "Mechanical properties of dried defatted spongy bone," *Acta Orthopaedica Scandinavica*, Vol. 47, No. 1, 1976, pp. 11-9.
- [21] Rohl, L., Larsen, E., Linde, F., Odgaard, A., and Jorgensen, J., "Tensile and compressive properties of cancellous bone," *Journal of Biomechanics*, Vol. 24, No. 12, 1991, pp. 1143-9.
- [22] Rohlmann, A., Zilch, H., Bergmann, G., and Kolbel, R., "Material properties of femoral cancellous bone in axial loading. Part I: Time independent properties," *Archives of Orthopaedic Trauma Surgery*, Vol. 97, No. 2, 1980, pp. 95-102.
- [23] Bohnen, I. M., Schaafsma, J., and Tonino, A. J., "Results and complications after posterior lumbar spondylodesis with the 'Variable Screw Placement Spinal Fixation System,'" *Acta Orthopaedica Belgica*, Vol. 63, No. 2, 1997, pp. 67-73.
- [24] Ebraheim, N. A., Rupp, R. E., Savolaine, E. R., and Reinke, D., "Use of titanium implants in pedicular screw fixation," *Journal of Spinal Disorders*, Vol. 7, No. 6, 1994, pp. 478-86.
- [25] Faraj, A. A., and Webb, J. K., "Early complications of spinal pedicle screw," *European Spine Journal*, Vol. 6, No. 5, 1997, pp. 324-6.
- [26] Kumano, K., Hirabayashi, S., Ogawa, Y., and Aota, Y., "Pedicle screws and bone mineral density," *Spine*, Vol. 19, No. 10, 1994, pp. 1157-61.
- [27] McAfee, P. C., Weiland, D. J., and Carlow, J. J., "Survivorship analysis of pedicle spinal instrumentation," *Spine*, Vol. 16, No. 8 Supplement, 1991, pp. S422-7.
- [28] Niu, C. C., Chen, W. J., Chen, L. H., and Shih, C. H., "Reduction-fixation spinal system in spondylolisthesis," *American Journal of Orthopaedics*, Vol. 25, No. 6, 1996, pp. 418-24.
- [29] Ohlin, A., Karlsson, M., Duppe, H., Hasserijs, R., and Redlund-Johnell, I.,

- “Complications after transpedicular stabilization of the spine. A survivorship analysis of 163 cases,” *Spine*, Vol. 19, No. 24, 1994, pp. 2774–2779.
- [30] Okuyama, K., Abe, E., Suzuki, T., Tamura, Y., Chiba, M., and Sato, K., “Can insertional torque predict screw loosening and related failures? An in vivo study of pedicle screw fixation augmenting posterior lumbar interbody fusion,” *Spine*, Vol. 25, No. 7, 2000, pp. 858–64.
- [31] Okuyama, K., Abe, E., Suzuki, T., Tamura, Y., Chiba, M., and Sato, K., “Posterior lumbar interbody fusion: a retrospective study of complications after facet joint excision and pedicle screw fixation in 148 cases,” *Acta Orthopaedica Scandinavica*, Vol. 70, No. 4, 1999, pp. 329–34.
- [32] Razak, M., Mahmud, M. M., Hyzan, M. Y., and Omar, A., “Short segment posterior instrumentation, reduction and fusion of unstable thoracolumbar burst fractures--a review of 26 cases,” *Medical Journal of Malaysia*, Vol. 55 Suppl. C, 2000, pp. 9–13.
- [33] Sales de Gauzy, J., Vadier, F., and Cahuzac, JP., “Repair of lumbar spondylolysis using Morscher material: 14 children followed for 1-5 years,” *Acta Orthopaedica Scandinavica*, Vol. 71, No. 3, 2000, pp. 292–296.
- [34] Schildhauer, T. A., Josten, C., and Muhr, G., “Triangular osteosynthesis of vertically unstable sacrum fractures: a new concept allowing early weight-bearing,” *Journal of Orthopaedic Trauma*, Vol. 12, No. 5, 1998, pp. 307–14.
- [35] Soini, J., Laine, T., Pohjolainen, T., Hurri, H., and Alaranta, H., “Spondylodesis augmented by transpedicular fixation in the treatment of olisthetic and degenerative conditions of the lumbar spine,” *Clinical Orthopaedics and Related Research*, No. 297, 1993, pp. 111–6.
- [36] Thalgot, J. S., LaRocca, H., Aebi, M., Dwyer, A. P., and Razza, B. E., “Reconstruction of the lumbar spine using AO DCP plate internal fixation,” *Spine*, Vol. 14, No. 1, 1989, pp. 91–5.
- [37] Wimmer, C., and Gluch, H., “Aseptic loosening after CD instrumentation in the treatment of scoliosis: a report about eight cases,” *Journal of Spinal Disorders*, Vol. 11, No. 5, 1998, pp. 440–3.
- [38] Chen, W. J., Niu, C. C., Chen, L. H., and Shih, C. H., “Survivorship analysis of DKS instrumentation in the treatment of spondylolisthesis,” *Clinical Orthopaedics and Related Research*, No. 339, 1997, pp. 113–120.
- [39] Davne, S. H., and Myers, D. L., “Complications of lumbar spinal fusion with transpedicular instrumentation,” *Spine*, Vol. 17, No. 6, Suppl., 1992, pp. S184–S189.
- [40] Guyer, D. W., Wiltse, L. L., and Peek, R. D., “The Wiltse pedicle screw fixation system,” *Orthopedics*, Vol. 11, No. 10, 1988, pp. 1455–1460.
- [41] Lonstein, J. E., Denis, F., Perra, J. H., Pinto, M. R., Smith, M. D., and Winter, R. B., “Complications associated with pedicle screws,” *Journal of Bone and Joint Surgery [Am]*, Vol. 81, No. 11, 1999, pp. 1519–1528.
- [42] McLain, R. F., Kabins, M., and Weinstein, J. N., “VSP stabilization of lumbar neoplasms: technical considerations and complications,” *Journal of Spinal Disorders*, Vol. 4, No. 3, 1991, pp. 359–65.

- [43] Mac Millan, M. M., Cooper, R., and Haid, R., "Lumbar and lumbosacral fusions using Cotrel-Dubousset pedicle screws and rods," *Spine*, Vol. 19, No. 4, 1994, pp. 430-434.
- [44] Steffee, A. D., and Brantigan, J. W., "The variable screw placement spinal fixation system. Report of a prospective study of 250 patients enrolled in Food and Drug Administration clinical trials," *Spine*, Vol. 18, No. 9, 1993, pp. 1160-1172.
- [45] West, J. L. 3rd, Ogilvie, J. W., and Bradford, D. S., "Complications of the variable screw plate pedicle screw fixation," *Spine*, Vol. 16, No. 5, 1991, pp. 576-579.
- [46] Whitecloud, T. S. 3rd, Butler, J. C., Cohen, J. L., and Candelora, P. D., "Complications with the variable spinal plating system," *Spine*, Vol. 14, No. 4, 1989, pp. 472-476.
- [47] Zucherman, J., Hsu, K., White, A., and Wynne, G., "Early results of spinal fusion using variable spine plating system," *Spine*, Vol. 13, No. 5, 1988, pp. 570-579.
- [48] Lee, T. C., "Complications of transpedicular reduction and stabilization of the thoracolumbar spine," *Journal of the Formosan Medical Association*, Vol. 94, No. 12, 1995, pp. 738-41.
- [49] Wetzel, F. T., Brustein, M., Phillips, F. M., and Trott, S., "Hardware failure in an unconstrained lumbar pedicle screw system. A 2-year follow-up study," *Spine*, Vol. 24, No. 11, 1999, pp. 1138-43.
- [50] van Royen, B. J., de Kleuver, M., and Slot, G. H., "Polysegmental lumbar posterior wedge osteotomies for correction of kyphosis in ankylosing spondylitis," *European Spine Journal*, Vol. 7, No. 2, 1998, pp. 104-10.
- [51] Berlemann U., Cripton P., Nolte L. P., Lippuner K., and Schlapfer F., "New means in spinal pedicle hook fixation. A biomechanical evaluation," *European Spine Journal*, Vol. 4, No. 2., 1995, pp. 114-22.
- [52] Law, M., Tencer, A. F., and Anderson, P. A., "Caudo-cephalad loading of pedicle screws : mechanisms of loosening and methods of augmentation," *Spine*, Vol. 18, No. 16, 1993, pp. 2438-43.

Session III: Cages and Interbody Fusion Devices

Steven M. Theiss¹

Extrusion of Interbody Fusion Devices—Clinical Examples

Reference: Theiss, S. M., “Extrusion of Interbody Fusion Devices—Clinical Examples,” *Spinal Implants: Are We Evaluating Them Appropriately? ASTM STP 1431*, M. N. Melkerson, S. L. Griffith, and J. S. Kirkpatrick, Eds., ASTM International, West Conshohocken, PA, 2003.

Abstract: Extrusion of lumbar interbody fusion devices is a rare, though well-described, complication. Extrusion has been seen with a variety of interbody devices and surgical techniques. It is most commonly seen when implants are placed using a posterior approach. Extrusion results from instability of the final construct following implantation, or misplacement of the device. Instability can result from placement of an undersized implant or excessive resection of the facet joints. In each case, an error in surgical technique can be identified which leads to the extrusion. A design flaw of the implant is generally not the cause for the extrusion.

Keywords: interbody fusion, fusion cage, extrusion, lumbar, PLIF

Lumbar interbody fusions have been performed for many years, using a variety of techniques. Yet recently, these techniques have gained considerable popularity due to the widespread use of interbody fusion devices. These devices are popular because they avoid many of the common pitfalls of lumbar fusion. Specifically, these devices result in a lower pseudarthrosis rate, shorter hospitalization and less surgical morbidity compared with other techniques of lumbar interbody fusion [1]. Yet, as with any surgical implant, these devices are also associated with their own set of complications. Among these complications is cage extrusion or migration. Decidedly, this complication is rare. In a two-year prospective study of BAK implants, Kuslich et al. reported a migration rate of 2.7%, with only about one half of these implants requiring surgical revision [1]. Migration of cages, though, is not limited to any single device, and has not been attributed to any specific design flaw of the implant [2]. Because this complication is rare, much of what we have learned about the reasons for migration, and the strategies for revision, has been gleaned from small clinical series and case reports [2–5]. There are some common themes, though, that are evident. Implant migration or extrusion is most always a result of instability of the final construct. This review will summarize the existing knowledge as to the cause of migration, as well as give clinical examples of this complication.

¹Assistant Professor, Department of Surgery, Division of Orthopedic Surgery, University of Alabama at Birmingham, Birmingham, AL 35294.

One common reason for cage extrusion is inadequate tensioning of the secondary spine stabilizing structures. The immediate stability of interbody fusion cage constructs has been extensively studied. These studies have suggested that the stability of these implants, when inserted as stand alone devices either anteriorly or posteriorly, is comparable to other interbody fusion techniques consisting of bone graft and internal fixation [1,6]. However, the ultimate stability of stand alone fusion cages depends on the proper tensioning of the surrounding structures, particularly the disc annulus and the longitudinal ligaments [3]. In cases of cage extrusion, a common technical error is the inadequate tensioning of these secondary stabilizing structures, most commonly due to an undersized implant. This is seen mostly with posterior insertion. McAfee et al. reported on four patients who required cage removal after the cages migrated posteriorly into the spinal canal after posterior insertion. Not only did the undersized implant lead to ligamentous laxity and instability, but it also did not allow proper capture of the vertebral endplate by the treads of the implant [3]. Kuslich et al., in their 2-year follow-up of 947 patients in a multicenter prospective trial, cited initial instability due to an undersized implant as the primary cause for migration [1]. This concept is illustrated by the case of OC. OC is a 45 year old male who presented with mechanical low back pain, without radiation into his lower extremities. Radiographic studies showed two level degenerative disc disease at L4, L5 and L5, S1 with concordant discography. After failing prolonged nonoperative management, the patient underwent two level posterior lumbar interbody fusion (PLIF) at the symptomatic levels. Machined femoral allograft cages were used at each level, with a single implant placed at L4, L5. Despite using the largest implant available at L4,L5, the implant did not adequately distract the vertebral interspace. The patient had an unremarkable course immediately postoperatively. On his first postoperative visit, radiographs revealed extrusion of the implant at L4, L5 posteriorly into the spinal canal (Figures 1 and 2). The patient did relate a history of prolonged vomiting from narcotic analgesics shortly after discharge, associated with repeated forcible lumbar flexion. He began to complain of increased back pain shortly thereafter, but he did not have any neurologic symptoms as a result of the extrusion. The patient eventually required revision surgery. An error of surgical technique, rather than a design flaw of the implant, was responsible for this complication.

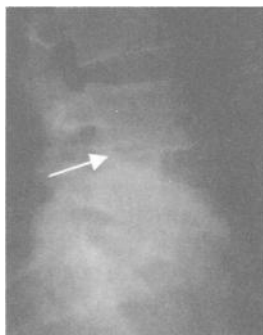


Figure 1



Figure 2

Figures 1 and 2—*The immediate postoperative lateral radiograph shows good placement of the interbody fusion device. At 2 weeks postoperatively, the implant at L4, L5 is extruded posteriorly. The arrow in each figure indicates the posterior edge of the implant.*

A second cause of cage extrusion is iatrogenic instability of the final construct from inappropriate resection of the posterior elements. Again, this complication is exclusively related to posterior insertion of the implants. Posterior insertion of interbody fusion devices often requires a wide laminectomy to avoid excessive retraction of the neural elements. Laminectomy with resection of greater than 50% of the facet joints, results in instability of the spinal motion segment [7]. Thus, in those instances when this is required for safe insertion of the fusion cages, stability of the construct depends on the stabilizing effects of the implants. Goh et al. studied the stability of bilateral cylindrical interbody implants following bilateral facetectomy. They found, after cage insertion, a significant reduction of stability in flexion compared with an intact motion segment prior to any intervention [8]. It is precisely this mode of instability that leads to posterior extrusion of the implant. Torsional stiffness was only restored with insertion of oversized cages, a scenario that would not be desirable clinically. This concept is illustrated by the case of WW who had single level degenerative changes and spinal stenosis at L4, L5 below a previous interbody fusion at L3, L4. She underwent a posterior decompression with a single level posterior interbody fusion using paired metallic fusion cages (Fig. 3). A bilateral facetectomy was performed to insert the cages. During the subsequent postoperative period, the patient developed a progressive deformity of the fusion level, with extrusion of an implant laterally, which resulted in compression of the adjacent nerve root (Fig. 4). This was eventually revised with posterior instrumentation to stabilize the instrumented interspace. Again, this mechanism of extrusion is directly attributable to a technical error of insertion, rather than a design flaw of the implant.

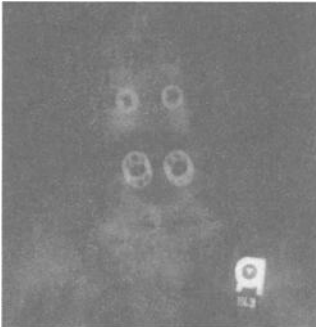


Figure 3

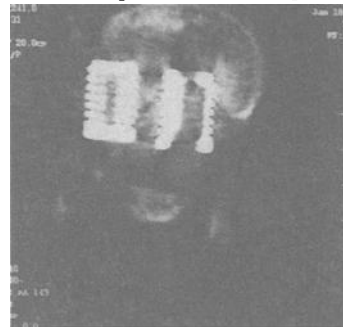


Figure 4

Figures 3, 4—*Immediate postoperative AP after implantation of two interbody fusion devices inserted at L4, L5 below a previous fusion. Note the bilateral facetectomy at this level in Figure 3. Early in the postoperative period, a cage extruded laterally into the neuroforamen, as shown on this CT myelogram.*

Finally, extrusion can result from misplacement of cages. This mode of extrusion is not limited to posterior insertion. In fact, it is the most common cause of migration after anterior insertion; either through an open or laparoscopic approach [3,9]. Misplacement usually results in cages inserted too far laterally to properly engage the vertebral bodies. A cage in an excessively lateral position is one with its center lateral to the medial border of the adjacent pedicle on an AP radiograph [3]. Extrusion then occurs in the lateral direction, due to an inadequate lateral bone bridge in the vertebral body to support the implant. Extrusion laterally can be associated with encroachment on the adjacent neuroforamen (Fig. 4). To avoid lateral placement, it is critical to locate the midline of the spine prior to insertion. If lateral extrusion occurs, it is usually necessary to remove the cage and decompress any compromised neurologic structures [3].

Extrusion of interbody fusion cages is a well-described, rare, clinical problem. However, a technical surgical error can be identified in virtually all cases. This consists either of malposition of the implant or instability of the interspace following implantation of the device. Instability can result from placement of an undersized implant that does not adequately capture the vertebral endplates or properly tension the soft tissue stabilizing structures. Excessive resection of the facet joints also results in instability that cannot be restored even with accurate placement of the fusion devices. Misplacement of the cages also causes extrusion by not adequately capturing the vertebral bodies. The reported cases of extrusion, the etiology and the treatment is summarized in Table 1. Extrusion, however, is not a result of a design flaw of the implant. Therefore, routine testing of interbody implants in a pushout or pullout mode does not seem relevant to described clinical scenarios. By adhering to strict surgical technique, extrusion of implants can almost always be avoided.

Authors	# of migrations	Time to migration	Etiology	Revision
Kuslich et al.	2.7%	0-3 months	misplaced, undersized	yes 1.2% no 2.5%
Uzi et al.	2	10d, 2 mo	facet resection	yes
McAfee et al.	5		misplaced undersized	yes
Elias et al.	2			yes
Glassman et al.	1	3 mo	undersized pseudo smooth implant	yes

Table 1

Table 1—*Reported cases of cage extrusion, the etiology of extrusion, as well as the treatment, are summarized*

References

- [1] Kuslich, S. D., Ulstrom, C. L., Griffith, S. L. et al., "The Bagby and Kuslich Method of Lumbar Interbody Fusion: History, Techniques, and 2-Year Follow-up Results of a United States Prospective, Multicenter Trial," *Spine* 1998, 23, pp. 1267–1278.
- [2] Uzi, E. A., Dabby, D., Tolessa, E., Finkelstein, J. A., "Early Retropulsion of Titanium-Threaded Cages After Posterior Lumbar Interbody Fusion: A Report of Two Cases," *Spine*, No. 26, 2001, pp. 1073–1075.
- [3] McAfee, P. C., Cunningham, B. W., Lee, G. A., et al., "Revision Strategies for Salvaging or Improving Failed Cylindrical Cages," *Spine*, Vol. 24, 1999, pp. 2147–2156.
- [4] Elias, W. J., Simmons, N. E., Kaptain, G. J., et al., "Complications of Posterior Lumbar Interbody Fusion When Using a Titanium Threaded Caged Device," *Journal of Neurosurgery*, Vol. 93, (1 Supplement), 2000, pp. 45–52.
- [5] Glassman, S. D., Johnson, J. R., Raque, G., et al., "Management of Iatrogenic Spinal Stenosis Complicating Placement of a Fusion Cage," *Spine*, 1996, Vol. 21, pp. 2383–2386.
- [6] Brodke, D. S., Dick, J. C., Kunz, D. N., et al., "Posterior Lumbar Interbody Fusion: A Biomechanical Comparison, Including a New Threaded Cage," *Spine*, No. 22, 1997, pp. 26–31.
- [7] Boden, S. D., Martin, C., Rudolph, R., et al., "Increase of Motion Between Lumbar Vertebrae after Excision of the Capsule and Cartilage of the Facet: A Cadaver Study," *Journal of Bone and Joint Surgery*, Vol. 76, 1994, pp. 1847–1853.
- [8] Goh, J. C. H., Wong, H., Thambyah, A., and Yu, C., "Influence of PLIF Cage Size on Lumbar Spine Stability" *Spine*, Vol. 25, 2000, pp. 35–40.
- [9] McAfee, P.C., "Interbody Fusion Cages in Reconstructive Operations on the Spine," *Journal of Bone and Joint Surgery*, Vol. 81-A, 1999, pp. 859–880.

Shannon S. Springer,¹ Sean F. Campbell,² Rodney L. Houfburg BS,³ Jennifer Pavlovic,⁴ and Adam Shinbrot⁵

“Is Push-out Testing of Cage Devices Worthwhile in Evaluating Clinical Performance?”

Reference: Springer, S. S., Campbell, S. F., Houfburg, R. L., Pavlovic, J., and Shinbrot, A., “**Is Push-out Testing of Cage Devices Worthwhile in Evaluating Clinical Performance?**” *Spinal Implants: Are We Evaluating Them Appropriately*, ASTM STP 1431, M. N. Melkerson, S. L. Griffith, and J. S. Kirkpatrick, Eds., ASTM International, West Conshohocken, PA, 2003.

Abstract: Interbody cages are successfully used clinically to support the spine’s anterior column to facilitate fusion of the motion segment. A standard, “Static Push-Out Test Method for Intervertebral Body Fusion Devices,” is under consideration by ASTM. The objective of this testing was to determine the loads required to extract interbody fusion cages from a simulated spinal motion segment (Grade 20 polyurethane foam model). The results obtained using the foam model were compared to results done using intact cadaver spinal motion segments (thoracic and lumbar). These data are contrasted with incidences of cage expulsion mentioned in the literature. Testing revealed a difference in the expulsion strength between the foam and cadaveric models. Differences between the 13 × 20 mm and the 9 × 20 mm cages were also found. The literature search revealed that anteriorly implanted cages may retropulse into the spinal canal due inadequate annular tension, undersized cages, and destabilization from laminectomy and partial facetectomy. The danger of retropulsion may be alleviated by the addition of posterior instrumentation (rods and screws). Standardized testing is a valuable tool in differentiating among designs but does not represent clinical failures.

Keywords: cage, pullout strength, push-out, expulsion, retropulsion, interbody fusion devices

Introduction

Interbody cages are successfully used clinically to support the spine’s anterior column to facilitate fusion of the motion segment. The mechanical performance of these intervertebral devices is important and differs among designs. Push-out testing may

¹ BME, Centerpulse Spine-Tech Inc., 7375 Bush Lake Rd., Minneapolis, MN 55439.

² BS, Centerpulse Spine-Tech Inc., 7375 Bush Lake Rd., Minneapolis, MN 55439.

³ BS, Centerpulse Spine-Tech Inc., 7375 Bush Lake Rd., Minneapolis, MN 55439.

⁴ PhD, Centerpulse Spine-Tech Inc., 7375 Bush Lake Rd., Minneapolis, MN 55439.

⁵ BS, Centerpulse Spine-Tech Inc., 7375 Bush Lake Rd., Minneapolis, MN 55439.

allow for an objective measure of cage purchase before bony ingrowth occurs. A standard, "Static Push-Out Test Method for Intervertebral Body Fusion Devices," is under consideration by the ASTM. The intent of this standard is "to allow for a consistent, repeatable comparison of different intervertebral body fusion device assemblies in this specific loading mode." [1] Described here are tests that meet this proposed standard.

The objective of this testing was to determine the loads required to extract interbody fusion cages from a simulated spinal motion segment (Grade 20 Polyurethane foam model). The results obtained using the foam model were compared to results done using intact cadaver spinal motion segments (thoracic and lumbar). These data are contrasted with incidences of cage expulsion mentioned in the literature.

Methods

Cadaveric Model

Fresh-frozen spines were separated into motion segments. Soft tissue was removed from the segments to enable secure potting in diestone material. The bone mineral densities (g/cm^2) of each vertebral body were measured in the anterior-posterior plane at all levels (T5-S1) using DEXA scan to ensure bone quality within the normal range. Six potted functional spinal units (FSU) were implanted with a single 13×20 mm BAK/L Interbody Fusion SystemTM (Centerpulse Spine-Tech, Inc.) cage per manufacturer instructions with the appropriate surgical instruments. The reconstructed FSUs were placed in a specially designed pullout test fixture that allowed an axial compressive force to be applied to the FSU. A calibrated helical spring was compressed between two free moving parallel plates. The parallel plates were positioned on top of the motion segment assembly. An axial compressive load of 956 N was applied and verified using an MTS 810 servo-hydraulic test frame. The actuator of the MTS was aligned perpendicularly to the face of the cage to ensure a pure axial tensile load to be applied. A threaded pullout fixture was inserted into the inner web of the cage and rotated 90 degrees to engage the cage. The cage was then pulled out with the MTS machine in load control at a loading rate of 4.5 N/sec to a maximum of 1779 N. Data from the load and displacement channels were collected.

Foam Model

Three sizes of cage (9×20 mm, 11×20 mm, and 13×20 mm) (Fig. 1) were implanted into Grade 20 polyurethane foam. Grade 20 foam was used to simulate dense cancellous bone. The foam was machined into blocks that fit into a specially designed pre-load fixture (Fig. 2). The fixture allowed a 445 N pre-load to be applied to the cage via a calibrated spring. A single BAK/L cage (Centerpulse SpineTech, Inc.) of each size was implanted a total of six times in the foam blocks (Fig. 4) using the manufacturers standard surgical instructions with the appropriate surgical instruments. The BAK/L cages were reused after no damage was noted upon visual inspection. A threaded push-out fixture (Fig. 3) was used to apply an axial force to the face of the cage. An MTS 858 Mini Bionix was used to perform the test in displacement control at a rate of 5 mm/min to

a maximum displacement of 10 mm. Data from the load and displacement channels were collected.

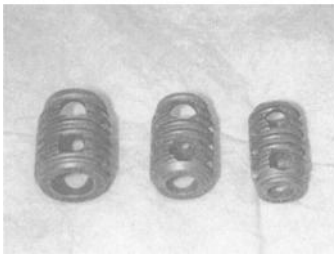


Figure 1 - BAK/L cages – 13 mm, 11 mm, 9 mm

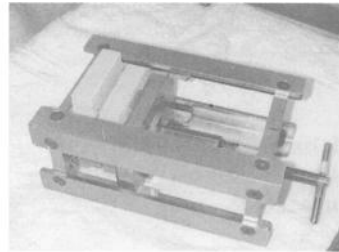


Figure 2 - Pre-load fixture

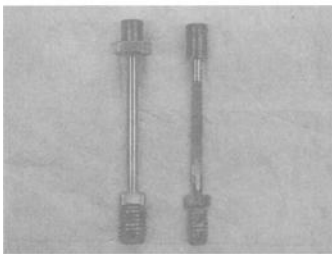


Figure 3 - Push-out Fixtures with BAK/L cages.

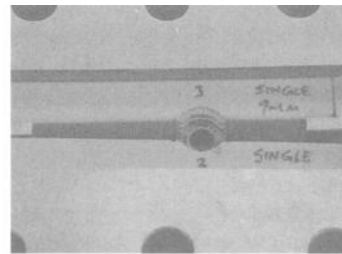


Figure 4 - Implanted 9mm BAK/L cage.

Statistics

The expulsion load (pullout in the cadaveric model and push-out in the foam model) was determined in each model. Data comparing the 13 × 20 mm cage implanted in the cadaveric model vs. foam model was analyzed using a student's t-test. An analysis of variance was used to establish the difference, if any, among the 9 × 20 mm, 11 × 20 mm and the 13 × 20 mm cages implanted in the foam model. A sample size of six was used, which is considered adequate according to guidelines set forth by ASTM.

Results

The DEXA scans showed bone densities that were representative of the normal range (Table 1).

The 13 × 20 mm cage implanted in the foam had greater mean expulsion strength than the same size cage implanted in the cadaver FSUs. There was a slight statistical difference between the two models ($p = 0.018$). Figure 5 presents the expulsion strengths (mean ± 1 SD). The table presents the normalized mean expulsion strengths (mean ± 1 SD) for both models.

Table 1 - Bone Mineral Densities

Spine Number	Level	Bone Density (g/cm ²)
1	L4-L5	1.171-1.132
4	L2-L3	1.184-1.309
3	T11-T12	1.040-0.933
1	T8-T9	1.063-0.996
4	T6-T7	1.024-1.064

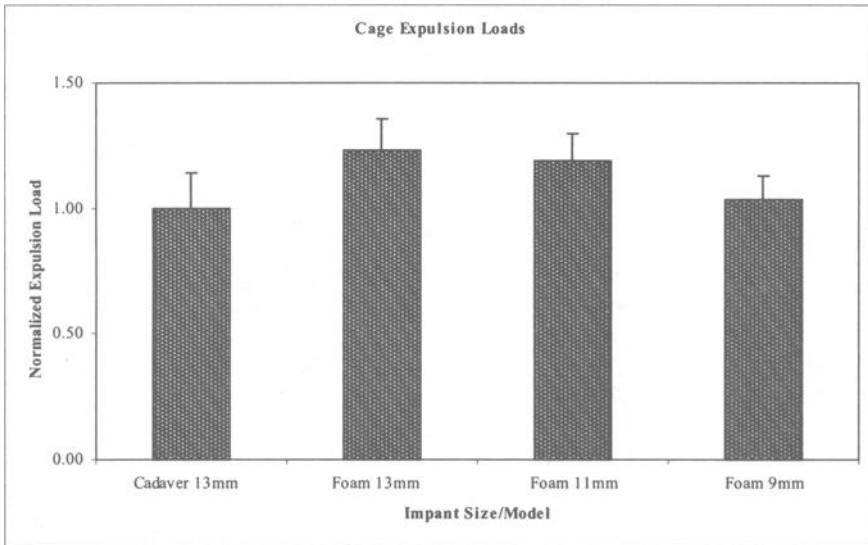


Figure 5 - Cage Expulsion Loads – Normalized loads ± 1 SD

Table 2 - Normalized Means and Standard Deviation for Expulsion Loads

	Cadaver 13x20mm	Foam 13x20mm	Foam 11x20mm	Foam 9x20mm
Mean	1.00	1.23	1.19	1.03
Standard Deviation	0.14	0.13	0.11	0.10

In the foam model there was no statistical difference between the 13 × 20 mm and 11 × 20 mm comparison and the 11 × 20 mm and 9 × 20 mm comparison. A statistical difference was found between the 9 × 20 mm and 13 × 20 mm cages. An example of an expelled cage is shown below (Fig. 6).

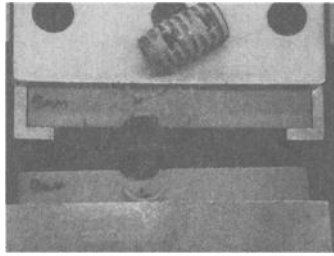


Figure 6 - *Expulsed cage*

Discussion

This study has shown that use of the ASTM draft F-04.25.02.02 for testing the expulsion loads of interbody fusion devices allows differences to be detected among device designs. The test method laid out in the standard has several differences from implantation done in a clinical setting due to the controlled environment in which the testing takes place. The standard allows for ideal placement in a bone substrate that is uniform in consistency with a consistent known pre-load. In a clinical setting surgeons have none of these advantages. The standard also allows an axial force to be applied perpendicularly to the face of the cage to initiate the expulsion. In a clinical setting many factors contribute to the expulsion or migration of a cage from its original orientation. The technique in the draft does not mimic the mechanisms responsible for cage expulsions in the clinical setting.

The foam model portion of this study was done in displacement control as recommended in the ASTM draft F-04.25.02.02. The cadaveric portion of this study, which was done before the ASTM draft was written, was tested in load control. The pre-load fixture and machined foam blocks used in this study were also developed before the ASTM draft was written. The 10 mm displacement limit was used as a safety factor to ensure that the peak expulsion loads would be measured. All of the peak loads occurred within the first 3 mm, the displacement limit stated in the draft standard. These variations from the standard do not take away from the conclusion stated above, that the draft standard allows differences to be detected among device designs.

It has also shown that by following the guidelines of the proposed standard a foam model may be used as a reasonable facsimile for expulsion testing in cadaveric FSU. The difference seen between the cadaver and foam models may be due to the difference in the actual bone density of the spinal FSUs and the higher density (grade 20) foam used. Polyurethane foam is readily available in many grades (densities). The use of grade 15 polyurethane foam may improve the correlation between the foam model and the cadaveric model.

There are few reported instances of cage expulsion of posteriorly implanted cages from the disc space in a clinical setting. Cage expulsion is described secondary to destabilization of the motion segment following laminectomy and partial facetectomy [2]. McAfee suggests other factors contributing to the retropulsion of cages are failure to achieve adequate distraction of the annulus fibrosis, using undersized cages and improper placement. Inadequately sized cages coupled with insufficient annular tension allow the cage to migrate into the spinal canal with flexion-extension movement [2–3]. McAfee also proposes cages placed too far laterally may break through the lateral annulus fibrosis and impinge the nerve root [3]. Eshkenazi and Dietl suggest the destabilization of the

motion segment may be overcome by adding posterior instrumentation to increase the stiffness in axial compression [2,5].

Push-out loads do not represent clinical failures but do give an objective measure of cage purchase before bony ingrowth occurs. The retropulsion of cages in a clinical setting is often due "to technical error at the time of placement [4]." Proper annular distraction, a correctly sized cage, and posterior instrumentation alleviate the danger of cages migrating into the spinal canal [3].

References

- [1] ASTM International, "Static Push-Out Test Method for Intervertebral Body Fusion Devices," F-04.25.02.02, ASTM International, West Conshohocken, PA.
- [2] Eshkenazi A. Uzi, Dabby, D., Tolessa, E., Finkelstein, J. A., "Early Retropulsion of Titanium-Threaded Cages After Posterior Lumbar Interbody Fusion: A Report of Two Cases," *Spine*, Vol. 26, No. 9, May, 2001, pp. 1073–1075.
- [3] McAfee, P. C., Cunningham, B. C., Lee, G. A., Orbegoso C. M., Haggerty, C. J., Fedder, I. L., Griffith, S. G., "Revision Strategies for Salvaging or Improving Failed Cylindrical Cages," *Spine*, Vol. 24, No. 20, 1999, pp. 2147–2153.
- [4] Theiss, S. T., "Extrusion of Lumbar Interbody Fusion Cages: Clinical Examples," ASTM Symposium on Spinal Implants: Are We Evaluating Them Appropriately? Dallas, Texas, November, 2001.
- [5] Dietl, R. H.-J., Krammer, M., Kettler, A., Wilke, H.-J., Lutz, C., Lumenta, C. B., "Pullout Test With Three Lumbar Interbody Fusion Cages," *Spine*, Vol. 27, No. 10, May, 2002, pp. 1029–1036.

John M. Dawson¹ and Steven L. Griffith²

A Comparison of Two Strength-Testing Methodologies for Interbody Structural Allografts for Spinal Fusion

Reference: Dawson, J. M. and Griffith, S. L., “A Comparison of Two Strength-Testing Methodologies for Interbody Structural Allografts for Spinal Fusion,” *Spinal Implants: Are We Evaluating Them Appropriately? ASTM STP 1431*, M. N. Melkerson, S. L. Griffith, and J. S. Kirkpatrick, Eds., ASTM International, West Conshohocken, PA, 2003.

Abstract: To maintain an intervertebral disc space during fusion, a structural allograft, typically utilizing dense cortical bone, must sustain functional loads. Difficulty with surgical placement of structural allografts has resulted in reports of intraoperative graft fracture but no data have been generated to quantify insertional loads. In this study, simulated intraoperative and immediate postoperative strengths of allograft femoral rings were quantified. Three types of processed allograft were used: Tutoplast[®] processed bone, frozen-thawed and freeze-dried. To replicate postoperative *in vivo* functional loading, axial compressive strengths were evaluated by crushing femoral rings between flat platens under displacement control. To replicate surgical placement into an intervertebral space, samples were oriented so that the ring would be loaded transversely and an “insertion” displacement was imposed at 1m/sec. In axial compression, all three allograft types sustained loads far greater than estimated *in vivo* spinal loads. In insertion loading, all allograft types yielded substantially smaller strengths. Because intraoperative insertional loads are unknown and subjective to individual surgeon technique, the adequacy or inadequacy of any group is unclear. Testing guidelines should be developed upon both anticipated *in vivo* loading and intraoperative demands.

Keywords: orthopaedic medical devices – bone, allograft, compressive strength, strength testing

Background

Allograft bone is used routinely in many spinal fusion procedures. There are several methods with many steps for processing allograft bone used in the industry today, including freezing, freeze-drying, or Tutoplast[®] processing (Tutogen Medical, Inc.). The Tutoplast process destroys and removes cells but preserves the collagen and mineral

¹ Director, Spine Biomechanics Research, Centerpulse SpineTech Division, 7375 Bush Lake Road, Minneapolis, MN 55439

² Vice President, Scientific Affairs, Centerpulse SpineTech Division, 7375 Bush Lake Road, Minneapolis, MN 55439

components. The tissue is chemically unchanged during its treatment, which includes delipidization, osmotic treatment (washing), oxidation treatment with hydrogen peroxide, alkaline treatment with sodium hydroxide, and dehydration with organic solvents.

The biomechanical fitness of an allograft is of paramount importance. Some investigators have found that the biomechanical properties of allografts are minimally affected by freezing. In contrast, freeze-drying diminishes some mechanical characteristics [1]. Freeze-thaw injury is thought to be due to mechanical disruption by the growth of ice crystals [2]. Regardless of the process used to prepare the allograft, it must be able to sustain functional loads during and after biologic incorporation. Though a graft may fail due to biologic factors, frequently mechanical failure is manifest [3]. Biomechanical performance is dictated by the mechanical properties of the graft, the interfaces between the graft and host bone, and the load environment. Biomechanical properties include the graft's material properties (elastic modulus, strength, and fatigue resistance) and geometry.

Not well understood is the axial compressive strength required after implantation. Summarizing the findings of others, White [4] reported the axial compressive strengths of lumbar vertebral bodies to be $6113\text{N} \pm 1425\text{N}$ (range, 4971N to 8572N). Hochschuler [5] cited strengths from 2400N to 6500N. Nachemson [6] reported compression loads during various activities at the L3 disc for various postures, including supine (300N), standing (700N), walking (850N), jumping (1100N), and lifting (2100 to 3400N). Hochschuler [5] reported compressive strengths of 55,000N to 63,000N for femur ring allografts. During incorporation, cortical bone allografts will decrease in mass and increase in porosity. These changes manifest in decreases in mechanical strength of 50% in the first year; the physical properties and strength return to normal after about two years but a donor graft is never fully remodeled [7]. These data suggest that the compressive strength of a lumbar femoral-ring allograft, at implantation, is at least six times greater than the strength of the adjacent vertebral bodies and at least sixteen times greater than the loads it may experience. If the graft strength is diminished by a factor of two during incorporation, its strength will still exceed vertebral body strength and lumbar loads by factors of 3 and 8, respectively.

A femoral ring graft must be able to withstand the forces applied to it during its implantation as well as during its service *in situ*. The strength required for implantation is not known. In the present study, graft strength was appraised in two ways. Insertion loading of a femoral ring was done to assess the strength of the graft during insertion. Axial loading of a femoral ring was done to determine the ultimate axial compressive strength of the graft during functional loading.

Methods

Sample Treatment

Allograft samples were obtained from tissue banks accredited by the American Association of Tissue Banks. All samples were weighed and photographed prior to testing. Geometric dimensions (maximum outer diameter, minimum wall thickness, and

axial thickness) were measured with electronic calipers and recorded. The axial thickness of all grafts was approximately 10mm. The geometry of a graft is important because it may be accepted or rejected for patient use based on its size and perceived strength. Samples were individually soaked in tap water with added salt (for a minimum of 0.9% NaCl by weight) for at least one hour prior to testing. Tutoplast specimens of femoral shaft were from different lots (representing different donors). Frozen-thawed and freeze-dried samples were not traceable and lot histories (expiration dates, for example) were unknown.

Insertion Testing

To replicate the implantation of a graft by tapping into an intervertebral disc space, samples were supported on the fixed platen of an MTS 858 Bionix so that the allograft ring would be loaded transversely (Figure 1). A compressive displacement of 2 mm was imposed at a rate of 40 mm/sec. This rate was selected to simulate impact loading. The actuator of the load frame contacted the samples with a round bone tamp with a diamond-textured face or a custom bifurcated bone tamp with a smooth surface (Figure 1). Tutoplast specimens were tested with both types of bone tamps (six samples for both), but freeze-dried and frozen-thawed samples were tested with the round bone tamp only (five and six samples, respectively). No particular anatomic orientation was maintained during insertion testing. Instead, each specimen was placed so that its maximum outer diameter was perpendicular to the direction of loading. This reflects its orientation during surgery. Actuator displacement and reactive force were recorded at 0.264 msec intervals (the minimum time interval possible with the data acquisition apparatus). Failure load, which was defined as the maximum observed load, was recorded for each specimen. The failure load was based upon the raw data (time, displacement, force output from the test machine) and not derived from a regression analysis of the data.

Axial Compressive Testing

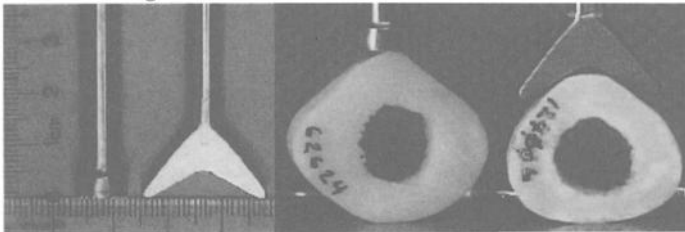


Figure 1 - Round (left) and bifurcated (right) bone tamps used as loading fixtures and the manner of loading the allograft samples

To measure the axial compressive strength of the femoral ring allografts, a compressive axial displacement of 5 mm was imposed at a rate of 3 mm/min. Samples were simply supported between two flat, smooth platens (Fig. 2) with the diameter of the allograft ring parallel to the platen. Actuator displacement and reactive force were

recorded at 0.010 second intervals.

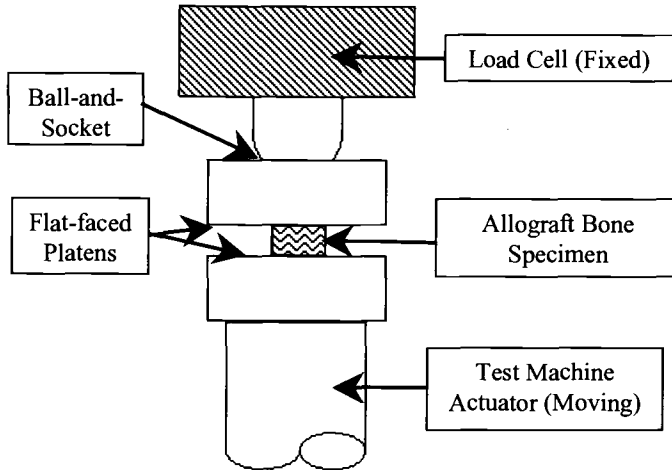


Figure 2 - Schematic representation of axial compression testing setup

Data Analysis

For both insertion and axial compression tests, an analysis of variance was performed to investigate differences in weight, wall thickness, and failure load among the allograft types. To isolate differences between allograft types, paired comparisons were then made.

Results

Allograft Insertion Tests

The characteristics of the allograft samples used for insertion testing and the results of testing are presented in Table 1. The groups appeared the same with regard to weight and were not statistically different ($p > 0.05$). The freeze-dried mean minimum wall thickness was significantly greater than that of either Tutoplast group ($p = 0.01$); the wall thickness of the frozen-thawed group was not different than that of the freeze-dried or the Tutoplast groups; the wall thicknesses of the Tutoplast groups were not different.

The failure load was estimated from a minimum of 35 data points (freeze-dried sample #1) to a maximum of 57 data points (frozen-thawed sample #2) because the failure load always occurred before the maximum compressive displacement (2mm) was achieved. Failure load of the frozen-thawed group was significantly different ($p < 0.001$) than the others. Tutoplast and freeze-dried samples behaved similar to each other. For all groups, the samples typically failed by radial cracking. Usually, it was observed that a specimen broke at the point of support on the fixed platen. Also common was a break

under the point of contact of the fixture. The locations of cracks at the right and left lateral aspects varied. No relationship between minimum wall thickness and insertion failure load could be found. There appears to be no advantage to using a bifurcated tamp in lieu of a round one because the mean failure load of that group was the smallest (but not statistically different from the Tutoplast samples tested with the round tamp).

Table 1 - *Insertion Sample Characteristics and Strengths (Mean ± 1 SD)*

Graft Type	N	Loading Fixture	Failure Load, N	Minimum Wall Thickness, mm	**Weight, g
Tutoplast	6	Round	205 ± 99	5.84 ± 0.44	9.6 ± 0.7
Tutoplast	6	Bifurcated	184 ± 55	5.62 ± 0.83	8.9 ± 0.6
Freeze-dried	5	Round	208 ± 24	6.94 ± 0.66	9.5 ± 0.7
Frozen-thawed	6	Round	891 ± 190	6.33 ± 0.50	8.8 ± 0.6

*Weight prior to re-hydration.

Allograft Axial Compression Testing

The characteristics of the allograft samples used for axial compression testing and the results of testing are presented in Table 2. The samples differed significantly in size with the frozen-thawed samples being largest in cross-section and the freeze-dried samples being smallest. The frozen-thawed samples exhibited the greatest failure loads and the freeze-dried samples exhibited the least. To eliminate differences in strength solely due to differences in size, the failure load was normalized by the cross-sectional area for each specimen. The cross-sectional area (mm²) was approximated by: Cross-Sectional Area = π t (D - t); where t = minimum wall thickness (mm) and D = maximum outer diameter (mm). When load/area was compared among the three groups, the frozen-thawed group was significantly strongest (p<0.003). There was no difference between the Tutoplast and freeze-dried groups. The frozen-thawed samples typically crushed at the superior and inferior faces; the Tutoplast and freeze-dried samples typically fractured throughout the specimen thickness.

Table 2 - *Axial Compression Sample Characteristics and Strengths (Mean ± 1 SD)*

Graft Type	N	Failure Load, N	Cross-Sectional Area, mm ²	Failure Load ÷ Area, MPa	* Weight, g
Tutoplast	5	57,867 ± 10387	424 ± 65	137 ± 16	5.3 ± 0.3
Freeze-dried	6	48,999 ± 4,025	279 ± 47	149 ± 4.9	8.5 ± 0.4
Frozen-thawed	6	73,659 ± 4,532	494 ± 36	178 ± 17	8.8 ± 1.5

* Weight prior to re-hydration.

Discussion

Allograft Insertion Testing

The data acquisition rate was less than optimal and is a limitation of this study. However, the test was able to discriminate between graft types and the test was adequately repeatable (as demonstrated by reasonable standard deviation of the results). Tutoplast and freeze-dried samples demonstrated equivalent strengths. Frozen-thawed samples were stronger. However, because required intraoperative insertion forces are unknown, it is not possible to determine if one or more groups are adequately - or inadequately - strong in insertion loading. A limitation of this study was that the allograft rings were supported by a rigid platen. In practice, these grafts would be inserted between two vertebral bodies. With increasing insertion depth, the vertebral bodies would offer increasing resistance. The magnitudes of the forces acting against a graft during insertion and their points of contact are highly variable based on surgical technique. Data describing the clinical modes of failure are presently unavailable. Grafts broken intraoperatively (including notes on any distractive techniques used) should be saved for later analysis. This critical clinical information is needed to correlate the *in vitro* tests with actual failures before developing a corresponding guide.

Allograft Axial Compression Testing

The axial compressive strengths reported here (48,999 to 73,659N) compare favorably with the maximum compressive failure loads for fresh femoral ring grafts (55,000 to 63,000N) reported by Hochschuler [3]. As they and others have noted, the axial compressive strength of vertebral bodies is in the range of 2400N to 6500N. It may be concluded that the Tutoplast, frozen-thawed, and freeze-dried groups all possess adequate initial compressive strength despite their apparent differences. Furthermore, considering the biological remodeling that is anticipated as the graft incorporates, all of the allografts tested should be able to sustain the anticipated loads seen *in situ* in the spine.

Conclusion

In axial compression, all three allograft types sustained loads far greater than estimated *in vivo* spinal loads. In insertion loading, frozen-thawed samples were stronger than Tutoplast and freeze-dried samples, which were equivalent. Because intraoperative insertional loads are unknown, the adequacy or inadequacy of any group remains unclear. Testing guidelines should be developed upon both anticipated *in vivo* loading and intraoperative demands.

References

- [1] Pelker R. R., and Friedlaender, G. E., "Biomechanical aspects of bone autografts

- and allografts," *Orthopaedic Clinics of North America*, Vol. 18, No. 2, 1987, pp. 235–239.
- [2] Malinin, T. I., "Acquisition and Banking of Bone Allografts," *Bone Grafts and Bone Substitutes*, M. B. Habal and A. H. Reddi, Eds., W. B. Saunders Company, Philadelphia, PA, 1992.
- [3] Davy, D. T., "Biomechanical issues in bone transplantation," *Orthopaedic Clinics of North America*, Vol. 30, No. 4, 1999, pp. 553–563.
- [4] White, A. A., and Panjabi, M. M., "Physical properties and functional biomechanics of the spine," *Clinical Biomechanics of the Spine, Second Edition*, JB Lippincott Company, Philadelphia, PA, 1990.
- [5] Hochschuler, S. H., Griffith, S. L., Weinhoffer, S. L., and Friedrich, T. E., "Compressive strengths of hollow, allograft bone cylinders proposed for lumbar interbody fusion," *Proceedings of the Annual Meeting of the North American Spine Society*, San Diego, CA, 1993.
- [6] Nachemson, A., "The load on lumbar disks in different positions of the body," *Clinical Orthopaedics and Related Research*, No. 45, 1996, pp. 107–122.
- [7] Kalfas I. H., "Structural Bone Graft Materials: Autograft, Allograft, and Synthetics," *Symposium on Anterior Column Support: Implications in Cervical and Thoracolumbar Spine Surgery*, Nassau, Bahamas, 1996.

Session IV: Functional Spinal Devices and/or Artificial Disks

Gerd Huber,^{1,2,3} Berend Linke,¹ Michael M. Morlock,³ and Keita Ito¹

The Influence of *In Vitro* Testing Method on Measured Intervertebral Disc Characteristics

Reference: Huber, G., Linke, B., Morlock, M. M., and Ito, K., “The Influence of *In Vitro* Testing Method on Measured Intervertebral Disc Characteristics,” *Spinal Implants: Are We Evaluating Them Appropriately*, ASTM STP 1431, M. N. Melkerson, S. L. Griffith, and J. S. Kirkpatrick, Eds., ASTM International, West Conshohocken, PA, 2003.

Abstract: Time-dependent behavior of functional spinal units, especially the anterior column, may interact with experimental methods when measuring their mechanical properties. Since they are tested using different load cycles, the comparison of results is difficult. The goal of this study was to determine the response of anterior column spinal units (body-disc-body units) to load cycles varying in waveform and cycle duration using an experimentally based mathematical model.

Specimen specific transfer function models were formulated for seven ovine lumbar anterior column units by fitting high order exponential functions to axial stress-relaxation measurements. Using axial load cycles with different waveforms and cycle durations, nine simulations in the time domain with each transfer function model were performed. For each simulation, the neutral zone, peak to peak, and hysteresis were evaluated.

The neutral zone and hysteresis were significantly dependent on the waveform of the load cycle. The differences of peak to peak for sinusoidal and triangular waveforms were low. All these characteristics were significantly dependent on the cycle duration. For example, comparison of 1 s to 20 s cycle durations exhibited neutral zone and hysteresis differences of 61–69% and 100%, respectively. Consequently, loading protocols should be chosen carefully and should be clearly reported.

Keywords: intervertebral disc, *in vitro* testing, neutral zone, peak to peak, hysteresis area, stress relaxation, dynamic model

Introduction

Cyclic *in vitro* mechanical measurements of functional spinal units (FSUs) are performed to estimate mechanical properties of natural passive spinal structures in order to improve general understanding of their biomechanical performance and function. Furthermore, the comparison of implant performance to each other and to the intact and/or injured condition are performed by *in vitro* measurements as well.

¹ AO Research Institute, Clavadelerstrasse, 7270 Davos, Switzerland.

² TUHH, Mechanic Section, Schwarzenbergstrasse 95, 21073 Hamburg, Germany.

³ TUHH, Biomechanics Section, Denickestrasse 15, 21073 Hamburg, Germany.

For this purpose, various specialized testing apparatuses with different loading protocols adapted to particular investigations have been developed [1–5]. Although most cyclic measurements are performed between predefined load limits, other parameters are not as consistent, e.g. waveform and frequencies. Of the various waveforms, sinusoidal force control loading is generally considered to be the most physiological. Although smooth load cycles with only a single characteristic frequency is applied, the control algorithm is demanding. On the other hand, actuators with constant velocities, e.g., stepper motors, combined with force triggers are more practical. Control algorithms are easier to realize, stable, and well suited for measurement of specimens with distinct nonlinear stiffnesses. However, with these devices, a smooth waveform is not possible, and as the actuator changes velocities at the trigger points, either triangular or trapezoidal waveforms are applied (Fig. 1). Another often varied parameter in mechanical *in vitro* measurements is cycle duration. This is perhaps due to the lack of distinct natural loading frequencies of the spine *in vivo* and limited actuator capacity.

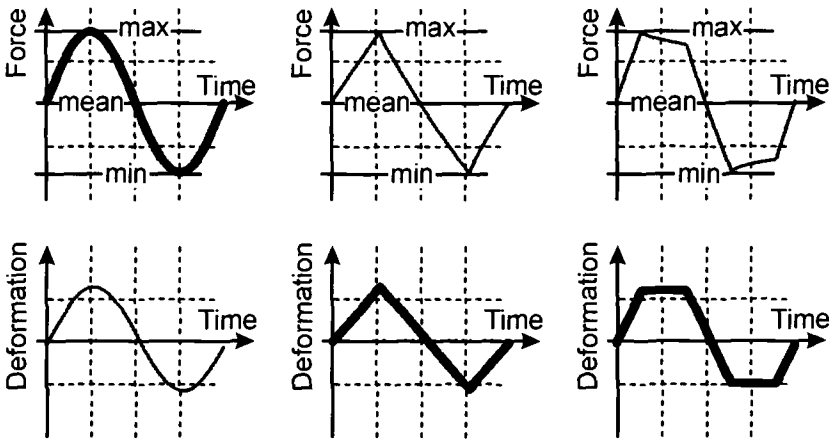


FIG. 1 — Loading cycle waveforms. The bold line waveforms indicate the actual control algorithm, i.e., force controlled or displacement controlled with force trigger, and the normal line waveforms represent the corresponding response of the specimen.

In addition to load application methods, the dynamics of the system to be tested must be considered. FSUs, especially their anterior column, consist of poroelastic and viscoelastic structures. Consequently, their time-dependent behavior may interact with experimental methods when measuring its mechanical properties. The extent of these interactions for load cycles, varying in waveforms and cycle duration, should be investigated. However, influence of the time-dependent behavior on measurement method is difficult to evaluate due to variability of specimens. Furthermore, if the same specimen is used to test different load cycles in series, specimen degeneration is difficult to prevent with the extended test procedures resulting from long repeated cycle durations and intermittent specimen recovery. Whereas, test processing with different load cycles on

different specimens is strongly influenced by inter-specimen variation and immense numbers of specimens are required.

Aim of the Study

Aim of the study was to determine the response of anterior column units (vertebral body-disc-vertebral body unit) to load cycles varying in waveform and cycle duration using an experimentally based mathematical model.

Materials and Methods

To minimize the influence of intra- and inter-specimen variability, first a mathematical model for each specimen was developed based on a mechanical relaxation test. Then these models were numerically simulated to calculate the response of each disc to load cycles, varying in waveform and cycle duration.

Experimental

Seven fresh frozen ovine lumbar FSUs from 5 different Swiss alpine sheep (female, virgin, mature) were used for the investigation. After dissection, the specimens were wrapped with moistened (Ringer's solution) gauze, sealed in double plastic bags and stored at -22°C . Eight hours before testing they were ambiently thawed to room temperature, and all muscles and posterior elements, including facet joints and posterior column ligaments, were removed prior to testing. The anterior and posterior longitudinal ligaments were kept intact. Both vertebrae of each anterior column unit were potted into trued up metal holders using non-surgical grade polymethylmethacrylate (BERACRYL, Troller, Fulenbach, Switzerland). During preparation, potting and measurement the specimens were kept moist (Ringer's solution) and whenever possible wrapped in gauze and cling wrap.

Axial stress-relaxation measurements (Fig. 2) for each specimen were done using a universal testing frame (BIONIX 858, MTS, Eden Prairie, MN). The pots were rigidly attached to the testing frame, constraining all other degrees-of-freedom except axial displacement. The internal force and displacement transducers and the corresponding software for actuator control and data acquisition (TestStar II and TestWare SX, MTS, Eden Prairie, MN) were used.

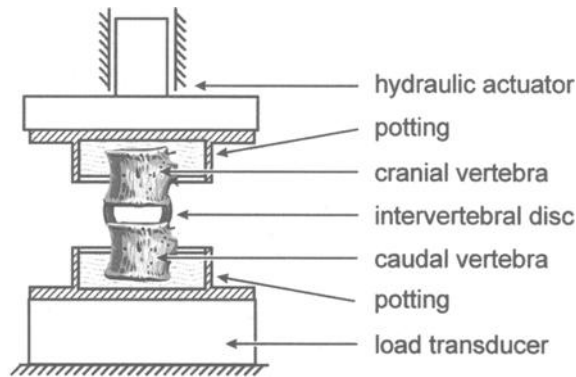


FIG. 2 — Sketch of the experimental setup for axial stress-relaxation measurements.

The displacement step for the stress-relaxation was 0.5 mm for all specimens. Pilot measurements exhibited that this magnitude of step led to peak forces of about 900 N, which is equal to 1.5 times sheep body weight. This is assumed to be a reasonable load, as *in vivo* studies with baboons and humans [6–8] have showed similar load-bodyweight relations to occur during normal activities and are sufficiently below causing irreversible damage to the specimen.

Prior to testing the specimens were allowed to reach a load-free equilibrium for 2700 s. Then, the 0.5 mm displacement step was applied. In practice an ideal displacement step cannot be applied, but the hydraulic actuator was able to reach the plateau within 50 ms without overshoot. The displacement was kept constant for 3600 s. Data were acquired at 100 Hz, 60 s prior to and 60 s after the step and at 2 Hz for the remainder of the measurement duration. Since the force gradient at the beginning of the relaxation curve is high, an internal 5 kHz peak detector was used to identify the peak force as well as its temporal position.

Numerical

The generic mathematical disc model is equal to an extensive serial and parallel arrangement of linear springs and linear dampers (Kelvin models in series). The stress relaxation behavior of these n dampers and $n+1$ springs can be described by the given series expansion of exponential terms (Eq 1).

$$F(t) = a_0 + \sum_{i=1}^n a_i \cdot e^{-\frac{t}{\tau_i}} \quad (1)$$

This exponential equation expresses the relaxation force (F) dependent on time (t), quasi-static end value (a_0), amplification parameters (a_i), and time constants (τ_i). To determine the model parameters specific for each specimen, this exponential equation was curve fit to the relaxation measurement of that specimen. Since no unique number of material properties exists to describe the behavior of the disc [9], the number (n) of sensible

parameters was also part of a least square optimization. For this optimization, an extensive number ($n = 1000$) of logarithmic spaced time constants between 100 ms and 20 h were pre-assigned. Furthermore, the relaxation measurements were re-sampled to a logarithmic scaled time axes with 3000 time steps (m). This led to time increments between 10 ms at the beginning of the relaxation curve and a time increment of 8 s at the end. This new time scale and pre-assigned time constants enabled the separation of the exponential terms and the amplification parameters (Eq 2).

$$\begin{pmatrix} F(0) \\ F(t_1) \\ \dots \\ F(t_m) \end{pmatrix} = \begin{bmatrix} 1 & 1 & 1 \\ 1 & e^{-\frac{t_1}{\tau_1}} & e^{-\frac{t_1}{\tau_n}} \\ \dots & \dots & \dots \\ 1 & e^{-\frac{t_m}{\tau_1}} & e^{-\frac{t_m}{\tau_n}} \end{bmatrix} \cdot \begin{pmatrix} a_0 \\ a_1 \\ \dots \\ a_n \end{pmatrix} \tag{2}$$

To calculate the parameters a_i a least square optimization algorithm (MATLAB™, MathWorks, Natick, MA) was used to solve the linear equations (Eq 2) with the constraint that $a_i \geq 0$. Then these parameters were used to formulate a transfer function model (G, Eq. 3) for each disc representing its dynamic behavior. The transfer function corresponds to the “Laplace-transformed” relaxation function divided by the “Laplace-transformed” 0.5 mm step input [10].

$$G = \frac{1}{0.5} \cdot \left(a_0 + \sum_{i=1}^n \frac{a_i \cdot s \cdot \tau_i}{s \cdot \tau_i + 1} \right) \tag{3}$$

Using these transfer function models, representing the specific behavior of each disc, dynamic simulations were performed. A sinusoidal force controlled loading cycle (SINE) and two displacement controlled loading cycles driven by constant velocities combined with force triggers were simulated with each model. The latter was represented by a triangular (TRI) and a trapezoidal (TRAP) displacement loading with 50 % standstill time at the force trigger-point. Consequently, the three waveforms had different strain rates, singularities (i.e. force trigger actions), and hold periods while maintaining similar maximum force amplitude and cycle duration.

Because of the indirect control method of the two latter waveforms, only time-domain analyses could be performed. Time domain simulations (SIMULINK™, MathWorks, Natick, MA) for three discrete cycle durations with each load protocol (nine simulations per specimen) were done. The shortest cycle duration was $T = 1$ s, which represents the typical cyclic loading due to walking. $T = 20$ s was also examined as it is in the range often used for cyclic *in vitro* measurements [11–15]. The slowest cycle duration of $T = 400$ s was used as it is near to the time needed if loads are increased in three or four steps with 30 s in-between relaxation periods [16–18].

For the simulations of the different waveforms and durations, loading protocols with identical minimum and maximum load limits were used. For the sinusoidal load cycles this corresponds to the magnitude of the oscillation (mean compression plus/minus amplitude of sinusoidal waveform) while for the triangular and trapezoidal load cycles this corresponds to the force trigger (causing abrupt changes in displacement rates). To

avoid tension of the specimen, the uncompressed equilibrium state was chosen as one limit and a compression of 900 N as the other. The maximum compression was identical to the average peak force used in the relaxation measurements (1.5 times sheep body weight, Fig. 4).

To compare the variant hysteresis loops caused by the different waveforms and cycle durations [19] of each specimen, three characteristics were calculated from each simulation (Fig. 3). These were the neutral zone (NZ), peak to peak (PP) and the hysteresis (HYS). The NZ was defined as the difference between the unloading phase and the loading phase at mean force (mean between both limits). This characteristic was adapted from the common definitions used for specimen bending [20]. PP was the motility of the specimen due to the load amplitudes and HYS was the area in-between one load-displacement loop. To diminish the influence of transient response, the characteristics were calculated from the third simulated load cycle, as also recommended for *in vitro* measurements [20].

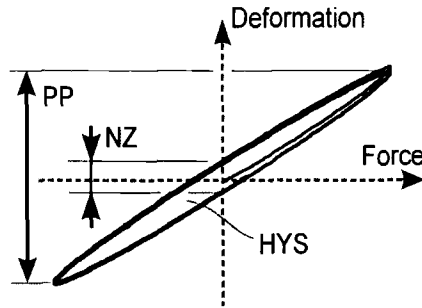


FIG. 3 — Characteristics determined for each loading simulation.

To adjust for inter-specimen variability, each characteristic was normalized by the mean of that characteristic for the nine simulations (3 waveforms \times 3 durations) of that specimen. The used transfer function model is linear. Thus displacement and force changes are proportional. Consequently, PP and NZ are proportional to the span between the load limits and HYS is proportional to square of this span. Thus, all simulation results were independent of the mean force and the normalized data were independent of the span between force limits. Hence the normalized mean group values and the intra-group variance per waveform and cycle duration were independent of the load amplitude used.

Statistical Analyses

Two multivariate analyses of variance (MANOVA) with linear models were performed for each of the three characteristics. Both raw data and normalized data were analyzed to compare the effect of inter-specimen variability to waveform and duration effects. The influence of cycle duration, waveform, and their interaction were examined. For pair wise comparison within one cycle duration or within one waveform, the Tukey-HSD post-hoc test was used. A significance level of $p < 0.05$ was used to reject the null hypothesis. Significant difference of characteristics as result of different waveforms are

shown in the bar charts of the mean values (Figs. 5–7). The significance levels for the comparison of cycle durations are shown in tables (Table 1–3).

Results

Creep Tests and Individual Disc Models

In general, ovine spinal specimens are quite uniform due to the similar age, weight, size, and living conditions of the sheep from which the specimens are harvested. However, as anticipated, inter-specimen variability in stress relaxation behavior was observed (Fig. 4). The greatest variability was observed in the peak reaction force, and there was also some smaller variability in the relaxation time constant. By identifying individual parameters out of the relaxation measurements and building specimen specific models, this variability was carried over to the simulation results.

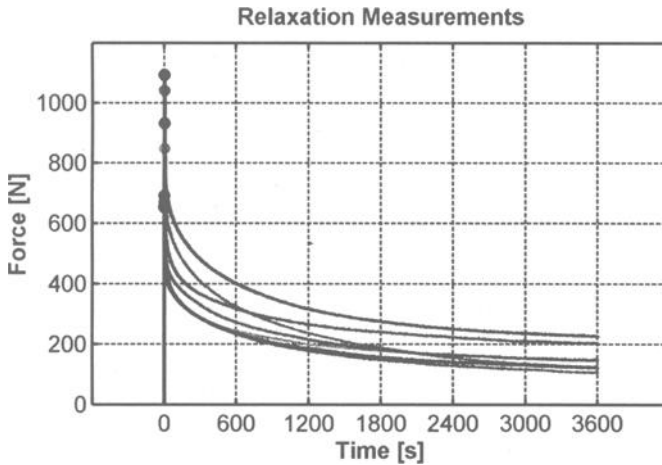


FIG. 4 — *Measured relaxation curves of the seven specimens.*

During each model development, most of the 1000 possible parameters a_i obtained by the optimization process were zero, and the corresponding time constants were not processed further. Overall, the specimen specific model development resulted in parameter sets of 8 to 11 parameters, a_i , and their corresponding time constants. Non-structural models as those identified in this study are not necessarily unique. Thus, it is not possible to compare the parameters of the different models directly. However, it is possible to compare the output of each model to the relaxation data used to develop that model (Table 1). The maximum difference between any measurement and its corresponding model simulation averaged 2.8% (range 1.4–3.8%). The mean difference (root mean square of the differences) over the entire relaxation period average 0.5%. These differences were much smaller than the differences observed between characteristics from the different loading protocols (see below).

TABLE 1 — Comparison of stress relaxation behavior for each single disc between measured specimens and its analytical model.

	Unit	Number of Specimen						
		1	2	3	4	5	6	7
Highest difference	N	4.0	4.2	6.6	5.0	7.9	5.2	4.2
Mean difference	N	1.0	1.0	1.1	1.0	1.2	1.1	1.0
Highest difference	%	3.0	2.7	3.5	3.8	3.0	2.5	1.4
Mean difference	%	0.5	0.5	0.5	0.6	0.5	0.4	0.3

Peak to Peak

In general, lower PP was observed with shorter cycle durations (Fig. 5). For all waveforms, the increase of cycle duration from T = 1 s to T = 20 s and from T = 20 s to T = 400 s lead to 21–28 % higher PP than the faster cyclic loading (shorter cycle duration). For the raw data, only the PP differences between T = 400 s and T = 1 s were significant for all waveforms, whereas for normalized PP, each cycle duration for all waveforms were significantly different (Table 1). Measurements with trapezoidal load cycles lead to lower PP than measurements with sinusoidal or triangular load cycles. This influence was more distinct for long cycle durations. For the evaluated range, statistically significant differences were 8% for T = 20 s and 14% for T = 400 s.

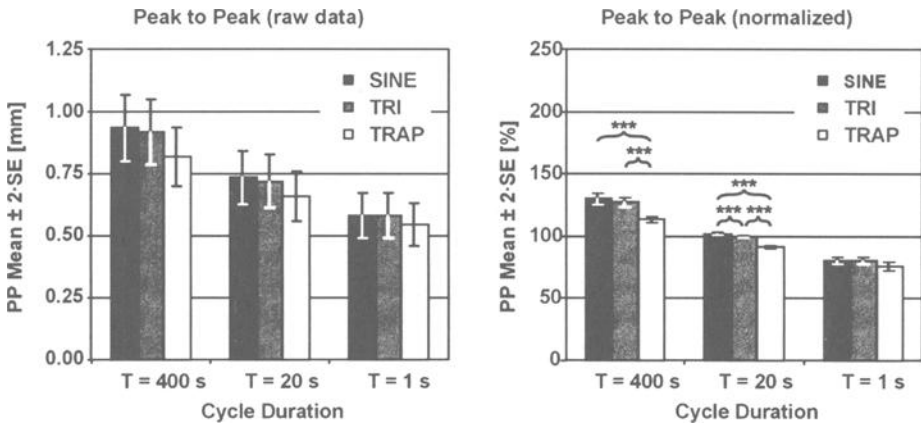


FIG. 5 — Averaged raw and normalized PP (plus/minus two standard errors), n=7 for all durations and waveforms - (* p < 0.05, ** p < 0.01, *** p < 0.001).

Table 2 — Comparison of influence of cycle duration for PP (raw and normalized data).

PP ^a	400 s versus 20 s		400 s versus 1 s		20 s versus 1 s	
	raw data	normalized	raw data	normalized	raw data	normalized
SINE	n.s.	***	***	***	n.s.	***
TRI	*	***	***	***	n.s.	***
TRAP	n.s.	***	**	***	n.s.	***

^a n.s. not significant, * p < 0.05, ** p < 0.01, *** p < 0.001

Neutral Zone

For the NZ, the differences were more distinct. Cycle durations of 20 s compared to 1 s increased the NZ by 91–100 % and cycle durations of 400 s compared to 20 s lead to 61–69% higher values (Fig. 6). This effect was not only significant for the normalized values, but also for the raw data (Table 2). Thus, even the high inter-specimen variability, as seen in the figure of the relaxation measurements (Fig. 3) had a lower influence on measured NZ, than those due to different waveforms. The NZ resulting from triangular waveforms especially differed from those of the other waveforms. Differences of over 30 % were observed. Again, these differences were only statistically significant for normalized data.

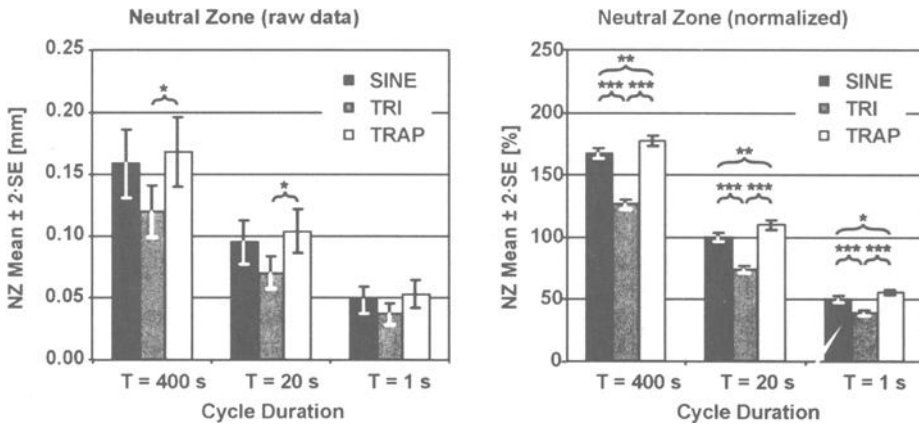


FIG. 6 — Averaged raw and normalized NZ (plus/minus two standard errors), n=7 for all durations and waveforms (* p < 0.05, ** p < 0.01, *** p < 0.001)

Table 3 — Comparison of influence of cycle duration for NZ (raw and normalized data).

NZ ^a	400 s versus 20 s		400 s versus 1 s		20 s versus 1 s	
	raw data	normalized	raw data	normalized	raw data	normalized
SINE	***	***	***	***	**	***
TRI	***	***	***	***	*	***
TRAP	***	***	***	***	**	***

^a n.s. not significant, * $p < 0.05$, ** $p < 0.01$, *** $p < 0.001$

Hysteresis Area

Since the findings for PP and NZ were homogeneous, as expected, the differences were more pronounced when examining HYS (Fig. 7), because the enclosed area of one cycle is roughly proportional to PP and to NZ. The influence of the cycle duration was significant for raw and normalized HYS (Table 3). In terms of waveform, the differences between triangular and the other two waveforms for $T = 20$ s and $T = 400$ s were statistically significant.

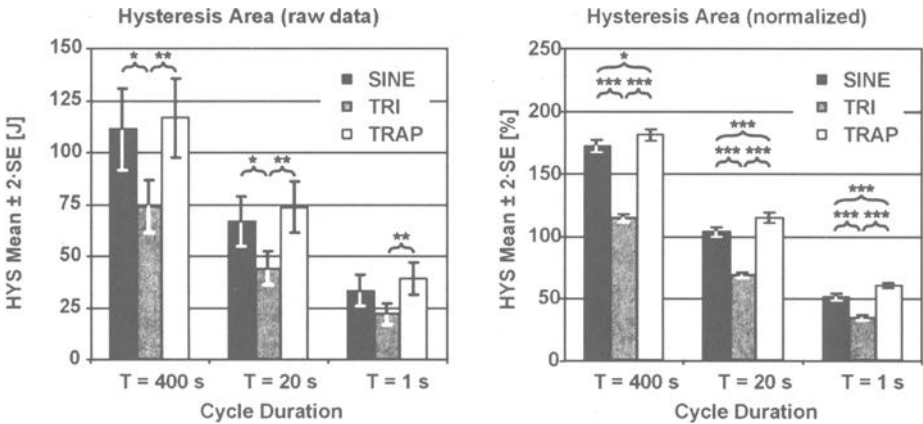


Figure 7 — Averaged raw and normalized HYS (plus/minus two standard errors), $n = 7$ for all durations and waveforms (* $p < 0.05$, ** $p < 0.01$, *** $p < 0.001$)

Table 4 — Comparison of influence of cycle duration for HYS (raw and normalized data).

HYS ^a	400 s versus 20 s		400 s versus 1 s		20 s versus 1 s	
	raw data	normalized	raw data	normalized	raw data	normalized
SINE	***	***	***	***	**	***
TRI	***	***	***	***	**	***
TRAP	***	***	***	***	**	***

^a n.s. not significant, * p < 0.05, ** p < 0.01, *** p < 0.001

Discussion and Conclusions

In general, for all of the investigated parameters, the variability between specimens was found to be greater than the differences resulting from waveform. Nevertheless, once normalized for inter-specimen variability, NZ and HYS showed consistent significant differences between waveforms. In contrast, the influence of specimen variability on NZ and HYS was less than that of cycle duration and for all waveforms, NZ and HYS were significantly affected by cycle duration. The effect of waveform and duration on PP was mixed. PP was occasionally influenced by waveform and cycle duration, but the differences caused by different waveforms were small and that due to cycle duration were not as distinct as for the other characteristics investigated. Hence, if PP is the main outcome variable of interest, comparisons between different loading protocols may be valid.

A unique experimental-mathematical technique was used to avoid inter-specimen variability, but this was not without certain limitations. In non-structural models, description of the transfer function is not necessarily unique. There may be other sets of parameters or other equations fitting the measured data in a similar manner. Therefore, extrapolation of the measurements by simulating load patterns longer than 3600 s or in the opposite direction simulating high frequencies, e.g., in the range of the sample frequency, may be unwise. In addition, only a linear uniaxial theory was used in this investigation, and the effects from non-linearities in stiffness are not simulated. However, to minimize such inaccuracies, the maximum loads in the simulation were chosen to be similar to the measured peak loads, such the linearization was local to the latter. If necessary, the model may be easily expanded for non-linearities in stiffness, but relaxation measurements with different step amplitudes must than be carried out to identify the model parameters. This was not done as with larger steps, progressive stiffening of the disc was expected and such a model would have led to even more distinct differences in characteristics.

In addition to load magnitude, load/motion directions can also vary in the disc. Bending motions (e.g., flexion-extension) are more common for *in vitro* measurements than axial compression. Nevertheless, it is reasonable to assume that the experimentally determined time dependency of the intervertebral disc (due to viscoelasticity of the annulus and poroelasticity of the nucleus) is not altered greatly by load direction. Hence,

similar results for other directions are expected, and to verify this assumption, *in vitro* tests in multiple directions should be conducted.

With respect to specimens, this study used only the anterior column of ovine FSUs. Ovine specimens were used because of their availability and uniformity (e.g., body weight, age, no natural history of spinal degeneration, etc.). Although inter-species transfer of knowledge is of concern, transfers of qualitative knowledge or phenomena to human spines is often generally accepted. Moreover, this investigation was based on relaxation measurements using the intervertebral disc rather than the entire FSU with posterior elements. For entire FSUs, posterior elements are expected to decrease the evaluated influences as they are stiffer and less time-dependent in their properties. Similarly, FSUs with fixation implants will further decrease these effects, but if comparison to intact FSUs from another study are used, these findings should be taken into account.

In summary, a substantial influence, of *in vitro* loading method on resulting measured characteristics of anterior column units, was demonstrated. Thus, results should either only be directly compared for similar loading protocols or these differences should be taken into consideration. Inferences of *in vitro* results to *in vivo* situation should also consider differences in loading. Furthermore, the dependency of the examined characteristics on different load cycles exhibits the dynamic behavior of anterior column units. Consequently, for *in vitro* FSU investigation, within the analyzed range of cycle durations, the general assumption of quasi-static cyclic measurements is difficult to justify. Therefore, *in vitro* loading protocols should be chosen carefully and cycle durations and waveforms used should be clearly reported.

References

- [1] Adams, M. A. and Dolan, P., "A Technique for Quantifying the Bending Moment Acting on the Lumbar Spine *in vivo*," *Journal of Biomechanics*, Vol. 24, No. 2, 1991, pp. 117–125.
- [2] Wilke, H.-J., Claes, L., Schmitt, H. and Wolf, S., "A Universal Spine Tester for *in vitro* Experiments with Muscle Force Simulation," *European Spine Journal*, Vol. 3, 1994, pp. 91–97.
- [3] Crawford, N. R., Brantley, A. G. U., Dickman, C. A. and Koeneman, E. J., "An Apparatus for Applying Pure Nonconstraining Moments to Spine Segments *In Vitro*," *Spine*, Vol. 20, No. 19, 1995, pp. 2097–2100.
- [4] Linke, B., Sellenschloh, K., Huber, G., Schneider, E., Weltin, U., "A New Method of Pre-clinical Spine Implant Testing in Six Degrees of Freedom—Based on the Hexapod Principle," *Journal of Biomechanics*, Vol. 31, (S1), 1998, p. 41
- [5] Schreiber, U., Bence, T., Bader, R., Beisse, R., Grupp, T., Mittelmeier, W. and Steinhäuser, E., "Validation of a Newly Developed Experimental Setup for Segmental Spinal Testing," *Journal of Biomechanics*, Vol. 34 (S1), No. 19, 2001, pp. 65–66.
- [6] Nachemson, A., "The Load on Lumbar Disks in Different Positions of the Body," *Clinical Orthopaedics*, Vol. 45, 1966, pp. 107–122.

- [7] Ledet, E., Gatto, C., McVoy, J., Brunski, J., Donzelli, P., Sachs, B., "Real-Time *In Vivo* Loading in the Baboon Lumbar Spine Using an Interbody Implant Load Cell," *Proceeding of the 46th Annual Meeting, Orthopaedic Research Society*, 2000, p. 384.
- [8] Wilke, H.-J., Neef, P., Hinz, B., Seidel, H., Claes, L., "Intradiscal Pressure Together with Anthropometric Data—A Data Set for the Validation of Models," *Clinical Biomechanics*, Vol. 16 (S1), 2001, pp. S111–S126.
- [9] Burns, M. L. and Kaleps, I., "Analysis of Load-Deflection Behavior of Intervertebral Disc under Axial Compression Using Exact Parametric Solutions of Kelvin-Solid Models," *Journal of Biomechanics*, Vol. 13, 1980, pp. 959–996.
- [10] Fliege, N., "Systemtheorie," Teubner, Stuttgart, 1991.
- [11] Coe, J. D., Warden, K. E., Sutterlin, C. E., McAfee, P. C., "Biomechanical Evaluation of Cervical Spinal Stabilization Methods in a Human Cadaveric Model," *Spine*, Vol. 14, No. 10, 1989, pp. 1122–1131.
- [12] Shea, M., Edwards, W. T., Colothiaux, P. L., Crowell, R. R., Nachemson, A. L., White III, A. A. and Hayes, W. C., "Three-dimensional Load Displacement Properties of Posterior Lumbar Fixation," *Journal of Orthopaedic Trauma*, Vol. 5, No. 4, 1991, pp. 420–427.
- [13] Zdeblick, T. A., Warden, K. E., Zou, D., McAfee, P. C., and Abitbol, J. J., "Anterior Spinal Fixators – A Biomechanical *In Vitro* Study," *Spine*, Vol., 18, No. 4, 1993, pp. 513–517.
- [14] Richman J. D., Daniel T. E., Anderson, D. D., Miller, P. L. and Douglas, R. A., "Biomechanical Evaluation of Cervical Spine Stabilization Methods Using a Porcine Model," *Spine*, Vol. 20, No. 20, 1995, pp. 2192–2197.
- [15] Wilke, H.-J., Kettler, A., Claes, L. E., "Are Sheep Spines a Valid Biomechanical Model for Human Spines?," *Spine*, Vol., 22, No. 20, 1997, pp. 2365–2374.
- [16] Clausen, J. D., Ryken, T. C., Traynelis, V. C., Sawin, P. D., Dexter, F. and Goel, V. K., "Biomechanical Evaluation of Caspar and Cervical Spine Locking Plate System in a Cadaveric Model," *Journal of Neurosurgery*, Vol. 84, 1996, pp. 1039–1045.
- [17] Rathonyi, G. C., Oxland, T. R., Gerich, U., Grassmann, S., Nolte, L.-P., "The Role of Supplemental Translaminar Screws in Anterior Lumbar Interbody Fixation: A Biomechanical Study," *European Spine Journal*, Vol. 7, 1998, pp. 400–407.
- [18] Cripton, P. A., Bruehlmann, S. B., Orr, T. E., Oxland, T. R. and Nolte, L.-P., "*In vitro* Axial Preload Application during Spine Flexibility Testing: Towards Reduced Apparatus-Related Artifacts," *Journal of Biomechanics*, Vol. 33, 2000, pp. 1559–1568.
- [19] Huber, G., Ito, K., Linke, B., Schneider, E., Morlock, M., "The Influence of Intervertebral Disc Time-dependent Properties on *in-vitro* Testing," *Journal of Biomechanics*, Vol. 34 (S1), 2001, pp. S13–S14.
- [20] Wilke, H.-J., Wenger, K. and Claes, L., "Testing Criteria for Spinal Implants—Recommendations for the Standardization of *in vitro* Stability Testing of Spinal Implants," *European Spine Journal*, Vol. 7, No. 2, 1998, pp. 148–154.

David B. Spenciner¹, P.E., James A. Paiva¹, and Joseph J. Crisco, Ph.D.²

Testing of Human Cadaveric Functional Spinal Units to the ASTM Draft Standard, “Standard Test Methods for Static and Dynamic Characterization of Spinal Artificial Discs.”

Reference: Spenciner, D.B., Paiva, J.A., and Crisco, J.J., “Testing of Human Cadaveric Functional Spinal Units to the ASTM Draft Standard, ‘Standard Test Methods for Static and Dynamic Characterization of Spinal Artificial Discs,’” *Spinal Implants: Are We Evaluating Them Appropriately*, ASTM STP 1431, M.N. Melkerson, S L. Griffith, and J.S. Kirkpatrick, Eds., ASTM International, West Conshohocken, PA, 2003

Abstract:

The development of replacement intervertebral discs has recently received significant attention in the new product arena. Presently, ASTM International is considering a standard for the evaluation of artificial discs. The purpose of this study was to evaluate human functional spinal units (FSUs) and intervertebral discs using the methods and equipment in the proposed standard and then to compare the results with existing literature.

FSUs and intervertebral discs were tested in axial rotation, anterior and posterior compressive shear, and axial compression. The stiffness values of the intervertebral discs were $1.8 \pm 1.1 \text{ N} \cdot \text{m}^\circ$ in axial rotation, $368.2 \pm 98.6 \text{ N/mm}$ in anterior compressive shear, $483.5 \pm 62.9 \text{ N/mm}$ in posterior compressive shear, and $1287.5 \pm 271.3 \text{ N/mm}$ in axial compression. These results are reasonable in comparison with the existing literature but there are notable differences. We conclude that the mechanical properties of the intervertebral disc are not sufficiently defined and further testing is warranted.

Keywords:

biomechanics, lumbar spine, intervertebral disc, mechanical properties

¹ Test Facility Manager and Project Leader, respectively, RIH Orthopaedic Foundation, Inc., 1 Hoppin Street, Coro West Suite 404, Providence RI 02903.

² Associate Professor, Department of Orthopedics and Division of Engineering, Brown Medical School / Rhode Island Hospital and Brown University, 1 Hoppin Street, Coro West Suite 404, Providence RI 02903.

Introduction:

On October 19, 1934, as part of the orthopedic section of the American College of Surgeons annual meeting, Robert Joplin, M.D. stated, "In attempting to analyze the etiological factors which make up the clinical orthopedic problem of this day and age, the spine plays a major role."^[1] This observation remains true today as back pain has the highest prevalence of any joint pain across all age groups and races^[2]. Although in 1995, spine arthroplasty accounted for less than 1% of all arthroplasty procedures^[3], interest in spinal artificial discs has increased substantially, as evidenced by the rapid growth in new product development. Concurrently, an ASTM subcommittee was created to discuss appropriate test methodology. At the present time, there is no universally accepted test methodology for evaluating these devices.

At the ASTM subcommittee level, orthopedic engineers and clinicians have labored to create a standardized test methodology for evaluating spinal artificial discs. The current draft (Revision F), "... is intended to provide a basis for the mechanical comparison among past, present, and future non-biologic intervertebral artificial discs." This draft is based on the recently approved ASTM standard F 2077-00, "Test Methods for Intervertebral Body Fusion Devices" and employs virtually identical test methods and equipment. In fact, the ASTM subcommittee considered adopting one standard test method for both the intervertebral fusion device and the spinal artificial disc. The proposed ASTM standard contains a description of test methodology for static and high cycle fatigue testing of artificial intervertebral discs in axial compression, 45° compressive shear, and axial torsion with an axial compressive preload. In the existing literature, several researchers have reported the mechanical properties of human cadaveric discs using a variety of test methods and equipment. In this study, we tested human cadaveric FSUs and intervertebral discs with the test methodology and equipment specified in the proposed standard. Our goal was to determine whether the current draft standard methodology produces stiffness and failure values consistent with existing literature.

Materials and Methods:*Specimen Preparation*

A total of 19 FSUs from nine human cadaveric lumbar and thoracolumbar spines were utilized in this study (Table 1). Specimens were stored fresh frozen and visually screened for gross anatomical defects. After the two initial specimens were tested, screening was expanded to also include radiography and bone densitometry on all of the remaining specimens. Exclusion criteria were compression fractures, degenerative disc disease, and osteoporotic bone.

Table 1--Age, gender, and levels of specimens tested

Specimen	Age (years)	Gender	Levels
A	69	Female	L2-L3, L4-L5
B	68	Female	T12-L1, L2-L3
C	65	Male	T12-L1, L2-L3
D	71	Female	T12-L1, L2-L3
E	62	Male	T12-L1, L2-L3
F	66	Male	T12-L1, L2-L3, L4-L5
G	69	Male	T12-L1, L2-L3
H	70	Female	T12-L1, L2-L3
I	40	Female	T12-L1, L2-L3

Single FSUs were first isolated and then all residual musculature was removed taking care to preserve the ligamentous structures. Throughout specimen preparation and testing, the FSUs were kept moist by a wrapping of saline-soaked gauze.

To facilitate testing, the FSUs were potted in a urethane molding compound in 12.70 cm by 12.70 cm by 2.54 cm deep aluminum cans. The FSUs were oriented such that the vertical axis through the center of the cans was coincident with the intersection of the midsagittal plane of the disc and a coronal plane posterior to the anterior wall of the disc by 2/3 of the disc depth. The vertical axis through the center of the cans was perpendicular to the mid-plane of the intervertebral disc. The vertebral bodies were potted to the pars interarticularis to provide secure fixation without constraining motion at the facets or spinous processes. The cans were then attached to aluminum interfacial blocks. The urethane, cans, and interfacial blocks served as the rigid connection between the FSU and the fixtures.

All specimens were tested in an intact condition (FSU) and as isolated intervertebral discs after removal of the posterior elements. This structural condition was termed the "anterior column unit" (ACU) and comprised removal of all ligamentous connections between the spinous processes, laminae, and transverse processes. Additionally, total resection was performed on the inferior facet of the superior vertebral body, the superior facet of the inferior vertebral body, and the spinous processes. Bony and ligamentous resection was sufficient to prevent contact between the two vertebral bodies during testing. The only structures remaining intact were the anterior longitudinal ligament, the intervertebral disc, and the posterior longitudinal ligament.

Mechanical Testing

The potted FSUs were placed into fixtures in a biaxial servohydraulic load frame. The fixtures were designed and built to comply with the requirements of Draft F of the "Standard Test Methods for Static and Dynamic Characterization of Spinal Artificial Discs" dated February 2001. The fixtures permitted testing in four mechanical modes: axial rotation (Figure 1), 45° anterior compressive shear, 45° posterior compressive shear (Figure 2), and axial compression (Figure 3). The axial rotation fixtures comprised a

plate that attached the bottom can to the load/torque cell and a hollow pushrod that attached the top can to a universal joint connected to the actuating piston of a servohydraulic load frame. The compressive shear fixtures utilized the same push rod, but with a 45° bottom plate attached to the load/torque cell via a X-Y table and a hemispherical interface with the top can. The same fixtures were utilized for anterior compressive shear as posterior compressive shear, the only difference being in the orientation of the FSU or ACU. The axial compression fixtures were identical to the axial rotation fixtures except that the top can was connected to the push rod with a hemispherical interface. Digital data from the load, actuator position, torque, and rotary position channels were acquired at 100 Hz for all tests.

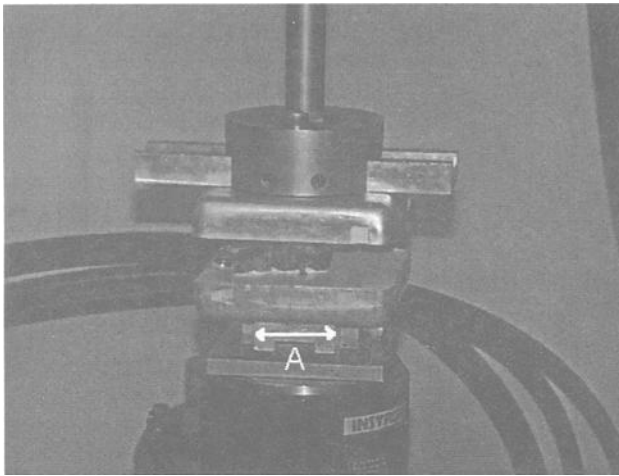


Figure 1--*Axial Rotation Test Set-up (Dimension A = 5.08 cm)*

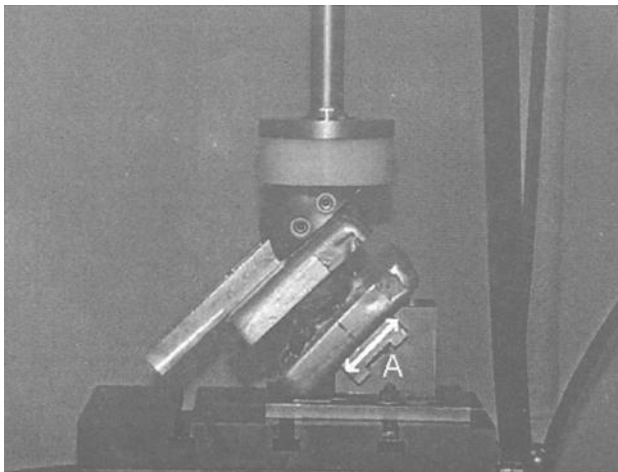


Figure 2--*Posterior Shear Set-up (Dimension A = 5.08 cm)*

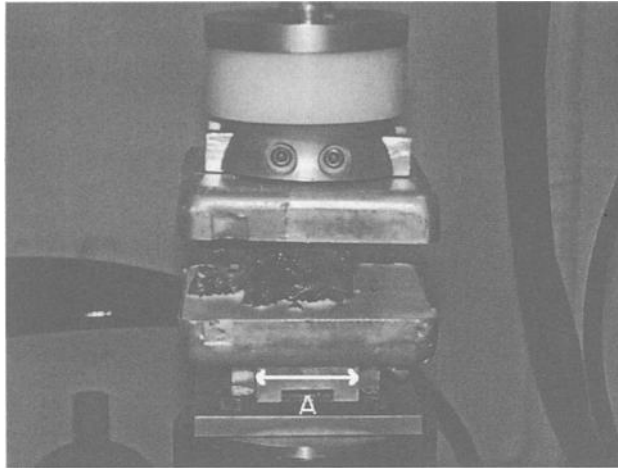


Figure 3--Axial Compression Set-up (Dimension $A = 5.08$ cm)

Left and right axial rotation testing comprised sinusoidal cycling in torque control with a mean of $0 \text{ N}\cdot\text{m}$ and amplitude of $\pm 5 \text{ N}\cdot\text{m}$ at 0.25 Hz . An axial compressive preload of 500 N (in load control) was applied during axial rotation. Compressive shear testing comprised sinusoidal cycling in load control between 50 N and 500 N at 0.25 Hz . In posterior compressive shear testing, the superior vertebral body translated posteriorly and in anterior compressive shear testing, the superior vertebral body translated anteriorly. In both compressive shear modes, the mid-plane of the disc was at a 45° angle to the load application axis. Axial compression testing comprised sinusoidal cycling in load control between 50 N and 500 N at 0.25 Hz . Each of these tests included sub-failure fatigue of the FSU or ACU for ten cycles (nine cycles to precondition each FSU or ACU and then one cycle for which data were collected). Not all specimens were tested in all mechanical test modes (Table 2).

After non-destructive testing was complete, all 19 ACUs were tested to failure in one of the mechanical test modes (using the same fixtures as were used for the non-destructive tests). Assignments to the various test modes were designed to ensure that the groups were comparable with respect to levels tested, donor age, and donor gender. Five ACUs were each tested to failure in axial rotation, anterior compressive shear, and axial compression while four ACUs were tested to failure in posterior compressive shear. A constant rotation rate of $1^\circ/\text{s}$ was employed for the axial rotation failure testing. A constant displacement rate of $25 \text{ mm}/\text{min}$ was used for the testing to failure in axial compression and both modes of compressive shear. Both of these rates are the maximum acceptable values in the proposed standard.

Data Analysis

The data from the tenth cycle of the sub-failure tests were reduced with a custom-designed LabView™ program³ to determine stiffness, range of motion (ROM), and neutral zone (NZ). Final stiffness (defined as the slope of the best-fit line to the final linear region of the load vs. displacement plot or torque vs. rotation plot) was determined for all four mechanical testing modes. ROM was determined for all four mechanical test modes, but NZ was determined only for axial rotation. ROM was defined as the total rotation (for axial rotation) or total linear displacement (for both modes of shear and for axial compression) at the maximum applied torque or load. NZ was defined as the amount of rotation between the intersection of the stiffness best-fit lines and the zero-load axis. Data from all three disc levels were pooled. A paired Student's t-test was performed to determine if the differences between the FSUs and the ACUs were statistically significant for stiffness, ROM, and NZ. To determine differences between anterior and posterior compressive shear, an unpaired Student's t-test was performed on the ROM and stiffness data for both FSUs and ACUs. A p value of 0.05 was set *a priori* in both cases.

In the failure tests, the ultimate load or torque was defined as the maximum applied load or torque without failure. The mean and standard deviation for the ultimate loads and ultimate torque were calculated.

Results:

Our summary data (Table 2) showed statistically significant changes in the mechanical properties between the FSUs and the ACUs (with the exception of the NZ during axial rotation).

³ National Instruments, Austin TX

Table 2—Results (average \pm one standard deviation) of sub-failure cyclic testing and statistical comparison between FSU and ACU properties

Test Mode	Mechanical Property	FSU	ACU	n	p Value
Axial Rotation	Stiffness (N· m/°)	3.7 \pm 3.3	1.8 \pm 1.1	19	<0.01
	ROM (°)	3.8 \pm 2.1	7.0 \pm 3.4	19	<0.01
	NZ (°)	0.3 \pm 0.8	0.6 \pm 1.0	19	0.11
Anterior Shear	Stiffness (N/mm)	587.9 \pm 192.0	368.2 \pm 98.6	7	0.01
	ROM (mm)	1.1 \pm 0.3	1.7 \pm 0.5	7	0.01
Posterior Shear	Stiffness (N/mm)	536.6 \pm 94.8	483.5 \pm 62.9	8	0.03
	ROM (mm)	1.1 \pm 0.2	1.2 \pm 0.2	8	0.01
Axial Compression	Stiffness (N/mm)	1403.0 \pm 266.5	1287.5 \pm 271.3	19	<0.01
	ROM (mm)	0.4 \pm 0.2	0.5 \pm 0.2	19	0.03

Stiffness

For axial rotation, the average stiffness decreased 50 percent after removal of the posterior elements. The stiffness data in left and right directions were pooled after it was determined (using a paired Student's t-test) that they were statistically equivalent ($p = 1.00$ for FSUs and $p = 0.67$ for ACUs). The stiffness values ranged between 1.27 N· m/° and 7.51 N· m/° (with one datum at 16.2 N· m/°) for FSUs and between 0.7 N· m/° and 4.9 N· m/° for ACUs.

In anterior compressive shear, the average stiffness showed a 40 percent decrease after removal of the posterior elements. The stiffness values ranged between 447.4 N/mm and 1005.0 N/mm for FSUs and between 231.0 N/mm and 524.0 N/mm for ACUs.

The average stiffness for posterior shear decreased 10 percent after removal of the posterior elements. The stiffness values ranged between 410.5 N/mm and 685.4 N/mm for FSUs and between 416.0 N/mm and 596.4 N/mm for ACUs.

The average stiffness for axial compression decreased 8 percent after removal of the posterior elements. The stiffness values ranged between 924.0 N/mm and 1816.0 N/mm for FSUs and between 766.0 N/mm and 1606.5 N/mm for ACUs.

Range of Motion and Neutral Zone

For axial rotation, there was an 83 percent increase in the average ROM after removal of the posterior elements. The ROM values ranged between 0.6° and 8.1° for FSUs and between 2.5° and 15.9° for ACUs. Analysis of the NZ data showed that there was not a statistically significant change after removal of the posterior elements. However, this is likely due to the small rotation values.

In anterior compressive shear, the average ROM increased 56 percent after removal of the posterior elements. The ROM values ranged between 0.5 mm and 1.3 mm for FSUs and between 1.2 mm and 2.6 mm for ACUs.

The average ROM increased 15 percent after removal of the posterior elements for posterior compressive shear. The ROM values ranged between 0.8 mm and 1.4 mm for FSUs and between 0.9 mm and 1.5 mm for ACUs.

There was an 11 percent increase in the ROM after removal of the posterior elements in axial compression. The ROM values ranged between 0.1 mm and 0.7 mm for FSUs and between 0.1 mm and 0.8 mm for ACUs.

In comparing anterior compressive shear and posterior compressive shear in FSUs, we found that there was not a statistically significant difference between the ROM data nor between the stiffness data ($p = 0.962$ and $p = 0.514$, respectively). However, in ACUs there were significantly higher ROM and stiffness values ($p = 0.032$ and $p = 0.017$, respectively) in anterior compressive shear than in posterior compressive shear.

Failure

In axial rotation, the ultimate torque values ranged between 19.8 N·m and 35.0 N·m. In anterior compressive shear, the ultimate load values ranged between 525 N and 1208 N, while in posterior compressive shear, they ranged between 854 N and 2212 N. In axial compression, the ultimate load values ranged between 2831 N and 5167 N (Table 3).

Table 3—Results (average \pm one standard deviation) of testing to failure for ACUs.

Test Mode	Levels Tested (n)	Ultimate Load or Torque (N or N·m)
Axial Rotation	T12/L1 (2), L2/L3 (2), L4/L5 (1)	24.8 \pm 6.0
Anterior Compressive Shear	T12/L1 (2), L2/L3 (3)	975 \pm 270
Posterior Compressive Shear	T12/L1 (2), L2/L3 (2)	1539 \pm 679
Axial Compression	T12/L1 (2), L2/L3 (2), L4/L5 (1)	3952 \pm 1067

Discussion:

This study was performed to determine whether testing human intervertebral discs with the equipment and methodology described in the most recent ASTM spinal artificial disc draft standard would produce results that were in agreement with data available in the literature. To do so, we measured the load-displacement and torque-rotation properties of FSUs and ACUs in axial rotation, anterior compressive shear, posterior compressive shear, and axial compression.

We compared our results to those in the literature and found that our average stiffness values in axial rotation was approximately half the values reported by Farfan, et al.[4] and Markolf[5] and comparable to the values reported by Goodwin, et al.[6], Haughton, et al.[7], and Abumi, et al.[8] (Table 4) One possible explanation for these differences is the use of different instantaneous axes of rotation for the various studies. Our ultimate torque values were approximately 20% lower than the value reported by Farfan, et al.[4]

Table 4—*Axial rotation data*

Authors	Region	Stiffness (N· m/°)	Ultimate Torque (N· m)
Current study	T12-L5	1.8 ± 1.1	24.8 ± 6.0
Farfan, et al.[4]	Lumbar	4.1 ± 1.6	31
Markolf[5]	T12-L1	4.0	...
Goodwin, et al.[6]	Lumbar	2.1	...
Haughton, et al.[7]	Lumbar	2.9	...
Abumi, et al.[8]	Lumbar	1.1	...

We were unable to locate any studies that utilized anterior compressive shear testing in which the load was applied at 45° to the mid-plane of the disc (Table 5). Our study produced results higher than those reported by Markolf[9] and by Berkson, et al.[10], both of whom tested in pure anterior shear. The results from Berkson, et al. are of initial stiffness and they applied a 400 N compressive axial preload. Our mean ultimate load was several times as much as the value reported by Markolf, but this is likely due to the difference in the direction of the load application used to produce shear.

Table 5—*Anterior shear data*

Authors	Region	Stiffness (N/mm)	Ultimate Load (N)
Current study	T12-L5	368.2 ± 98.6	975 ± 270
Markolf[9]	Thoracolumbar	260	150
Berkson, et al.[10]	Lumbar	105.4 to 147.5	...

Likewise, there is little existing posterior shear data (Table 6). As with anterior shear, posterior shear has been typically performed via pure shear, rather than through compressive shear. Our study produced stiffness values approximately three times those reported by Berkson, et al.[10] Since they calculated intact stiffness values and applied pure shear, we expected our values to be higher.

Table 6—*Posterior shear data*

Authors	Region	Stiffness (N/mm)	Ultimate Load (N)
Current study	T12-L5	483.5 ± 62.9	1539 ± 679
Berkson, et al.[10]	Lumbar	131.1 to 168.6	...

Our values for final stiffness and ultimate load in axial compression were in between values in the existing literature from Berkson[10], Virgin[11], two studies by Hirsch[12, 13], Brown[14], and three studies by Markolf[5, 15, 16]. (Table 7) Our mean ultimate

load was in between values reported by Brown[14] and Markolf[16], but more than the value reported by Virgin[11].

Table 7—Axial compression data

Authors	Region	Stiffness (N/mm)	Ultimate Load (N)
Current study	T12-L5	1287.5 ± 271.3	3952 ± 1067
Berkson, et al.[10]	Lumbar	800	...
Virgin[11]	Lumbar	2500	778 ± 170
Hirsch[12]	Lumbar	609	...
Hirsch, et al.[13]	Lumbar	700	...
Brown, et al.[14]	Lumbosacral	2900 ± 500	5207 ± 534
Markolf[5]	T12-L1	2250	...
Markolf, et al.[15]	Thoracolumbar	4160	...
Markolf, et al.[16]	T12-L1	1800	1800

Direct comparison of our data with the existing literature was hampered by the difference in testing methods, varied data analyses, and limited number of publications. For example, in 1970 Farfan et al.[4] and in 2000 Race, et al.[17] (who tested bovine intervertebral discs) showed that the stiffness of the intervertebral disc was higher with higher loading rates, which is attributed to the viscoelastic (i.e. loading rate sensitive) properties of the disc. The displacement rates in our failure tests were the maximum allowed by the draft ASTM standard. There are significant differences between the methods specified by ASTM and the methods used to produce the existing data. It has been shown that the mechanical properties of FSUs are dependent on the test methods. In 1998, Grassmann et al.[18] found that the ROM in axial rotation with constrained loading was less than the maximum rotation measured in unconstrained loading (despite there being a lack of statistical significance). In contrast, Charriere, et al.[19] found a statistically significant lowering in the stiffness for constrained loading. While the proposed ASTM standard requires compressive shear, most researchers have focused on pure shear. In 45° compressive shear testing, the applied load is initially composed of equal components of compression and shear at the disc. Therefore, compared with pure shear, we would expect that compressive shear stiffness values would tend to be higher than pure shear values. Also, many researchers have evaluated other bending motions such as flexion/extension and lateral bending. As these motions are not evaluated by the currently proposed ASTM standard, we did not include them in this study. The largest difference in the data analysis between researchers was in the calculation of stiffness values. For this calculation, researchers have reported either initial, overall, or final stiffness values. Lastly, while much data has been published on the mechanical properties of the intact FSU, relatively few studies have evaluated the properties of ACUs. Of those that have evaluated the human intervertebral disc, most have focused on axial compression.

Limitations relating directly to the specimens themselves include the small number of samples, advanced age of the donors, the inclusion of three different disc levels (T12/L1, L2/L3, and L4/L5), and the unequal number of samples at the different specimen levels. It is well accepted that the mechanical properties of the human FSU change somewhat

with age and level (Wilke et al.[20] and Panjabi[21]) and therefore it seems reasonable that the mechanical properties of the human ACU change somewhat with age and level.

There were three major limitations of our study regarding complete duplication of the equipment and methodology in the proposed standard. In the proposed standard, polyacetal interfacial blocks are used for cyclic testing (to avoid wear on the device) and metallic blocks are used for static testing (so that stiffness measurements reflect that of the device). In this study, urethane potting compound and aluminum interfacial blocks were used to pot and test the specimens. Also, our specimens (including cans and interfacial blocks) were much taller than artificial spinal discs. For compressive shear, we were forced to mount the bottom fixture on an X-Y table so that the load could be applied properly (i.e. through the center of the disc). Lastly, our axial torsion fixtures fully constrained all off-axis motion while the proposed standard specifies that flexion/extension and lateral bending motion shall be unconstrained. We expect that constraining the motion in these directions would produce a higher stiffness value.

These findings provide insight into the appropriateness of the currently proposed ASTM draft standard equipment and methodology. Although our stiffness values were higher in anterior compressive shear and posterior compressive shear, our stiffness values in axial rotation and axial compression were comparable to the existing literature values. Some of the differences may be explained by variations in testing methodology and data analysis. At this point, it would be premature to recommend changes to the proposed standard. However, the results of this study suggest that if a more comprehensive characterization of the human intervertebral disc is desired, further testing, such as flexion/extension, lateral bending, combined moments, and shear is warranted.

Acknowledgements:

This study was supported by the RIH Orthopaedic Foundation, Inc and University Orthopedics, Inc. The technical assistance of Molly Miller and Drew Harry is also gratefully acknowledged.

References:

- [1] Joplin, R. B., "The Intervertebral Disc", *Surgery, Gynecology and Obstetrics*, F. Martin, Ed., Franklin Martin Memorial Foundation, 1935, pp. 591-599.
- [2] Praemer, A., Furner, S. and Rice, D., "Selected musculoskeletal conditions: Back and other joint pain." *Musculoskeletal Conditions in the United States*, American Academy of Orthopaedic Surgeons, Rosemont, IL, 1999, pp. 27-33.
- [3] Praemer, A., Furner, S. and Rice, D., "Arthroplasty and total joint procedures", *Musculoskeletal Conditions in the United States*, American Academy of Orthopaedic Surgeons, Rosemont, IL, 1999, pp. 121-138.
- [4] Farfan, H. F., Cossette, J. W., Robertson, G. H., Wells, R. V. and Kraus, H., "The effects of torsion on the lumbar intervertebral joints: the role of torsion in the production of disc degeneration", *J Bone Joint Surg [Am]*, 1970, 52(3), pp. 468-97.
- [5] Markolf, K. L., "Deformation of the thoracolumbar intervertebral joints in response to external loads: a biomechanical study using autopsy material", *J Bone Joint Surg [Am]*, 1972, 54(3), pp. 511-33.
- [6] Goodwin, R. R., James, K. S., Daniels, A. U. and Dunn, H. K., "Distraction and compression loads enhance spine torsional stiffness", *J. Biomechanics*, 1994, 27(8), pp. 1049-57.
- [7] Haughton, V. M., Lim, T. H. and An, H., "Intervertebral disk appearance correlated with stiffness of lumbar spinal motion segments", *AJNR Am J Neuroradiol*, 1999, 20(6), pp. 1161-5.
- [8] Abumi, K., Panjabi, M. M., Kramer, K. M., Duranceau, J., Oxland, T. and Crisco, J. J., "Biomechanical evaluation of lumbar spinal stability after graded facetectomies", *Spine*, 1990, 15(11), pp. 1142-7.
- [9] Markolf, K. L., "Stiffness and damping characteristics of the thoracic-lumbar spine." in *Bioengineering approaches to the problems of the spine*. 1970 b, Washington, DC., National Institutes of Health.
- [10] Berkson, M. H., Nachemson, A. and Schultz, A. B., "Mechanical properties of human lumbar spine motion segments. Part II: Responses in compression and shear; influence of gross morphology", *Journal of Biomechanical Engineering*, 1979, 101, pp. 53-57.

- [11] Virgin, W. J., "Experimental investigations into the physical properties of the intervertebral disc." *J. Bone Joint Surg.*, 1951, 33-B(4), pp. 607-611.
- [12] Hirsch, C., "The reaction of intervertebral discs to compression forces." *J. Bone Joint Surg.*, 1955, 37-A(6), pp. 1188-1196.
- [13] Hirsch, C. and Nachemson, A., "New observations on the mechanical behavior of lumbar discs", *Acta Orthopaedica Scandinavia*, 1954, 23(4), pp. 254-283.
- [14] Brown, T., Hansen, R. J. and Yorra, A. J., "Some mechanical tests on the lumbosacral spine with particular reference to the intervertebral discs." *J. Bone Joint Surg.*, 1957, 39-A(5), pp. 1135-1164.
- [15] Markolf, K. L. and Morris, J. M., "The structural components of the intervertebral disc. A study of their contributions to the ability of the disc to withstand compressive forces", *J Bone Joint Surg Am*, 1974, 56(4), pp. 675-87.
- [16] Markolf, K. L. and Steidel, R. F., "The dynamic characteristics of the human intervertebral joint." in *ASME Winter Annual Meeting*, 1970 a, New York, NY, The American Society of Mechanical Engineers.
- [17] Race, A., Broom, N. D. and Robertson, P., "Effect of loading rate and hydration on the mechanical properties of the disc", *Spine*, 2000, 25(6), pp. 662-9.
- [18] Grassmann, S., Oxland, T. R., Gerich, U. and Nolte, L. P., "Constrained testing conditions affect the axial rotation response of lumbar functional spinal units", *Spine*, 1998, 23(10), pp. 1155-62.
- [19] Charriere, E., Beutler, T., Caride, M., Mordasini, P., Dutoit, M., Orr, T. and Zysset, P., "Mobility of the L5-S1 spinal unit: A comparative study between an unconstrained and a semi-constrained system." in *47th Annual Meeting, Orthopaedic Research Society*, 2001, San Francisco, CA, Orthopaedic Research Society.
- [20] Wilke, H. J., Wenger, K. and Claes, L., "Testing criteria for spinal implants: recommendations for the standardization of in vitro stability testing of spinal implants", *Eur Spine J*, 1998, 7(2), pp. 148-54.
- [21] Panjabi, M., Yamamoto, I., Oxland, T. and Crisco, J., "How does posture affect coupling in the lumbar spine?" *Spine*, 1989, 14(9), pp. 1002-11.

R. G. Hudgins¹ and Q.-B. Bao²

Durability Test Method for a Prosthetic Nucleus (PN)

Reference: Hudgins, R. G., and Bao, Q.-B., “Durability Test Method for a Prosthetic Nucleus (PN),” *Spinal Implants: Are We Evaluating Them Appropriately, ASTM STP 1431*, M. N. Melkerson, S. L. Griffith, and J. S. Kirkpatrick, Eds., ASTM International, West Conshohocken, PA, 2003.

Abstract: Durability is critical for permanent spinal implants. Proposed test methods suggest that prosthetic intervertebral discs (PIDs) having fixation plates for vertebral attachment should be tested at a 45° angle to create combined compression-shear loads. Generally, a prosthetic nucleus (PN) does not have fixation plates and does not transmit shear loads as high as PIDs; thus, loading PNs through fixation plates would not mimic physiological conditions. Currently, most PNs are fatigue tested using compression only. A test method and fixture are proposed for testing a PN in a saline bath at 37 °C under combined compression-flexion-extension loading simulating physiological conditions. A multi-station test fixture, mounted in a servo-pneumatic test frame, was used to conduct the tests under load control. The fixture has a top platen to apply a controlled compression load and a bottom test bed that rotates on a horizontal axis at a set frequency creating a flexion/extension motion. Compression loads were monitored for each station, and the rotation and moment were monitored for the test bed. A software control algorithm coordinated the compression stroke of the test frame with the test bed rotation so that the maximum compression load occurred near the peak rotation angle. The PN compression load range was approximately 200 N–550 N applied at 1.5 Hz, and the test bed rotation was -3.6° to +2.3° to simulate lumbar flexion/extension motion during vigorous walking. The peak compression stress component was approximately 1 MPa, and the peak flexion/extension component was approximately 1 MPa giving a maximum combined stress on the implant edge of 2.0 MPa. Specimens were examined and photographed with magnification, and masses were monitored to assess implant wear. No cracks were observed on any of 6 implants tested to 12.7 million cycles, and the average total mass loss was approximately 6.9 mg (stdev = 4 mg). Testing continues.

¹ Project Manager, Disc Dynamics, Inc., 5909 Baker Road, Suite 550, Minnetonka, MN 55345.

² VP, R&D, Disc Dynamics, Inc. 5909 Baker Road, Suite 550, Minnetonka, MN 55345.

Keywords: prosthetic intervertebral disc nucleus, fatigue, wear, permanent set, in situ curable polyurethane, test fixture

Introduction

Durability is a critical issue for any permanently implanted medical device. A Prosthetic Nucleus, PN, is a permanent orthopedic implant, and its durability must be examined. Currently, there are no established standards or methodologies for testing a PN. Proposed test methods, such as "Standard Test Methods for Static and Dynamic Characterization of Spinal Artificial Discs," Draft H (April, 2002), are more appropriate for total prosthetic intervertebral discs (PIDs). The proposed test method suggests that PIDs, having fixation plates for vertebral attachment, should be tested at a 45° angle to create combined compression-shear loads. Generally, PNs do not have fixation plates, and loading PNs through fixation plates for mechanical tests would not mimic physiological service conditions. Currently, one PN was fatigue tested using axial compression loads [1], and a second PN was tested using hydrostatic compression in a fixture that allowed vertical compression motion [2]. Fatigue tests using axial or hydrostatic compression do not simulate the bending stresses that PNs see physiologically. Therefore, it is reasonable to add a horizontal rotation onto an axial compression load for simulating physiologically relevant loading modes of compression-flexion-extension for durability and wear evaluations.

This research presents a specially designed test fixture, test method, and data analysis method for fatigue and wear testing a PN. Specifically, the fixture, test method, and data analysis method will be discussed in relation to physiological loading and kinematics. Wear data will be presented on a mass loss basis. Wear particle analysis will be addressed in further research.

Methods

Test Fixture

A test fixture was developed for fatigue and wear testing a PN in a saline bath at 37° C under combined compression-flexion-extension loading simulating physiological conditions. A six-station test fixture, mounted in a servo-pneumatic test frame, was used to conduct the tests under load control (Fig. 1). A side view illustration (Fig. 2) of the test fixture shows relative positions of the fixture's design features. A cup (Fig. 3) made of high molecular weight polyethylene, UHMWPE, was designed to hold the test specimen in the test cell. A loading nose (Fig. 4) made of UHMWPE was fitted to the upper compression anvil. The cup and loading nose, having an as machined finish, were designed to allow the PN to undergo free radial expansion. The fixture had a top platen that applied a compression load and a bottom test bed that rotated on a horizontal axis at a set frequency that created a flexion-extension motion. The test bed's center of rotation, CR in Fig. 2, was aligned with the bottom of each test specimen. The rotational and vertical loading frequencies could be varied as desired, and the rotation angle could be varied from approximately $\pm 2^\circ$ to $\pm 15^\circ$. The controlled load was applied to the top platen, and compression loads were monitored

for each station. The load for each PN was adjusted independently using the adjustable upper compression anvil attached to the load cell. The test bed rotation and

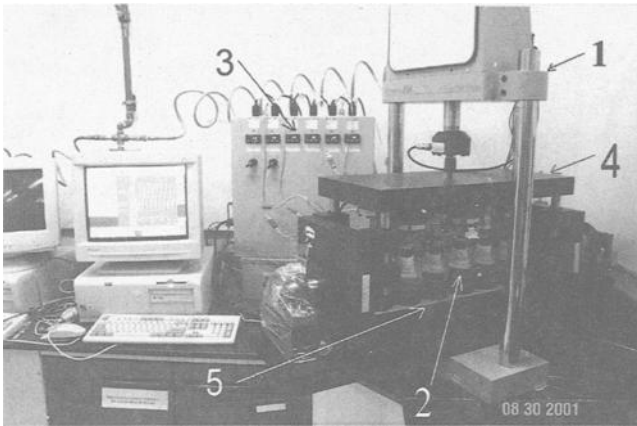


Figure 1 — Fatigue fixture 1) pneumatic test frame, 2) test cells with UHMWPE specimen cups, 3) temperature controllers, 4) loading platen, 5) rotating bed supporting test cells

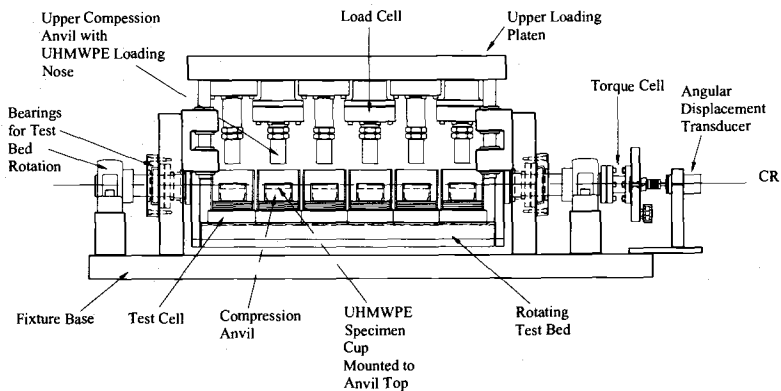


Figure 2 — Side view of test fixture showing the test bed's center of rotation.

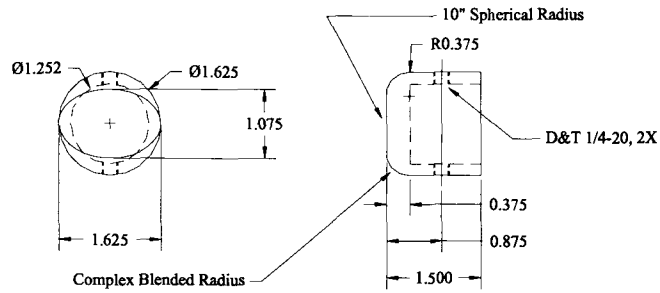


Figure 3 — Loading nose for attachment to upper compression anvil (dimensions given in inches for machining purposes).

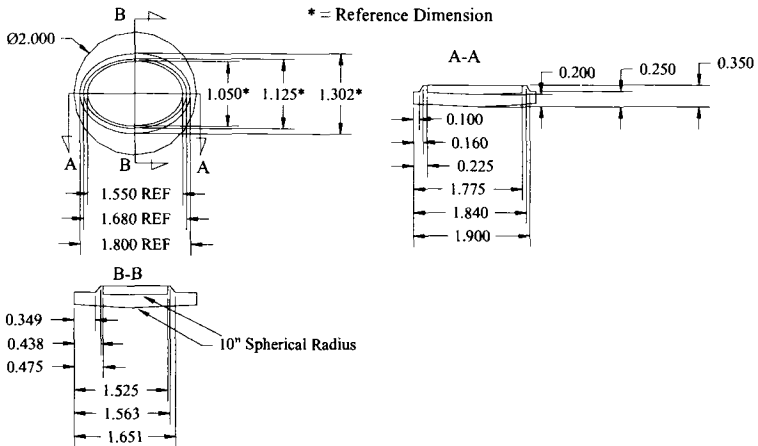


Figure 4 — Loading nose for attachment to upper compression anvil (dimensions given in inches for machining purposes).

torque were monitored. The torque required to rotate the test bed produced the flexion-extension moment applied to the PN specimens. The machine was computer controlled using software that coordinated the compression stroke with the test bed rotation so that the maximum compression force occurred at a desired rotation angle.

Test Method

Specimen Preparation — PN test specimens were made using a custom delivery system. The system used a polymer application device to deliver a proprietary, in-situ curable polyurethane into an implant balloon to create a PN. The test specimens were made using a wooden mold saturated with water, and a water bath maintained at $37^{\circ}\text{C} \pm 2^{\circ}\text{C}$. The wooden mold cavity simulated a typical implant geometry, and the mold volume was approximately 4.4 ml. The water saturated oak mold and water bath were used to simulate physiological implantation conditions.

Nine specimens were prepared. Six specimens were used for the fatigue and wear test, and 3 specimens were retained as controls for long term mass changes due to hydration. All test specimens were preconditioned for approximately 22 days in saline at 37°C to reach saline absorption equilibrium. The mass of the specimens was measured periodically during the preconditioning period to verify constant mass indicating saline absorption equilibrium. The specimens were elliptically shaped having a major axis (lateral dimension) of approximately 33 mm and a minor axis (anterior/posterior dimension) of approximately 20 mm. The approximate cross-sectional area of the specimens was 525 mm^2 ; the height was approximately 10 mm, and the average mass was 4.9127 g.

Test Conditions — Six PN implants were tested using combined cyclic axial compression flexion-extension loads. All specimens were tested in normal saline at $37^{\circ}\text{C} \pm 2^{\circ}\text{C}$. The axial compression load was applied at a nominal frequency of 1.5 Hz $+0.07/-0.02$ Hz, and the maximum compression load was $550\text{ N} \pm 25\text{ N}$, and the minimum compression load was $200\text{ N} \pm 50\text{ N}$. The upper compression anvil was adjusted for each specimen to obtain the closest maximum compression force to the nominal load as possible. The flexion angle applied was -3.6° to $+2.3^{\circ}$ relative to the vertical giving 5.9° for a total range of motion. The resulting flexion-extension moment was -8.6 Nm to $+5.2\text{ Nm}$ per specimen.

Analytical Methods

Physical Analysis — Specimens were periodically weighed during the fatigue and wear test to determine the mass loss and wear rate. Wear rate was determined as the mass change per million cycles. A bulk saline absorption coefficient was determined from saline absorption data using three control PNs for extended submersion. The bulk absorption coefficient was used to estimate the theoretical, pristine mass of the 6 test specimens during the test period. The wear was estimated as the difference between the theoretical, pristine mass and the actual mass of the PN specimen. The bulk absorption coefficient was determined for the specimens after the first 525 hours of immersion in saline at 37°C till termination of the wear test. The first 525 hours of immersion allowed the specimens to reach near mass equilibrium and a linear

absorption behavior. The relative mass change, m_r , for each control specimen was calculated as

$$m_r = \frac{m - m_0}{m_0} \quad (1)$$

where m is the mass at a time of interest and m_0 is the original mass of the specimen. The relative mass change versus time was plotted and the slope from 525 hours immersion till 2,900 hours immersion at test termination was determined. The slope of the absorption curve gives the bulk absorption coefficient, γ , and it is expressed as

$$\gamma = \frac{m_r}{\Delta t} \quad (2)$$

where Δt was determined as a time of interest, t , minus 525 hours. Thus, the theoretical mass, m_{TH} , was determined for each PN specimen during wear testing from the linear relation

$$m_{TH} = \gamma m_0 t + m_{t=525} \quad (3)$$

where $m_{t=525}$ is the mass of the individual specimen at 525 hours immersion. The wear mass, m_w , was determined from

$$m_w = m_{TH} - m_f \quad (4)$$

where m_f is the final mass of the wear tested PN at the end of the test.

Specimens were also photographed using magnification up to 126 × to document the surface condition. Finally, the height of each PN was measured during each physical inspection over the course of the test. The permanent set for each specimen was determined by the difference in the original height and the height at the time of inspection.

Stress Analysis — Stresses are calculated based upon the axial deformation and the curvature induced from the rotation. Axial strain, E_A , (large strain definition, Boresi and Sidebottom [3], Ward [4])

$$E_A = \varepsilon_A + \frac{1}{2} \varepsilon_A^2 = \frac{1}{2} \left[\left(\frac{h_1}{h_0} \right)^2 - 1 \right] \quad (5)$$

where ε_A is the engineering strain, displacement/original height, along the centroidal axis from compression, h_1 is the deformed height, and h_0 is the original height of the specimen. Linearization of equation 5 results in the typical definition of engineering or small strain. Bending strain is determined by the curvature of the flexed body. Curvature, κ , is given by

$$\kappa = \frac{1}{\rho} \quad (6)$$

where ρ is the radius of curvature. The radius of curvature (Figure 5) is

$$\rho = L3 - b \quad (7)$$

and the symbols are defined in the figure. The quantity $L3$ is expressed as

$$L3 = \frac{h_1 + h_2}{\sin \theta} \quad (8)$$

where θ is the rotation angle. Solving for h_1 from equation 5 in terms of E_A , then

recognizing that h_2 can be expressed as $b(\sin\theta)$ and substituting into equation 8 $L3$ becomes

$$L3 = \frac{h_0 \sqrt{2E_A + 1}}{\sin \theta} + b \tag{9}$$

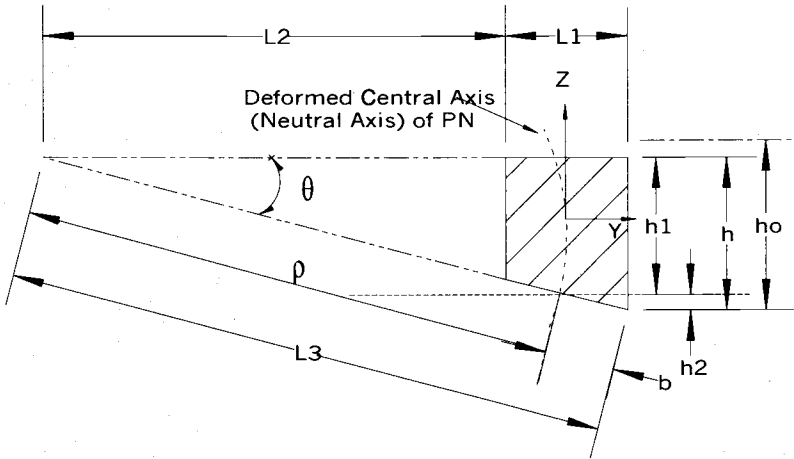


Figure 5 — Idealized geometry for determining the radius of curvature.

Next, using equations 9 ad 7, the curvature can be expressed as

$$\kappa = \frac{\sin \theta}{h_0 \sqrt{2E_A + 1}} \tag{10}$$

The bending stress or flexural stress, σ_f , from Eulerian bending theory as given by Popov [5] is

$$\sigma_f = \frac{My}{I_x} = E\kappa y \tag{11}$$

where M is the moment, y is the distance from the geometric center of the specimen to the anterior or posterior edge of the specimen, I_x is the cross-sectional moment of inertia, and E is the PN's compression modulus. The total stress, σ_t , is the superposition of the flexural stress and the axial compression stress [5]

$$\sigma_t = \sigma_f + \sigma_c \tag{12}$$

where σ_c is the compression stress, the compression force divided by the cross-sectional area.

The torque, T , required to rotate the test bed of the machine is a measured output from the test fixture. Thus, the bending stress estimate can be checked by calculating the flexural moment from the stress relationships and comparing the calculated flexural moment to the measured torque. The flexural moment relationship is based upon the

material properties, specimen geometry, and curvature from the rotation; the same quantities necessary to determine the flexural stress. The flexural moment for one specimen, M_n , is given as

$$M_n = E\kappa I_x \tag{13}$$

and the flexural moment can be used to calculate the torque to rotate the test bed as

$$T = \sum M_n \tag{14}$$

sum of the individual flexural moments to verify the analytical results.

Results

The preconditioning period was sufficient to allow the mass of the test specimens to reach near equilibrium (Fig. 6) before the fatigue and wear test began. The bulk absorption coefficient was determined from the data in Fig. 7. The absorption coefficient was determined using average relative change in mass of the mass control specimens, specimens PN 7 – PN 9, while specimens PN 1 – PN 6 were undergoing fatigue and wear testing. The absorption coefficient, based on the original mass, was 1.066×10^{-6} g/g/hr. Figure 8 shows the theoretical, pristine masses of PN test specimens 1–6 along with actual masses of the control specimens. The theoretical, pristine masses follow the trend of the control masses.

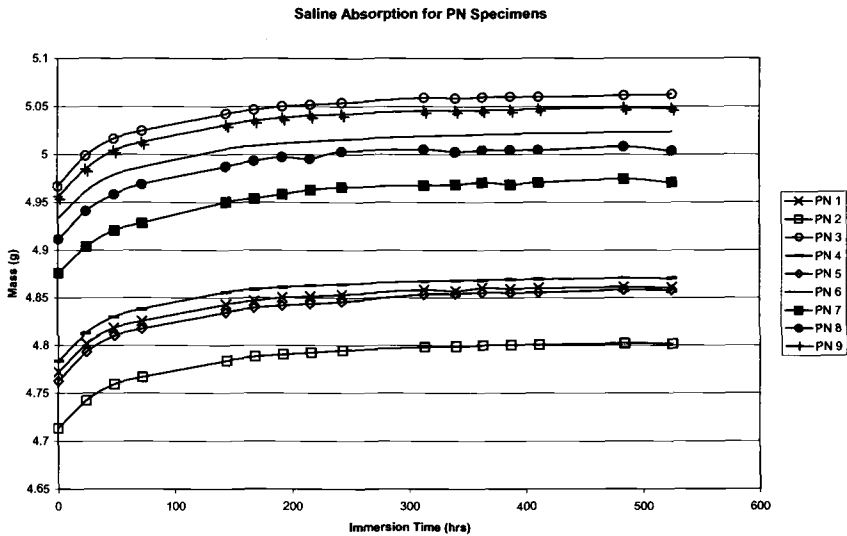


Figure 6 — Saline absorption data indicating mass equilibrium of all test and control specimens.

The fatigue and wear test was suspended at 12.7 million cycles. The average wear of the specimens at 12.7 million cycles was 6.9 mg with a standard deviation of 4.0 mg. Table 1 gives the wear mass for each specimen. The average wear rate over the test duration was approximately 0.5 mg/million cycles. Figures 9 and 10 show a typical

surface condition. Some wear was noted on PN surfaces as evidenced by abrasions and pitting. No cracks or balloon tears were observed in any of the six PNs. Permanent set was experienced by all PN specimens. The permanent set is shown in Fig. 11 as the

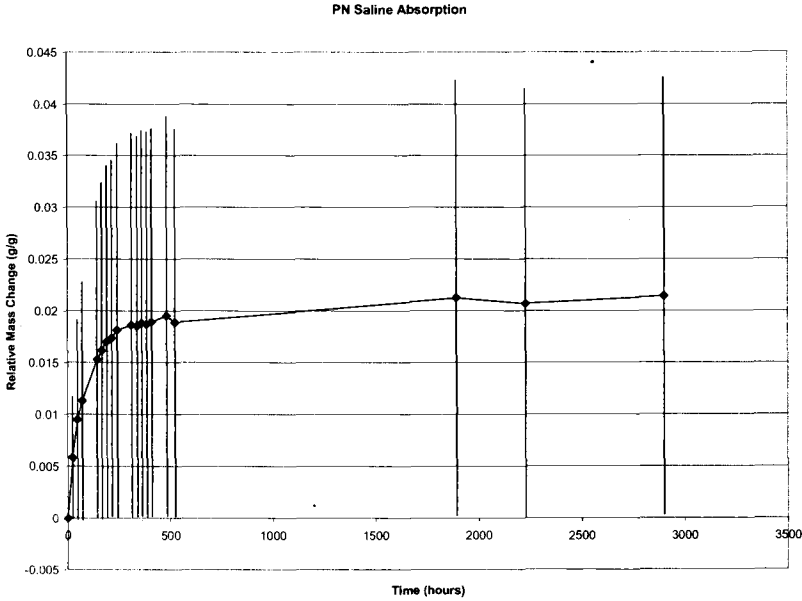


Figure 7 — Saline absorption data used to calculate bulk diffusion coefficient. Data is the average of the relative mass changes for the control PNs, and error bars indicate ± 1 standard deviation.

average with ± 1 standard deviation bars. The axial compression stress at the maximum compression load was approximately 1.0 MPa. The maximum applied stress from the combined compression/flexion loads was approximately 2.0 MPa (the compression stress due to bending on the outer edge of the implant was approximately 1.0 MPa). The maximum applied stress from the compression/extension load was 1.5 MPa (the compression stress due to bending on the outer edge of the implant was approximately 0.5 MPa). Comparison of calculated torque from summing the flexural moments for each specimen and experimentally measured torque at peak loading was within 10%. The calculated torque was 8.8 Nm and the measured torque was 9.5 Nm.

Table 1 — PN Wear at 12.7 million cycles.

Test Specimen	Wear Mass (mg)
PN 1	Gained Mass
PN 2	1.6
PN 3	Gained Mass

PN 4	7.1
PN 5	7.6
PN 6	11.2

Saline Absorption

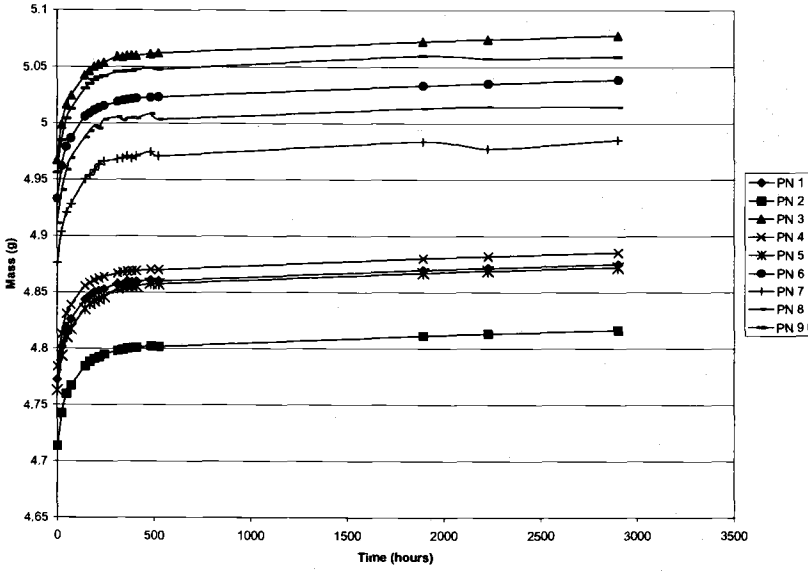


Figure 8 — Theoretical masses of specimens 1-6 based upon the bulk diffusion coefficient, and the actual masses of control specimens 7-9.

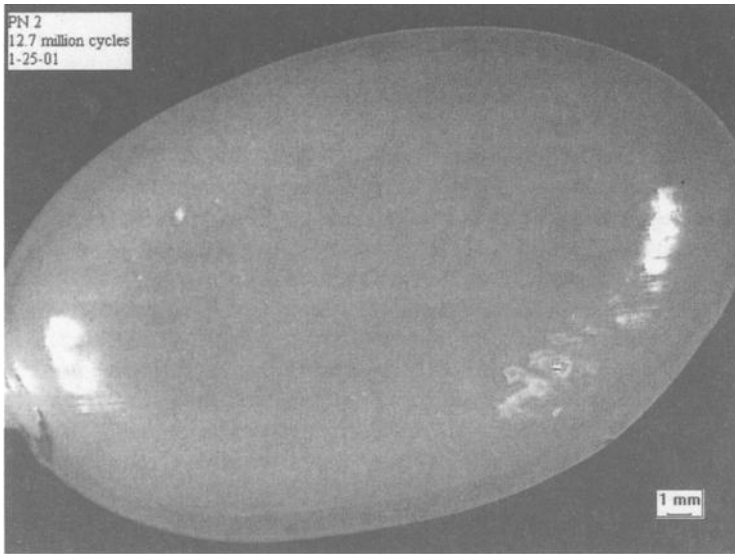


Figure 9— *Typical surface of test specimen at 12.7 million cycles. Light spots on upper left of PN indicate wear, and they occur in a location of high bending stress.*

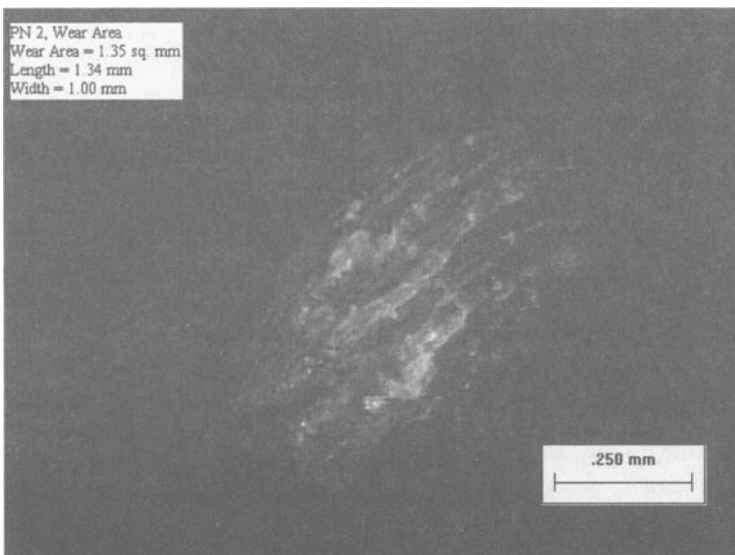


Figure 10— *Magnified view (X 126) of wear area on surface of test specimen.*

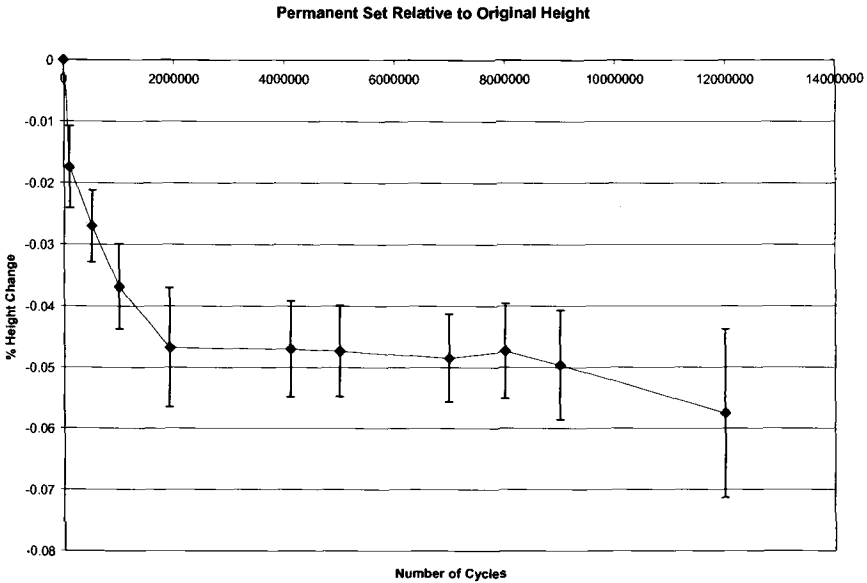


Figure 11 — Permanent set as a function of test cycles with error bars indicating ± 1 standard deviation.

Discussion

The test fixture used in this fatigue and wear study was capable of producing loads and rotations that were similar to physiological compression/flexion and compression/extension conditions. This loading was felt to be more indicative of a PN's performance than axial compression alone, and more physiologically relevant than loading a PN through fixed endplates at a 45° angle. Physiologically, the annulus provides radial constraint for the nucleus, and it is expected to share some of the spinal load along with a PN implant. The split-half specimen cups were designed to avoid radially constraining the PN during the loading cycle. Therefore, the unconstrained test condition required the PN to bear the entire test load. Hence, a rigorous test condition resulted. The fixture was also capable of producing specimen wear. Wear patterns exist around the edges of the implant. The fixture and test method also allowed the PN's permanent height loss to be tracked and the applied stresses to be estimated.

Wear was estimated as the difference between a theoretical, pristine mass and the actual mass of the specimen at inspection. Generally, the theoretical, pristine mass estimate seemed to have worked well for most specimens. However, two PNs continued to gain mass during the fatigue and wear test. The mass gained was greater than the theoretical, pristine mass so the wear of these two PNs could not be determined. However, the wear of the PNs was low compared to the variation of saline absorption. Thus, the wear rate analysis only estimates the average wear of the PNs. A definitive mass loss from wear will be determined by exhaustively drying the specimens to remove all moisture. The difference in the initial dry mass and the final

dry mass will be the ultimate measure of total wear. The specimens are still being tested on a periodic basis and then stored in saline at 37° C for further fatigue and wear. Thus, the definitive wear mass will be determined later. Definitive mass loss measurements made by exhaustive drying cannot be performed during the inspection intervals because the PNs absorb 2% or more of their original mass in saline. Thus, repeated drying and hydration for mass measurements would make fatigue and wear tests prohibitively long. Given the limitations of the wear estimate, the total wear was low over the test duration. No cracks or balloon tears were found in any of the PNs during surface inspection and photography.

A large portion of the permanent set (height loss), 4.7%, occurred in the first 2.8 million cycles. This average height loss remained approximately constant from 2.8 million cycles to about 7 million cycles. Although permanent set continues beyond 12.7 million cycles, the amount of permanent set, less than 8% maximum, is not excessive.

The stress analysis was based on linear concepts. The overall PN deformation was relatively small, but physiologically relevant, and allowed use of linear analysis. Larger deformations would have caused significant nonlinear material behavior, and short beam theory that includes warping of the bent beam cross-section would be necessary to achieve more analytical precision. However, given the physiological deformation range applied to the PN and the polymer's material properties, the linear analysis was sufficient to produce calculated torques close to the actual measured torques. The peak applied stresses of 2.0 MPa for compression/flexion and 1.5 MPa for compression/extension were greater than the intradiscal nucleus pressures measured *in vivo* for walking of 0.65 MPa [6]. The data of Hinz et al. [7] combined with the data of Smeathers [8] also supports applied stress levels of approximately 0.5 MPa to 0.6 MPa for brisk walking. Total range of motion for the pelvis during walking ranges from about 3.8 degrees to 4.6 degrees according to Stokes et al. [9], Vogt and Banzer [10], and Thurston and Harris [11]. The pelvic rotation would be expected to approximate the rotation at L5-S1 during normal walking. A treadmill study by Syczewska et al. [12] and a 3 dimensional study of walking by Callaghan et al. [13] show amplitudes of approximately 2 degrees and 6.5 degrees flexion/extension respectively for the lumbar spine. Thus, the maximum applied stresses were 2.3–3.2 times greater than typical intradiscal pressures during walking, and the range of motion was sufficient to cover a wide range of physiological conditions. The stresses were also supported by the PN without any load sharing achieved through radial constraint of a surrounding annulus.

Conclusions

A test fixture was developed that produced combined compression-flexion-extension loading without requiring rigid fixation of the test specimen to the test fixture. Stress analysis procedures were found adequate for the physiological deformation range applied to the PN. Implant wear and permanent set were observed during the test. The test parameters mechanically and thermally simulated physiological service conditions. Estimated implant wear was low, and permanent set was reasonable. No cracks or balloon tears were detected in any of the six test specimens over the reported 12.7 million test cycles.

References

- [1] Bain, A. C. and Norton, B. K., "Comparison of the Pre- and Post-Fatigue Viscoelastic Properties of a Prosthetic Disc Nucleus," *Society for Biomaterials, 27th Annual Meeting Transactions*. Saint Paul, MN, 24–29 April, 2001.
- [2] Bagga, C. S., Williams, P., Higham, P. A., and Bao, Q. B., "Development of Fatigue Test Model for a Spinal Nucleus Prosthesis with Preliminary Results for a Hydrogel Spinal Prosthetic Nucleus," *ASME/AICHe/ASCE Summer Bioengineering Conference*, Sunriver, OR, 1997.
- [3] Boresi, A. P. and Sidebottom, O. M., *Advanced Mechanics of Materials*, John Wiley and Sons, Inc. New York, 1985, pp. 43–44.
- [4] Ward, I. M., *Mechanical Properties of Solid Polymers*, John Wiley and Sons, Inc. New York, 1985, pp. 29–31.
- [5] Popov, E. P., *Introduction to Mechanics of Solids*, Prentice-Hall, Inc., Englewood Cliffs, New Jersey, 1968, pp. 255, 381.
- [6] Wilke, H., Neef, P., Caimi, M., Hoogland, T., and Claes, L., "New In Vivo Measurements of Pressures in the Intervetebral Disc in Daily Life," *Spine*. 1999, Vol. 24, No. 8, pp. 755–762.
- [7] Hinz, B., Seidel, H., Brauer, D., Menzel, G., Bluthner, R., and Erdmann, U., "Bidimensional Accelerations of Lumbar Vertebrae and Estimation of Internal Spinal Load During Sinusoidal Vertical Whole-body Vibration: a Pilot Study," *Clinical Biomechanics*, 1988, No. 4, pp. 241–248.
- [8] Smeathers, J. E., "Measurements of Transmissibility for the Human Spine during Walking and Running," *Clinical Biomechanics*, 1989, Vol. 4, pp. 34–40.
- [9] Stokes, V. P., Anderson, C., and Forsberg, H., "Rotational and Translational Movement Features of the Pelvis and Thorax During Adult Human Locomotion," *Journal of Biomechanics*. 1989, Vol. 22, No. 1, pp. 43–50.
- [10] Vogt, L. and Banzer, W., "Measurement of Lumbar Spine Kinematics in Incline Treadmill Walking," *Gait and Posture*, 1999, Vol. 9, pp. 18–23.
- [11] Thurston, A. J. and Harris, J. D., "Normal Kinematics of the Lumbar Spine and Pelvis," *Spine*. 1983, Vol. 8, No. 2, pp. 199–205.
- [12] Syczewska, M., Oberg, T., and Karlsson, D., "Segmental Movements of the Spine During Treadmill Walking With Normal Speed," *Clinical Biomechanics*. 1999, Vol. 14, pp. 384–388.
- [13] Callaghan, J. P., Patla, A. E., and McGill, S. M., "Low Back Three-dimensional Joint Forces, Kinematics, and Kinetics During Walking," *Clinical Biomechanics*. 1999, Vol. 14, pp. 203–216.

**Session V: Suggested Test Methods,
Models, Fixtures, or Needed
Improvements**

Elizabeth A. Friis,¹ C. Douglas Pence,² Charles D. Graber,² Jorge A. Montoya³

Mechanical Analogue Model of the Human Lumbar Spine: Development and Initial Evaluation

Reference: Friis, E. A., Pence, C. D., Graber, C. D., and Montoya, J. A. “**Mechanical Analogue Model of the Human Lumbar Spine: Development and Initial Evaluation,**” *Spinal Implants: Are We Evaluating Them Appropriately? ASTM STP 1431*, M. N. Melkerson, S. L. Griffith, and J. S. Kirkpatrick, Eds., ASTM International, West Conshohocken, PA, 2003.

Abstract

Mechanical testing of spinal instrumentation on cadaveric spine segments can be challenging. In this study, a mechanical analogue lumbar spine model was developed to be similar in rigidity to that of cadaveric spine segments. Three models of an adult human lumbar spine were built from composite vertebrae, ligaments and discs created individually to reproduce the nonlinear mechanical properties of human components. These models and three calf lumbar spines were loaded in a biaxial mechanical test system in axial compression, torsion, right and left lateral bending, flexion and extension. Rigidities were calculated in the secondary linear load-displacement region. Load-displacement behavior was nonlinear for both analogue and calf spines. There was good reproducibility between the models. Average axial rigidity of the analogue spines was 86 N/mm versus 231 N/mm for the calf spines, possibly due to the calf flat-back. In the remaining loading modes, the analogue spine was 26–65% more rigid than young calf spines. Comparisons to human cadaveric spine segments are underway.

Keywords: spine, mechanical analogue, spine testing, spine model, lumbar spine

Introduction

Mechanical testing of spinal instrumentation on cadaveric spine segments can be challenging. Problems with testing include changing mechanical properties of the biological specimens with time, difficulty in applying instrumentation (such as strain gages) to the segments in a timely fashion, and great variability between specimens. The purpose of this study was to develop and test mechanical analogue lumbar spine segments that model the rigidity of normal human spine segments. Unlike cadaveric spine segments, the analogue models can be easily instrumented with transducers and its properties do not degrade with time. In theory, the models can also be made with a much tighter reproducibility than that found in cadaveric specimens.

¹Assistant Professor, University of Kansas, Mech. Engrg., 3013 Learned Hall, Lawrence, KS 66045.

²Clinical Assoc. Prof., KUSM-W, Dept. of Surgery, Section of Orthop. and Biomech. Tech., respectively Ortho. Res. Inst., Inc., 929 N. St. Francis, Wichita, KS 67214.

⁴Product Engineer, Stryker Howmedica Osteonics, 59 Route 17 South, Allendale, NJ 07401.

Limitations of Biological Models

There are severe limitations in the use of biological models in testing for the effects of spinal instrumentation. With time after thaw and exposure to air, the soft tissues and hard tissues change in properties, thus altering the rigidity response of the spine segment.⁹ Wilke et al.¹⁵ recently quantified the effect of exposure and time after thaw to mechanical response of the spine segment. They showed that the most critical factor in determining the amount of change in a spine segment is the length of exposure. In addition, while working with human cadaveric specimens, one assumption that is often avoided in the literature is documentation of the amount of time from expiration of the donor to freezing. The likely variation in this time could greatly affect the mechanical properties of the cadaveric specimen before testing even initiates. This problem can be easily controlled with animal models, but not with human cadaveric specimens. Wilke et al.¹⁶ showed that formalin fixation forms crosslinks in the soft tissues and significantly alters the mechanical response of the spine. He suggested that fixed specimens should not be used in biomechanical testing as they were not appropriate models of *in vivo* mechanical behavior. The application of spine instrumentation and various transducers such as strain gages can be time consuming. Without formalin fixation, there is a high risk of degenerative changes over the preparation and testing time. Cadaveric spines also display significant variation, so direct comparison of results are difficult. Finally, cadaveric spines are often osteoporotic and have variable states of degeneration making them less suitable for mechanical testing and comparative analysis. These limitations greatly hinder the use of cadaveric spine models in testing.

Use of Animal Models in Spine Testing

Wilke et al.^{13,14} showed similar mechanical properties, such as range of motion and stiffness in certain segments, between human and calf FSUs. This suggested that calf spines can be used as a substitute for human spines in some *in vitro* tests. Furthermore, Kettler and associates⁸ concluded that FSUs and polysegmental spines (five segments), at least qualitatively, have similar mechanical properties. Therefore it is reasonable to compare polysegmental calf spines to human FSUs. Many researchers have used the calf spine model in evaluating the effect of spinal instrumentation. In addition, Wilke et al. tested sheep spine segments and showed similarity to human cadaveric spines.¹³

Mechanical testing of spine stabilization (implant) devices is very limited at the present date due to the special problems of testing biological structures controlled by soft tissues. As stated previously, these problems include changing mechanical properties of the biological specimens with time, difficulty in applying instrumentation to the segments in a timely fashion, and great variability between specimens. For example, in a study of intervertebral disc pressures, investigators have found up to 500% variation in normal disc pressures between different cadaveric specimens.² Variation in the size of the specimens and the quality of the bone stock and soft tissues can also be tremendous. Such variations make it quite difficult to detect and statistically validate changes due to the presence of instrumentation in cadaveric spine specimens. Use of a validated, anatomically correct mechanical analogue spine in spinal instrumentation testing would provide consistent, repeatable and comparable results while maintaining accuracy.

Use of Synthetic Models in Lumbar Spine Testing

Synthetic models of the lumbar spine have also been used in testing although none to date but the one proposed in this application provide both correct anatomy and rigidity. An ASTM Standard F1717-01 dictates that two polyethylene blocks with a space in between be used for the static and fatigue testing of spinal implant constructs in a full corpectomy model. This standard is thought to represent a worst-case scenario for testing of implants, but gives no information about the effect of the instrumentation on the spine itself. Dick³ extended this idea to evaluate five different brands of cross-link spinal instrumentation to determine which design characteristics were most desirable mechanically. Five different rigid pedicle screw systems were tested. Each was loaded under compression, torsion, right/left lateral bending and under flexion/extension. Each test was performed over five full cycles of sinusoidal loading with data derived from the fifth cycle. The model used for the insertion of the pedicle screws was a pair of polyurethane foam vertebrae L3 and L4 (Sawbones[®], Pacific Research Laboratories, Vashon Island, WA). A primary advantage of using the polyurethane vertebrae over human cadaveric vertebrae was that there was no specimen degradation or inter-specimen variability during testing, which was encountered with animal and human spine models. The testing model used by Dick et al. is similar to the commonly used ASTM Standard F-117-96, but had a more physiological alignment of the pedicle screws.³ The polyethylene blocks do not reproduce the complex geometry of the spine crucial for the accurate insertion of pedicle screws. However, neither of these synthetic models have ligamentous representation and again represent a worst case testing scenario without the capability of assessing the effect of the instrumentation on the spine itself.

Wilke et al.¹⁹ developed a modular mechanical model of the spine that could be adapted to approximate the mechanical properties of various spinal levels and pathologic conditions in single- or multi-segmental forms. The model was compared to human L4-L5 specimens in flexion and extension, axial rotation and lateral bending. This model showed comparable ranges of motion to those of human specimens in all directions and was also characterized by increasing stiffness with increasing load as well as hysteresis. Wilke stated that "This model can be used as a standard for the comparison of different spine testers. As a substitute for cadaveric specimens in implant testing, these models provide the advantages of availability, consistent properties, and adaptability, and avoid the risks associated with handling human tissue."¹⁹ The downside to the Wilke et al. model was that it was not anatomically correct and did not allow for measurement of disc pressures, thus limiting the use of the model in measuring parameters such as change in facet joint load and disc pressures.

Experimental Method

First generation mechanical analogue lumbar spine segments were developed by using composite materials technology applied in a novel manner. The approach used was to design and fabricate each component of the spine segment with sizes and nonlinear mechanical properties similar to those of a normal human spine. These individual components were then connected together with an anatomically appropriate angle of lordosis. This general technique can be compared with methods of building models in the finite element method. Methods of fabrication and properties of each component are given as follows.

Mechanical Analogue Vertebrae

The synthetic vertebrae of the analogue spines were synthetic analogue vertebrae T12 through L5 (Pacific Research Laboratories Inc., Vashon, WA) with an articulation to a polyurethane foam portion of the top of S1. The analogue vertebrae (as supplied by Pacific Research Laboratories) consist of a shell of E-glass filled epoxy to represent cortical bone and polyurethane foam to model the cancellous bone. Cortical bone in the synthetic analogue vertebrae was simulated by the same E-glass-filled epoxy used to represent cortical bone in third generation composite femurs also made by Pacific Research Laboratories. Typical properties for the E-glass-filled epoxy are 90 MPa strength and 12.4 GPa stiffness in tension, 120 MPa strength and 7.6 GPa stiffness in compression.²⁰ The density of the polyurethane foam can be varied to represent different qualities of cancellous bone.¹¹ A 0.32 g/cm³ density cellular polyurethane foam was used to model normal cancellous bone of the vertebrae. Typical compressive properties of this foam are 5.4 MPa for compressive strength, 137 MPa for compressive elastic modulus.²⁰ These analogue bones were joined together using mechanical analogue ligaments and discs designed specifically for the analogue spine. Special care was made to ensure that the facet joints were in proper articulation, creating an angle of lordosis between 30 and 60 degrees.

Mechanical Analogue Ligaments

Mechanical analogues of the anterior longitudinal ligament (ALL), posterior longitudinal ligament (PLL), interspinous ligament (IL), supraspinous ligament (SL), and ligamentum flavum (LF) were iteratively designed individually, specifically to match the mechanical properties of normal human fresh ligaments.

The experimental procedure for the development of each of the spinal ligaments consisted of five phases: (1) Acquisition of mechanical property and cross-sectional area data for each human biological ligament from the literature. (2) Development of artificial composite analogue ligaments that display nonlinear mechanical behavior. (3) Uniaxial tensile testing of composite ligaments as described in the literature for biological ligaments. (4) Com-

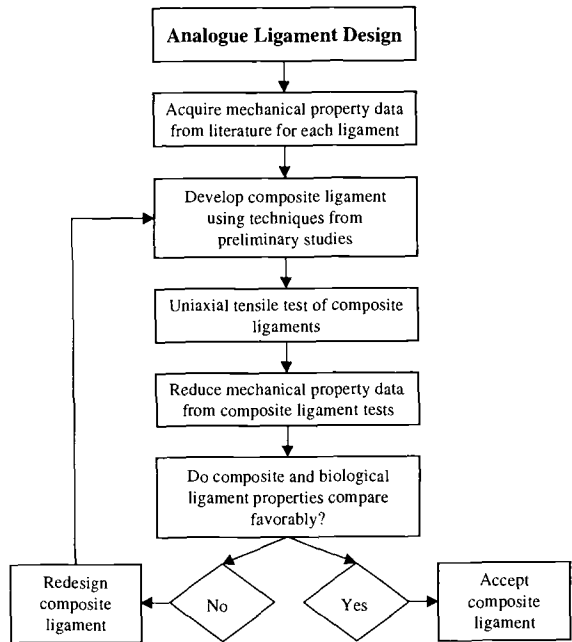


Figure 1. Iterative design process for synthetic analogue ligaments. The same general process was used in the development of analogue intervertebral discs.

parison of composite ligament mechanical properties to biological ligament mechanical properties. (5) Iterative design of composite ligaments [restarting at #2] as required to create ligaments with mechanical properties that are comparable to those of biological ligaments. These steps are outlined in Figure 1. Final materials used in the construction of the ligaments were chosen by trial and error evaluation of many different types of materials that exhibited nonlinear load-deformation characteristics in tension. Criteria for selection included nonlinear behavior range, thickness, strength, interface with silicone matrix, availability, and reproducibility.

The ALL was composed of five alternating layers of 1/8 inch gage polyester fabric mesh (3 layers) and partially stretched (10 percent strain) 1/16 inch gage metal screen wire at a 45° bias (2 layers) embedded in Grade 65 HTV silicone rubber (A-PSE-65 Prosthetic Silicone, Factor II Inc., Lakeside, AZ). The ALL dimensions used were 3.5 mm thick, 15.75 mm wide, and 25 cm length. The PLL was composed of one layer of fabric mesh and one layer of highly stretched (30 percent strain) metal screen wire at a 45° bias embedded in Grade 65 silicone rubber. The PLL dimensions were 1.75 mm thick, 9.0 mm wide, and 25 cm length. The remaining ligaments (IL, SL, and LF) were all 7.5 mm wide and 3.35 mm thick and were composed of moderate durometer silicone sheet (Grade 30). The cross sectional areas of each individual ligament were equal to those reported in the literature for the lumbar spine.¹² The length of these ligaments depended on the connection space between the individual vertebrae. Facet capsulary ligaments were composed of silicone adhesive with fabric mesh embedded and wrapped around the facet joints. The cartilage was simulated by pure silicone interfaces. Each ligament was iteratively designed and developed so that its load-displacement properties were similar to those reported in the literature for the specific ligament for typical physiological levels.^{5,12} In particular, the nonlinear load characteristics of the ALL and PLL were reproduced to some extent in the analogue components. Testing of analogue ligaments was done in a manner similar to that reported in the literature for cadaveric tissues.⁶ Initial stiffnesses were approximately 35 MPa up to 0.8 percent strain and 153 MPa up to 2 percent strain for the ALL and PLL, respectively. Secondary stiffnesses were approximately 65 MPa and 250 MPa for the ALL and PLL, respectively.

Mechanical Analogue Intervertebral Discs

Intervertebral discs were made from molds created to have the shape of the individual disc for the specified level. Molds were created by first forming a wax replica of the individual disc then using the lost-wax method to form a polymethyl methacrylate mold around the wax replica. The discs were made by forming a one-quarter inch thick outer layer of Grade 65 HTV silicone with an outer ring of screen wire mesh oriented at a 45° bias embedded in the silicone. The wire mesh was wrapped around the upper and lower regions of the analogue annulus to connect into the analogue nucleus pulposus. The inner region of the disc (or the analogue nucleus pulposus) was composed of a lower durometer silicone (A-PSE-30 Prosthetic Silicone, Factor II Inc., Lakeside, AZ). Each intervertebral disc was iteratively designed and developed so that its load-displacement properties were similar to those reported in the literature. Figure 2 shows typical load-displacement data for two discs as compared to data reported in the literature.^{7,11} Note that the nonlinear load characteristics of the intervertebral discs were reproduced in the analogue components.

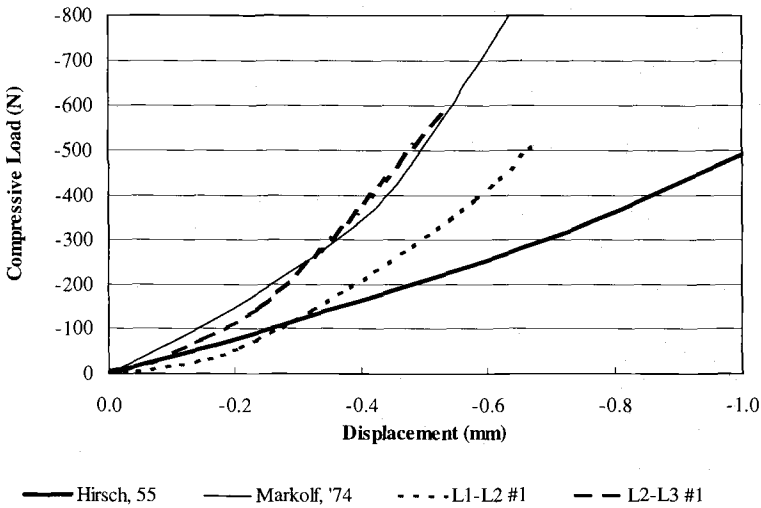


Figure 2. Typical load-displacement data for two intervertebral discs compared to data as reported in the literature.^{7,11}

Assembly of the Lumbar Analogue Spine Model

Mechanical analogue lumbar segments were formed by adhering the various parts together (at anatomically correct locations) using RTV aerospace grade silicone rubber (Gray RTV 157 Silicone Adhesive, General Electric, Waterford, NY). In the two models that were built, angles of lordosis of 54 degrees and 45 degrees were achieved. Higher strength attachment of the intervertebral discs to the vertebral bodies (i.e., closer to natural strength) was achieved by first using high strength epoxy to adhere one Velcro pad side to the bottom and top of the disc. Fibrous attachment of the disc to the endplate was then achieved by adhering the molded intervertebral disc to the Velcro pad with high strength RTV silicone adhesive. The Velcro pad provided interdigitation of the silicone with the endplate, thus modeling the natural fibrous attachment at the endplate-disc junction.

To prepare for mechanical testing, the vertebral bodies were potted in special jigs so that the segment was axially aligned from the center of the body of T12 to the middle-top of the body of S1 (the normal axis of alignment in standing) to form a complete lumbar segment.¹ The final assembly consisted of the seven composite vertebral bodies (T12-S1), one anterior longitudinal ligament, one posterior longitudinal ligament, one ligamentum flavum, ten interspinous and one supraspinous ligament, six intervertebral discs and twelve capsular facet ligaments.

Preliminary Validation

In this study, preliminary evaluation of the validity of the lumbar analogue spine model was performed using mechanical rigidity testing and directly comparing results

from the analogue models to fresh frozen calf spines. Calf spines were used for preliminary validation because the variance in their mechanical behavior is much lower than human spines. As reviewed previously, calf spines have been favorably compared to human cadaveric spines for the purposes of mechanical testing.¹⁷ Spinal operations and instrumentation are typically used on middle-aged or younger patients. Most testing with this analogue model will examine these types of operations and instrumentation. It is difficult to obtain human cadaveric spines in the middle-age ranges. Older aged specimens would have even more variable (and perhaps less representative) properties. Calf spines are also much less expensive than human spines and more readily obtained. Human cadaveric specimens of middle age are currently requested for use in further validation.

Rigidity testing consisted of load control testing in flexion, extension, torsion, axial compression, right lateral bending (RLB) and left lateral bending (LLB). Bending moments of 3 N-m and axial loads of 600 N, load and moment ranges were applied.

These values were in the middle of those used by other investigators, as reported in the literature.^{4,18} Figure 3 shows the model being tested in flexion using a four centimeter offset to produce bending moments. Therefore, the testing methods used did not provide a pure bending, but instead a combined bending and axial compression. At the time of testing, the capability of testing in pure bending was not available to the authors. Specimens were cyclically loaded with $R = +0.1$ for five cycles at a rate of 0.5 Hz. Load-

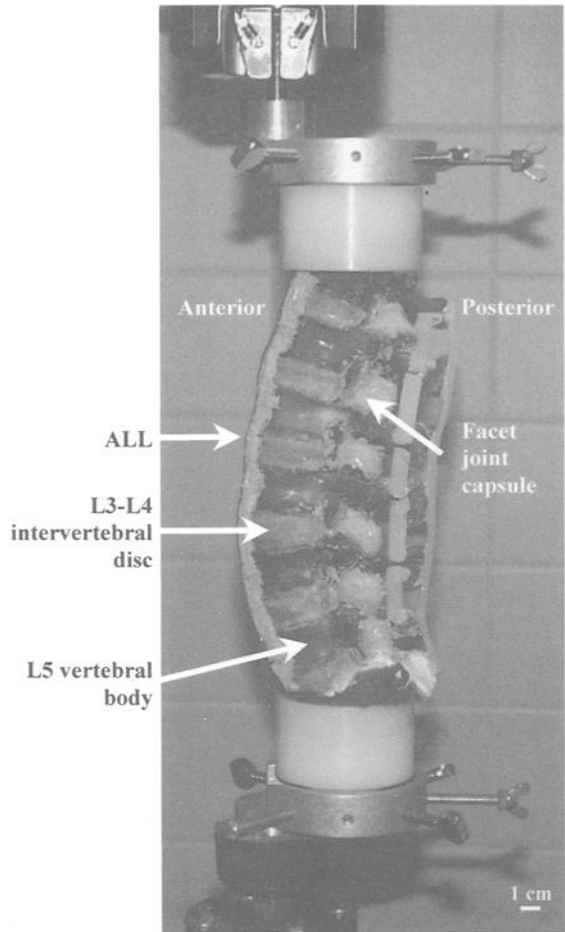


Figure 3. Analogue lumbar spine specimen tested in flexion. The top was loaded through a ball and socket, thus providing full freedom of rotational movement. A four-centimeter offset was used in all modes of bending.

displacement data was collected for all cycles. The slope of the secondary linear region (the "EZ" region) was measured from the fifth cycle. In the testing mode available, specimens could not be loaded from, for example, flexion through extension, so reliable data in the low load regimen (the "NZ" region) could not be measured.⁶

Three fresh frozen calf spines were obtained from a supplier who routinely supplies calf spines to industry for testing spine instrumentation (Green Village Packing, Green Village, NJ). The calf spines were dissected down when partially frozen and potted and tested after they were completely thawed. All testing was completed within eight hours of thawing.⁹ Calf spines were tested in flexion, extension, torsion, axial compression, right lateral bending and left lateral bending in a manner identical to that used to test the analogue models. Data was collected and analyzed in the same technique as with the analogue spines.

Results

The lumbar analogue spine model showed good reproducibility between tests on the same model and between two different models. The load-displacement behavior was nonlinear and displayed hysteresis. The analogue spine model has been found to have rigidity values in the same general range as fresh-frozen calf spines. Calf spines have been shown in the literature to have motion segment properties in flexion, extension, LBR, and LBL that are in the same general range as fresh human spine segments.^{14,17} Table 1 gives average "EZ" rigidities of these specimens and percent differences for two analogue models in comparison to three calf spines tested in an identical manner. Figures 4 and 5 show this rigidity data in graphical format. For the four modes of bending and torsion, the analogue spine segment was consistently more rigid with the average percent difference between approximately 25 and 65 percent. In axial compression, the calf spine was much stiffer than the analogue spine with a 155% difference. This large difference in axial compression may possibly be attributed to the very low angle of lordosis (i.e., "flat back") of the young calf spines.

Table 1 - Average rigidities in the "EZ" region for both the lumbar calf and analogue spine specimens. Note the large difference in axial rigidity that may be due in part to the "flat back" nature of the calf spine.

Average Rigidity in "EZ" Region						
Mode of Loading				Lateral Bending	Lateral Bending	
Specimen Type	Axial (N/mm)	Flexion (N-m/deg)	Extension (N-m/deg)	Right (N-m/deg)	Left (N-m/deg)	Torsion (N-m/deg)
Lumbar Calf	219.5	0.653	0.536	0.683	0.618	0.341
Lumbar Analogue	86.2	1.888	0.855	0.923	0.855	0.590
Average Percent Difference	-154.7	65.4	37.3	26.1	27.7	42.2

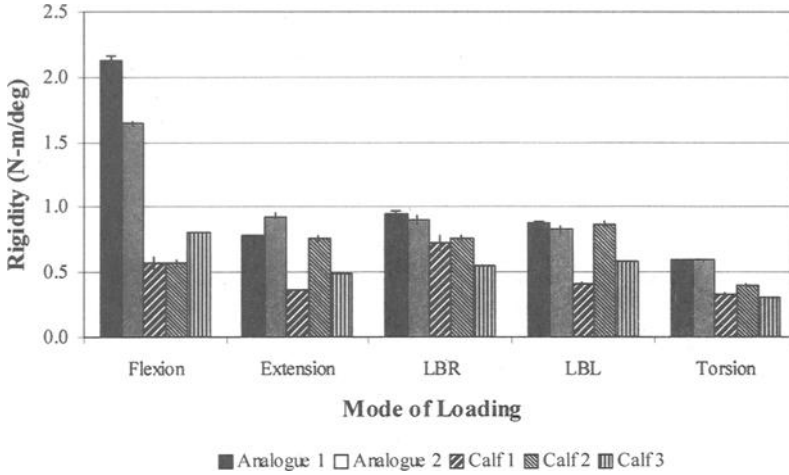


Figure 4. Bending rigidities measures for two human mechanical analogue spines in comparison to three calf spines. (LBL = left lateral bending, LBR = right lateral bending)

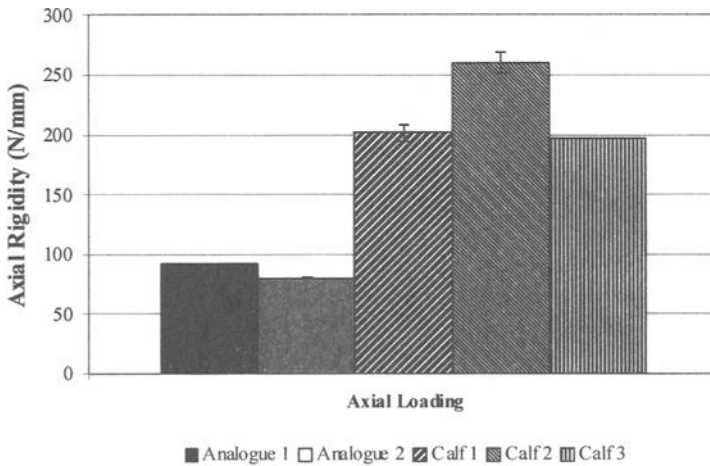


Figure 5. Axial rigidity measures for two human mechanical analogue spines in comparison to three calf spines. The large differences may be due in part to the “flat back” nature of the calf spines.

Discussion

As shown in Table 1 and Figures 4 and 5, the analogue spine segment was consistently more rigid for the four modes of bending and torsion, with the average percent difference between 25 and 65 percent. Wilke et al.¹⁴ reported the greatest similarity between human and calf functional spine unit biomechanical properties in axial rotation and lateral bending. These modes of loading also demonstrated the greatest similarity in the present study between calf spines and analogue models. The relatively large percent variations in secondary stiffness are not unlike those differences found in Wilke's comparative study.¹⁴ The tissues of a calf are immature and would naturally exhibit different mechanical properties than an adult human spine. The calf spine also has a very low angle of lordosis or is "flat backed" in comparison to a typical human spine. With a low angle of lordosis the specimen rigidity in the secondary or "EZ" region would be increased the most axial compression. As the angle of lordosis increases (i.e., the curvature of the structural body increases), the lower stiffness ligaments assume a larger role in resistance to deformation under higher loads.

One would not expect young calf spines to be the absolute standard for which a model of a human cadaveric spine is developed. The purpose of this initial development and evaluation was to test if the rigidity of the analogue model was in the general range of another model used for biomechanical testing of spinal devices. Calf spines are easy to obtain and relatively consistent in mechanical properties because of the narrow range of size and weight of the animals. Human cadaveric spines have been shown to exhibit a wide range of data. Even data generated in one laboratory with similar age group specimens and consistent loading techniques has been shown to vary widely. One design goal of the mechanical analogue lumbar spine segment is to make a consistent model on which the effect of devices and surgical techniques on the spine segment can be tested without the wide natural variance in spine properties clouding the effect of the procedure. One use of the mechanical analogue spine model would be as an initial step in first understanding the general nature of a technique or problem. The natural variance in normal spines is an important factor to consider and the effects of these variances can be better studied once the general nature of a problem is understood. Future work with the analogue models can include development of "nonstandard" specimens. Variations in models can be made by altering component material properties, load-deformation response, and bone and ligament orientations. Examples of model variations include low density vertebral bodies to simulate osteoporosis, changes in the nonlinear stiffness of discs to simulate degeneration at single or multiple levels, increased laxity in ligaments represented by an increase in the load-deformation response, and laxity of facet capsules through material property modifications.

The rate of testing used in this study was 0.5 Hz, similar to a physiological rate of loading during normal movement and a typical rate of loading used in the quasistatic testing of cadaveric specimens. As the rate of loading increases, one would expect a change in the mechanical response of the models and the biological specimens. Further work on development of the analogue spine model would include comparison at different loading rates. Similarly, the loads and moments applied to the analogue model in this study were not at the maximum levels that could be applied before failure of the model.

Further development will include determination of failure of the analogue models under quasistatic loading and in fatigue at physiological load levels.

The anatomically correct adult human lumbar spine model discussed in the present work is in its infancy. In the initial stages of research and development, however, the results presented in this article show it to be in the general range of mechanical behavior of calf spine segments. Research in progress includes comparison to human cadaveric spine segments and the development and application of a pressure-measuring mechanical analogue intervertebral disc. Iterative redesign and complete validation of the anatomically correct mechanical analogue spine would allow it to be used in the study many clinical questions and aid in the design and development of spinal instrumentation.

Conclusion

Mechanical testing of spine stabilization (implant) devices is very limited at the present date due to the special problems of testing biological structures controlled by soft tissues. Development and complete validation of the anatomically correct mechanical analogue spine would open the doors for examining a multitude of other clinical questions. Surgical procedures such as laminectomy and discectomy could easily be performed on the analogue spine. Further validation of the current model with comparison to human cadaveric specimens is required. Future testing will include application of pure bending such that both the NZ and EZ regions of load-deformation behavior can be compared.

The anatomically and mechanically suitable analogue spine segment would allow researchers and manufacturers to test devices and the effect of surgical procedures in a more reproducible model than is currently available. This capability would assist in the design and development of better implants for many different applications in spine surgery. It is anticipated that the need for adequate analogue spine segments and Functional Spine Units (FSUs) will be realized even more in the coming years by both the FDA and medical device companies for both design of spinal instrumentation and fatigue testing of these implants.

Acknowledgments

The authors gratefully acknowledge partial funding of this work by EBI, L.P. and the cooperation of Pacific Research in molding vertebrae.

References

- [1] Bernhardt M., "Normal Spinal Anatomy: Normal Sagittal Plane Alignment," *The Textbook of Spinal Surgery*, Philadelphia, JB Lippincott, 1997.
- [2] Cunningham B. W., Yoshihisa K., McNulty P. S., Cappuccino A., McAfee P. C., "The Effect of Spinal Destabilization and Instrumentation on Lumbar Intradiscal Pressure: An In Vitro Biomechanical Analysis," *Spine*, Vol. 22, 1997, p. 2663.
- [3] Dick J. C., Zdeblick T. A., Bartel B. D., Kunz D. N., "Mechanical evaluation of cross-link designs in rigid pedicle screw systems," *Spine*, Vol. 22, 1997, p. 4.
- [4] Glazer PA, Colliou O, Klish SM, Bradfore DS, Bueff HU, Lotz JC: Biomechanical analysis of multilevel fixation methods in the lumbar spine. *Spine*, Vol. 22, 1997 p. 2.

- [5] Goel V. K., Voo L M., Weinstein J. N., Liu Y. K., Okuma T., Njus G.O., "Response of the ligamentous lumbar spine to cyclic bending loads," *Spine*, Vol. 13, No. 3, 1988, pp. 294–300.
- [6] Goel V. K., Weinstein J. N., "Biomechanics of the Spine: Clinical and Surgical Perspective," CRC Press, Inc., Boca Raton, FL, 1990.
- [7] Hirsch C., "The reaction of intervertebral discs to compression forces." *J Bone Joint Surg*, Vol. 37A, 1955, p.118.
- [8] Kornblatt M. D., Casey M. P., Jacobs R. R., "Internal fixation in lumbosacral spine fusion," *Clin Orthop*, Vol. 203, 1986, pp. 141–150.
- [9] Lucas G. L., Cooke F. W., Friis E A., *A Primer of Biomechanics*, New York, Springer, 1999.
- [10] Markolf K. L., Morris J. M., "The structural components of the intervertebral disc," *J. Bone Joint Surg*, Vol. 56A, 1974, p. 675.
- [11] Szivek J. A., Thomas M., Benjamin J. B., "Characterization of a synthetic foam as a model for human cancellous bone," *J Appl Biomater*, Vol. 4, No. 3, 1993, pp. 269–272.
- [12] White A. A., Panjabi M M., *Clinical Biomechanics of the Spine*, 2nd Ed., J. B. Lippincott, Philadelphia, PA, 1990.
- [13] Wilke H. J., Kettler A., Claes L. E., "Are sheep spines a valid biomechanical model for human spines?" *Spine*, Vol. 22, 1997, p. 20.
- [14] Wilke H. J., Krischak S., Claes L E., "Biomechanical comparisons of calf and human spines," *J Ortho Research*, Vol. 14, 1996, pp. 500–503.
- [15] Wilke H. J., Jungkunz B., Wenger K., Claes L. E., "Spinal segment range of motion as a function of in vitro test conditions: effects of exposure period, accumulated cycles, angular-deformation rate, and moisture condition," *Anat Rec*, Vol. 251, No. 1, 1998, pp. 15–19.
- [16] Wilke H. J., Krischak S., Claes L. E., "Formalin fixation strongly influences biomechanical properties of the spine," *J Biomech*, Vol. 29, No. 12, 1996, pp. 1629–1631.
- [17] Wilke H. J., Krischak S. T., Wenger K. H., Claes L. E., "Load-displacement properties of the thoracolumbar calf spine: experimental results and comparison to known human data," *Eur Spine J*, Vol. 6, No. 2, 1997, pp. 129–37.
- [18] Wilke H. J., Wenger K., Claes L., "Testing criteria for spinal implants: recommendations for the standardization of in vitro stability testing of spinal implants," *Eur Spine J*, Vol. 7, No. 2, 1998, pp.148–154.
- [19] Wilke H. J., Russo G., Schmitt H., Claes L. E., "A mechanical model of human spinal motion segments," *Biomed Tech (Berl)*, Vol. 42, No. 11, 1997, pp. 327–331.
- [20] <http://www.sawbones.com/>, Pacific Research Laboratories reported data.

Denis J. DiAngelo¹ and Kevin T. Foley²

An Improved Biomechanical Testing Protocol For Evaluating Multilevel Cervical Instrumentation In A Human Cadaveric Corpectomy Model

Reference: DiAngelo, D. J., and Foley K. T., “An Improved Biomechanical Testing Protocol For Evaluating Multilevel Cervical Instrumentation In A Human Cadaveric Corpectomy Model,” *Spinal Implants: Are We Evaluating Them Appropriately? ASTM STP1431*, M. N. Melkerson, S. L. Griffith, J. S. Kirkpatrick, Eds., ASTM International, West Conshohocken, PA, 2003.

Abstract: Spinal instrumentation is commonly used to stabilize the multi-level strut-grafted cervical spine. There are no standard tissue-based testing protocols for evaluating spinal devices. An improved biomechanical testing protocol was developed to study the strut-graft mechanics of the instrumented cervical spine in flexion and extension. The biomechanical stability of two different anterior cervical plating systems were evaluated and compared to the harvested condition. A force sensing strut-graft (fssg) was used to measure the axial compressive load. Parameters of stiffness, segmental vertebral motion, and strut-graft loads were statistically compared with a one-way anova ($p < 0.05$) to determine differences between the spine conditions. Applying a bending moment distribution across the cervical spine resulted in a motion response that closely matched the in vivo case. Fssg loads were affected by plate application and specific plate design features. The testing protocol has been used to study the biomechanical stability of various multi-level strut-graft cervical instrumentation. Information of strut-graft loads aided in better understanding graft-plate load-sharing mechanics and clinically-observed multi-level instrumentation failure mechanisms.

Keywords: biomechanical testing, spinal instrumentation, corpectomy, cervical spine, biomechanics, anterior cervical plate, instrumented strut-graft mechanics

¹Associate Professor, School of Biomedical Engineering, The University of Tennessee Health Science Center, 899 Madison Avenue, Suite 801, Memphis, TN 38163

²Associate Professor, Department of Neurosurgery, The University of Tennessee Health Science Center, Memphis, TN

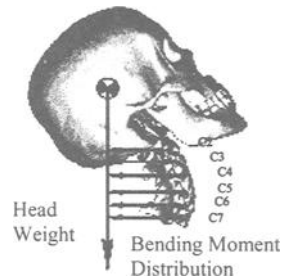
Introduction

Strut-graft fusion with instrumentation is intended to restore the mechanical integrity of the operated spine and decrease graft-related complications. The incidence of graft complications and the nonunion rate of strut-graft fusion increase as the number of spinal levels increases. The mechanism(s) of failure occurring in these scenarios is poorly understood and little is known about the load-sharing mechanics between the strut-graft and instrumentation. Biomechanical testing on human cadaveric tissue offers a practical means for evaluating and ranking different surgical techniques. However, there are no standard tissue-based testing protocols for evaluating spinal devices. Further, in vitro tests can be performed under load control, displacement control, or more recently, hybrid control (combinations of load and displacement) through the use of multi-axis, robotic controllers [9,16,17,37].

The cervical spine consists of a series of free vertebral bodies that exhibit complex, coupled motions and loading behaviors [38]. For the sub-axial cervical spine, in vivo motion is greatest in the sagittal plane with more rotation occurring in extension than flexion.[38] Only small amounts of muscle activity are needed to maintain the head’s orientation in an erect neutral position. Thus, muscle-induced compression is small and head weight is the typical physiologic force that acts on the cervical spine. Flexion or extension of the head induces a bending moment distribution throughout the cervical spine that increases caudally and acts in combination with the compressive (head weight) force (Figure 1). In vitro testing methods should replicate this motion response.

The objective of this study was to identify the appropriate loading conditions that would replicate the in vivo motion response of the cervical spine, and thus to develop a biomechanical testing protocol for evaluating multilevel surgical devices and techniques used to treat the injured or diseased spine. A comparative study of two different anterior cervical plating systems is given to demonstrate the features of the improved testing method.

Figure 1 - In Vivo Sagittal Motion and Mechanics of the Cervical Spine. This computer model illustration depicts the caudally increasing bending moment distribution (2-5 Nm), greatest at the C5-C6 level, created by continuous rotations with like polarity at each vertebral level (40° flexion or extension) with an axial compressive load (50 N head weight) [6,7,11,23].



Methods

Biomechanical Testing Apparatus

A single controlled degree of freedom testing apparatus called a single actuator adaptable programmable testing apparatus (SAAPTA) was used in this study [3,6,7]. The rigid, three-column frame housed a (servo motor) load actuator (Industrial Device Corp., Novato, CA) connected to a robotic controller (Adept Inc., San Jose, CA). A single axis load cell (Transducer Technologies, Temecula, CA) was in-line with the shaft of the load

actuator. The other end of the single axis load cell was coupled to end mounting fixtures that regulated the end motion and loads applied to the spinal construct. A six-axis force sensor (JR3 Inc., Woodland, CA) was rigidly fixed to the base of the test frame to which the opposite end of the spine was rigidly fixtured and attached. The multi-axis load cell reported the three orthogonal forces and moments transferred through the spine in real-time.

End Mounting Configurations

A sequence of tests were previously performed to analyze different mounting configurations and appropriate ranges of load and motion in order to identify a particular set of end conditions that produce normal motion of the intact spine tissue [6]. The “gold standard” of motion was replication of positions considered normal by anatomists, physical therapists, and neurosurgeons (Figure 1). Three different mounting configurations were evaluated: pinned-pinned (PP), pinned-fixed (PF), and translational / pinned-fixed (TPF) (Figure 2). For the first two conditions, the lower mounting fixtures were either unclamped and free to rotate, or fixed. The upper mounting fixtures converted the single controlled input from the load actuator to either a rotational input alone or a coupled motion input (unconstrained translations and/or rotation in the sagittal plane) and a combined loading state (axial compressive force alone or with a flexion/extension bending moment).

For the TPF case, the upper fixture consisted of a linear bearing and splined shaft assembly that mounted in a rotating joint attached to the actuator (Figure 3). The linear bearing provided a virtually frictionless method for the splined shaft to move relative to the actuator, thus minimizing the shearing forces. The flexion/extension axis of the spine was placed eccentric to the load axis of the actuator and induced a compressive load and flexion/extension bending moment to the upper pot. The specimens were mounted in an inverted neutral orientation with the T1 pot attached to the upper fixture and the C2 pot mounted to the lower base fixture, thereby inducing a greater moment at T1 than C2. Specimens with gross alignment deformities were not used.

A rotational displacement transducer (RDT) (Data Instruments, Acton, MA) was attached to the rotational joint connected to the actuator; this transducer measured the global rotation of the spine. A translational displacement transducer (TDT) (Data Instruments, Acton, MA) was inserted into a custom designed plate between the upper pot and splined shaft connection; the TDT measured changes in the moment arm length.

Non-Destructive Testing Protocol

All tests were performed under displacement control with the sub-axial (C2-T1) cervical spine positioned either in-line (PP; PF) or eccentric (TPF) to the center-line of the vertical actuator shaft. The actuator was programmed to output a triangular shaped displacement-time waveform of 6.4 mm/sec. For each configuration, an increasing incremental displacement was applied until a target moment at T1 between 3 to 4 Nm was reached, or was stopped if any of the following limits were reached: 40° of sagittal plane rotation; 5 Nm bending or torsional moment at T1, or axial compressive load of

500 N for the P-P and P-F configurations or 75 N for the TPF configuration. These values were based on our preliminary test findings [6] and agreed with the limits used by other researchers.[27,29] The spines were preconditioned with five cycles before formal testing. Each test trial included three loading cycles; the third cycle was analyzed.

For the PF configuration, minimal displacement of the actuator quickly produced a high compressive load that exceeded the allowable load limit and induced minimal amounts of vertebral motion. The PP configuration produced an unordered, bipolar motion response similar to that associated with the first mode of column buckling. Further, for both the PP and PF configurations, a non - physiologic internal moment was created in the spine. However, with the TPF configuration, all vertebral bodies moved continuously with the same polarity of rotation. A distributed moment was applied throughout the cervical spine. As such, the TPF configuration satisfied the external loading criteria necessary to replicate the in vivo motion response of the cervical spine.

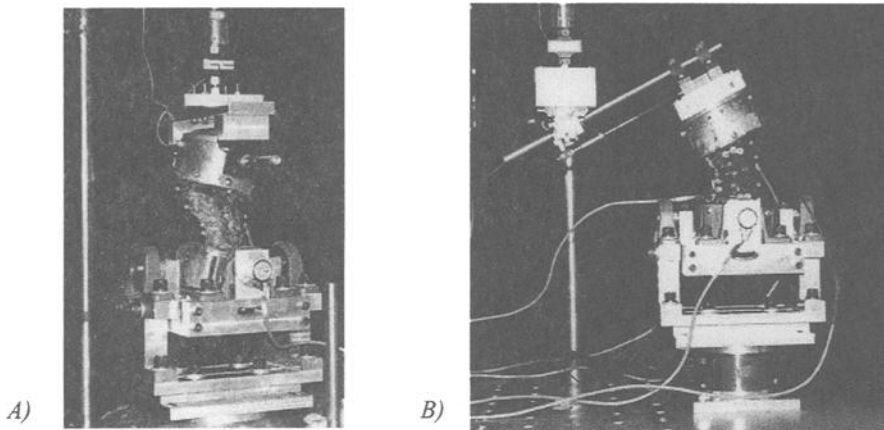


Figure 2 — End Mounting Configurations. A) The PP or PF configuration and B) TPF configuration.

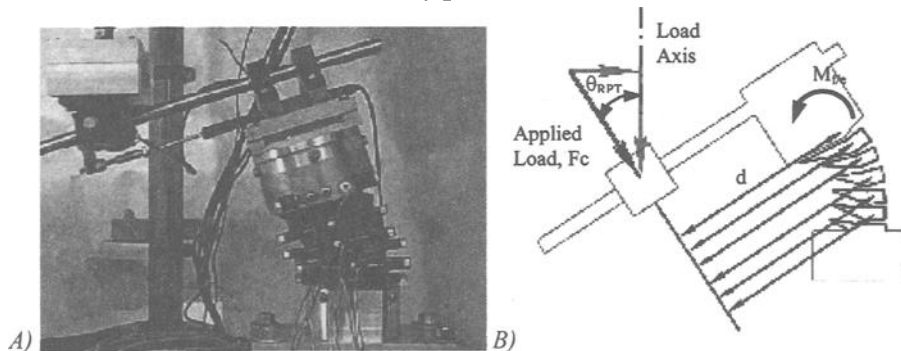


Figure 3 - A) Photograph of a spine mounted in the testing apparatus (SAAPTA). B) Schematic of mounted spine. With the flexion/extension axis of the spine placed eccentric to the load axis of the actuator, a compressive load (F_c) and flexion/extension bending moment (M_{fe} , where $M_{fe} = F_c * d$) were induced.

Improved Testing Protocol

The improved biomechanical testing protocol was modified to study the effects of spinal instrumentation on the strut-graft mechanics of the multilevel corpectomy spine. For the purpose of this paper, the biomechanical results of a comparative study between a constrained anterior cervical plate (CACP) and a semi-constrained translational anterior cervical plate (TACP) are given.

Specimen Preparation and Spine Conditions

Ten fresh human cadaveric cervical spines (C2-T1) were procured from the Medical Education Research Institute (Memphis, TN). The average age and gender of the harvested spines used was 74.2 ± 11.9 years (5 male and 5 female). The spines were harvested and immediately double wrapped in plastic bags and stored at -20°C until preparation. Before preparation the spines were thawed in a refrigeration system for 12 hours. All spines were screened with anteroposterior and lateral radiographs to exclude any with gross osteopenia or anatomic abnormality. Bone density measurements were not done. However, any specimen that was unable to provide adequate screw purchase, as determined the surgeon, was not used.

All spines were evaluated sequentially in five different conditions. They included the harvested (H), strut-graft alone (GA), strut-graft with constrained anterior cervical plate (CACP), and strut-graft with translational anterior cervical plate (TACP). Five spines were tested with the translational plate and five spines with the constrained plate. The Orion™ cervical plating system (Medtronic – Sofamor Danek, Memphis, TN) was used for the CACP conditions and the Premier™ plating system (Medtronic – Sofamor Danek, Memphis, TN) was used for the TACP condition. The two plate designs are shown in Figure 4.

An existing tissue procurement protocol used by our laboratory in other in vitro studies was implemented [9,15]. Prior to testing, the free ends of the vertebral bodies of C2 and T1 were mounted in cylindrical pots using an alignment frame that positioned the cervical spine specimen in a neutral upright orientation. The flexion/extension axis was estimated at the anterior aspect of the facet joint of each vertebra. After testing of the intact spine (H), all spines underwent a corpectomy from C4-C6. The three level corpectomy was performed using standard spinal instruments including a high-speed drill. The corpectomy trough was made 15 mm wide and included resection of the posterior longitudinal ligament. After corpectomy testing, the superior end plate of C7 and inferior end plate of C3 were mortised (1–2 mm depth) to accommodate the force sensing strut-graft (FSSG) (Figure 5A).

Following SG spine testing, the spines were separated into two groups and instrumented with either a constrained anterior cervical plate (CACP, Figure 5B) or a translational anterior cervical plate (TACP, Figure 5C). The plates were appropriately sized by the surgeon and applied according to the manufacturer's specifications from C3 to C7. Standard unicortical screw placement was used with both plate types. With the CACP arrangement, the screws were constrained from translating or pivoting relative to the plate (Figure 4A). A similar screw plate connection was used at the caudal screw attachment site of the TACP. However, at the cephalad screw site, the screws were

positioned at a distance of 2 mm from the outer edge of a slot and were free to travel vertically in either direction. Throughout the entire testing sequence the spines were kept moist at regular intervals with a normal saline mist.

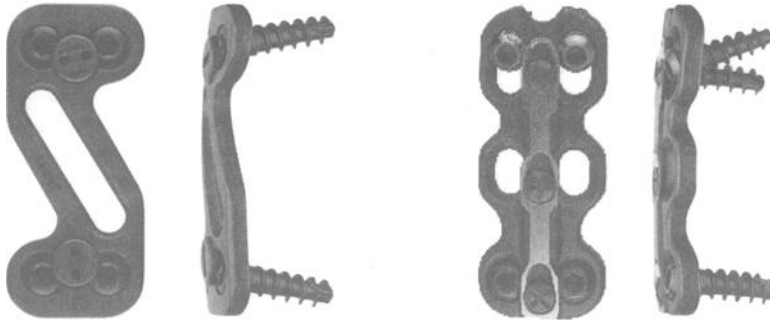
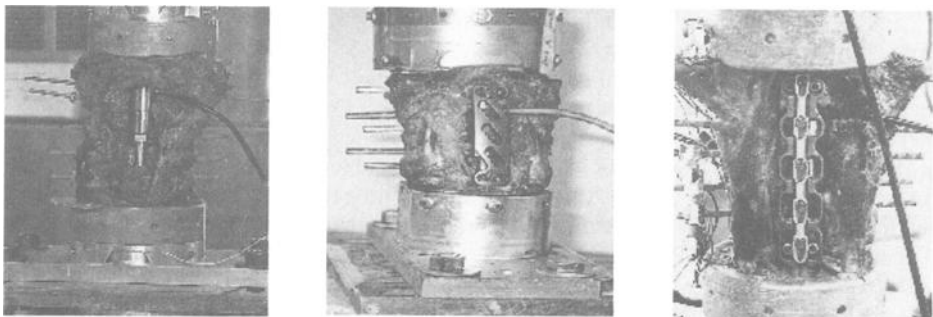


Figure 4 - Anterior cervical plate designs. A) Constrained anterior cervical plate (Orion™, Medtronic Sofamor Danek, Memphis, TN). Upper and lower screws are constrained in location and trajectory. and B) Translational anterior cervical plate (Premier™, Medtronic Sofamor Danek, Memphis, TN). Upper screws are free to translate and pivot in a slot. Lower screws are constrained in location and trajectory.



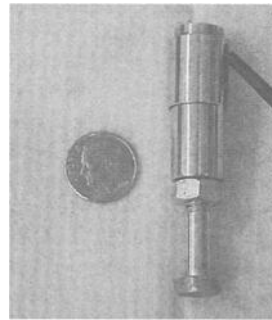
A) Graft-Alone (GA) B) Strut-Graft with CACP C) Strut-Graft with TACP

Figure 5 - Spine Conditions. Mounted spines after A) insertion of strut-graft, B) application of constrained anterior cervical plate, and C) application of translational anterior cervical plate.

Force Sensing Strut-Graft

A custom-designed compression-only FSSG was designed to measure the load transferred through the strut-graft (Figure 6). The length was adjusted until contact at the end plates occurred and a compressive load of 20 N was reached (i.e., approximately 50% of head weight). Output from the FSSG was amplified, then processed and displayed within custom data acquisition routines developed in Labview (National Instruments, Austin, TX). The testing protocol was modified to include the FSSG load in the control strategy; the test was stopped if the FSSG load exceeded 250N.

Figure 6 - A custom designed compression-only force sensing graft was developed to function directly as a typical fibular allograft strut. The FSSG consisted of male end cap, a female end cap, and a button load cell (Cooper Instruments, Warrenton, VA). The male end cap was modified to permit variable length adjustments (40-125mm) that could be locked in position.



Non-contact Motion Measurement System

A three-dimensional (3-D) non-contact real-time measurement system was used to track segmental cervical motion for each testing condition.[8,9] For the two-dimensional motion analysis, target arrays consisting of two light emitting diodes were rigidly attached to each spinous process (Figure 3A). The individual motion segment unit (MSU) rotations were then expressed relative to the subjacent vertebral body using principles of rigid body mechanics.

Data Management and Analysis

Signals from the transducers were collected with a dedicated analog to digital (A/D) data acquisition system (National Instruments, Inc., Austin, TX) and sampled at 10 hz. The data were processed using custom-designed software routines (Labview, National Instruments) and collected in a spreadsheet file for later computational processing and statistical analysis (Sigma Stat, Jandel Scientific, San Rafael, CA).

The moment applied to the spine at T1 (M_a) was calculated from the in-line load cell (F_a), the total rotation of the upper pot (θ_{rdi}), and the displacement offset ($d_a - d_{dt}$) between the upper pot and load axis: $M_a = F_a(d_a - d_{dt})/\cos(\theta_{rdi})$, where d_a is the initial offset distance between the load axis and the center of the upper pot. For each test trial, the vertebral rotation and applied moment data were combined to calculate global (C2-T1) spine stiffness. Moment values of the altered spines at common end limits of motion were normalized to the harvested condition to control intrinsic differences in the specimens and compared using a one-way ANOVA with a Tukey test ($p < 0.05$).

The FSSG loads were measured before and after plate attachment and at end limits of motion common to all spines. A one-way ANOVA with a Tukey test ($p < 0.05$) was used to determine the statistical differences in the strut-graft pre-load, strut-graft end-load, and changes in strut-graft load for the GA, CACP, and TACP conditions.

For each test trial, the relative change in the local (C3-C7) motion of the surgical site to the global (C2-T1) motion was evaluated, as well as the relative changes in the rotational motion at each MSU. A one-way ANOVA with a Tukey test ($p < 0.05$) was used to statistically analyze the normalized motion data.

Results

Mean Relative Rotations and Normalized Motion

The mean relative MSU rotations for the H condition are shown in Figure 7. The motion profile of the cervical spine tested *in vitro* in combined flexion and extension was similar to that of published *in vivo* data [1,12,22,38], as shown in Figure 7B; the highest range of flexion/extension motion occurred at the C5-C6 MSU, as was observed by Lysell [23].

The distributions of the mean relative MSU rotations for the instrumented spine conditions are shown in Figure 8. Application of a constrained plate shifted motion from the operated region to the end segments (C2-C3 and C7-T1) (see Figure 8A). For the CACP spine, the rotation of C2-C3, as a fraction of the total spine rotation, was 32% in flexion and 36% in extension and at C7-T1 was 40% in flexion and 20% in extension. The percent motion contribution of these segments in the H spine were 12% in flexion and 14% in extension at C2-C3 and 16% in flexion and 8% in flexion at C7-T1. For the TACP (Figure 8B), a similar increase in motion compensation occurred at the adjacent segments, but to a lesser extent than for the CACP spine. The percent of the total rotation of C2-C3 was 20% in flexion and 13% in extension and at C7-T1 was 22% in flexion and 32% in extension.

The mean local rotation values of the operated region (C3-C7) for the altered spine conditions are shown in Figure 9. Application of a constrained plate reduced extension motion across the operated region from 70% of the total (C2-T1) motion in the harvested case to 29%. This decrease was significantly lower than that for the GA spine ($p < 0.001$) and TACP spine ($p = 0.03$). The spread in the data limited significance from occurring in the normalized flexion motion.

Cyclic FSSG Loads

The cyclic loading responses of the FSSG for both plated spine conditions are shown in Figure 10. Three parts of the loading curve were analyzed: 1) the initial FSSG preload prior to and following plate attachment, 2) the FSSG load at end limit of 8 degrees, and 3) the change in FSSG load from the resting position to end limit of flexion or extension. A loading range of 5 to 50 N was considered an acceptable, physiologic limit for the FSSG to experience, as it approximates typical head weight. For the CACP spine, the upper limit of this range was exceeded during both flexion and extension. However, for the TACP spine condition, the cyclic FSSG load remained within the physiologic range.

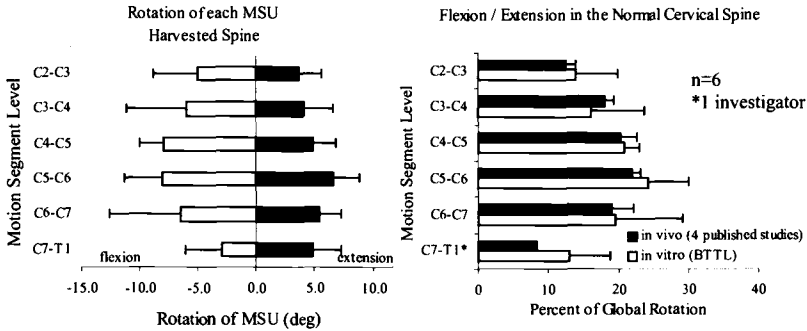


Figure 7 - Relative MSU Rotations – H Spine. A) Mean flexion and extension rotational values at each MSU level of harvested condition. The greatest motion occurred at C5-C6 MSU. B) Combined flexion/extension rotations for the in vitro H spine compared to published in vivo data [1,12,22,38].

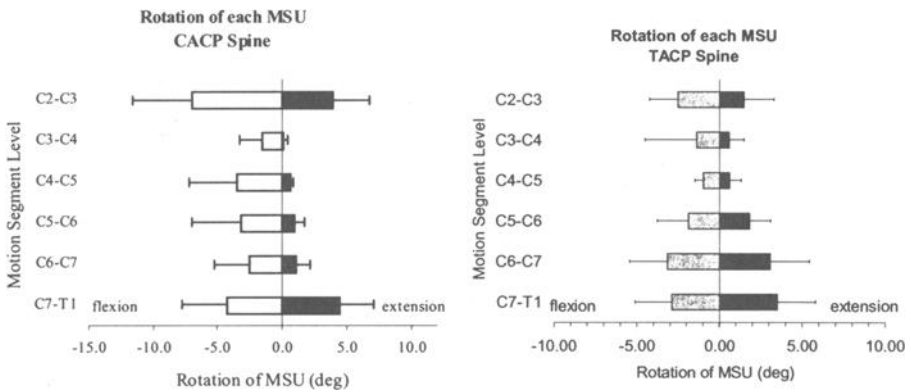


Figure 8 - Relative motion segment unit (MSU) rotations of the A) CACP spine and B) TACP spine.

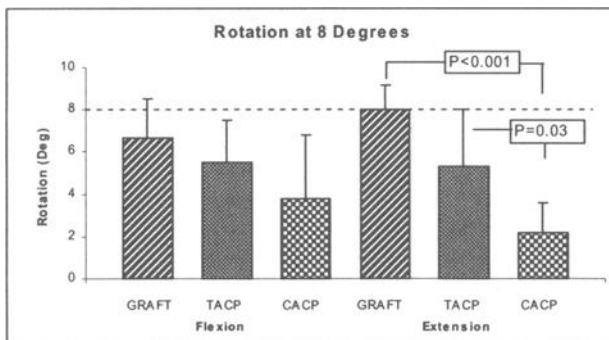


Figure 9 - Normalized motion at 8 degrees for the GA, TACP, and CACP conditions. (Means plus one standard deviation are shown.)

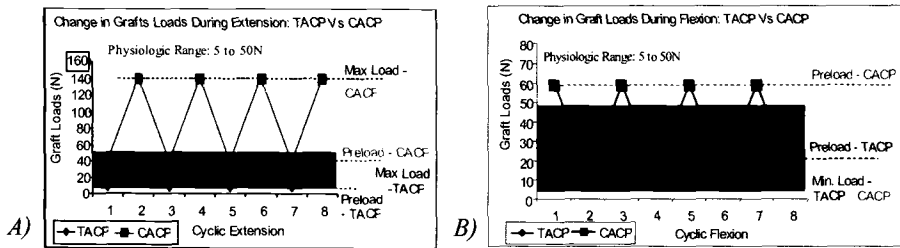


Figure 10— Cyclic FSSG Loads of TACP versus CACP in A) Flexion and B) Extension.

Preload, End Limit, and Change in FSSG Loads

The average preload value for the GA condition was 21.1 N using the combined values for flexion and extension. Following GA testing and application of the translational plate, the average strut-graft preload was 14.4 ± 10.9 N. Application of the CACP significantly increased the average preload to 49.4 ± 19.5 N relative to the TACP ($p < 0.001$) and the GA constructs ($p < 0.001$). This change was due to the divergent (cephalad-to-caudal) nature of the fixed angle screws of the CACP. Importantly, there were no significant differences in FSSG preload between the TACP and GA constructs ($p = 0.49$), indicating neutral application of the plates, as intended.

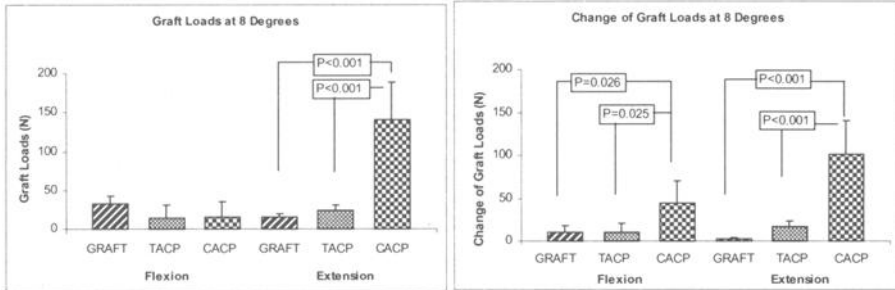
The strut-graft loads are shown in Figure 11. The mean values of the maximum FSSG loads at the end limit of motion (8 degrees of flexion and 8 degrees of extension) are shown in Figure 11A. As would be expected, when placed alone, the strut-graft was loaded in flexion and unloaded in extension. With both plates, these load transfer patterns were reversed. The CACP construct produced significantly higher strut-graft loads in extension than the TACP spine ($p < 0.001$) and GA spine ($p < 0.001$). Importantly, there was no significant difference in maximum strut-graft loads in extension between TACP and GA constructs. In flexion, there were no significant differences in the maximum strut-graft loads between the CACP, TACP, and GA constructs.

The mean values of the change in FSSG load from the preload condition to an end limit of 8 degrees global rotation are shown in Figure 11B. No significant differences occurred between the TACP and GA constructs in either extension or flexion. However, the relative change in the FSSG loads was significantly different for the CACP spine compared to the GA spine in flexion ($p = 0.026$) and extension ($p < 0.001$) and the TACP spine in flexion ($p = 0.025$) and extension ($p < 0.001$).

Normalized Moment

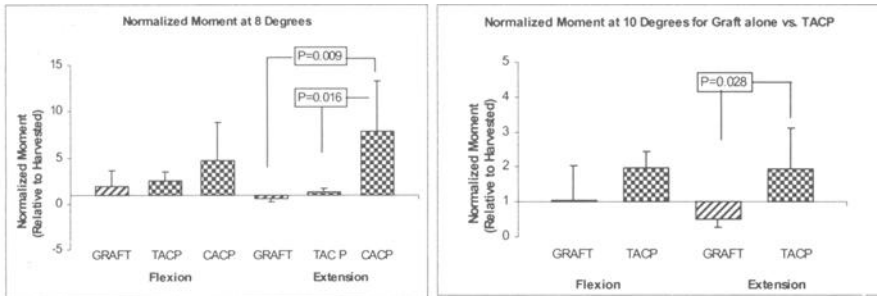
A typical viscoelastic hysteresis response was observed in all the stiffness curves, indicating minimal tissue/ligamentous relaxation had occurred throughout the testing sequence. The normalized moment values were compared at 8 degrees of global rotation. The CACP spine was significantly stiffer than the GA spine ($p < 0.009$) and the TACP spine ($p = 0.016$) (Figure 11). Although there was an increasing trend in the global moment when going from the GA to the TACP to the CACP condition in flexion, the spread in the data limited significance from occurring. A separate comparison between the GA and TACP spines conditions was possible at 10 degrees (see Figure 12). At this

extension limit, a significant difference occurred between the GA and TACP spine conditions ($p = 0.028$).



A) FSSG Load at the Limit of Motion B) Change in FSSG Loads.

Figure 11 - FSSG loads at the A) End limit of motion and B) Change in FSSG loads for the GA, TACP, and CACP conditions. (Means plus one standard deviation are shown.)



A) Normalized Moment at 8 degrees B) Normalized Moment at 10 degrees

Figure 12 - Normalized moment at A) 8 degrees of flexion and extension and B) 10 degrees of flexion and extension for the GA, TACP, and CACP conditions. (Means plus one standard deviation are shown.)

Discussion

Biomechanical Testing Apparatus

Physiologically relevant studies of tissue-implant mechanics require testing systems that replicate the complex, coupled physiologic motions and loads of human joints. With respect to the cervical spine, a series of free bodies must be analyzed for different motion/load end conditions that are prescribed or controlled by the testing device. The motions of interior spinal bodies are measured, but cannot be controlled.

Simple mechanical devices continue to be used that incrementally apply pure static moments to the spine [25]. More commonly, however, programmable testing systems are

employed. Smith et al. [34] used a material testing system (MTS) machine to study spine mechanics; the mounted specimen was highly constrained (no motion was permitted above or below the area of interest) and did not replicate physiologic motion or loading conditions. Custom fixtures must be added to standard machine testing machines to permit coupled motions, but often remain limited to simple loading scenarios, i.e., tension/compression, pure torsion, four point bending. Weinhoffer et al. [36] added a slotted plate fixture to an MTS actuator to enable spinal rotation with non-vertical translation. As the actuator moved down, the upper pot attachment was free to rotate but was constrained to follow a slotted path. The orientation of the slot imposed a specific horizontal versus vertical translational relationship of the upper spinal body that, in turn, was non physiologic. Kunz et al. [21] modified a two DOF MTS machine by adding a third rotational DOF to the base of the device. The device was used for pure moment testing with or without an axial compressive load. James et al. [20] presented a 2 DOF spine tester that regulated axial rotation with either flexion/extension or lateral bending. Independent control of each motor prevented force feedback or force limit control features. Shea et al. [33] developed 3 degrees of freedom (DOF) testing apparatus for planar analysis of spine biomechanics that provided independent control of the displacement output of each axis, but no force feedback control schemes were provided. Wilke et al [37] developed a spine tester that applied pure moments to the superior end of a spinal construct in three orthogonal directions through the use of counter balanced stepper motor units attached to the superior end of a spinal construct. The testing protocol was limited to pure moment loads only. More recently, Gilbertson et al. [17] employed robotics technology to study single MSU lumbar spine mechanics. Extensive modifications to the manipulator itself (at significant expense) were required and in the end the test system was limited to quasi-static analysis or "pure moment" load control schemes.

Strut-Graft Loads

Few investigators have studied the effects of multilevel instrumentation on strut-graft loading mechanics. The optimal compressive load needed to promote bone fusion in the presence of spinal instrumentation is unknown. Rapoff et al. used a calf spine to study load-sharing mechanics in a strut-plate model [32]. The graft-plate construct was modeled as two parallel linear springs; the forces in each were estimated as a function of their displacement changes. Although the plate was found to load-share with the graft, the spines were tested in compression only using a single-level fusion model. Extrapolation from this single-level study to the multilevel situation should not be done without experimental confirmation. Harris et al. [18] used a single level bovine spine model to study the strain patterns in a cervical strut fixed with two different anterior plate designs. For compression loading only, addition of the plates was found to reduce the load supported by the strut-graft. Weinhofer et al. [36] inserted a pressure transducer catheter into the lumbar disk to record changes in disk pressure for different spine conditions, but tested under flexion loading only. Although strain readings demonstrate changes in the loading conditions, no direct relationship exists that characterizes the loading state on the spinal body. Olsewski et al. used a small, compression-only load cell for the measurement of strut-graft loads and a strain gauge technique for measurement of the facet joint load [26]. The loads applied to a single-level strut were estimated using

the load cell for conditions of flexion testing via an eccentrically applied compressive load. As the strut height increased, the level of load borne by the facets decreased, suggesting that excessive distraction of the vertebral segments changed the load-sharing between the posterior elements and the strut, increasing the chances for collapse and potential pseudo-arthrosis. Unfortunately, none of these studies can be properly extrapolated to the understanding of the biomechanics of multilevel strut-grafts or the effects of instrumentation on these grafts.

We have previously developed a multi-axis force sensing strut graft that not only measured tension/compression, but also measured the lateral bending moment, flexion/extension bending moment, and axial torque. The device was used to characterize the strut-graft loading mechanics of anterior, posterior, and combined anterior-posterior cervical instrumentation in a corpectomy model [9,15]. It was determined that the greatest amount of load sharing between the strut-graft and instrumentation occurred in flexion and extension and was compressive. The bending and torsional moments transferred through the strut-graft were minimal (i.e., less than 15% of applied moment). We have since modified the force sensing strut-graft to measure compression only. Other researchers have since begun using similar compressive force sensing strut-grafts to characterize the load sharing mechanics of cervical instrumentation [24]. Aside from differences in testing method (they used load control versus our displacement control), a preload of 50 to 150N was used compared to our preload of 20N. We used a strut-graft pre-load of 20 N or approximately half of head weight that was created by decompressing the spine and tensioning the surrounding tissue. On average, an additional 10 to 50N of load may act on the strut-graft via plate attachment. Using a preload of 20N, the strut-graft load did not exceed the end plate failure strength when tested within our load limits (i.e., 3 to 4 Nm flexion/extension bending moment).

In addition to measuring the strut-graft loads, the internal vertebral disc pressure could also be analyzed. Cripton et al. [4] measured the internal lumbar disc pressure using a needle mounted pressure transducer inserted into the disc space to study posterior lumbar instrumentation. However, in our model, a discectomy was performed and a strut-graft inserted into the region. In the proposed study, measurement of internal disc pressure could be used to better understand the loading mechanics at the adjacent segments.

Biomechanical Testing Protocols

Although a variety of different testing methods have been used to study cervical spine mechanics, the two most common methods are load control and displacement control [16]. Under load control, a pure or constant moment is incrementally applied to the spine and the spine is typically loaded in one plane of motion at a time (i.e., sagittal, frontal, or transverse). Under displacement control, the translational and rotation motions of the vertebrae are controlled. Our biomechanical testing apparatus can be controlled under either load, displacement, or a hybrid control (displacement with force feedback). In this study the displacement of the spine was controlled and, using custom fixtures, a "moment distribution" was induced throughout the spine. Other parameters were also monitored to establish the upper motion limit that included the applied moment, applied load, and strut-graft load. A limit value was assigned to each parameter and the test was stopped if any limit checks were exceeded. This arrangement is vastly different than and superior to

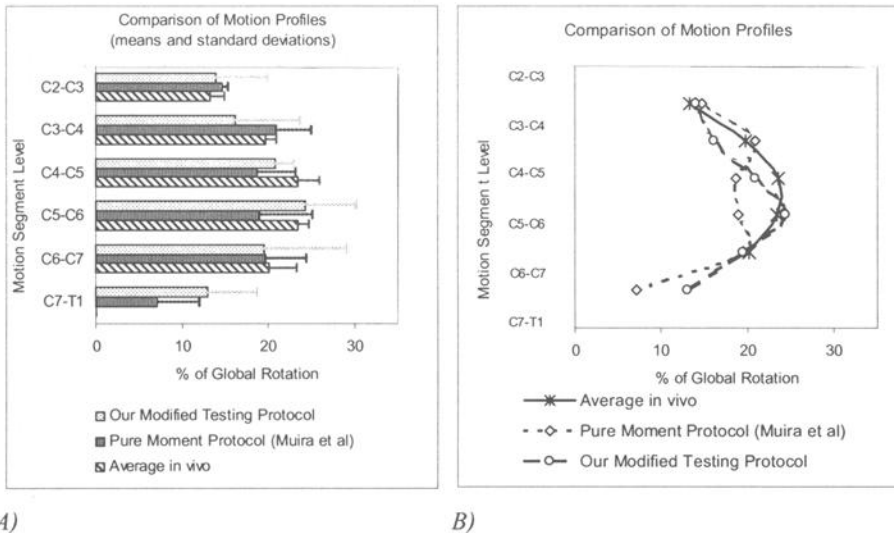
pure-moment methods where there is no limit check on the resultant motion or strut-graft load. Further, pure moment protocols typically use moment values in the range of 1 to 2 Nm. However, when analyzing spinal instrumentation, this load level may not be sufficient to induce measurable differences in the motion response.

A question arises as to which testing method better replicates the in vivo motion behavior of the cervical spine. Miura et al. recently described a method to simulate in vivo cervical spine kinematics using a preload and pure moment protocol [25]. The technique of a follower load was used in conjunction with a pure moment. A critical detail of the follower load concept is to pass a compressive load through the centers of rotation of each motion segment unit (MSU). In their study, the IAR was placed near the lateral masses and remained fixed for the flexion and extension tests. However, this IAR position was based on three cited studies [2,13,35], none of which performed an error analysis on the propagation of error associated with the theoretical calculation itself, nor were the instant centers determined over small ranges of motion that typically occur between two adjacent MSUs (i.e., 2 to 3 degree increments). We have previously shown that the error in calculating the location of the instant axis of rotation (IAR) can be large (as high as +/- 10mm) for small angular changes (2 to 3 degrees) and that the IAR position is significantly different in flexion than in extension [10]. The motion response using their pure moment protocol with a follower load is shown in Figure 13, along with an average in vivo data set [12,14,19,22,30,31], and MSU rotational patterns from our testing protocol. They concluded that since the amounts of rotation at each cervical MSU were not significantly different from a collection of in vivo data, the protocol was acceptable. However, the combined mean flexion/extension rotational values did not always follow the in vivo pattern and in some instances went in the opposite direction or remained constant across multiple MSU levels (see Figure 13B) at the region where the predominant amount of motion occurs in the cervical spine (i.e., C4-C5 and C5-C6). The trend in their data suggests that if the sample size were increased, significant differences would exist between their in vitro data and the in vivo data.

The follower load concept was developed by Patwardhan et al. [28] to allow the intact spine to withstand greater compressive loads without buckling. A compressive load is applied along the bending axis of the spine to simulate the net resultant action of muscles on either side of the spine. The follower load has been successfully used to demonstrate how the intact multi-segmental spine can withstand large compressive loads without buckling [28]. Our modified testing protocol was designed to study the multilevel instrumented cervical spine in a corpectomy model. It remains unknown as to the level of strut-graft load experienced in vivo during the bone remodeling phase. Further, in the instrumented condition, a collar or halo is often used for extra stabilization. Hence, between the instrumentation and halo or collar, it is not known how much additional muscle force is needed to stabilize the spine or whether an excessively large compressive load occurs. Use of the follower load to study the multi-level instrumented corpectomized spine may artificially add more stability to the spine than occurs in vivo. Other investigators [5,24] studying the mechanics of the instrumented strut-grafted spine have used the follower load to apply a pre-load (100 to 150N) to the grafted spine, then add the plate to the grafted construct. By doing so, any additional graft load due to the plate application (which can be as high as 100 to 150N) will be additive to the existing 100 N pre-load. The end resultant is that the strut-graft load approaches the failure strength of cancellous bone before any moment has been applied to the spine. If the

vertebral end plates are mortise to accommodate the strut-graft, then the level of strut-graft load quickly approaches the failure strength of the cancellous bone.

Lastly, when studying long segment plating systems in a corpectomy model the predominant load on the strut-graft occurs in flexion and extension. Similarly the predominant change in motion at the screw plate junction between a translational plate and a constrained plate occurs in flexion and extension. Testing in lateral bending may show measurable differences, but they will not be as significant as those that occur in flexion and extension. As a result, when analyzing long segment anterior cervical instrumentation in a corpectomy model, flexion/extension tests must be done. Lateral bending and axial rotation tests could be done but are not essential.



A) Figure 13 – Combined Flexion/Extension Motion: A) Average in vivo versus in vitro motion responses for pure moment loading [25] and modified testing protocol. Average values from several in vivo studies are plotted for comparison. [12,14,19,22,30,31]

Conclusion

An improved biomechanical testing protocol was developed that replicated the physiologic flexion and extension motion response of the cervical spine. Aspects of the protocol were demonstrated through an analysis of two different anterior plating systems having unique screw-plate features. We have also used the protocol to study other multilevel cervical spine instrumentation [9,15]. Information regarding strut-graft loads aided in better understanding graft-plate load-sharing mechanics and failure mechanisms of the instrumented multilevel corpectomized spine. Further, analysis of the motion distribution across the operated site and segments adjacent to the fused region were useful parameters to characterize the different screw-plate design features.

Acknowledgments

An engineering research grant from The Whitaker Foundation. Tissue procurement was coordinated through Medical Education and Research Institute (MERI, Memphis, TN). W. Liu, Ph.D. and K. Olney, B.Sc. for assistance with biomechanical tests.

References

- [1] Amevo B., Macintosh J. E., Worth D., and Bogduk N., "Instantaneous axes of rotation of the typical cervical motion segment: I. An empirical study of technical errors," *Clin Biomech*, 1991, Vol.6, pp. 31–37.
- [2] Amevo B., Worth D., Bogduk N., "Instantaneous axis of rotation of the typical cervical motion segments: A study in normal volunteers. *Clin. Biomech.*, Vol. 6, 1991, pp. 111–117.
- [3] Chen J., "Development of a flexible biomechanical testing apparatus," MS Thesis, UT-Memphis, 1996.
- [4] Crompton P. A., Gautham M. J., Wittenberg R. H., Nolte L. P., "Load sharing characteristics of stabilized lumbar spine segments," *Spine*, 2000, Vol. 25, No.2, pp. 170–179.
- [5] Crompton P. A., Miura T., Panjabi M. M., "The effects of physiologic compressive preload on the in vitro flexibility of the lower cervical spine," *Proceedings of the 2001 Cervical Spine Research Society*, Poster #35, pp. 214–215.
- [6] DiAngelo D. J., Faber H. B., Dull S. T., Jansen T. H., "Development of an in vitro experimental protocol to study the extensional mechanics of the cervical spine," 1997 *ASME Advances in Bioengineering*, November, 1997.
- [7] DiAngelo D. J., Jansen T. H., Eckstein E. C., Foley K. T., Dull S. T., "Measurements for the in vitro failure of multi-level instrumented cervical spine," 1997, *ASME Advances in Bioengineering*, November, 1997.
- [8] DiAngelo D. J., Vossel K. A., Jansen T. H., "A multi-body optical measurement system for the study of human joint motion," 1998, *ASME Advances in Bioengineering*, November, 1998.
- [9] DiAngelo D. J., Foley K. T., Vossel K. A., Rampersaud Y. A., Jansen T. H., "Anterior Cervical Plating Reverses Load Transfer Through Multilevel Strut-Grafts," *Spine*, 2000, Vol. 25, No.7, pp. 783–795.
- [10] DiAngelo D. J., Vossel K. A., Foley, K. T., "The instant axis of rotation of the cervical spine in flexion and extension," *Proceedings of the 2000 Cervical Spine Research Society*, Poster #30, pp. 203–204.
- [11] Dimnet J., Pasquet A., Krag M.H., Panjabi M., "Cervical spine motion in the sagittal plane: kinematic and geometric parameters," *J Biomech*, Vol. 15, No.12, 1982, pp. 959–969.
- [12] Dvorak J., Froehlich D., Penning L., Baumgartner H., and Panjabi M., "Functional radiographic diagnosis of the cervical spine: Flexion /extension," *Spine*, 1988, Vol. 13, pp. 748–55.
- [13] Dvorak J., Panjabi M. M., Novotny J. E., et al., "In vivo flexion/extension of the normal cervical spine," *J Orthopedic Res*, 1991, Vol. 9, pp. 828–834.
- [14] Dvorak J., Panjabi M. M., Grob D. et al., "Clinical validation of functional flexion/extension radiographs of the cervical spine," *Spine*, 1993, Vol. 18, pp. 120–127.

- [15] Foley K. T., DiAngelo D. J., Rampersaud Y. R., Vossel K. A., and Jansen T. H., "The In Vitro effects of instrumentation on multilevel cervical strut-graft mechanics," *Spine*, Vol. 24, No. 22, 1999, pp. 2366–2376.
- [16] Goel V. K., Wilder D. G., Pope M. H., Edwards W. T., "Biomechanical testing of the spine. Load-controlled versus displacement-controlled analysis," *Spine*, 1995, Vol. 20, No. 21, pp. 2354–2357.
- [17] Gilbertson L. G., Doehring T. C., Livesay G. A., Rudy T. W., Kang J. D., Woo S. L., "Improvement of accuracy in a high-capacity, six degree-of-freedom load cell: application to robotic testing of musculoskeletal joints," *Ann Biomed Eng*, 1999, Vol. 27, No. 6, pp. 39–843.
- [18] Harris M. B., Thomas K. A., Ingram C. M., "The effect of anterior thoracolumbar plate application on the compressive loading of the strut graft," *Spine*, Vol. 21, No. 13, 1996, pp. 1487–1493.
- [19] Holmes A., Wang C., Han Z.H., et al., "The range and nature of flexion-extension motion in the cervical spine," *Spine*, 1994, Vol. 19, pp. 2505–2510.
- [20] James K. S., Wenger K. H., Schlegel J. D., Dunn H. K., "Biomechanical evaluation of the stability of thoracolumbar burst fractures," *Spine*, Vol. 19, No.15, 1994, pp. 1371–1740.
- [21] Kunz D. N., McCabe R. P., Zdeblick T. A., Vanderby R., "A multi-degree of freedom system for biomechanical testing," *J Biomechanical Engineering*, Vol. 116, 1994, pp 371–373.
- [22] Lind B., Sihlbom H., Nordwall A., and Malchau H., "Normal range of motion of the cervical spine," *Arch Phys Med Rehabil*, Vol. 70, 1989, pp 692–695.
- [23] Lysell E., "Motion in the cervical spine: An experimental study on autopsy specimens," *Acta Orthop Scand*, 1969, Vol. 123, pp. 1–61.
- [24] Miura T., Panjabi M. M., Crompton P. A., "Stability of Three Strut-Graft Constructs for Multi-Level Cervical Corpectomy," *Proceedings of the 2001 Cervical Spine Research Society*, Paper #18.
- [25] Miura T., Panjabi M. M., Crompton P. A., "A method to simulate in vivo cervical spine kinematics using a compressive preload," *Spine*, 2002, Vol. 27, No.1, pp. 43–48.
- [26] Olsewski, J. M., Garvey T. A., Schendel M. J., "Biomechanical analysis of facet and graft loading in a smith-robinson type cervical spine model," *Spine*, 1994, Vol. 19, No. 22, pp. 2540–2544.
- [27] Parsons J. R., Zimmerman M. C., Lee C. K., Langrana N. A., "Examination of the failure mode of several cervical spine fixation devices," *ASME Advances in Bioengineering*, 1993, BED-Vol. 24, pp. 175–178.
- [28] Patwardhan A. G., Havey R. M., Ghanayem A. J., et al., "Load carrying capacity of the human cervical spine in compression is increased under a follower load," *Spine*, 2000, Vol. 25, pp. 1548–1554.
- [29] Pelker R. R., Duranceau J. S., Panjabi M. M., "Cervical spine stabilization. A three-dimensional, biomechanical evaluation of rotational stability, strength, and failure mechanisms," *Spine*, 1991, Vol. 16, No. 2, pp. 117–122.
- [30] Penning L., "Normal movements of the cervical spine," *Am J Roentgenol*, 1978, Vol. 130, pp. 317–326.
- [31] Ordway N. R., Seymour R. J., Donelson R. G., et al., "Cervical flexion, extension, protrusion, and retraction. A radiographic segmental analysis," *Spine*, 1999, Vol. 24, pp. 240–247.

- [32] Rapoff A. J., O'Brien T. J., Ghanayem A. J., Zdeblick T. A., "Anterior cervical graft and plate load sharing," *Proc. of the 1997 Cervical Spine Research Society*.
- [33] Shea M., Edwards W. T., White A. A., Hayes W. C., "Variations of stiffness and strength along the human cervical spine," *J Biomech*, 1991, Vol. 24, pp. 95-107.
- [34] Smith S. A., Lindsey R. W., Doherty B. J., Alexander J., and Dickson J. H., "An in vitro biomechanical comparison of the orosco and ao locking plates for anterior cervical spine fixation," *J Spinal Disorders*, 1995, Vol. 8, No. 3, pp. 220-223.
- [35] van Mameren H., Sanches H., Beurgens J., et al., "Cervical spine motion in the sagittal plane. II Position of segmental averaged instantaneous centers of rotation: A cineradiographic study," *Spine*, 1992, Vol. 17, pp. 467-474.
- [36] Weinhoffer S. L., Guyer R. D., Herbert M., Griffith S. L., "Intradiscal pressure measurements above an instrumented fusion: a cadaveric study," *Spine*, 1995, Vol. 20, No. 5, pp. 526-531.
- [37] Wilke J. H., Wolf S., Claes L. E., Arand M., Wiesend A., "Influence of varying muscle forces on lumbar intradiscal pressure: an in vitro study," *J Biomech*, 1996, Vol. 29, No. 4, pp. 549-555.
- [38] White A., Panjabi M., "Clinical Biomechanics of the Spine," J.B. Lippincott Co., Philadelphia, 1990.

Berend Linke,¹ Georg Meyer,¹ Stefan Knöller,² and Erich Schneider,¹

Influence of Preload in Flexibility Testing of Native and Instrumented Lumbar Spine Specimens

Reference: Linke, B., Meyer, G., Knöller, S., and Schneider, E., “**Influence of Preload in Flexibility Testing of Native and Instrumented Lumbar Spine Specimens,**” *Spinal Implants: Are we evaluating them appropriately? ASTM STP 1431*, M. N. Melkerson, S. L. Griffith, and J. S. Kirkpatrick, Eds., ASTM International, West Conshohocken, PA, 2003.

ABSTRACT: In-vitro investigations on spine specimens are usually performed to evaluate the biomechanical behavior of the native spine, or to determine the stabilizing effects of different types of implants. These investigations are currently performed by the application of pure moments in the anatomic directions. The inclusion of an additional preload is heavily discussed, but seldom used in the experiments. Investigators often mention that different preloads have an influence on the results, but a detailed analysis of the influence on specific outcome parameters is still missing. The aim of this study was to show the effects of preload on the load-displacement behavior of spine specimens and to give basic data upon which investigators of future studies may decide on the necessity of its inclusion, depending on their specific question. A six degree-of-freedom loading device has been developed and was used to load the specimens. It has a parallel architecture and is equipped with a hybrid position/force controller. Sixteen human lumbar spine specimens L1-L3 were investigated. The spines were tested native and in two stabilized corpectomy situations. An anterior stabilization with VestroFix and SynEx was used with and without posterior USS fixation. Compressive preloads of 0N - 400N were applied and the flexibility tests carried out. The orientation of the preload was changing in accordance to the movement of the specimen.

A general reduction of the range of motion (ROM) of up to 40% due to 400 N of preload was observed. It could be shown, that this is not a general stiffening effect in the case of a strong sigmoid shape of the hysteresis curve. Whenever the low-stiffness (LS) is considerably lower than the high-stiffness (HS), HS is not affected by preload, but LS is strongly increased (50– 80% in native case). With increasing rigidity of additional instrumentation the stiffening effect is reduced on LS and increased on HS. The stiffness-ratio ($SR = HS/LS$) is reduced to about 50% due to 400 N preload in the native case. If implants are evaluated by an instrumented-to-native (I/N) comparison, the effect of preload on the I/N

¹ AO Research Institute, Clavadeler Strasse, CH-7270 Davos, Switzerland.

² Department of Orthopedic Surgery, Hugstetter Strasse 55, D-79106 Freiburg, Germany.

ratio of the characteristic parameters is only minimal and specific to the instrumentation used.

KEYWORDS: spine, preload, in-vitro testing, flexibility testing, six degree-of-freedom, loading device

Introduction

In-vitro investigations on spine specimens are usually performed to evaluate the biomechanical behavior of the native or injured spine or to determine the stabilizing effects of different types of implants in a specific injury model. These investigations are performed by the application of pure moments in the anatomic directions (flexion/extension, lateral bending, axial rotation). The inclusion of an additional preload is heavily discussed, but seldom used in such experiments. Investigators often mention that different preloads have an influence on the results, but a detailed analysis of the influence on specific outcome parameters is still missing.

In the seventies and eighties some investigators already addressed the effect of preload with respect to the load-displacement behavior of native spine specimens in in-vitro investigations. Panjabi et al. [1] used dead weights placed on top of the specimens to produce a preload of 400 N and found an increase of the range of motion (ROM) in flexion and lateral bending when 10 Nm of bending moment was applied. Contrary to this they found a decrease in ROM for axial rotation. Miller and Skogland [2] placed the insertion point of the preload force at the center of the upper vertebra and found a decrease in ROM in flexion, lateral bending and axial rotation, but still an increase in extension. Yamamoto et al. [3] used 50 N, 100 N and 150 N of preload and found no effect on the flexibility of the specimens.

Later in the nineties other investigators found more consistent effects of preload on the ROM of native spine specimens. Janavic et al. [4] used very high values of preload and found a decrease in ROM in flexion/extension, lateral bending and axial rotation of 60% up to 80%. Goodwin et al. [5] used 100 N to 425 N. They only tested in axial rotation, but additionally to the intact situation they also investigated three types of injury models. For all situations they found an increase in the overall stiffness, which is equivalent to a decrease in ROM. In comparison of the injured situation to intact, the data showed an increase of the ratio injured/intact due to the preload for all injury models. This means that the stiffening effect was observed to be stronger for the injured specimens. Hoffer et al. [6] studied the effect of preload on native and specimens instrumented with a cage using 300 N and 600 N. They did not find an effect of the preload in the intact situation for flexion/extension and lateral bending, but a decrease in ROM for axial rotation. The ratio of ROM cage/intact increased with preload for axial rotation, which means that the effect of preload was stronger for the intact situation. In flexion the ratio decreased, which means that the effect of preload was stronger for the instrumented situation.

Other studies as well addressed the effect of preload in spine flexibility testing, but with another focus. E.g. Patwardhan et al. [7] introduced the concept of a follower

load to overcome the problem of load direction when the specimen deforms, Wilke et al. [8] started to simulate the individual muscle groups acting at the spinal column and very recently Cripton et al. [9] investigated the difference of the effect of preload using 4 different types of preload application. They were able to show that a decrease in flexibility could be produced if the preload remains aligned along the axis of the spine throughout the motion. If the preload does not follow the axis of the spine and remain aligned with the axis of gravity the flexibility of the spine increases. These findings are in good agreement with the other studies mentioned and gives an explanation for the inconsistency outlined before. In general also Adams [10], Edwards [11], and Goel et al. [12] mentioned the necessity of using preloads in in-vitro experiments on spine specimens, without giving more detailed data. An investigation of Wilke et al. [13] reported of an inconsistency of in-vitro determined loads on a posterior instrumentation when compared to the data that was measured in-vivo by Rohlmann et al. [14]. The lack of an application of preload in the in-vitro experiments was suspected to be the reason for the inconsistency.

A further motivation for the investigation presented here is given by the studies of Nachemson [15] and Wilke [16]. They demonstrate a high pressure in the intervertebral disc of a human being in-vivo. These findings underline the importance of including a compressive preload in in-vitro experiments.

Summarizing all these studies it can be stated, that only the effect of preload on the ROM or the overall stiffness, respectively, has been investigated. A consensus can be found, that the application of preload has a stiffening effect in all principal loading directions, if the direction of the force is remaining aligned with the spine. The frequently observed increase in ROM can be considered to be due to a type of preload application, where the direction of force is not changing throughout the motion of the specimen (Cripton et al. [9]). The effect of preload on the sigmoid shape of the hysteresis curve, which is an important characteristic, however has not been addressed so far. Also the importance of an inclusion of the preload in cases where the stabilizing properties of spinal instrumentation are investigated by instrumented-to-native comparison has not been studied thoroughly.

The aim of this study is to demonstrate the effects of preload on the load-displacement behavior of spine specimens and to give basic data upon which investigators of future studies may decide on the necessity of its inclusion depending on their specific question.

Materials and Methods

Specimens and Preparation

A total of 16 fresh frozen human cadaver lumbar spine specimens (L1-L3) was used for the investigation. The specimens were sealed in double plastic bags and stored at -22°C . The BMD was evaluated by QCT (Densiscan 1000, SCANCO Medical AG, Basserdorf, Switzerland) and DEXA ($\text{BMD}_{\text{QCT}} = 0.27 \pm 0.08 \text{ g/cm}^3$, $\text{BMD}_{\text{DEXA}} = 0.93 \pm 0.24 \text{ g/cm}^2$) in all specimens. Bone abnormalities were excluded by a series of AP and lateral radiographs of all specimens. Four hours before testing the specimens were thawed and carefully freed from all musculature while preserving the osteoligamentous structures. The conditions for the handling of cadaver specimens formulated by Wilke et

al. [17] were followed throughout all the steps in the preparation phase. Cancellous bone screws were introduced into both endplates of the L1 and L3 vertebrae, and embedded into PMMA material. A special jig was used during the curing phase to ensure a horizontal orientation of the L2 vertebra and a parallel orientation of both fixtures at the same time. Plasticine was molded at places where space was needed for positioning of the implants (Figs. 1 and 2). After the PMMA was cured completely, the plasticine was removed.

To simulate the clinical case of a lumbar instability as seen in burst fractures or tumors of the spine, a corpectomy was performed. To obtain a representative clinical situation, corpectomy of the lumbar vertebral body L2 was done. The corpectomy was performed by cutting the intervertebral discs L1/2 and L2/3. The vertebral body L2 was resected with an oscillating saw ensuring that the anterior longitudinal ligament was preserved. A thin cortical layer remained at the anterior ligament. At the posterior aspect an approximately 1 cm wide piece of bone remained anterior to the spinal canal. Care was also taken not to interfere with the facet joints and ligamentous structures. The corpectomy defect was restored using the titanium cage SynEx (STRATEC Medical, Oberdorf, Switzerland) and two stabilization systems were applied. In case (V) a purely ventral instrumentation was used (VentreFix, STRATEC Medical, Oberdorf, Switzerland), in case (C) a combined stabilization was performed by additional application of a dorsal instrumentation (USS-Fracture System, STRATEC Medical, Oberdorf, Switzerland), (Fig. 3). The VentroFix was fixed to the vertebral bodies L1 and L3 by two cancellous bone screws each, the USS was applied on both sides of the spinal processes.



FIG. 1—Screws for support in embedding material and plasticine space-holders.

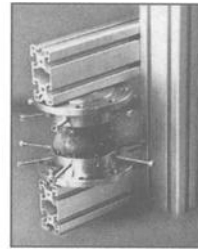


FIG. 2—Specimen in embedding jig.



FIG. 3—Specimen after corpectomy, restoration with SynEx and combined ventral and dorsal instrumentation.

Loading Device

The specimens were loaded in a six-degree-of-freedom (6DOF) loading device [18]. It consisted of six hydraulic actuators that were mounted between a mobile platform and the fixed base in a parallel mechanical structure (Fig. 4). By adjusting the length of each actuator the platform could be moved in six degrees-of-freedom ($T_x, T_y, T_z, \varphi_x, \varphi_y, \varphi_z$), by adjusting the force that each actuator applies to the platform, the platform could be loaded in six degrees-of-freedom ($F_x, F_y, F_z, M_x, M_y, M_z$). To determine the load on the specimen, a task co-ordinate system was specified (Fig. 5). Its origin was located in the center of the middle vertebra and its axes were directed as proposed in [17], with the x-axis pointing forward, the y-axis pointing to the left and the z-axis pointing cranial. The origin of the task co-ordinate system was called the "Reference Point on the Specimen." All displacement and load data were calculated with respect to this point. The displacements of the top vertebra were calculated with respect to the bottom vertebra, but expressed in co-ordinates of the task co-ordinate system, which moves with the bottom vertebra. Due to this definition a flexion/extension movement was almost a pure rotation and shear was not produced. For the description of the angular orientation of the lower part of the specimen that was attached to the mobile platform with respect to the upper part that was attached to the fixed crosshead, the RPY (roll-pitch-yaw) angle convention [19] was used. The load was determined by a six component load transducer (MKA 4kN 250 Nm, Huppert GmbH, 71083 Herrenberg, Germany) to which the specimen was directly attached. The displacement was determined by six LVDTs (MTU-200-G, 200 mm, Messring GmbH, 80608 Munich, Germany) mounted in-line with each cylinder and calculation of the translation and rotation of the platform iteratively by a Newton-Raphson algorithm [20]. Using a hybrid position/force controller, similar to that proposed in [21] it was possible to choose either position or load control in each degree-of-freedom in the task co-ordinate system. All experiments were performed with the rotational degrees-of-freedom in position control and all translational degrees-of-freedom in force control. This choice of control modes enabled a free movement of the center of rotation and an application of preload while angular stability was preserved. The applied preload was directed in negative z-direction, pointing through the origin of the task co-ordinate system. Position and load data in six degrees-of-freedom each was recorded with a sampling frequency of 50 Hz.

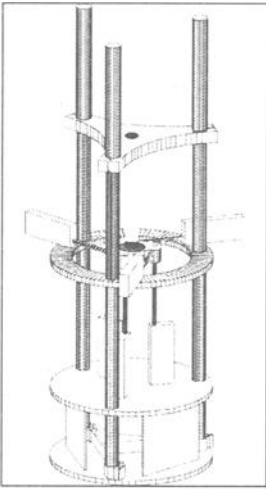


FIG. 4—6DOF loading device in parallel mechanical architecture [16].

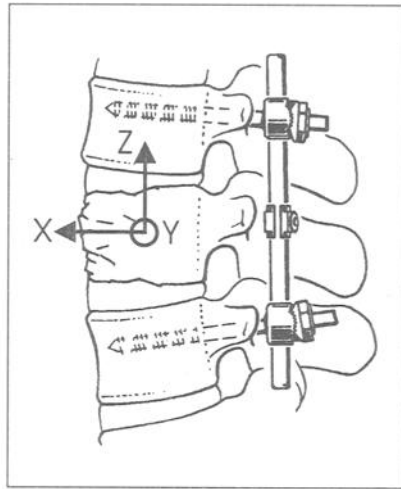


FIG. 5—Task co-ordinate system with respect to the specimen.

Test Protocol

The specimens were mounted on the 6DOF simulator with the fixtures oriented parallel and without any preload. First the native specimen (N) was tested, followed by tests with corpectomy, SynEx and purely ventral stabilization (V) and combined stabilization (C). In one half of the specimens (V) was tested after (N), followed by (C), in the other half (C) was tested after (N), followed by (V).

In each stage of instrumentation flexibility tests were carried out by application of moments in the three principal directions separately (flexion/extension – left/right lateral bending – left/right axial rotation). The loads were applied continuously with a sinusoidal shape, a magnitude of approximately ± 7.5 Nm and a frequency of 1/20 Hz. For a discussion on the effect of the shape and the frequency of the signal on the outcome of flexibility tests on spinal motion segments please refer to [22] and [23]. The torque was produced by controlled sinusoidal angular movement so that the maximum torque of 7.5 Nm was reached, while the center of rotation was free to move and angular stability in the non-loaded rotational directions was preserved. The exact displacement rate resulted from the respective angular amplitude used for the test and the frequency of 1/20 Hz. Four cycles of movement were performed in each individual test of which the last three were used for the evaluation.

Each of the 9 flexibility tests was performed without a preload and with 100 N, 200 N and 400 N of compressive preload. 400 N was chosen as the upper limit, as this magnitude was used in other studies e.g., [1], [5], [9] and is assumed to represent upper body weight. In vivo measurements of intradiscal pressure suggest higher loads up to 3 kN, which appears not to be appropriate for in-vitro testing due to the lack of musculature. The 36 experiments in one specimen were carried out within 8 hours.

Data Analysis

The results of the flexibility tests were evaluated by determination of characteristic values of the hysteresis curve of the respective main motion. The coupled motion in the translational directions and the coupled loads in the rotational directions were not evaluated. One of the derived characteristic values was ROM according to standard procedure described by Panjabi [24] and Wilke et al. [17]. Due to the procedure of load application, the maximum torque applied was not exactly 7.5 Nm in all cases, but usually a little higher. In these cases the ROM was not calculated from the maximum load, but from the intersection of the curve at 7.5 Nm on the “loading-slope,” not on the “relaxation-slope.” The validity of this procedure is shown in Fig. 6. Regardless of the maximum torque, which is achieved for the two sample trajectories in each part of the figure, the results are the same on the “loading-slope.” On the “relaxation-slopes” the results are different due to the viscoelasticity of the biological tissue.

Three more characteristic values were the stiffness in the high-stiffness area (HS), the stiffness in the laxity area (LS) (Fig. 7) and the “stiffness-ratio” (SR). The high-stiffness was evaluated as the mean slope of the “loading-slope” between -7.5 to -6.0 Nm and 6.0 – 7.5 Nm, which was a range of 10% of the whole curve width on each side. The mean value of the two high-stiffness values at positive and negative loads was defined as the value HS. The low-stiffness was evaluated as the mean slope between -0.75 and 0.75 Nm, which was also a range of 10% of the whole curve width. The mean value of the two low-stiffness values from the respective “loading-slopes” of the curve was defined as the value LS. The “stiffness-ratio” (SR) describes the sigmoidity of the hysteresis curve, it was defined as the ratio HS/LS . Similar values were already mentioned by Wilke (S1, S2 and “Steifigkeitsquotient” in [25], LZS, EZS and “Sigmoidity” in [17]), but to the authors knowledge these were never used in an evaluation. The difference of HS to the Wilke proposal was, that it was only evaluated on the respective “loading-slopes” and not on the “relaxation-slopes” as in [25] and [17].

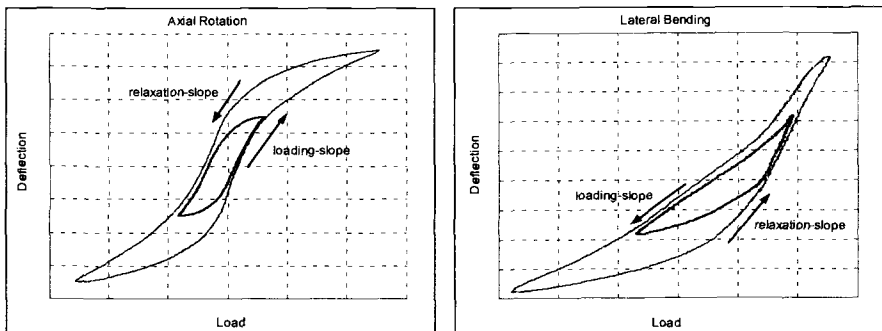


FIG. 6—Hysteresis curves of the same specimen with different load amplitudes

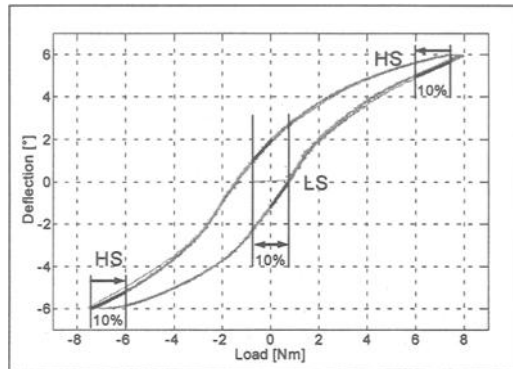


FIG. 7—Definition of HS and LS in a hysteresis curve.

Presentation of the data and statistical evaluation

Four types of diagrams are used: The raw data of ROM is presented as box-plots to show the variance of the results due to the wide range of bone quality of the specimens. For ratios of ROM with preload with respect to the unloaded case all values are presented. QMQ-plots, showing the 25% and 75% quartiles and the median with respect to the applied load, are introduced to visualize qualitative trends for the parameters ROM, HS and LS relative to the unloaded case as well as SR. Median-plots, showing only the median with respect to the applied load, are used further to qualitatively compare trends of HS and LS relative to the unloaded case and of the ratios with respect to native (I/N) of ROM, HS and LS. To test for significance of the visualized trends, paired t-test on the differences between the groups 0 N (unloaded case) and 400 N (maximum load applied) was used. The significance level was chosen to be $p = 0.05$.

Results

Absolute Values, Without Preload

The absolute values of ROM (given as the sum of positive and negative ROM) in the unloaded case are presented in Fig. 8 for the native situation and for the situation with combined ventral and dorsal instrumentation. In the native case the large variance of the data ranging from 2–22° was obvious. In the combined stabilized situation values were in the range of 0.4–14°.

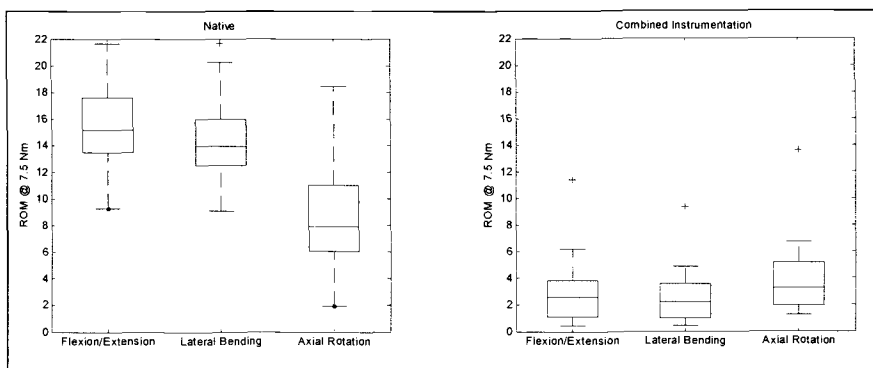


FIG. 8—ROM in unloaded case, absolute values.

The absolute values for HS were in the range of 0.9–6 Nm/° for the native situation and between 1.4–25 Nm/° for the combined stabilized situation. Again the large variance of the data was obvious. For LS the absolute values ranged from 0.2 Nm/° to 6 Nm/° in native, for the combined stabilized situation hardly any sigmoidity of the hysteresis curves was present and thus the values for LS equaled those of HS. The stiffness ratio ranged from 1–9 in native and was equal to 1 in most of the combined stabilized cases.

Relative Reduction Due to Preload

Because the aim of this study was to show the influence of preload on the characteristic parameters derived from the hysteresis curves, the values were normalized to the unloaded case. In individual cases a reduction of ROM due to 400 N preload of 60% occurred, as can be seen in Fig. 9. Taking all specimens into account, a significant reduction of up to 40% of ROM at a 400 N preload ($p < 0.01$) was observed. Fig. 10 shows the respective QMQ-plots. In Fig. 11 it can be seen, that HS was not significantly affected by preload in the native case, the increase for the instrumented situations was significant ($p < 0.01$). For LS a strong increase due to preload was observed (50–80% in native), all effects were significant with $p < 0.01$. The respective QMQ-plot is presented in Fig. 12. The stiffness ratio $SR = HS/LS$, dropped significantly ($p < 0.02$) to about 50% in the native situation (flexion/extension: 53%, lateral bending: 63%, axial rotation: 53%), as can be seen in Fig. 13.

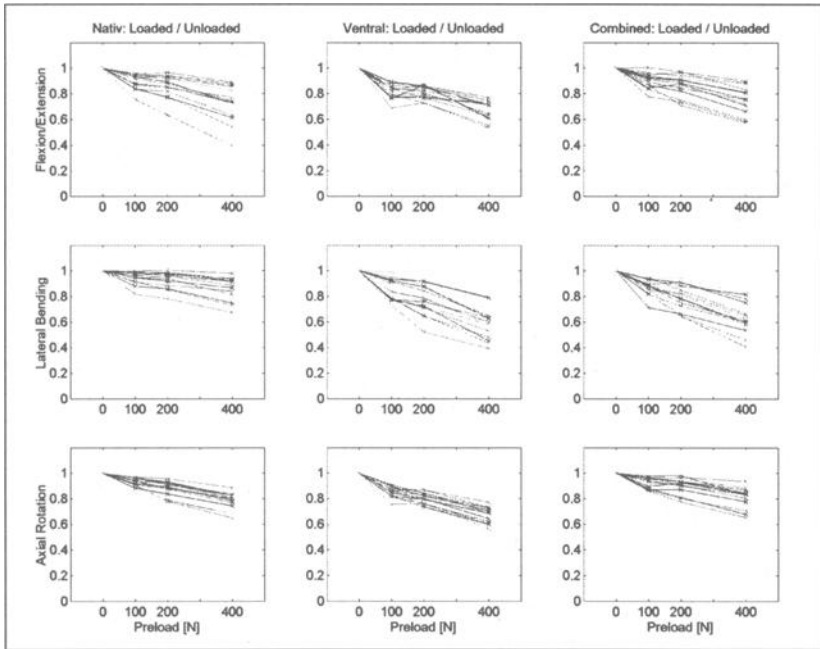


FIG. 9—ROM relative to unloaded case, individual values of all specimens.

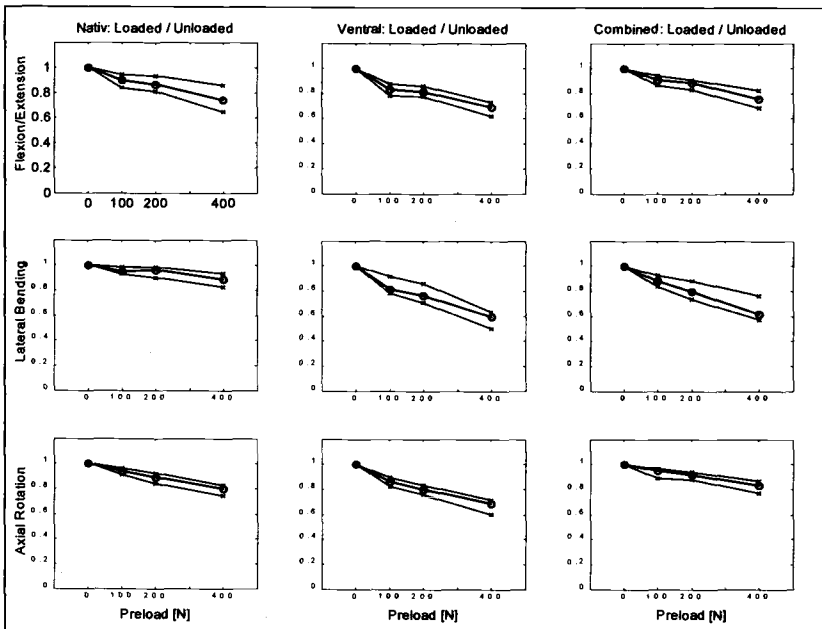


FIG. 10—ROM relative to unloaded case, Median (o) and Quartiles (x).

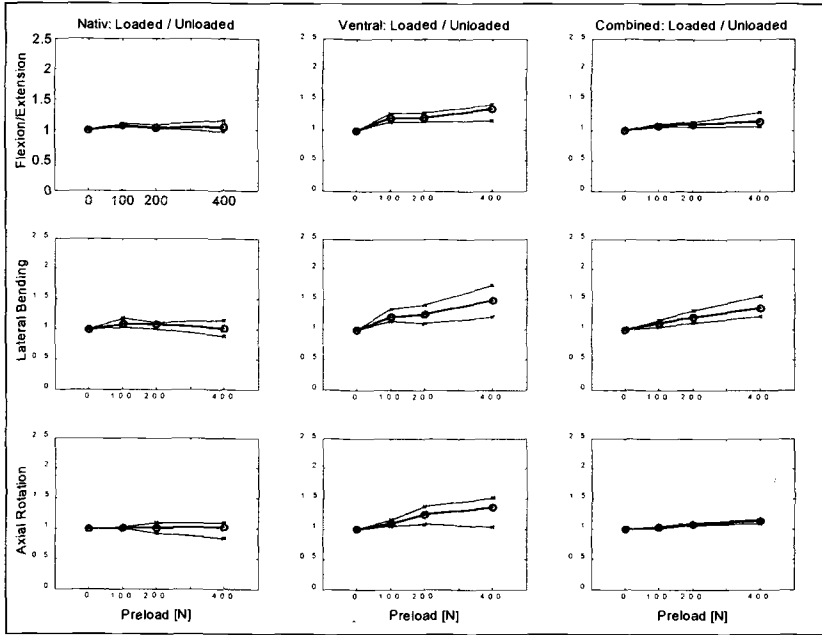


FIG. 11—HS relative to unloaded case, Median (o) and Quartiles (x).

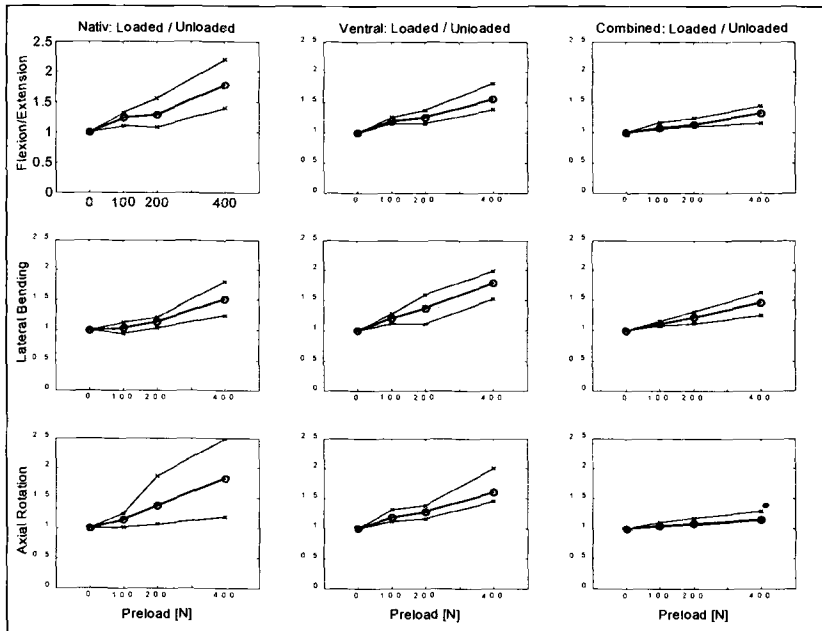


FIG. 12—LS relative to unloaded case, Median (o) and Quartiles (x).

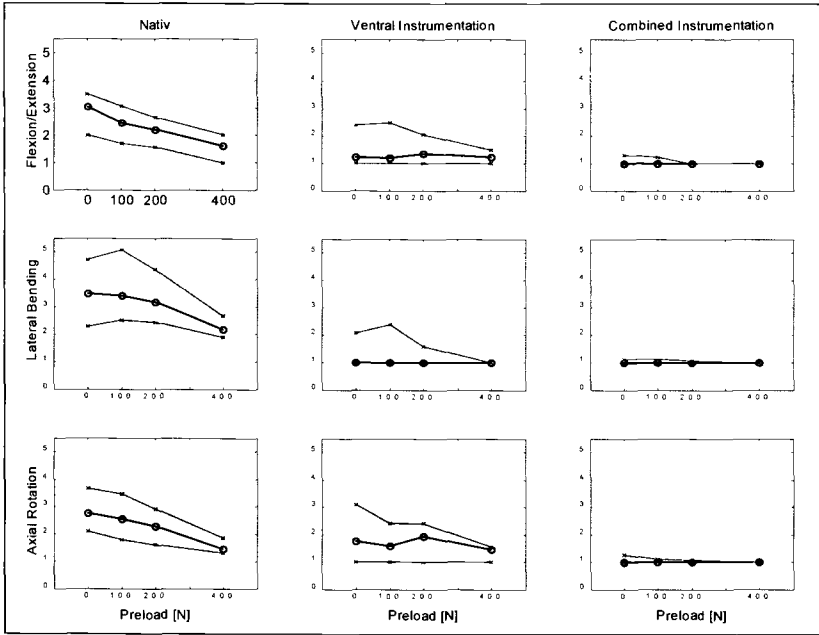


FIG. 13—Stiffness-Ratios, Median (o) and Quartiles (x).

Discussion

The results showed will be interpreted in three separate sections. The effect of preload on the ROM of native spine specimens has already been addressed in several other studies, therefore the findings of this study will be related to them and the impact of the type of load application will be discussed especially. The effect of preload on the shape of the hysteresis curve (defined by the parameters HS, LS and SR) has not been addressed in the literature so far. The respective results will therefore be discussed independently. The effect of preload on the stabilizing capabilities of specific implants (defined by the instrumented-to-native ratio of all parameters) will be discussed in the third section. At the end a summary of results and interpretation is given.

Range-of-motion (ROM)

The results of this study show a similar trend of the effect of preload on the ROM for native as well as for instrumented specimens. In general a reduction of ROM was observed. An obvious difference with respect to the loading direction or with respect to the stage of instrumentation was not found. More specifically a reduction of about 25% for flexion/extension, 20–30% for axial rotation, 15% for lateral bending in native and 40% for lateral bending with instrumentation was observed.

The findings for axial rotation are in good agreement with most of the studies reported in the literature [1], [2], [4], [5] as the explicit type of load application does not have a strong impact in this loading mode. The different results presented by Panjabi et al. [1] for flexion/extension and lateral bending are considered to be due to the difference

in the type of load application of the study, as it has been show in [9]. Studies using a similar type of load application as in this investigation [2,4,9] also report of a reduction of ROM for flexion/extension and lateral bending. The much stronger reduction found in [4] is due to the much higher load that was applied. The results of [3] where no effect was found for any loading direction cannot be explained, but these findings are not in agreement with the rest of the studies. The test setup of Patwardhan et al. [7] to introduce the concept of a follower load was different to the one used here, but the results can as well be interpreted as a reduction of ROM for flexion/extension due to the application of a compressive preload.

Shape of the Hysteresis Curve

To characterize the shape of a hysteresis curve the parameters HS, LS, and SR have been introduced. The effect of preload on these parameters has not been addressed in the literature so far. The data given here therefore cannot be discussed with respect to other studies, but is an addition to the literature.

The general reduction of ROM is typically interpreted as an overall effect of stiffening. It can be seen in Figs. 11 and 12, that this is not always true. In the case of a strong sigmoid shape of the hysteresis curve, which is typically present in native specimens the low-stiffness (LS) is considerably lower than the high-stiffness (HS). In these cases HS is not affected by preload, but LS is strongly increased (50–80% in native case, $p < 0.01$). With increasing rigidity of additional instrumentation the stiffening effect is reduced on LS and increased on HS. HS is not influenced by preload in native, but 35–50% increased with ventral instrumentation. For LS the strong effect of stiffening in native mode is reduced with increasing rigidity of the instrumentation. For a clearer visibility of that effect, the median curves of Figs. 11 and 12 for all loading directions are compared in one diagram for native and one for ventral stabilization in Fig. 14. It is obvious, that in native mode only LS is affected by preload, but not HS. In the instrumented situation both parameters are similarly increased with preload.

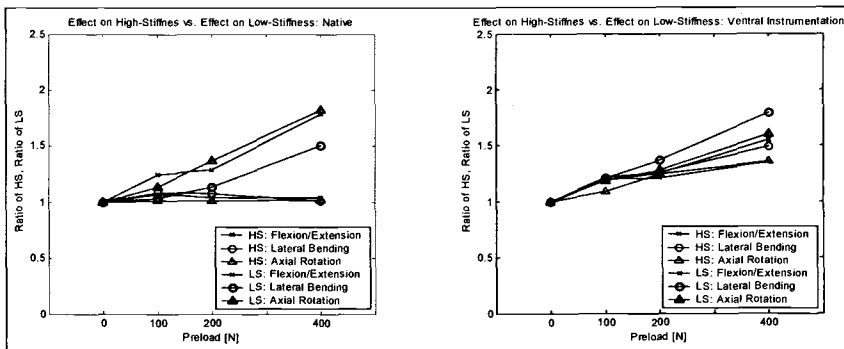


FIG. 14—HS and LS relative to unloaded case, Median.

The same observation can also be expressed by the stiffness-ratio (SR). In the native case the values of HS and LS differ strongly, resulting in a SR of 3–4. With increasing preload the degree of sigmoidity of the hysteresis curve is reduced. LS is increased whereas HS remains constant, resulting in a drop of SR to about 1.5–2 with 400

N preload ($p < 0.02$ for native). SR is almost meaningless in the instrumented situation, because most values are very close to 1. In these cases, LS and HS are similarly increased with preload.

Stabilizing Capabilities by Instrumented-to-Native Comparison

The stabilizing capabilities of implants are most often characterized by the instrumented-to-native ratio (I/N) of ROM. This is done to reduce the inter specimen variability. It has been pointed out earlier, that the effect of preload on ROM is not very different for native compared to the instrumented situations. As a consequence it has to be expected, that the effect on a ratio of those measures will only be minor. In Fig. 15 the I/N ratios of ROM are presented for all preloads. Significant effects ($p < 0.05$) are indicated by solid lines, whereas not significant trends are indicated by dashed lines.

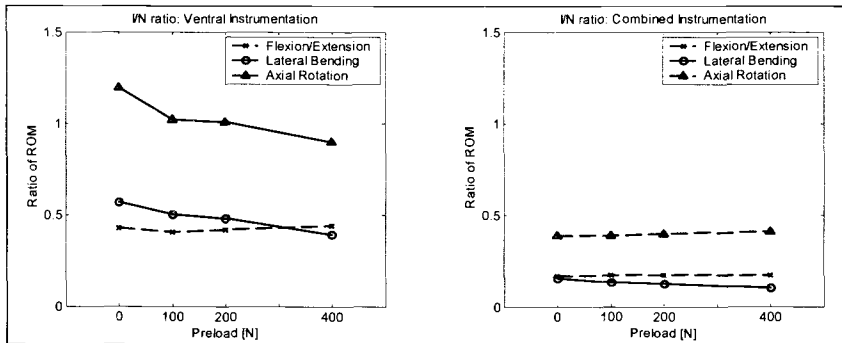


FIG. 15—Ratio of ROM with respect to native, Median.

A strong influence on the I/N ratio of ROM is not obvious. Significant influences are present, but they are specific to the implant and loading direction. In axial rotation it is decreased by 25% for the ventral instrumentation, but not for the combined instrumentation and in lateral bending by 30% for both instrumentations. In flexion/extension the I/N ratio of ROM is not affected. The effect of a compressive preload on this I/N ratio of ROM has also been studied by Hoffer et al. [6] for cage instrumentation. The results of that study do not correspond to the findings presented here. We found a significant effect for lateral bending; they only found it to be marginally significant. We did not find an effect for flexion/extension whereas they did. We found a decreasing effect in axial rotation only with one of the instrumentations; they found an increasing effect. An explanation for this discrepancy may be, that a comparison of rod fixations to cage instrumentation is not valid. Even the effects for ventral and combined instrumentation in this study are not equivalent.

In summary it can be concluded, that only a slightly effect of preload on the I/N ratio of ROM is present and that it is strongly dependant upon the specific instrumentation used.

The effects of preload on the I/N ratio for the parameters HS and LS are presented in Figs. 16 and 17.

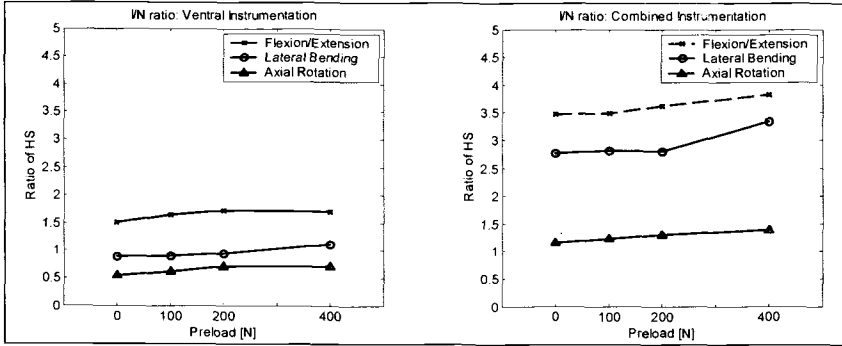


FIG. 16—Ratio of HS with respect to native, Median.

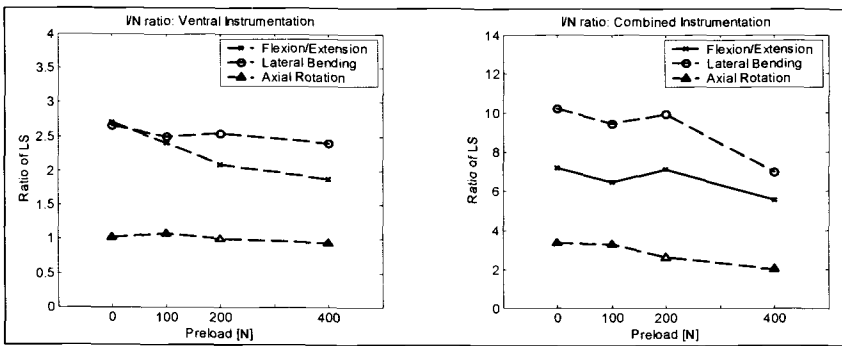


FIG. 17—Ratio of LS with respect to native, Median.

Strong influences on the I/N ratio of HS or LS are not obvious. Significant influences are present, but they are again specific to the implant and loading direction. The I/N ratio of HS is increased by about 20%, which could already be derived from Fig. 14, as HS is affected in the instrumented situation, but not in the native reference. The I/N ratio of LS is not significantly affected; only a trend of decrease can be seen. Even though this result was not to be expected from Fig. 11, a significant effect could not be detected due to the high variability of the 16 specimens.

The I/N ratio of SR is significantly increased for the combined instrumentation (40–80%), which is just a cause of the decreasing influence of the preload on SR for the native situation and the absence of an influence with the rigid instrumentation (see Fig. 13). This means that the influence of instrumentation on the shape of the hysteresis curve is strongest without the application of a preload.

Summary of Results and Interpretation

A reduction of ROM with increasing preload was observed. An obvious difference with respect to the loading direction or with respect to the stage of instrumentation was not found. As a consequence a strong influence on the instrumented-to-native (I/N) ratio of ROM is not present. The general reduction of ROM is typically interpreted as an overall effect of stiffening, which is not always true. In the native situation high-stiffness (HS) is not affected by preload, but low-stiffness (LS) is strongly increased. In the instrumented situation both parameters are similarly increased with preload.

With increasing preload the degree of sigmoidity of the hysteresis curve is reduced. The influence of instrumentation on the shape of the hysteresis curve is strongest without the application of a preload.

Conclusion

Preload has a significant effect on the characteristics of hysteresis curves derived from spine specimens in in-vitro investigations. A reduction in range of motion due to preload cannot be interpreted as a general effect of stiffening throughout the whole loading range.

Studies investigating the biomechanical behavior of native spine specimens must consider the influence of a preload. When instrumented-to-native ratios are used to evaluate the instrumentation, the effect of preload on these values is minimal and specific to the instrumentation used.

Acknowledgment

The provision of the SynEx, VestroFix and USS implants by STRATEC Medical, Oberdorf, Switzerland, is gratefully acknowledged.

References

- [1] Panjabi, M. M., Krag, M. H., White, A. A., Southwick, W. O., "Effects of preload on load displacement curves of the lumbar spine," *Orthopaedic Clinics of North America*, Vol. 8, 1977, pp. 181–192.
- [2] Miller, J. A., Skogland, L. B., "On the load-displacement behaviour of adolescent spinal motion segments—an experimental study using autopsy specimens," Ph.D Thesis, Sophies Mínde Orthopaedic Hospital, University of Oslo, Norway, 1980.
- [3] Yamamoto, J., Panjabi, M. M., Crisco, T., Oxland, T., "Three-dimensional movements of the whole lumbar spine and lumbrosacral joint," *Spine*, Vol. 14, 1989, pp. 1256–1260.
- [4] Janavic, J., Ashton-Miller, J. A., Schultz, A. B., "Large compressive preloads decrease lumbar motion segment flexibility," *Journal of Orthopaedic Research*, Vol. 9, 1991, pp. 228–236.
- [5] Goodwin, R. R., James, K. S., Daniels, A. U., Dunn, H. K., "Distraction and compression loads enhance spinal torsional stiffness," *Journal of Biomechanics*, Vol. 27, 1994, pp. 1049–1057.
- [6] Hoffer, Z., Oxland, T. R., Cripton, P. A., Sherman, J., Nolte, L.-P., "Compressive loading affects the stabilization provided by lumbar interbody cages," *Proceedings of the 44th Annual Orthopaedic Research Society*, New Orleans, 1998.

- [7] Patwardhan, A. G., Havey, R. M., Meade, K. P., Lee, B., Dunlap, B., "A follower load increases the load-carrying capacity of the lumbar spine in compression," *Spine*, Vol. 24, 1999, pp. 1003–1009.
- [8] Wilke, H.-J., Wolf, S., Claes, L., Arand, M., Wiesend, A., "Stability increase of the lumbar spine with different muscle groups. A biomechanical in vitro study," *Spine*, Vol. 20, 1995, pp. 192–198.
- [9] Cripton, P. A., Bruehlmann, S. B., Orr, T. E., Oxland, T. R., Nolte, L.-P., "In vitro axial preload application during spine flexibility testing: towards reduced apparatus-related artifacts," *Journal of Biomechanics*, Vol. 33, 2000, pp. 1559–1568.
- [10] Adams, M. A., "Spine update: mechanical testing of the spine," *Spine*, Vol. 20, 1995, pp. 2151–2156.
- [11] Edwards, W.T., "Biomechanics of posterior lumbar fixation: analysis of testing methodologies," *Spine*, Vol. 16, 1991, pp. 1224–1232.
- [12] Goel, V. K., Wilder, D. G., Pope, M. H., Edwards, W. T., "Controversy: biomechanical testing of the spine, load-controlled versus displacement-controlled analysis," *Spine*, Vol. 20, 1995, pp. 2354–2357.
- [13] Wilke, H.-J., Rohlmann, A., Neller, S., Schultheiß, M., Bergmann, G., Graichen, F., Claes, L., "Is It Possible to Simulate Physiologic Loading Conditions by Applying Pure Moments? A Comparison of In Vivo and In Vitro Load Components in an Internal Fixator," *Spine*, Vol. 26, 2001, pp. 636–642.
- [14] Rohlmann, A., Bergmann, G., Graichen, F., "Loads on an internal spinal fixation device during walking," *Journal of Biomechanics*, Vol. 30, 1997, pp. 41–47
- [15] Nachemson, A., "The load on lumbar disks in different positions of the body," *Clinical Orthopedics*, Vol. 45, 1966, pp. 107–122.
- [16] Wilke, H.-J., Neef, P., Caimi, M., Hoogland, T., Claes, L., "New in vivo measurements of pressures in the intervertebral disc in daily life," *Spine*, Vol. 24(8), 1999, pp. 755–762.
- [17] Wilke, H.-J., Wenger, K., Claes, L., "Testing criteria for spinal implants—recommendations for the standardization of in vitro stability testing of spinal implants," *European Spine Journal*, Vol. 7, 1998, pp. 148–154.
- [18] Linke, B., Sellenschloh, K., Huber, G., Schneider, E., Weltin, U., "A new method of pre-clinical spine implant testing in six degrees of freedom—based on the hexapod principle," *Journal of Biomechanics*, Vol. 31, Suppl. 1, p. 41, 1998.
- [19] Nikravesh, P. E., "Computer-aided analysis of mechanical systems," Prentice-Hall, New Jersey, 1988.
- [20] Yang, J. Geng, Z.J., "Closed form forward kinematics solution to a class of hexapod robots," *IEEE Transactions on Robotics and Automation*, Vol. 14, 1998, pp. 503–508.
- [21] Raibert, M. H., Craig, J. J., "Hybrid position/force control of manipulators," *Transactions of the ASME Journal of Dynamic Systems, Measurement, and Control*, Vol. 103, 1981, pp. 126–133.
- [22] Huber, G., Ito, K., Morlock, M. M., "Zeitabhängiges Verhalten von Bandscheiben: Modellrechnungen basierend auf in-vitro Relaxationsmessungen," Tagungsband: 2. Tagung der Deutschen Gesellschaft für Biomechanik, S. 83, Freiburg, 2001.
- [23] Huber, G., Ito, K., Linke, B., Schneider, E., Morlock, M. M., "The influence of intervertebral disc time-dependent properties on in-vitro testing," *Biomechanica IV*, 23.-25.9.2001, Davos, Switzerland, 2001.
- [24] Panjabi, M. M., "Biomechanical evaluation of spinal fixation devices: Part I. A conceptual framework," *Spine*, Vol. 13, 1988, pp. 1129–1134.
- [25] Wilke, H.-J., "Möglichkeiten und Grenzen der biomechanischen in vitro Testung von Wirbelsäulenimplantaten," Habilitationsschrift, Medizinische Fakultät der

Universität Ulm, Abteilung Unfallchirurgische Forschung und Biomechanik,
1996.

William L. Carson,¹ Marc A. Asher,² Oheneba Boachie-Adjei,³ and Behrooz Akbarnia⁴

Transverse Connectors: Clinical Objectives, Biomechanical Parameters Involved in Their Achievement, and Summary of Current and Needed In Vitro Tests

Reference: Carson, W. L., Asher, M., Boachie-Adjei, O., and Akbarnia, B., “**Transverse Connectors: Clinical Objectives, Biomechanical Parameters Involved in Their Achievement, and Summary of Current and Needed In Vitro Tests,**” *Spinal Implants: Are We Evaluating Them Appropriately*, ASTM STP 1431, M. N. Melkersen, S. L. Griffith, and J. S. Kirkpatrick, Eds., ASTM International, West Conshohocken, PA, 2003.

Abstract: The clinical objectives for using transverse connectors (TCs) on different implant constructs are compiled. Results from a survey of 2499 clinical cases, hand held-loaded models, linkage analysis, and finite element analysis were used to identify the important biomechanical characteristics and parameters of constructs affecting the need for a TC and of the TC itself that are involved in achieving the clinical objectives. These were compared to those tested in ASTM standards to evaluate existing and needed TC tests. Axial and torsional gripping characteristics of TC interconnections are adequately tested with ASTM F 1798-97. ASTM F 1717-01 axial test protocol can reveal the effect of TCs on the flexion fatigue life of longitudinal members, however the torsional test protocol results have questionable clinical relevance due to fixtures constraining 3 of 6 construct relative degrees-of-freedom. A substitute gimbal-gimbal or gimbal-pushrod fixture is proposed. The following are proposed to test TC characteristics that are not tested with current ASTM standards: an H construct for testing TC lateral bending characteristics, an unconstrained 3D test for transfixed thoracolumbar constructs having different combinations of hook-claw-wire and screw foundations, and a fixture to test torsional characteristics of constructs having sacroiliac foundations.

Keywords: Transverse connectors, spine implants, clinical objectives, biomechanical parameters, in vitro tests

¹ Ph.D., Professor Emeritus Mechanical and Aerospace Engineering, University of Missouri-Columbia, 2111 Fairmont, Columbia, Missouri, USA.

² M.D., Dept. of Surgery Orthopedic Section, The University of Kansas Medical Center, 3901 Rainbow Blvd., Kansas City, Kansas, USA.

³ M.D., The Hospital for Special Surgery, 523 East 72 Street, New York, New York, USA.

⁴ M.D., San Diego Center for Spinal Disorders, 4130 La Jolla Village Drive, Suite 300, La Jolla, California, USA.

1. Introduction

Transverse connectors between longitudinal members in spinal implant constructs vary widely in their design and biomechanical characteristics, most notably in their interconnection to the longitudinal member, and the transverse member itself. There continues to be a quest for the ultimate transverse connector, which can be easily placed as the last component(s) of a construct with little to no preplanning by the clinician, and which also has the appropriate biomechanical characteristics to function properly in all clinical situations. Clinicians are not in universal agreement when to or not to use transverse connectors in a particular construct. This is evidenced by similar clinical cases and constructs with and without transverse connectors, which for the most part produce seemingly similar clinical results.

There are two ASTM standards with protocols applicable to testing some biomechanical characteristics of transverse connectors: Guide for Evaluating the Static and Fatigue Properties of Interconnection Mechanisms and Subassemblies Used In Spinal Arthrodesis Implants (F 1798-97), and Test Methods for Spinal Implant Constructs in a Vertebrectomy Model (F 1717-01).

The goals of the work summarized in this paper were: 1) to identify the clinical objectives for transfixation along with the important biomechanical characteristics and associated parameters of transverse connectors that are needed to achieve these objectives, 2) to identify appropriate in vitro tests on or with transverse connectors to quantitatively evaluate their clinically important biomechanical characteristics, and 3) to evaluate if they are included in F 1798-97 or F 1717-01 and if not to propose fixtures for such tests.

“TC” will be used as the acronym for Transverse Connector in this paper.

2. Methods and Procedures

At recent Isola Study Group meetings clinicians were asked to discuss their reasons for using transverse connectors to identify the clinical objectives for transfixation. Objectives were also compiled from the literature [8 – 10]. Clinical objectives for transfixation are summarized in section 3 of this paper.

To identify and more thoroughly understand the biomechanical characteristics and associated parameters of transverse connectors that are important in various clinical constructs and foundations, the following three things were done. 1) The location and types of transverse connector failures that appeared in a multi-center retrospective survey [12] of 2499 cases involving spinal implant constructs used to treat a variety of pathologies were investigated. In addition the existence or not of fretting corrosion was observed from a study on the “Effects of Transverse Connector Design on Development of Late Operative Site Pain...” [13]. This information provided evidence as to the types of internal loads that transverse connectors were being subjected to as well as giving

some clues as to the types of external loads that would produce them. The transverse connectors used in these clinical cases were limited in type, primarily to Isola designs, which have their relative strengths/weaknesses that would have some influence on the types of clinical implant failure observed. Thus these studies did not necessarily identify all potential clinical modes of transverse connector failure. 2) To more thoroughly (bending, and torsion). The stability with and without a transverse connector was determined by observing the relative resistance to construct deflection as load was applied. To help identify important parameters, one or more of the transverse connector's interconnections were loosened to finger tight before loading. If the construct remained stable upon application of a particular component of external loading, the parameters (axial and/or torsional gripping for example) that were reduced to near zero by the interconnection loosening were not important for resisting that particular component of loading. When a component of relative motion (axial translation or rotation) was significant within the loosened interconnection (Figure 1), the corresponding gripping strength parameter was important for resisting the applied component of load. To get insight into the importance of the transverse member's axial and bending stiffness as well as the lateral bending strength of its interconnection to the longitudinal member, a 6 mm wide rubber band was stretched between and attached to the longitudinal members. The relative stretching and bending of this rubber band transverse connector (Figure 2) served to indicate the relative importance of a TC's axial stiffness and bending properties, respectively, to each component of applied load.

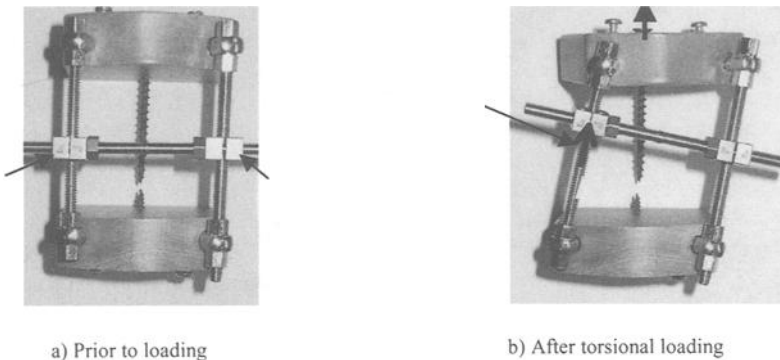


Figure 1 – Model illustrating importance of TC's axial grip to longitudinal member for resisting torsional load on a bilevel 40° pedicle screw angle construct when loss of torsional grip in two or more longitudinal member-to-screw interconnections exist, which results in an unstable mechanism to torsional load without a TC.

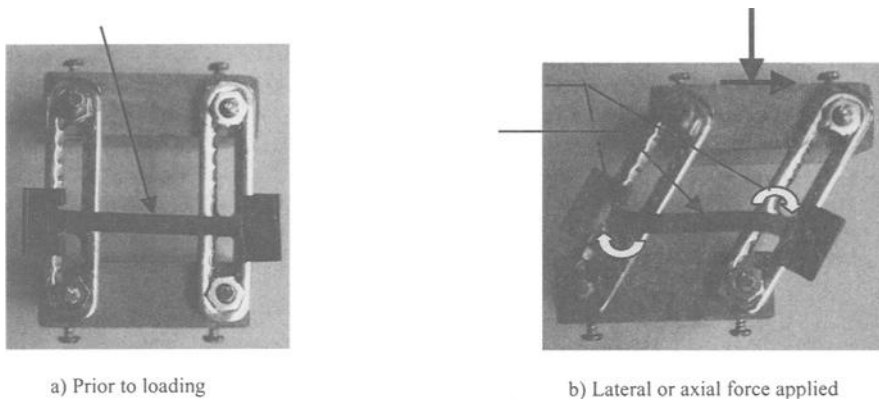


Figure 2 – Model illustrating importance of transverse member's lateral bending stiffness and TC's interconnection to longitudinal member lateral bending strength on a bilevel 0° pedicle screw angle construct, which results in an unstable mechanism to lateral and axial load without a TC.

3) To quantitatively evaluate the need for transverse connectors and the importance of associated parameters, finite element analysis of the internal forces and moments within 3D bilevel and trilevel pedicle screw spine instrumentation models when subjected to each of the six components of external loading were studied [4, 5, 6, 7]. In addition, linkage analysis was used [3] to identify the important parameters associated with transverse connectors in long constructs having less secure bone implant (hook-claw-wire) type foundations on each end. The important biomechanical characteristics and parameters are summarized in section 4 of this paper. There is no claim that the list of "important" parameters is all inclusive. Quantitative justifications such as magnitude comparison of the internal components of force and moment being transmitted through a transverse connector when a construct is subjected to different components of loading are not presented in this paper, but are contained in the references [4-7].

To identify appropriate in vitro tests and to evaluate if they are included in F 1798-97 and F 1717-01, the clinically observed modes of transverse connector assembly failure were compared to those observed when using the test protocols in these standards. Also, the important biomechanical characteristics and associated parameters listed in section 4 were compared to those being tested with the protocols in these two standards. Section 5 of this paper contains a summary of this analysis, as well as recommendations for fixtures to test those parameters and characteristics that are not part of F 1798-97 or F 1717-01.

3. Clinical Objectives of Transfixation

Clinical objectives for using transverse connectors are construct/foundation

dependent. Thus the following list of objectives has been subdivided into: constructs in general, thoracolumbar long constructs, and Luque-Galveston foundations.

3A. *Constructs in general:*

1. To create stable constructs (structures) that resist with appropriate stiffness all 3 dimensional force and moment components of applied load without having to rely upon load sharing by the anterior column.
2. To avoid mechanism constructs (Figure 3) that freely move due to little or no resistance to some 3 dimensional components of applied force and moment until load sharing stops the movement and resists the applied load.

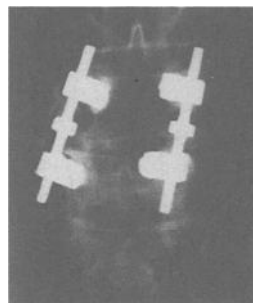


Figure 3 – *Clinical example of unstable 3D mechanism construct.*

3B. *Thoracolumbar long constructs:*

1. To increase torsional stiffness of the construct (resistance to axial torque).
2. To prevent lateral separation of rods and related hook dislodgment.
3. To create secure hook-claw foundations.
4. To increase resistance to pull out by triangulation of pedicle screws.
5. To increase stability of and reduce internal loads within screw foundations.

3C. *Luque-Galveston foundations:*

1. To reduce pull out of iliac posts.
2. To increase stiffness to lateral bending and thus control the piston effect.
3. To create secure sacroiliac foundations.

4. Construct Characteristics and Parameters Affecting the Need for Transfixation, and Transverse Connector Biomechanical Characteristics and Parameters Affecting the Achievement of Clinical Objectives

Construct characteristics and parameters affecting the need for transfixation, and the important biomechanical characteristics and parameters of transverse connectors affecting the achievement of their clinical objectives is dependent upon the type of construct on which transverse connectors are applied. Thus the following list has been subdivided into the following constructs: bilevel four pedicle screw constructs, constructs with single level insecure bone attachment (hook-claw-wire) at each end, thoracolumbar constructs having a less secure bone attachment type (hook-claw-wire) superior foundation and a pedicle screw inferior foundation, constructs with Luque-Galveston inferior foundation, and constructs in general. No additional biomechanical characteristics or parameters related to transverse connectors were observed in stabilizing multilevel pedicle screw constructs than observed in bilevel construct stabilization [5, 6]. One reason is that

constructs with three or more levels of pedicle screw fixation tend to be more stable than bilevel since each additional level of pedicle screw fixation acts as a transverse connector to the bilevel portion of the construct.

4A. Bilevel Four Pedicle Screw Constructs

Bilevel four pedicle screw construct characteristics and parameters affecting need for transverse connection are:

1. Resistance to screw rotation within bone which clinically can not be relied upon and decreases with time.
2. Load sharing by the anterior column may provide adequate stability to the construct without use of a TC, and is probably the reason for the clinical success of non-transfixed constructs that would otherwise be unstable.
3. Pedicle-to-pedicle angle [1, 2, 7]. 0° results in unstable mechanism constructs in the absence of resistance to screw rotation within bone (Figure 2). Posterior rectangular constructs can not resist lateral loading, and if displaced into a parallelogram configuration can not resist axial loading. Trapezoidal configurations can not resist lateral bending in addition to lateral and axial force. As pedicle-to-pedicle angle increases above 0° , construct stability (resistance to the aforementioned components of applied load) rapidly increases while internal forces and moments rapidly decrease both of which begin to asymptotically level off above 30° .
4. Torsional grip of screw anchor connection to the longitudinal member. Loss of torsional grip to the longitudinal member in two or more connections creates a 3D mechanism construct that can not resist torsional loading (Figure 1 and 3). This instability occurs regardless of pedicle angle.

Transverse connector biomechanical characteristics and parameters affecting the achievement of the clinically identified objectives are:

1. Transverse member's lateral bending stiffness. The rubber band simulated TC shown in Figure 2 deformed into an "S" shape, which illustrates zero lateral bending at the center of the transverse member with max lateral bending occurring adjacent to and at the center of each longitudinal member. The same "S" shape was observed when the rubber band simulated TC was attached to the torsionally unstable construct in Figure 1.
2. Transverse member's axial stiffness. As can be observed in Figures 1 and 2, there is some change in perpendicular distance between longitudinal members during displacement of the construct. However, the rate of change is relatively small at first since the TC's loosened connection was observed to slide freely along the longitudinal member for approximately +/- 1 cm before the construct began to increase its load resistance. Thus, axial stiffness of the transverse member is a parameter but of lesser importance than its bending stiffness.
3. Lateral bending strength of TC's interconnection to longitudinal member. As illustrated in Figure 2, the maximum lateral bending moment occurs at the TC's interconnection to the longitudinal member.
4. Axial grip of TC's interconnection to longitudinal member. Translation of the

loosened TC interconnection along the longitudinal rod as illustrated in Figure 1 has been the primary relative motion observed for each of the unstable mechanism constructs (Figures 1, 2) and corresponding components of applied load.

5. **Number of TCs.** One TC located anywhere between or outside of the instrumented levels is adequate to eliminate the unstable mechanism characteristics and associated high internal forces and moments. Two TCs at ends of construct versus one central TC has little to no effect on construct stiffness to axial, flexion-extension, or AP load [4, 9], but does produce some increase in construct stiffness to torsional, lateral bending, and lateral force [4, 9, 10].

4B. Single Level Insecure Bone Attachment (Hook-Claw-Wire) at Each End Type of Construct

Linkage analysis [3] and physical models (Figure 4) were used to identify the important transverse connector parameters associated with transfixing single level insecure bone attachment (hook-claw-wire) at each end type of construct. Based upon treating the construct as a 3 dimensional linkage with joints having resistance to relative rotation, the equation for torsional resistance T of these constructs in terms of the terminology defined in Figure 5 is:

$$T = (LR/LL)T_z + (2 * L3/LL)T_x \quad (1)$$

Transverse connector biomechanical characteristics and parameters affecting the torsional resistance of these constructs are:

1. Transverse connector's:
 - T_z, torsional grip to longitudinal rod.
 - T_x, torsional grip to transverse rod.
 - Transverse plane bending stiffness of the transverse member is required to transmit the action-reaction torque T_z between the TC's connectors.
 - Torsional stiffness of the transverse member is required to transmit the action-reaction torque T_x between the TC's connectors.
2. Dimensions and location of TCs:
 - LR, spacing between the two TCs measured along the longitudinal member. Based on the (LR/LL) factor in equation 1, the construct has greater torsional resistance when the TCs are further apart (greater LR) for a given torsional gripping strength T_z to the longitudinal rods.
 - L3, lateral distance between the longitudinal members. Based on the (2*L3/LL)

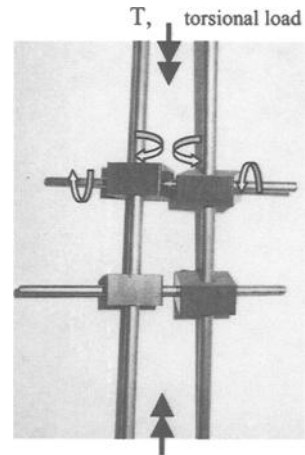


Figure 4 – Single level insecure bone attachment at each end type of construct with arrows showing relative rotation of upper TC's connectors about each longitudinal member and the transverse member when torsionally loaded. Note the similar rotation of the lower TC.

factor in equation 1, the construct has greater torsional resistance when the longitudinal members are further apart (greater L_3) for a given torsional gripping strength T_x to the transverse member.

LL , the longitudinal distance between the single levels of attachment to bone. Based on the (LR/LL) and $(2*L_3/LL)$ factors in equation 1, the shorter the distance between end foundations, the greater is the constructs torsional resistance for given torsional gripping strengths T_z and T_x .

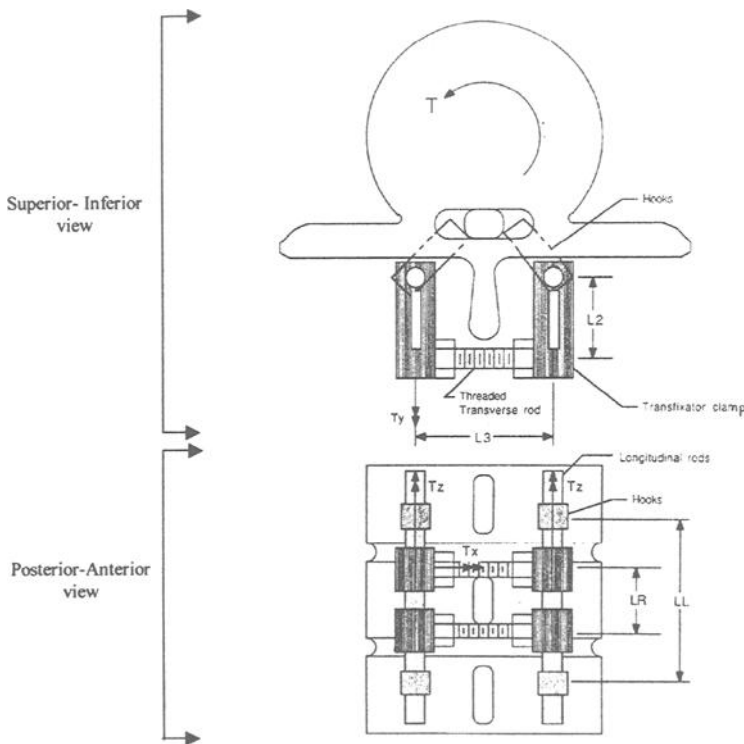


Figure 5 – Linkage model, definition of TC parameters and construct with single level hook at each end.

Physical models (Figure 4) with T_z or T_x independently set to zero as well as both simultaneously set to zero were torsionally loaded manually to confirm that existence of either T_z or T_x alone would produce a construct resistant to torsional load. This was done by drilling slip fit holes in the PVC blocks (simulated TC connectors in Figure 4) corresponding to the gripping strength T_z or T_x desired as zero, while using a press fit hole to create a non-zero gripping strength interconnection. Distances L_R and L_3 were also varied to confirm their relative influence on construct torsional resistance.

L_3 is clinically limited in magnitude by the patients anatomy, thus torsional grip T_x

to the transverse member and its torsional stiffness is less important than is torsional grip T_z to the longitudinal member and the corresponding transverse plane bending stiffness of the transverse member.

4C. *Thoracolumbar Constructs Having a Less Secure Bone Attachment Type (Hook-Claw-Wire) Superior Foundation and a Pedicle Screw Inferior Foundation*

The model shown in Figure 6 was used to investigate the need for and the biomechanical characteristics and parameters associated transverse connectors on thoracolumbar constructs. The model simulated constructs having a less secure bone attachment type (hook-claw-wire) superior foundation with a more secure pedicle screw bone attachment inferior foundation. The inferior foundation was four screw with 0° pedicle angle, similar to the lateral and axial load unstable two level four screw construct shown in Figure 2. Also, the results in Wood et al’s “Torsional Rigidity of Scoliosis Constructs” [8] paper were studied. They performed unconstrained torsional rigidity tests on four short (T2-T11) and four long (T2-L3) scoliosis constructs having different foundations (hooks only; hooks with concave side thoracic sublaminar wires; hooks with distal pedicle screw anchors; and hooks, distal pedicle screw anchors and concave thoracic sublaminar wires) with no, one upper, one lower, or two crosslinks.

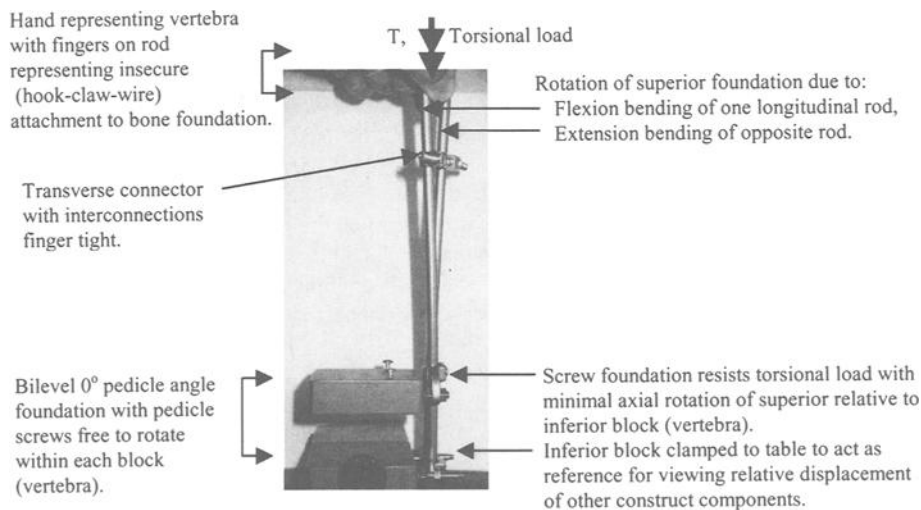


Figure 6 – *Thoracolumbar construct model with torsional load T applied.*

Lateral Load Instability - The model in Figure 6 with no transverse connector was found to be unstable to lateral force due to the inferior foundation being similar to the unstable mechanism construct in Figure 2. A single TC located at the superior end of the

construct as shown in Figure 6 with secure interconnections to each longitudinal member was able to stabilize the construct to lateral loading. This was true regardless of the TC's location along the longitudinal member. The following observations were also independent of TC location. When one TC interconnection to the longitudinal rod was loosened to finger tight, its primary relative motion was translation along the rod. When the TC was simulated with a rubber band, the same "S" shape bending-stretching characteristics were observed as shown in Figure 2 for the bilevel screw construct. Thus the same biomechanical characteristics and parameters affecting the need for transfixation and of the transverse connector itself listed in section 4A of this paper for lateral load resistance also apply to thoracolumbar constructs with bilevel pedicle screw foundations.

Torsional Load Stability - Wood et al [8] concluded that "one or two cross-links placed posterior fail to exert as much global torsional control as bilateral pedicle screws compared to all hook and wire foundation constructs". The torsional stabilizing ability of a bilevel screw foundation relative to that of a less secure (hook-claw-wire) foundation can be seen with the hand held model in Figure 6 by observing the minimal rotation within the inferior foundation compared to the significant relative rotation of and within the superior foundation. The torsional instability of constructs with insecure (hook-claw-wire) foundations at each end of the construct can be seen in Figure 4 by the large anterior displacement of the left and posterior displacement of the right rod at the superior end of the construct with corresponding opposite direction of rod displacement at the inferior end. Thus the need for transfixation to achieve torsional stabilization of thoracolumbar constructs is dependent upon the type of end foundations and the security of their attachment to the spinal column (bone).

The following is a summary of thoracolumbar foundation and construct biomechanical characteristics and parameters affecting the need for transfixation to achieve construct torsional stability:

1. 4 screw bilevel foundation, is resistant to torsion without transfixation unless two or more screw anchors have inadequate torsional grip on the longitudinal member as illustrated in Figures 1 and 3. Thus transfixation at a bilevel screw foundation is not mandatory if it and the correspondingly spanned vertebral column is stable to other components of load, and torsional grip of screw connectors to the longitudinal members is adequate.
2. Hook-claw-wire foundation. Hook-claw-wire interconnection security to bone in all three dimensions is more variable than that of a pedicle screw. Thus hook-claw-wire foundations are more in need of transfixation to keep hooks and claws from dislodging, rods from spreading, and to resist rotation at that level of the construct as shown by the hand held model in Figure 6.
3. Flexion-extension bending stiffness of the longitudinal rods. As can be observed in Figure 6, if a pedicle screw foundation that is stable itself to torsional load exists on one end of a thoracolumbar construct, the primary cause for relative rotation of the opposite end of the construct is flexion bending of one rod with corresponding extension bending of the opposite rod.

The important biomechanical characteristics and parameters of a transverse connector at the level of a less secure (hook-claw-wire) foundation to achieve increased

torsional stability of the construct are:

1. T_z, torsional grip to longitudinal rod.
2. Transverse plane bending stiffness of the transverse member that is required to transmit the action-reaction torque T_z between the TC's connectors.
3. T_x, torsional grip to transverse rod.
4. Torsional stiffness of the transverse member, which is required to transmit the action-reaction torque T_x between the TC's connectors.

The first two (T_z, and transverse plane bending stiffness of the TC cross member) are in general more significant as can be observed in Figure 6 by the greater rotation of the TC's connectors about the longitudinal rods than about its cross member. As another indication of the importance of TC torsional gripping strength to the longitudinal rods, Cook et al [13] observed corrosion at upper TC interconnections to the longitudinal rod when removing lower gripping strength TCs for late operative site pain. In comparison, there has been no late operative site pain in similar constructs having TCs with stronger gripping strength interconnections.

4D. *Constructs with Luque-Galveston Foundation*

Fatigue failure of the transverse member of TCs located at the level of Luque-Galveston Foundations have been clinically observed [12]. Failure has consistently been laterally located adjacent to the TC's connection to one of the longitudinal members (Figure 7). This location and mode of failure is consistent with the lateral bending moment profile illustrated in Figure 2b, zero at center of TC increasing to a maximum at each longitudinal member. Reversed lateral bending within the TC would occur as resistance to vertical force is shifted from one leg thus longitudinal member to the other during ambulation, which clinically is referred to as the "piston effect".

The important TC biomechanical characteristics and parameters involved in controlling the piston effect and preventing iliac anchor pull out are:

1. Axial gripping strength of TC's interconnection to the longitudinal rod.
2. Lateral bending strength of TC's interconnection to the longitudinal rod.
3. Lateral bending stiffness and fatigue strength of TC's transverse member.
4. Axial stiffness of the TC's transverse member.

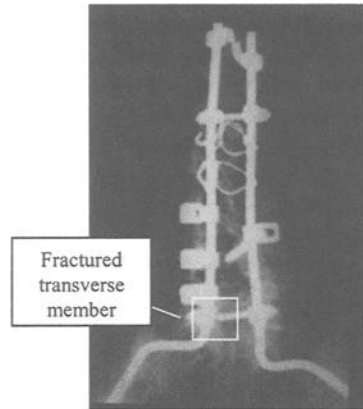


Fig. 7 — *Luque-Galveston foundation with fractured transverse member due to its lateral bending caused by construct piston effect.*

4E. Constructs in General

Fifty seven of the 111 component failures reported in the survey of 2499 clinical cases [12] were longitudinal rod fractures, 26 being adjacent to some type of connector including TCs. Connectors have also been observed during four point bend in vitro testing [12] to be detrimental to the flexion fatigue life of longitudinal members.

5. Existing and Needed Tests for Transverse Connectors in ASTM Standards

Summarizing the analysis presented in section 4 of this paper, the important transverse connector biomechanical characteristics and parameters for achievement of the clinical objectives presented in section 3 are:

1. Gripping strength of interconnections, axial and torsional to the longitudinal member, and to a lesser degree to the transverse member.
2. Lateral bending characteristics of transverse member and interconnections, static stiffness and strength, and fatigue strength of the transverse member and its interconnection to the longitudinal member.
3. Corrosion resistance of interconnections, particularly to longitudinal member.
4. Effect of TC connectors on longitudinal member's flexion bending fatigue life.
5. Transverse plane bending, and torsional characteristics of transverse member, stiffness and strength of the transverse member to transmit the action-reaction gripping torque T_z of interconnections on the longitudinal members, and to resist the action-reaction torque T_x about the transverse member of TC connectors.

The results of comparing these biomechanical characteristics and parameters to those tested in current ASTM standards are presented in the following subsections. Fixture modifications and/or additions are also proposed for those characteristics and parameters inappropriately or not tested in current standards.

5A. Axial and Torsional Grip to Longitudinal and Transverse Members.

The axial and torsional protocols in F 1798-97 are appropriate for testing TC interconnection gripping strength to longitudinal rods and the transverse member.

5B. Lateral Bending Characteristics of Transverse Connector Assemblies.

The flexion bending axial load test protocol on bilevel constructs that are symmetrical to the mid sagittal plane in F 1717-01 produce little to no load on and within the transverse connector(s) as verified by finite element analysis [4 – 7]. This type of test does however produce applicable characterization

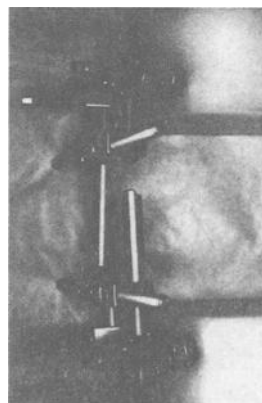


Fig. 8 – Flexion bending rod fatigue at TC connector produced with F 1717-01 axial load protocol.

of the effect of TC connections on the flexion bending fatigue life of longitudinal rods, fracture occurring adjacent to the TC connector (Figure 8) as has been observed clinically [12].

Figure 9 contains a schematic and photos of an H construct that Carson et al [11] have used to characterize TC static lateral bending stiffness and strength, and reversed lateral bending fatigue characteristics. As shown in the schematic of Figure 9, the reverse direction “lateral” bending moment is zero at the center of the transverse member and maximum at its interconnection to each longitudinal rod. The coronal plane shear load in the transverse member is constant over its length and is equal to the applied load F on the H construct. This shear load is the component of force that must be resisted by the axial gripping force of the TC interconnections to the longitudinal members. Thus the “combined” lateral bending and axial gripping characteristic of each TC interconnection to a longitudinal member is tested by this H construct. This in vitro construct has produced fatigue fracture of the transverse member at its entry into the connector to the longitudinal rod, which corresponds to the consistent clinical observation [12] of the lateral location of TC failure in Luque-Galveston foundations (Figure 7). This correlation implies that the in vivo lateral bending profile is similar to that created by the H construct.

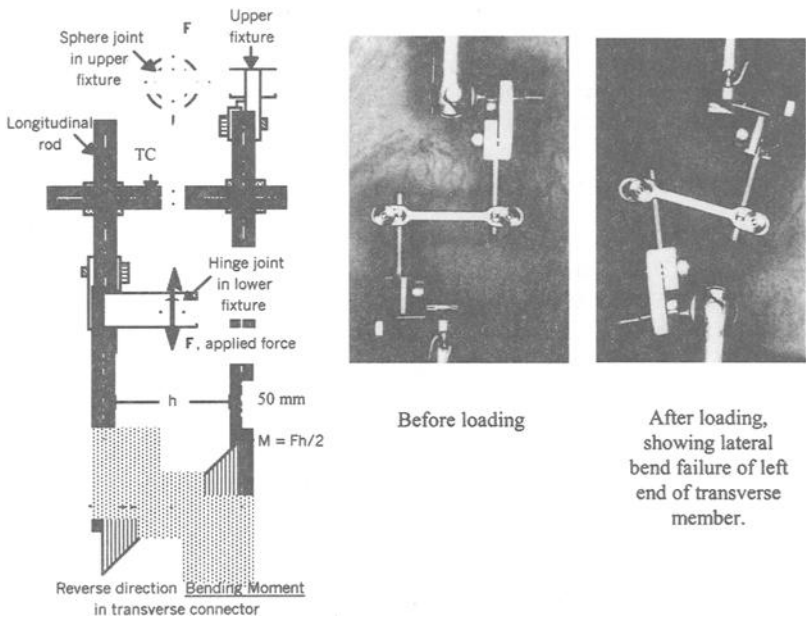


Fig. 9 — H construct used by Carson et al for testing reverse direction lateral bending characteristics of TCs [11].

The “transverse moment test apparatus for subassembly” in F 1798-97 (Figure 10) would produce the same bending moment and shear force profile on one half of a TC if the force is applied directly to a cross section of the transverse member located 25 mm from the longitudinal member. The primary advantage of an H construct is that no external load is applied on the transverse member, and thus no force application fixture is required on the transverse member that could influence its biomechanical characteristics. Thus the H construct produces a more clinically appropriate assessment of the lateral bending stiffness and strength of the entire transverse connector assembly. Also, the H construct avoids the practical difficulties associated with applying the force to TCs having some type of mid transverse member connection, and those of unsymmetrical design with portions of a connector being near the desired point of force application.

The H construct in Figure 9 simulates the TC being at the end of a construct since the longitudinal rod resists no force or moment on one side of each TC rod connector. It also produces no axial force in the cross member. Figure 11 contains a schematic of an alternate H construct assembly for lateral bending tests, which simulates the TC being located somewhere in the mid section of a construct. It creates a coronal plane shear load in the cross member equal to the applied load F , and an axial force in the cross member that increases with applied load as the construct elastically or plastically deforms. If the TC and corresponding construct is symmetrical, the TC would be subjected to the same reverse “lateral” bending moment profile that is shown in Figure 9.

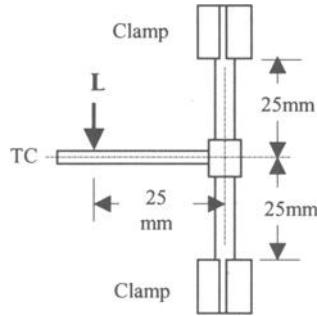


Fig. 10 – Transverse moment test apparatus for subassembly (Fig. 4 in F 1798-97).

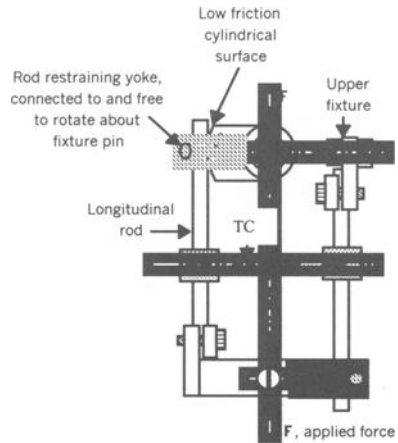


Fig. 11 – Alternate H construct to simulate TC located in the mid section of a construct for testing the TC’s lateral bending characteristics.

5C. *Torsional Loading Characteristics of Transverse Connector Assemblies.*

The pinned-pinned torsional with axial bias load symmetrical construct test protocol in F 1717-01 constrains three of the six relative degrees-of-freedom of superior relative to inferior vertebra motion. For this reason, torsional tests with F 1717-01 fixturing produces test results that are questionable relative to their clinical relevance [2]. Standardized test fixtures and a protocol to test the torsional capabilities of transfixied compared to non-transfixied bilevel constructs/foundations, and longer constructs having different combinations of hook-claw-wire and pedicle screw foundations needs to be developed. As an example, Wood et al [8] developed and used a system of fixtures to test the later. An alternative gimbal-gimbal fixture or gimbal-pushrod fixture that releases all six relative degrees-of-freedom have been proposed in an ASTM STP 1431 paper [2]. In addition, Figure 12 contains a fixture which would simulate and test the 3 dimensional 6 degree-of-freedom torsional resistance characteristics of constructs with transfixied sacroiliac foundations, such as the Luque-Galveston foundation.

5D. *Fretting-Corrosion Characteristics of Transverse Connector Assemblies.*

Fretting-corrosion of lower gripping strength transverse connector interconnections has been observed clinically, usually at upper transfixied hook-claw-wire foundations [13]. Hook-claw-wire foundations vary in configuration, and the security of their bone-implant interconnections. Therefore, they are more likely to initially rely on the transverse connector to resist torsion before deflection within the foundation locks it and commences to resist torsion. To simulate this clinical condition would require developing a torsionally loaded construct having an insecure bone to hook-claw-wire interconnection foundation. Carson et al [11] has observed fretting corrosion debris similar to that which occurs in vivo [13] during H construct lateral bend tests on transverse connectors when conducted in a Ringer's solution maintained at 37°C and $6 < \text{Ph} < 7$. The magnitude of fretting-corrosion was observed to be greater for connectors having lower gripping strength when tested under the same load.

The constrained pinned-pinned construct protocols in F 1717-01 would not be expected to produce fretting-corrosion in the axial-flexion test since the transverse connectors carry little to no load for that mode of testing. Fretting-corrosion might occur if the F 1717-01 torsion test protocol were conducted in a saline environment. However due to the constrained fixturing, TC internal loading would typically be less which would reduce the likelihood of observing fretting-corrosion.

Clinically [12, 13] and as observed when testing in saline environments [11], fretting-corrosion occurs within interconnections and is more prevalent the weaker their gripping strength. These observations give credibility to the use of gripping strength results from F 1798-97 as a predictor of the relative likelihood of interconnection fretting-corrosion within implants made of the same materials. Since this is only an indirect predictor, fatigue testing in a saline environment should be encouraged.

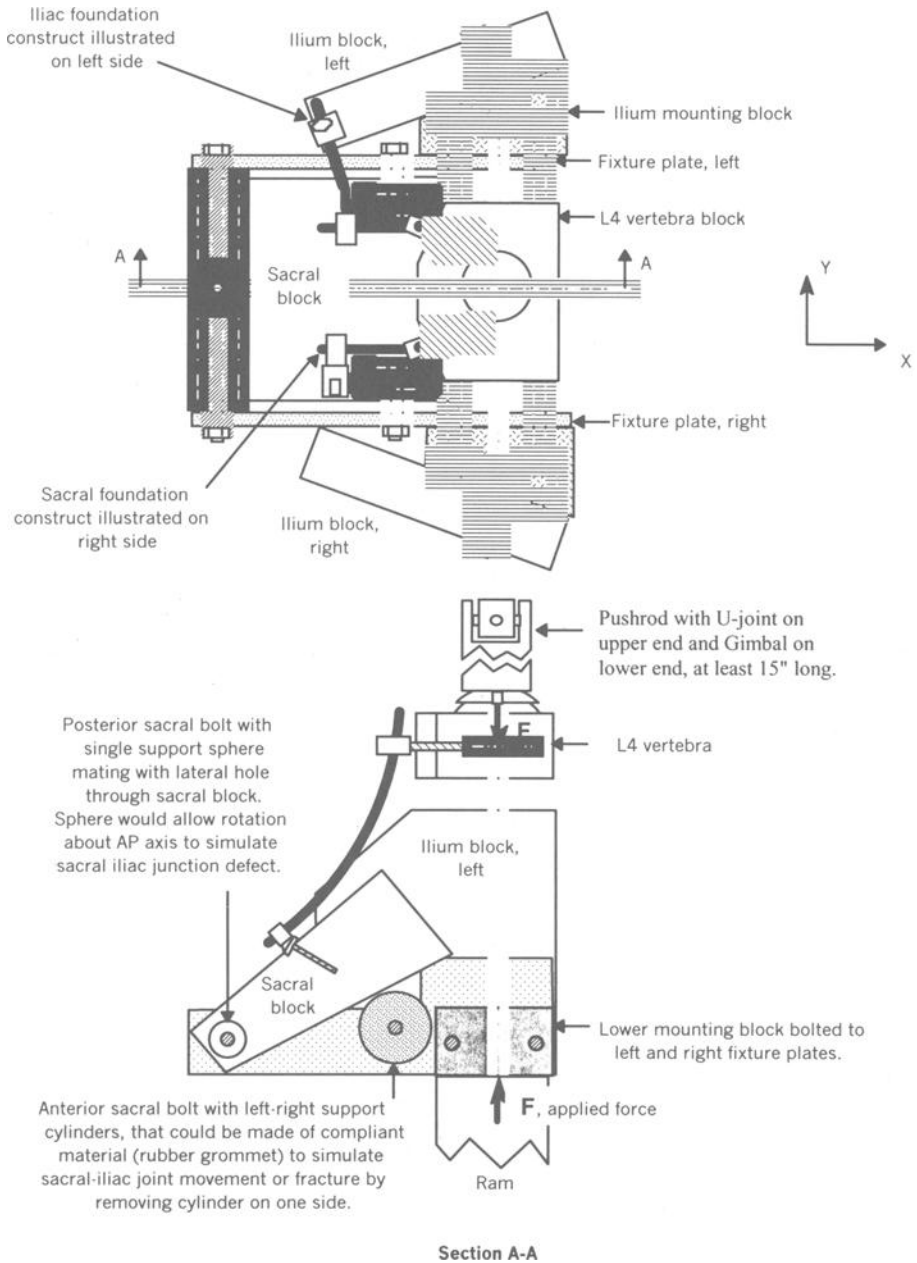


Figure 12 - Proposed universal fixture for testing long or short constructs with sacroiliac foundations in torsion and/or axial load.

6. Summary of Recommendations

The following is a summary of recommendations made in the body of this paper.

1. Substitute gimbal-gimbal or gimbal-pushrod fixtures [2] for the pinned-pinned fixtures used in F 1717-01 for axial and torsional testing.
2. Incorporate one of the proposed H construct assemblies illustrated in Figures 9 and 11 into a standard/guide to test transverse connectors for their lateral bending static and fatigue characteristics. Consider performing the tests in saline type environment to evaluate relative propensity to fretting-corrosion.
3. Develop a standard/guide to test constructs for their torsional load resistance characteristics in an unconstrained manner, such as in reference [8] or as shown in Figure 12 that also includes possible testing of sacroiliac foundations.

References

- [1] Carson, W. L., Duffield, R. C., Arendt, M., Ridgely, B. J., Gaines, R. W., "Internal Forces and Moments in Transpedicular Spine Instrumentation, The Effect of Pedicle Screw Angle and Transfixation—The 4R-4Bar Linkage Concept," *Spine*, September 1990, Vol. 15, No. 9, pp. 893–901.
- [2] Carson, W. L., "Relative 3 Dimensional Motions between End Vertebrae in a Bilevel Construct, The Effect of Fixture Constraints on Test Results," *Symposium on Spinal Implants: Are We Evaluating Them Appropriately*, ASTM STP 1431, M. N. Melkerson, S. L. Griffith, and J. S. Kirkpatrick, Eds., ASTM International, West Conshohocken, PA, 2003.
- [3] Voth, B. E., "Analytical and Experimental Evaluation of the Torsional Capabilities of Transfixed Rod-Hook Spine Implant Systems," BSMAE honors thesis, University of Missouri-Columbia, June 1989.
- [4] Sharma, M. S., "The Effect of Transverse Connector Articulation on Bilevel Spinal Implant Construct's Stability, and Internal Forces and Moments," M.S. thesis, University of Missouri-Columbia, May 1994.
- [5] Chen, Liu-Yuan, "Finite Element Analysis of Internal Forces and Moments in Bilevel and Trilevel Spine Instrumentation—The Effects of Pedicle Angle, Transfixation, Vertebra Offset and Variations in Vertebra Size," M.S. thesis, University of Missouri-Columbia, Dec. 1992.
- [6] Voth, B. E., "Finite Element Analysis of Internal Forces and Moments in Bilevel and Trilevel Spine Instrumentation – The Effects of Pedicle Angle, Transfixation, Vertebra Offset and Variations in Vertebra Size," M.S. thesis, University of Missouri-Columbia, Aug. 1991.
- [7] Ridgely, B. J., "Finite Element Analysis of Internal Forces and Moments in Bilevel Transpedicular Spine Instrumentation – The Effect of Pedicle Screw Angle and Transfixation," M.S. thesis, University of Missouri-Columbia, Aug. 1989.

- [8] Wood, K. B., Wentorf, F. A., Ogilvie, J. W. Kim, K. T., "Torsional Rigidity of Scoliosis Constructs," *Spine*, August 1, 2000, Vol. 25, No. 15, pp. 1893–1898.
- [9] Dick, J. C., Zdeblick, T. A., Bartel, B. D., Kunz, D. N., "Mechanical Evaluation of Cross-Link Designs in Rigid Pedicle Screw Systems," *Spine*, March 15, 2000, Vol. 25, No. 6S, pp. 13S–18S.
- [10] Lynn, G., Mukherjee, D.P., Kruse, R.N., Sadasivan, K.K., Albright, J.A., "Mechanical Stability of Thoracolumbar Pedicle Screw Fixation," *Spine*, March 15, 2000, Vol. 25, No. 6S, pp. 31S–35S.
- [11] Carson, W. L., Elphinston, J., "In Vitro Static and Fatigue Testing of SS and Ti Closed (Drop Entry) Threadless TRC, SS Open (Drop Entry) Threadless TRC, and SS Threaded TRC for ¼" Dia. Rods," Confidential report to AcroMed Corp., May 1997.
- [12] Carson, W. L., Asher, M., Boachie-Adjei, O., Lebowhl, N., Dzioba, R., Akbarnia, B., "History of Isola-VSP Fatigue testing results with Correlation to Clinical Implant Failures," *Symposium on Spinal Implants: Are We Evaluating Them Appropriately*, ASTM STP 1431, M. N. Melkerson, S. L. Griffith, and J. S. Kirkpatrick, Eds., ASTM International, West Conshohocken, PA, 2003.
- [13] Cook, S., Asher, M., Lai, S. M., Carson, W. L., "Effect of Transverse Connector Design on Development of Late Operative Site Pain: A Biomechanical and Clinical Study," *Symposium on Spinal Implants: Are We Evaluating Them Appropriately*, ASTM STP 1431, M. N. Melkerson, S. L. Griffith, and J. S. Kirkpatrick, Eds., ASTM International, West Conshohocken, PA, 2003.

William L. Dunbar Jr.,¹ Dan Cesarone,² and Hassan Serhan³

An Evaluation of the Influence of UHMWPE Test Block Design on the Mechanical Performance of Bilateral Lumbar Corpectomy Constructs

REFERENCE: Dunbar, W. L., Cesarone, D., Serhan, H., “An Evaluation of the Influence of UHMWPE Test Block Design on the Mechanical Performance of Bilateral Lumbar Corpectomy Constructs,” *Spinal Implants: Are We Evaluating Them Appropriately? ASTM STP 1431*, M. Melkerson, J. S. Kirkpatrick, and S. L. Griffith, Eds., ASTM International, West Conshohocken, PA, 2003.

ABSTRACT: The purpose of this study was to investigate how the design of corpectomy test blocks influences key strength parameters in bilateral lumbar construct testing. Two different test block designs were used with components from DePuy AcroMed’s Stainless Steel ISOLA™ Spinal System in the evaluation. Both test block designs were made to approximate the bending moment and pedicle screw angle in the lower lumbar spine. The first block type was fixed to the test frame by a pin that passed through the block as recommended in ASTM F1717-97. The second block type had a spherical indentation that mated with a spherical ball fixture (ball-socket connection). A battery of static and dynamic compression bending was performed for each block type. Static compression bending tests for the bilateral constructs yielded statistically different values ($p < 0.05$) for the yield strength, stiffness, and ultimate strength for the two test block types. Dynamic compression bending results showed a difference in runout load of 5.27 Nm between the two block types. The failure modes in static and dynamic compression testing were the same for each block type.

KEYWORDS: Spinal implant testing, lumbar, bilateral construct, corpectomy, test blocks

¹ MS, Senior Research Engineer, Research & Technology Group, DePuy AcroMed Inc., 325 Paramount Drive, Raynham, MA, 02766.

² Project Engineer, Customs & Specials Group, DePuy AcroMed Inc., 325 Paramount Drive, Raynham, MA, 02766.

³ Ph.D., Director, Research & Technology Group, DePuy AcroMed Inc., 325 Paramount Drive, Raynham, MA, 02766.

Introduction

The corpectomy testing specified in the ASTM standard F1717-97 provides a method to evaluate spinal systems and compare them to one another. For bilateral lumbar testing the standard specifies the use of ultra high molecular weight polyethylene (UHMWPE) blocks that are connected to the test frame through a pin (Fig. 1). This pin restricts the movement of the test sample to rotations about the pin and displacements perpendicular to the pin. An alternate test block design that connects to the load frame via a ball-socket joint would allow rotation in all three planes (Fig. 1). It is possible that such a test block could identify deficiencies in a spinal system that are not currently exposed or could provide an alternate means of testing spinal systems.

The objective of the work described here was to determine if such an alternate design of UHMWPE corpectomy test blocks would have an effect on the results of a lumbar bilateral corpectomy compression test battery of the stainless steel DePuy AcroMed ISOLA Spinal System.

Materials and Methods

Components from DePuy AcroMed's Stainless Steel ISOLA™ Spinal System were used for evaluation, including standard slotted connectors, 7.0 × 45 mm pedicle screws, 6.35 mm diameter rods, and transverse cross-connectors. All components were chosen from the same production lots. Two different types of UHMWPE test blocks were used for comparison. Both block types were made to approximate the bending moment and pedicle screw angle in the lower lumbar spine. The first block type was fixed to the test frame by a pin that passed through the block as currently recommended in ASTM F1717-96. The second block type had a spherical indentation in its end that mated with a spherical ball fixture (ball-socket connection). Figure 1 depicts the two block types. Bilateral corpectomy constructs were built with a gauge length of 76 mm as recommended in ASTM F1717-96.

A battery of static and dynamic compression bending was performed following ASTM F1717-96 using each UHMWPE block type (Fig. 2). All tests were performed at the DePuy AcroMed Research Laboratory (Raynham, MA) in ambient room conditions. Static compression bending was performed in displacement control at a rate of 25.4 mm/minute until failure occurred. Failure was defined as either fracture of a construct component or attainment of 50 mm displacement. Results from the two groups were compared using a Student's t-test and SigmaStat (SPSS Science, version 2.0) software. Dynamic compression bending tests were run with fixtures identical to those used in the static testing. Initial test loads were determined by examination of the static compression load-displacement curves. The R ratio (min/max load) was equal to 0.1 for each sample. Tests were run on a MTS Mini-Bionix load frame at a frequency of 5 Hz until failure occurred. A single load frame was used for all samples from each group. Failure of a construct was defined as an increase of 3 mm in the axial displacement of the test frame crosshead. If a failure had not occurred by two million cycles the test was stopped and the specimen was recorded as a non-failure. SN curves were created from the dynamic data through a natural logarithmic curve fit (Fig. 4).

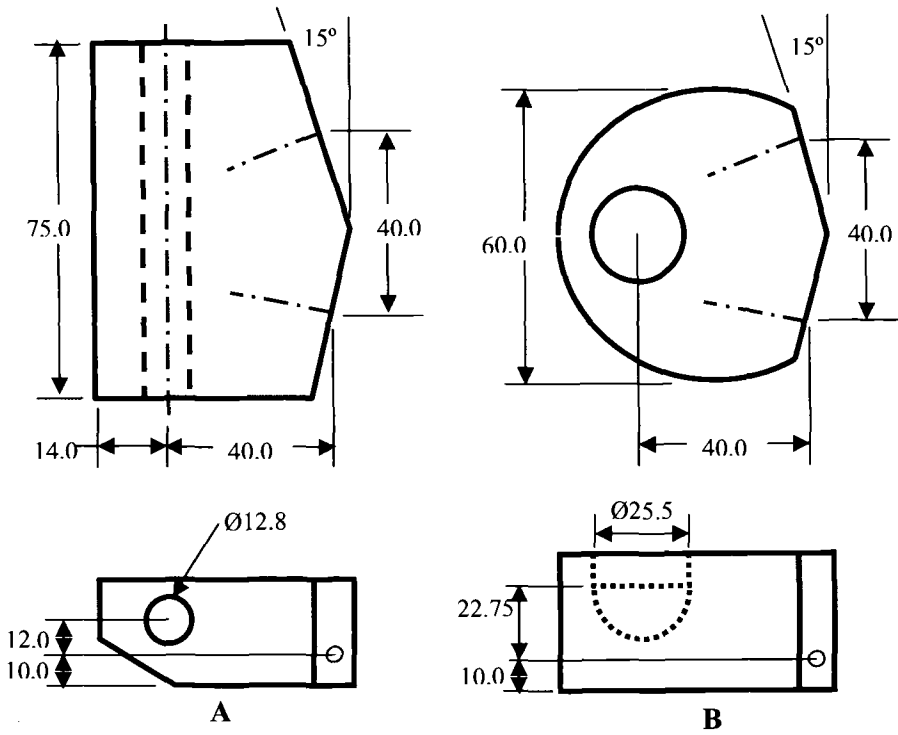


FIG. 1 – Test block geometry. A: Pinned, B: Ball-socket (dimensions are mm).

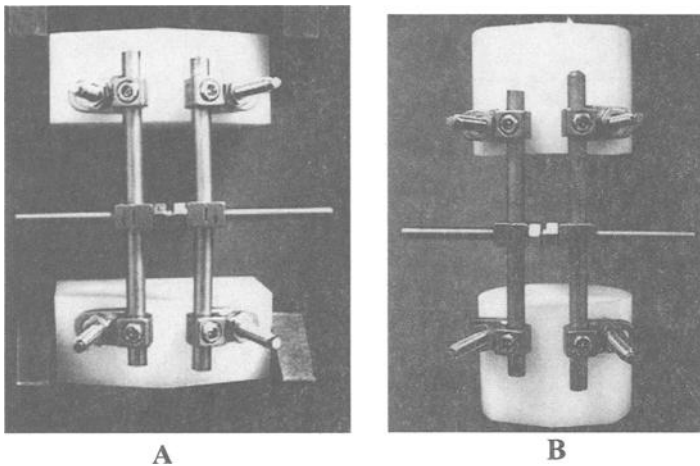


FIG. 2 – Compression test setup. A: Pinned, B: Ball-socket.

Results

Results for static compression testing are summarized in the following table.

TABLE 1—*Summary of static compression results.*

	Yield Strength (Nm)	Displacement @ Yield (mm)	Stiffness (Nm/mm)	Ultimate Strength (Nm)	Displacement @ Ultimate (mm)
Pinned (n=5)	55.2 ± 5.3 [†]	16.6 ± 3.5	3.55 ± 0.74	74.6 ± 0.8 [†]	50.2 ± 0.0
Ball-Socket (n=5)	47.1 ± 1.1	10.4 ± 1.3	5.57 ± 0.16 [†]	70.0 ± 0.8	47.1 ± 2.8

[†] Denotes statistically significant difference.

The yield strength for the constructs assembled with the pinned blocks was significantly higher ($p < 0.05$) than that for the ball-socket blocks. The stiffness for the constructs assembled with the pinned blocks was significantly lower ($p < 0.05$) than that for the ball-socket blocks. The ultimate strength for the constructs assembled with the pinned blocks was significantly higher ($p < 0.05$) than that for the ball-socket blocks. The yield point for both groups corresponded to yield of the longitudinal member. Representative force-displacement curves for each block type are shown below in Fig. 3.

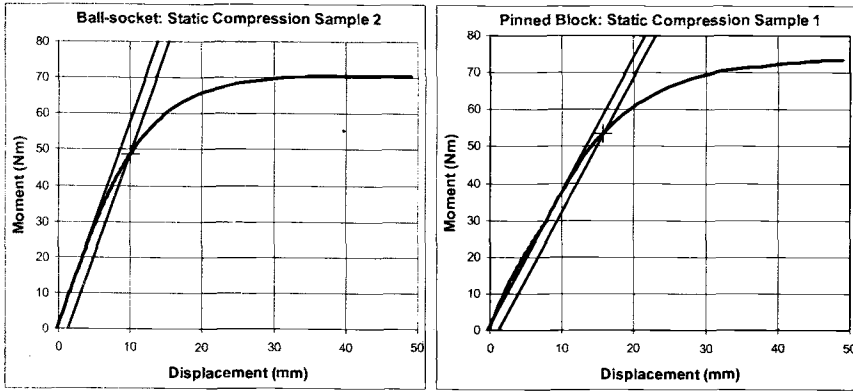


FIG. 3 – *Representative static compression force-displacement charts.*

Results for dynamic compression testing are summarized in the following table.

TABLE 2—*Dynamic Compression Results.*

Load (Nm)	Pinned		Ball-Socket	
	Cycles	Failure	Cycles	Failure
44.78	71,669	Rod at transverse rod connector (TRC)
39.53	165,327	Rod at TRC	92,303	Rod at TRC
36.89	120,164	Rod at TRC
34.26	167,624	Rod at TRC	197,848	Rod at TRC
31.62	211,169	Rod at TRC
28.99	238,017	Rod at TRC	245,229	Rod at TRC
26.35	333,639	Rod at TRC
23.72	644,167	Rod at TRC	2,000,000	No failure
21.08	1,018,712	Rod at TRC
18.45	2,000,000	No failure

The raw data show that all failures in each group occurred in the longitudinal member (rod) at the location of the transverse rod connector. The pinned block constructs achieved runout at 18.45 Nm while the ball-socket block constructs achieved runout at 23.72 Nm. Applying a statistical curve-fit to each data set (Fig. 4) yields a predicted runout at 5 million cycles of 21 Nm with 95% confidence intervals of 25 and 17 Nm for the pinned blocks. Similar analysis yields a predicted runout at 5 million cycles of 24 Nm with 95% confidence intervals of 28 Nm and 18 Nm for the ball-socket blocks.

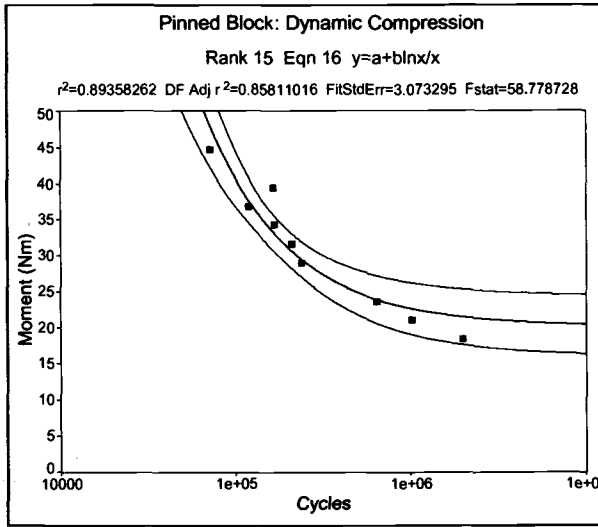


FIG. 4 — S-N curve for pinned block type.

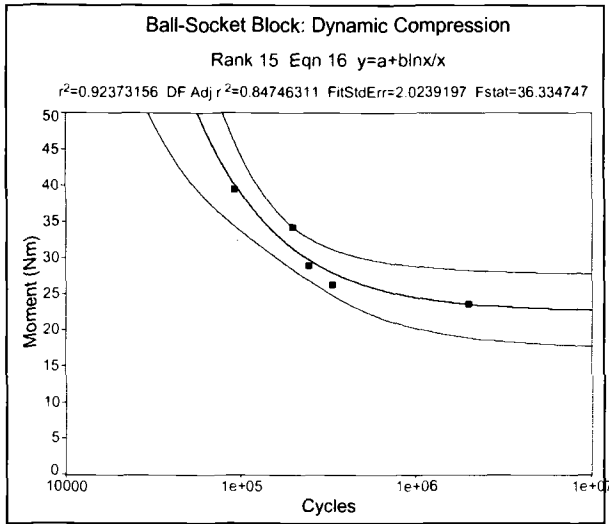


FIG. 4 — S-N curve ball-socket block type.

Discussion

Statistical analysis of the static compression results shows a difference in the results for each block type tested. The ball-socket blocks produced a stiffer construct, giving a lower yield strength and ultimate load. Dynamic compression results also appear to be different for the two block types.

All testing was conducted on the same load frames with calibrated load cells. The UHMWPE used in manufacture of the blocks had the same material properties for each block type. The pedicle screw angle, moment arm, and gauge length were identical for each block type. The tested components from each group were from the same production lots. The main difference between the two block designs, other than the manner in which the load was applied, was the distance between the center of rotation of the test fixture and the center of the screw hole in the blocks (Fig. 1). It was not possible to keep this distance constant, as the diameter of the pin fixtures (12.8 mm) and the diameter of the spherical ball fixture (25.5 mm) were different. The distance from where the load was applied (bottom of the pin hole and bottom of the socket) to the center of the screw hole was equal in each block type, resulting in the difference in the centers of rotation. Lowering the center of rotation in the ball-socket blocks to the currently prescribed center of rotation in the pinned blocks (12 mm from screw hole per ASTM F1717-96) was not possible as the spherical ball test fixture would then interfere with the screw holes.

The larger center of rotation in the ball-socket block type will result in a longer active moment arm as the block rotates during static compression testing. This longer active moment arm may explain why the yield strength and ultimate loads were lower for the ball-socket blocks than for the pinned blocks. To demonstrate the manner in which the active moment arm for each block type will change as the block rotates, the following idealized graph was constructed (Figs. 5 and 6). If the UHMWPE blocks and the pedicle

screws are assumed to be rigid, then it follows that the vertical distance between the center of rotation and the screw hole (distance a in Fig. 5), and the horizontal distance from the applied load to the longitudinal member (distance b in Figure 5) will remain constant as the block rotates.

Point 1: Center of Rotation
 Point 3: Location of Longitudinal Member
 Line b: Screw Hole

	Pinned	Ball-Socket
a	12.0	22.75
b	40.0	40.0
c	41.8	46.0

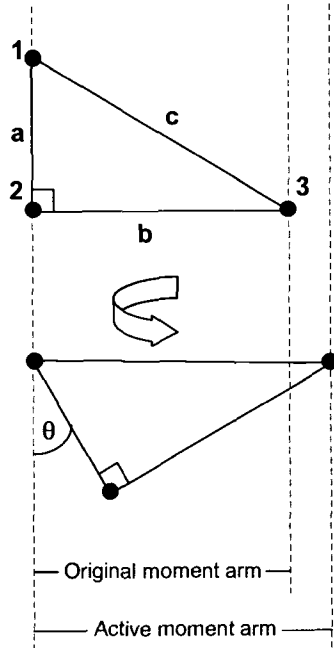


FIG. 5 – Demonstration of the change in active moment arm as test block rotates.

Calculating the active moment arm for the two block types as they rotate from 0 to 45 degrees as depicted above yields the following graph.

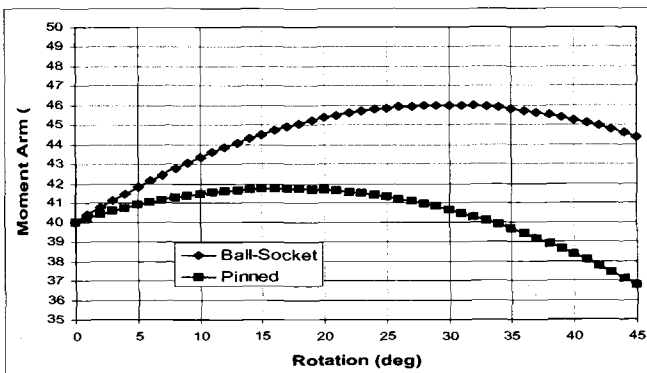


Figure 6 – Graph of active moment arm vs. block rotation.

The graph in Figure 6 shows that the active moment arms for the two block types quickly

diverge as the blocks rotate. At 30 degrees of rotation there is a 13% difference in the values of the active moment arms. Although this is a simplified analysis that does not consider the moment arm in three dimensions, it demonstrates how the active moment arm is effected by the location of the center of rotation for the two test block designs. This difference in active moment arm may explain the difference in static compression results for the two block types, as the results reported in Table 1 were calculated using the original moment arm for each block design and not the active moment arm.

In dynamic testing, the nature of how the load is applied in each block type may have influenced the results. The applied load in the pinned blocks is distributed equally across the entire length of the block (Fig. 1). This may isolate inconsistencies in the longitudinal members of the constructs and cause premature failure of the construct. Inconsistencies between longitudinal members in a construct may include slight differences in active length and stress concentrations introduced during assembly. For the ball-socket blocks, the load is centrally applied and equally distributed to the longitudinal members (Fig. 1). This will shield the same types of inconsistencies that may be highlighted by the pinned blocks.

Conclusions

The two test-block designs used in this study produced different results for static and dynamic compression testing of lumbar bilateral constructs. The screw angles and moment arms were the same in each block type, but the center of rotations and the planes in which rotation are restricted differed. It is concluded that the difference in center of rotation was the contributing factor to the differences in the results. Altering the diameter of the spherical ball fixture to match that of the pins prescribed in ASTM F1717-96 (12.8 mm) and matching the centers of rotation for each block (12 mm from the screw holes) may produce statistically equivalent results for the two block types in static compression testing. The ball-socket block type did not produce any failure modes different from those seen in the pinned block type. Any alternative test block design to be considered for inclusion in ASTM F1717 should be put through a similar comparison and shown to produce statistically similar results to the current test block design in order to maintain the ability to compare mechanical testing across current and future spinal systems.

Juay Seng Tan,¹ Brian K. Kwon,¹ Dinesh Samarasekera,¹ Marcel F. Dvorak,¹ Charles G. Fisher,¹ and Thomas R. Oxland¹

Vertebral Bone Density—A Critical Element in the Performance of Spinal Implants

Reference: Tan, J. S., Kwon, B. K., Samarasekera, D., Dvorak, M. F., Fisher, C. G., and Oxland, T. R., “**Vertebral Bone Density – A Critical Element in the Performance of Spinal Implants.**” *Spinal Implants: Are We Evaluating Them Appropriately*, ASTM STP 1431, M. N. Melkerson, S. L. Griffith, and J. S. Kirkpatrick, Eds., ASTM International, West Conshohocken, PA, 2003.

Abstract: The effectiveness of spinal implants in fixation is dependent upon the bone-implant interface, and thus on vertebral bone density. Current ASTM assessment methods use synthetic elements as vertebral surrogates and therefore, by definition, do not address important in vivo performance and failure characteristics. The purpose of this study is to contrast the mechanical behaviour of pedicle screws in cadaveric vertebrae versus synthetic surrogates. Short-term physiologic axial compression and bending moment were cyclically applied to pedicle screws inserted in lumbar vertebrae and UHMWPE. Kinematics of the pedicle screws in bone and in UHMWPE were significantly different in terms of the range of motion and pivoting and bending points on the screws. For the vertebral fixation, there was a trend towards a more rigid screw-bone interface with increasing bone mineral density. Devices tested using ASTM and ISO test standards may give clinicians and regulatory bodies a false sense of security with respect to implant performance due to their limited scope.

Keywords: bone mineral density, pedicle screw, mechanical testing, implant loosening

Introduction

Spinal instrumentation is commonly used to stabilize the spine in conditions of trauma, tumor, deformity, and degeneration. Various implant types are in existence, including pedicle screws, pedicle and laminar hooks, wires, cables, rods and plates, as well as anterior devices such as interbody cages. The pre-clinical assessment of these devices may involve many different types of testing, as described previously [1,2]. Within the last decade, ASTM standard test methods for spinal implants have been developed. One such Standard is the ASTM Test Methods for Static and Fatigue for

¹ Ph.D. Student, Orthopaedic Spine Surgeon, Research Assistant, Head of Division of Spinal Surgery, Orthopaedic Spine Surgeon, Head of Division of Orthopaedic Engineering respectively, Department of Orthopaedics, University of British Columbia, 3114-910 West 10th Avenue, Vancouver, BC Canada V5Z 4E3.

Spinal Implant Constructs in a Corpectomy Model (F 1717). The focus of this article is to address the relevance of F 1717 to the clinical situation.

In general, spinal instrumentation is effective in correcting deformity and stabilizing the spine, however, failures do occur. Clinical mechanisms of instrumentation failure are varied, but include intra-operative, or early post-operative fixation failure, late development of pseudoarthrosis with concomitant implant loosening, and disc or vertebra failure adjacent to the instrumentation [3–6]. Ideally, testing methods would address these failure mechanisms, but this can be a significant challenge. For example, adjacent segment effects represent both a biological and mechanical problem that may be difficult to simulate in a pre-clinical model. However, early fixation failure represents a series of failure modes that can be evaluated in a pre-clinical model, including both failure of the specific device or the interface between the device and the spine. Clinical investigation suggests that it is the interface between the device and the spine that is the most common site of early failure [3,5]. Essentially, this represents failure of the bone-implant interface.

Biomechanical studies have demonstrated that bone mineral density, and more so the presence of osteoporosis, is a critical factor in the success of achieving rigid fixation both for pedicle screws [7–13] and interbody cages [14,15]. In general, pedicle screw pull-out strength and toggle amplitude as well as interbody cage subsidence resistance and overall stabilisation have been shown to be linearly correlated to BMD.

The F 1717 uses synthetic elements as vertebral surrogates and therefore does not address the bone-implant interface. The F 1717 does evaluate the mechanical properties of the screw-rod constructs, particularly in fatigue failure. However, such failure is not a common mode of clinical failure [3–6]. Since cancellous bone has an elastic modulus that ranges between 0.01–1.0 GPa, whereas UHMWPE has a modulus of 1 GPa, the construct would be expected to behave differently if the bone was included in the assessment.

The primary purpose of this study was to contrast the mechanical behaviour of pedicle screws under short-term cyclic physiologic loads when inserted in cadaveric vertebrae versus synthetic surrogates. Secondly, the effect of bone mineral density on the pedicle screw behaviour was investigated, as was a novel model of simulating a situation where the screw-bone interface is recognised as being poor. In essence, we are questioning whether the fixation at the bone-implant interface can be measured during short-term cyclic testing.

Materials and Methods

Specimen Preparation

Eight lower lumbar cadaveric vertebrae (three L3s, three L4s, two L5s) from a previous endplate indentation study [16] were used in this study. All specimens had intact pedicles. Lateral DEXA bone mineral density (BMD) ranged from 0.30 to 1.04 g/cm² with a mean of 0.70 g/cm².

Pedicle screws of uniform size (USS diameter 6 mm and length 45 mm, Synthes Spine, Paoli, PA) were inserted into each pedicle. A single spine surgeon (BK) carried out all screw insertions for the specimens. Two types of pedicle screw hole preparation

were carried out in a randomised manner for each specimen. One side was prepared in the normal recommended fashion using a blunt pedicle probe to a depth of approximately 50 mm. The other side was prepared with an overdrilled hole using a 15/64 inch (5.95 mm) drill bit to a depth of 50 mm. The latter method was an attempt to create a "loosened" screw model. Accuracy of insertion was checked by direct palpation of the pedicle walls. Radiographs were taken in the cephalo-caudad (axial) direction to verify screw placement through the pedicle. Specimens were defrosted at room temperature for 4 to 5 hours before screw insertions were carried out. After the screws had been inserted, the specimens were soaked in saline solution and submerged in a water bath maintained at 37 °C for 16–24 hours before being tested.

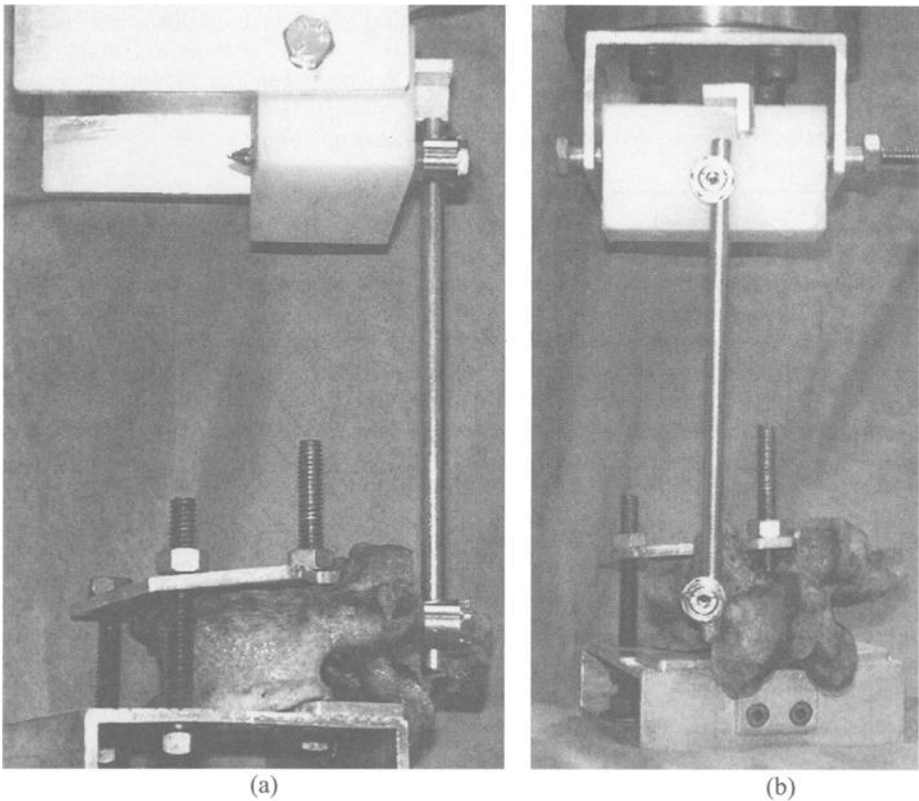


Figure 1—(a) Lateral and (b) frontal view of the testing jig. A single vertical rod connects the two pedicle screws, which in turn are inserted into a UHMWPE block superiorly and into the pedicle of a cadaveric specimen inferiorly. Other tests included a UHMWPE block inferiorly as well. The pedicle screws were placed parallel to each other and the connecting rod was aligned vertically before every test. The vertebral body was securely clamped to the base of the testing machine, whereas the UHMWPE was allowed to pivot about an axis 35 mm away from the vertical rod.

Pedicle Screw Loading

A custom built jig was used to test the pedicle screws with loads simulating physiological conditions. The basic test configuration was similar to the ASTM standard (F 1717), but a cadaveric vertebra replaced the inferior block and the dimensions were modified to reflect recent *in vivo* load data [17,18]. To allow comparison between screw fixation in a vertebra and UHMWPE, an inferior block of UHMWPE was used in other tests. A vertical connecting rod of length 140 mm was attached to the two pedicles screws, which were inserted in a UHMWPE block and in the pedicle of a cadaveric specimen respectively (Fig. 1). The inferior blocks and specimens were clamped rigidly to the base of the testing machine, which is a different setup from the ASTM standard. This fixation method was selected to prevent the specimen breakdown that would probably occur if a single loading point had been used for the vertebra. The design of a rigid inferior mount results in somewhat different moments being applied to the screw-vertebra interface, depending upon the vertebral material. A two-dimensional finite element analysis demonstrated this effect, which is shown in Fig. 2.

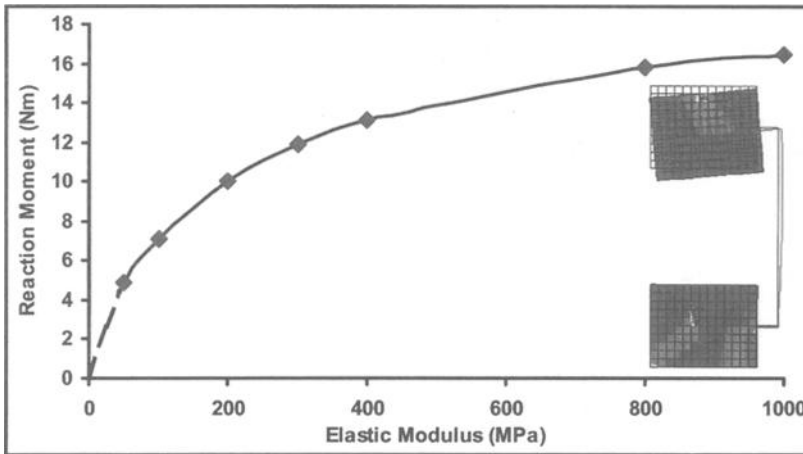


Figure 2—A two-dimensional finite element analysis determined the variation in ground reaction moments as a factor of elastic modulus of the lower block. The lower block was rigidly fixed in translation and rotation while the upper block was allowed to rotate.

The initial position of the specimen was such that the pedicle screw was in a horizontal position. The upper segment of the testing apparatus was attached to the actuator arm of the testing machine and was hinged to the UHMWPE block, allowing the block to freely rotate about a single axis. The horizontal distance between the hinge and the vertical rod was 35 mm. Liquid levels were used to ensure that the vertical connecting rod was in an absolute vertical position prior to toggle tests. A single UHMWPE block was used and the same pedicle screw was inserted in the block throughout all the tests.

The vertical load acting on the setup was cycled between an axial compression of 300 N and tension of 30 N at a rate of 0.5 Hz for 100 cycles using a servohydraulic test system (Instron 8874, Instron Corporation, Canton, MA). The moment arm of 35 mm resulted in a bending moment ($300 \text{ N} \times 35 \text{ mm} = 10.5 \text{ Nm}$) in the connecting rod in addition to the cephalo-caudad force. This ratio of axial load to bending moment was based upon *in-vivo* measurements [17,18].

Kinematics

Motion of the pedicle screws with respect to the inferior UHMWPE and the cadaveric specimens was detected using a high precision optoelectronic system (Optotrak 3020, Northern Digital Inc., Waterloo Canada) at a rate of 10 Hz, which gave twenty data points for each cycle. Two sets of marker carriers, each with four infrared LEDs, were mounted onto the rigid bodies: pedicle screw and bone or pedicle screw and UHMWPE block (Fig. 3). The three dimensional motion of these two rigid bodies with respect to one another was post processed.

A Cartesian local coordinate system was specified to describe the motion of the pedicle screws. The origin of the local coordinate system lay along the axis of the screw at the point where the connecting rod was attached to the pedicle screw. The z-axis always pointed away from the screw tip. The y-axis was parallel to the connecting rod and pointed upwards toward the direction of the superior pedicle screw. The direction of the x-axis was the vector cross product of the y- and z-axes.

The relative motions between the pedicle screw and the UHMWPE and between the pedicle screw and the vertebral bone were post processed from the three-dimensional motion data using custom software. The range and offset of the motion of the pedicle screw head were obtained from the average of the last five cycles (96th to 100th). These parameters gave an indication of dynamic motion under repetitive loading (range) and of settling or subsidence (offset). As the applied loads were in the sagittal plane (parallel to the pedicle screws), the resultant motions were primarily y translation and x rotation (Fig. 4). Furthermore, the translation of the screw tip was also calculated, which when combined with the translation of the screw head, allowed for an estimation of the instantaneous axis of rotation to be made.

Statistics

The range and offset of the motion of the pedicle screw head were compared between the three types of insertion: UHMWPE, normal insertion and overdrilling. An unpaired t-test was used to determine if there was any difference between the translation and rotation ranges and offsets between screws in UHMWPE and screws in bone inserted in the normal fashion. A paired t-test was used to compare between pedicle screws in normal and in overdrilled holes. Effects of BMD on translation and rotation offsets and ranges were determined for both normal insertion and overdrilling by calculating Pearson product-moment correlation coefficients between these factors and BMD. Statistical significance was assumed to be at the 95% level.

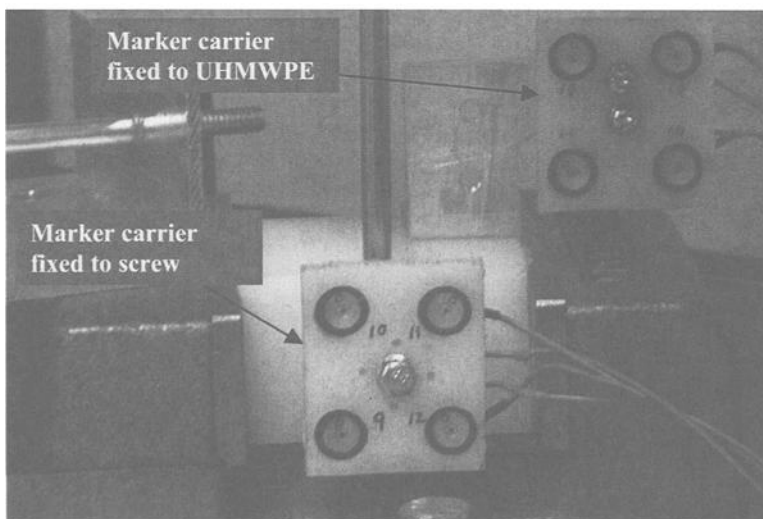
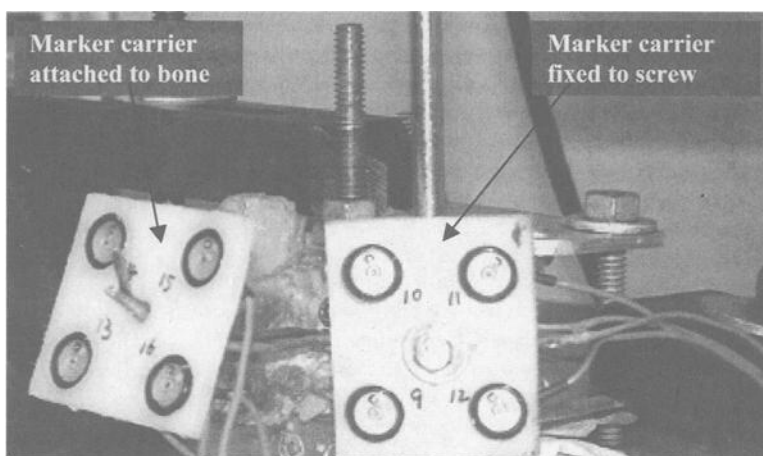
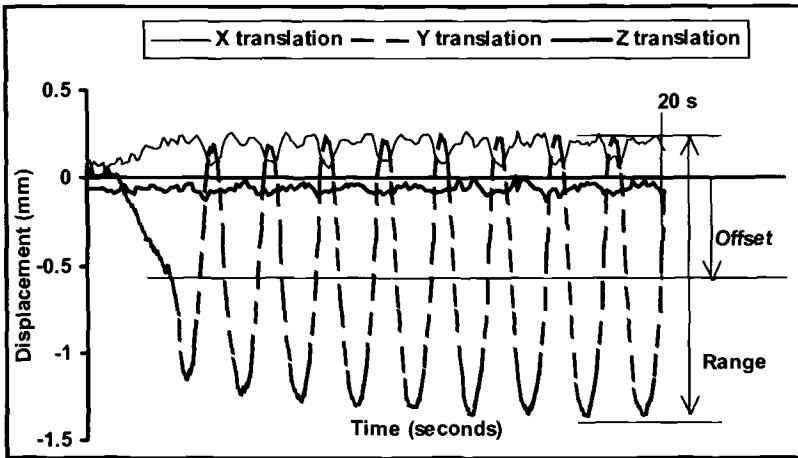
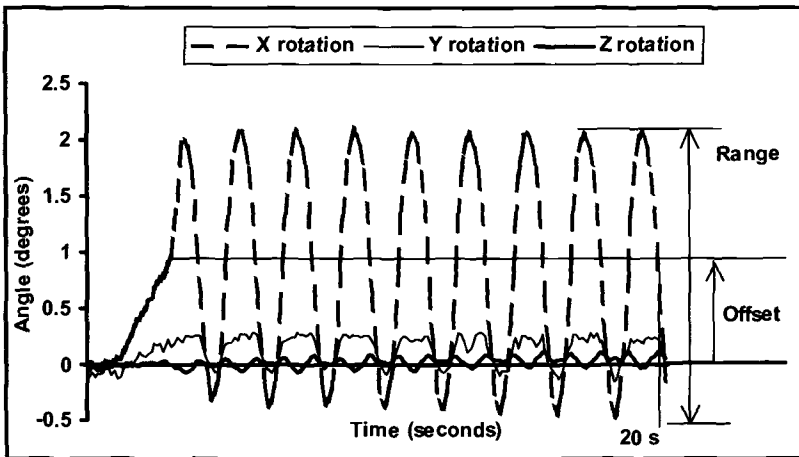


Figure 3—Two marker carriers, each with four infrared LEDs, were mounted onto the two rigid bodies, (a) pedicle screw and vertebral specimen (b) pedicle screw and UHMWPE block. A high precision optoelectronic system was used to capture the motion of each rigid body with time. Subsequent post processing determines the relative motion of the pedicle screw in bone and of the pedicle screw in UHMWPE.



(a)



(b)

Figure 4 – The (a) relative translations and (b) rotations between pedicle screw and bone in all six degrees of freedom for the first twenty seconds are presented in these two graphs. Translations in y of the screw head and rotations in x were the main motions measured, since the applied loads were in that plane. The other translations and rotations were not deemed significant as their magnitudes were much smaller. The range and offset of the y translation and x rotation are as shown on the graphs. Range and offset of the motion of the pedicle screw head were obtained from the average of the last five cycles (96th to 100th).

Results

Motion of Pedicle Screw

The motions reported here consist of the sagittal plane rotation of the screw with respect to the vertebra and the axial translation of the screw head. The other rotations and translations were measured, but were very small and therefore not deemed significant.

The range of motion of the pedicle screw in the UHMWPE block was small, averaging 0.2 mm and 0.9°. The range of motion in the bone was significantly higher, averaging 1.4 mm and 2.4° for normally inserted screws and 2.4 mm and 2.7° for screws in overdrilled holes (Fig. 5 and Table 1).

The offset of translation of pedicle screws in the UHMWPE block was -0.1 mm whereas the offset of the pedicle screws in bone was -0.5 mm and in the overdrilled holes was -1.2 mm. The offset of the rotation of pedicle screws in UHMWPE was 0.4° whereas the offset of the pedicle screws in bone was 0.4° and in overdrilled holes was 0.3°. Offset of the pedicle screws in bone resulted in enlarged insertion holes. There was a significant difference in translation range ($p < 0.005$), translation offset ($p < 0.05$) and rotation range ($p < 0.001$) between motion of screw in UHMWPE and bone, while rotation offsets were not different ($p > 0.95$). There was no significant difference in translation range ($p = 0.15$), translation offset ($p = 0.47$), rotation range ($p = 0.33$) and rotation offset ($p = 0.89$) between pedicle screws in normal and overdrilled holes.

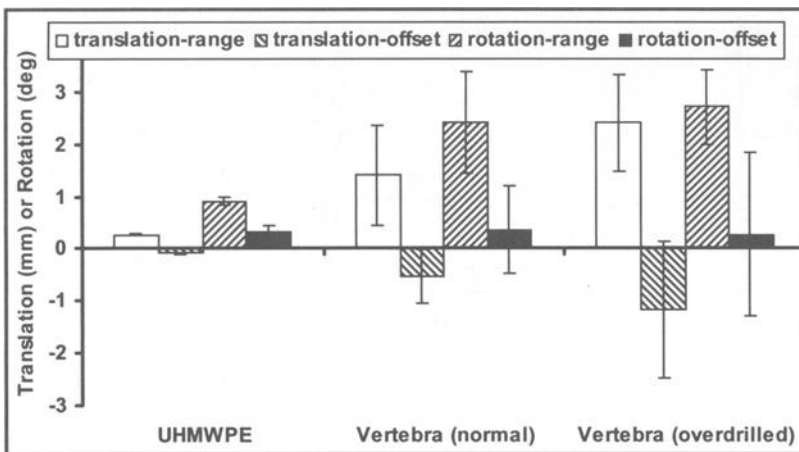


Figure 5 – The range and offset of the motion of the screw heads for screws inserted in a) UHMWPE, b) bone with normal insertion and c) bone with overdrilling. Error bars denote the standard deviation. n = 8 for each group.

Table 1 — Range and offset of translation and rotation in the sagittal plane.

	Y Translation-Range (mm)			X Rotation-Range (degrees)		
	Screw in UHMWPE (n=8)	Normal Insertion (n=8)	Overdrilled (n=8)	Screw in UHMWPE (n=8)	Normal Insertion (n=8)	Overdrilled (n=8)
Mean	0.2	1.4	2.4	0.9	2.4	2.7
s.d.	0.02	1.0	0.9	0.02	1.0	0.7
Max	0.3	3.1	3.9	0.9	3.9	4.1
Min	0.2	0.5	1.5	0.9	1.3	1.8
	Y Translation-Offset (mm)			X Rotation-Offset (degrees)		
	Screw in UHMWPE (n=8)	Normal Insertion (n=8)	Overdrilled (n=8)	Screw in UHMWPE (n=8)	Normal Insertion (n=8)	Overdrilled (n=8)
Mean	-0.1	-0.5	-1.2	0.4	0.4	0.3
s.d.	0.02	0.5	1.3	0.05	0.8	1.6
Max	-0.1	0.0	0.0	0.4	1.7	2.7
Min	-0.1	-1.6	-4.1	0.3	-1.3	-2.2

Table 2 — Correlation between range and offset of translation and rotation against BMD.

	p value	Correlation ^a	Correlation coefficient, r ²
Translation range	0.15	No	0.37
Translation offset	0.26	No	0.24
Rotation range	0.12	No	0.35
Rotation offset	0.69	No	0.03

^aA 95 % confidence level ($p < 0.05$) was used to decide if the data were significantly correlated.

Motion of Pedicle Screw in Bone; Effects of BMD

The correlation between bone mineral density and the range and offset of motion of the pedicle screw inserted in the normal fashion (Fig. 6 and Table 2) was not statistically significant. There was, however, a trend that the specimens with higher bone mineral density generally had lower translation and rotation ranges, whereas these ranges tended to be higher for specimens with lower bone mineral densities.

No direct correlation between magnitude of translation or rotation with BMD was found for the pedicle screws inserted into the overdrilled holes.

Center of Rotation

The kinematics of the pedicle screw in bone could be broadly categorised into two groups. For specimens with higher bone mineral density, the screws were pivoting about a point located somewhere between the screw tip and the screw head. Translations and rotations were generally smaller (Fig. 6 and 7). For specimens with lower bone mineral density, the motion of the screws underwent two stages. In the first stage, screw motion was characterized by vertical rigid body translation, with the screw head and screw tip

both translating along the y-axis together. In the second stage, the screw demonstrated a rotational motion, with the screw head and tip moving in opposite directions, indicative of a center of rotation somewhere between the screw tip and the screw head.

Overdrilling did not alter the kinematic patterns of the pedicle screws in the specimens. With overdrilling, pedicle screws in specimens with higher bone mineral density were observed to be pivoting about a point, without the translations as observed in the overdrilled specimens with lower bone mineral density. This was in spite of the observation that the magnitudes of range and offset in the overdrilled holes were not correlated with BMD.

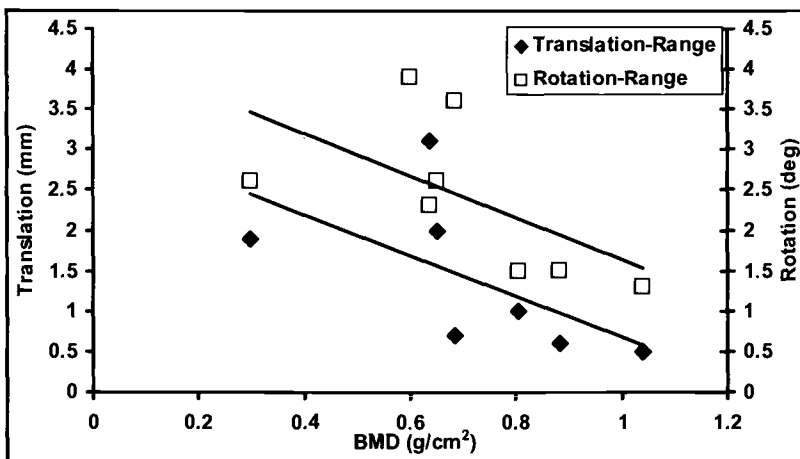


Figure 6 — Scatterplots of screw head translation and rotation ranges versus BMD for pedicle screws inserted with normal hole preparation. No significant linear correlations in translation range ($p = 0.15$, $r^2 = 0.369$) or rotation range ($p = 0.12$, $r^2 = 0.350$) with BMD were found but there was a trend of lower translations and rotations for specimens with higher BMD. No correlations were found for pedicle screws inserted in overdrilled holes.

Discussion

The testing methodology in this study applied similar loads and boundary conditions onto the two pedicle screws, one inserted in bone and the other inserted in UHMWPE. The results of this study showed clearly that the motion of the pedicle screw with respect to bone was significantly higher than its motion in a homogeneous block of UHMWPE. The higher stiffness of the UHMWPE results in less rotation of the screws and rod construct. Inspection of the specimens indicated that the pedicle screws caused permanent enlargement of the insertion holes of the pedicles. On the other hand, the pedicle screws inserted in the UHMWPE did not result in any observable damage to the latter.

The motion of the pedicle screw with respect to the UHMWPE at the screw head could be attributed to a) motion of the screw within the UHMWPE and b) bending of the screw outside the UHMWPE. Indeed, a combination of both scenarios, motion within

and bending outside the UHMWPE, could have occurred. Although no gross permanent damage to the UHMWPE was observed, such motion could also be partially attributed to load application within the elastic limit of the UHMWPE. As the portion of the pedicle screw embedded within the UHMWPE was not substantially loaded, it could be postulated that fatigue fracture of pedicle screws tested in UHMWPE would occur at the neck of the screw.

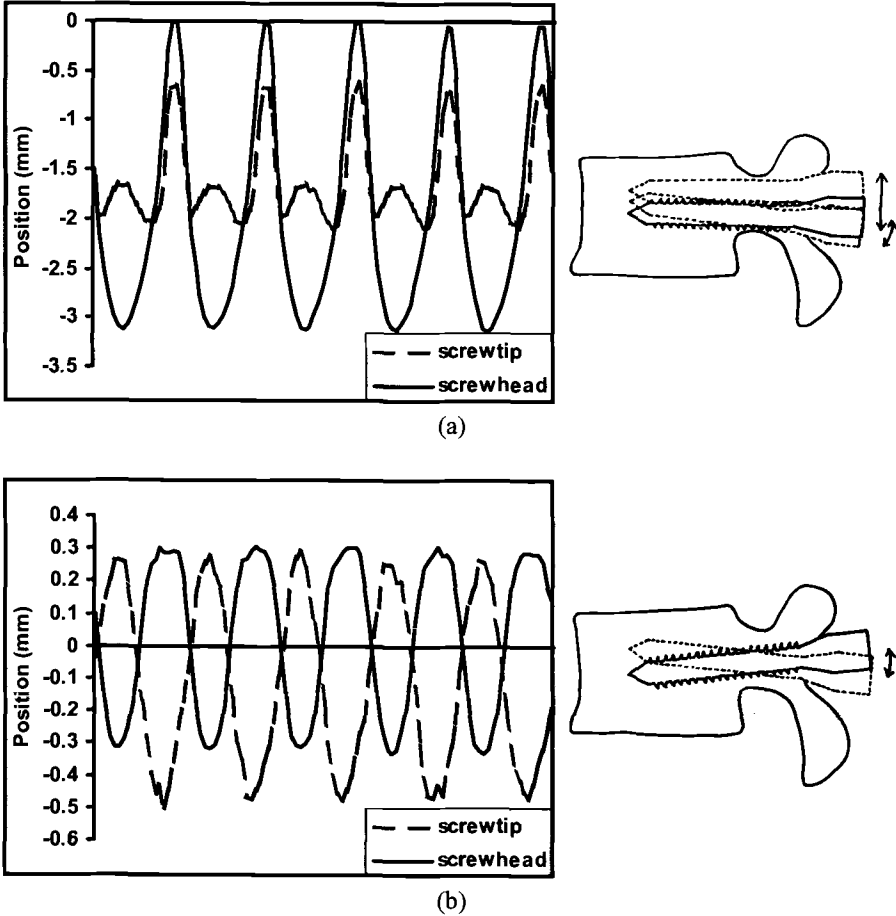


Figure 7 — Typical motion of pedicle screws inserted in the normal fashion at the screw head and screw tip during the last 5 cycles for specimens (a) with low BMD and (b) with high BMD. The motion pattern for screws in low BMD bone was in two stages, a rigid body translation and a rigid body rotation. While in high BMD bone, the screws were mainly in rigid body rotation, oscillating about a point some distance between the screw head and screw tip.

Motion of the pedicle screw with respect to the vertebra was largely attributed to the rigid body motion of the screws within the bone and not to the bending of the screw itself. This rigid body motion of the screw against the bone resulted in enlargement of the insertion hole and permanent damage to the internal trabecular structure of the vertebral body. The kinematics of the pedicle screws in the bone was consistent with the presence of a fulcrum between the head and tip about which the pedicle screws were oscillating. Description of this clinically relevant mode of failure may aid in the development of improved techniques of spinal fixation.

Bone mineral density appeared to have an effect on the kinematics of the pedicle screws. Although translation and rotation ranges were not significantly correlated with bone mineral density in this study, there was a trend to suggest this association. The small sample size in this study could have contributed to the failure to demonstrate a statistically significant correlation. Moreover, the BMD values used in the statistical analysis were of the vertebral bodies and did not include the quality of bone in the pedicle region. The same trend against BMD was observed in pull-out tests by many researchers [7-9, 11-13]. In those studies, specimens with higher BMD had higher pull-out force, while in the current study, there was a trend of lower translation and rotation ranges for specimens with higher BMD.

By studying the motion of the screw tip and screw head, it was revealed that for screws in vertebrae with higher bone mineral density, the screws were pivoting about a point between the screw head and the screw tip. For screws in vertebrae with lower bone mineral density, the screws underwent a rigid body translation followed by a pivoting motion. The former group of pedicle screws inserted in vertebrae with higher BMD could be considered to have achieved satisfactory early bone-implant fixation and they, in addition to the screws inserted in the UHMWPE, would have passed the ASTM test protocol. The latter group of pedicle screws inserted in vertebrae with lower BMD mimicked the clinical scenario of intra-operative or early post-operative bone-implant interface failure. Thus, bone mineral density indeed influenced short-term fixation and early failure of pedicle screws. This would not have been detected using the F 1717 test protocol. The damaging effects of metallic implants on bone have not been fully characterized or addressed in the F 1717. It is possible that some designs of pedicle screws could result in more damage to the trabecular structure than others. Therefore the fatigue life of an implant does not appear to be correlated to the ability of an implant to successfully develop a strong bone implant interface.

Overdrilling did not result in significantly higher translation or rotation ranges and offsets as compared to the screws inserted in the normal fashion. The kinematics of the pedicle screws was also not affected by overdrilling. Overdrilling furthermore caused the translation and rotation ranges and offsets to be independent of BMD, eliminating the trend of BMD effect observed for the normal screw insertions. Overdrilling the insertion holes resulted in a loosened screw model which otherwise could be achieved by a high number of cyclic motions on a screw inserted in a normal fashion.

Conclusion

This study contrasted, under short-term cyclic physiologic loads, the mechanical behavior of pedicle screws inserted in cadaveric vertebrae versus synthetic surrogates.

The kinematics of the screws inserted in bone and in UHMWPE were found to be different in terms of the range of motion, pivoting and bending points of the screws and in terms of the effects of bone mineral density. The kinematics of the screws in bone is more relevant to clinical modes of failure. The fixation at the bone-implant interface can be quantified during short-term cyclic testing when an appropriate model is used, as demonstrated in this study.

Acknowledgments

The implants used in this study were compliments from Synthes (Canada) Ltd.

Funding from the Canadian Institutes of Health Research and Synthes Spine are gratefully acknowledged.

References

- [1] Panjabi, M. M., "Biomechanical Evaluation of Spinal Fixation Devices," *Spine*, 1988, Vol. 13, No. 10, pp. 1129–1134.
- [2] Ashman, R. B., Bechtold, J. E., Edwards, W. T., Johnston II, C. E., McAfee, P. C., and Tencer, A. F., "In Vitro Spinal Arthrodesis Implant Mechanical Testing Protocols," *Journal of Spinal Disorders*, 1989, Vol. 2, No. 4, pp. 274–281.
- [3] Paramore, C. G., Dickman, C. A., and Sonntag, V. K., "Radiographic and Clinical Follow-up Review of Casper Plates in 49 Patients," *Journal of Neurosurgery*, 1996, Vol. 84, No. 6, pp. 957–961.
- [4] McAfee, P. C., Cunningham, B. W., Lee, G. A., Orbegoso, C. M., Haggerty, C. J., Fedder, I. L., and Griffith, S. L., "Revision Strategies for Salvaging or Improving Failed Cylindrical Cages," *Spine*, 1999, Vol. 24, No. 20, pp. 2147–2153.
- [5] Eck, K. R., Bridwell, K. H., Ungacta, F. F., Riew, D., Lapp, M. A., Lenke, L. G., Baldus, C., and Blanke, K., "Complications and Results of Long Adult Deformity Fusions down to L4, L5, and the Sacrum," *Spine*, 2001, Vol. 26, No. 9, pp. E182–E192.
- [6] Uzi, E. A., Dabby, D., Tolessa, E., and Finkelstein, J. A., "Early Retropulsion of Titanium-Threaded Cages after Posterior Lumbar Interbody Fusion," *Spine*, 2001, Vol. 26, No. 9, pp. 1073–1075.
- [7] Halvorson, T. L., Kelley, L. A., Thomas, K. A., Whitecloud III, T. S., and Cook, S. D., "Effects of Bone Mineral Density on Pedicle Screw Fixation," *Spine*, 1994, Vol. 19, No. 21, pp. 2415–2420.
- [8] Soshi, S., Shiba, R., Kondo, H., and Murota, K., "An Experimental Study on Transpedicular Screw Fixation in Relation to Osteoporosis of the Lumbar Spine," *Spine*, 1991, Vol. 16, No. 11, pp. 1335–1341.

- [9] Wittenberg, R. H., Shea, M., Swartz, D. E., Lee, K. S., White, A. A., and Hayes, W. C., "Importance of Bone Mineral Density in Instrumented Spine Fusions," *Spine*, 1991, Vol. 16, No. 6, pp. 647–652.
- [10] Zindrick, M. R., Wiltse, L. L., Widell, E. H., Thomas, J. C., Holland, W. R., Field, B. T., and Spencer, C. W., "A Biomechanical Study of Intrapeduncular Screw Fixation in the Lumbosacral Spine," *Clinical Orthopaedics and Related Research*, 1986, No. 203, pp. 99–112.
- [11] Pfeiffer, M., Gilbertson, L. G., Goel, V. K., Griss, P., Keller, J. C., Ryken, T. C., and Hoffman, H. E., "Effect of Specimen Fixation Method on Pullout Tests of Pedicle Screws," *Spine*, 1996, Vol. 21, No. 9, pp. 1037–1044.
- [12] Yamagata, M., Kitahara, H., Minami, S., Takahashi, K., Isobe, K., Moriya, H., and Tamaki, T., "Mechanical Stability of the Pedicle Screw Fixation Systems for the Lumbar Spine," *Spine*, 1992, Vol. 17, No. 3S, pp. S51–S54.
- [13] Okuyama, K., Sato, K., Abe, E., Inaba, H., Shimada, Y., and Murai, H., "Stability of Transpedicle Screwing for the Osteoporotic Spine," *Spine*, 1993, Vol. 18, No. 15, pp. 2240–2245.
- [14] Lund, T., Oxland, T. R., Jost, B., Crompton, P., Grassmann, S., Etter, C., and Nolte, L. -P., "Interbody Cage Stabilisation in the Lumbar Spine," *Journal of Bone and Joint Surgery*, 1998, Vol. 80-B, pp. 351–359.
- [15] Oxland, T. R., Lund, T., Jost, B., Crompton, P., Lippuner, K., Jaeger, Ph., and Nolte, L. -P., "The Relative Importance of Vertebral Bone Density and Disc Degeneration in Spinal Flexibility and Interbody Implant Performance," *Spine*, 1996, Vol. 21, No. 22, pp. 2558–2569.
- [16] Grant, J. P., Oxland, T. R., and Dvorak, M. F., "Mapping the Structural Properties of the Lumbosacral Vertebral Endplates," *Spine*, 2001, Vol. 26, No. 8, pp. 889–896.
- [17] Rohlmann, A., Bergmann, G., and Graichen, F., "Loads on an Internal Spinal Fixation Device During Walking," *Journal of biomechanics*, 1997, Vol. 30, No. 1, pp. 41–47.
- [18] Rohlmann, A., Graichen, F., Weber, U., and Bergmann, G., "Monitoring In Vivo Implant Loads with a Telemeterized Internal Spinal Fixation Device," *Spine*, 2000, Vol. 25, No. 23, pp. 2981–2986.

Author Index

A	Griffith, S. L., 92	
Akbarnia, B., 3, 191		H
Asher, M. A., 3, 47, 191		
B	Houfburg, R. L., 86	
Bao, Q. -B., 127	Huber, G., 101	
Beck, P., 40	Hudgins, R. G., 127	
Bibbs, M., 40		I
Boachie-Adjei, O., 3, 191	Ito, K., 101	
Boschert, P., 68		J
C	Jensen, L. M., 55	
Campbell, S. F., 55, 86		K
Carson, W. L., 3, 24, 47, 63, 191		
Cesarone, D., 209	Kirkpatrick, J. S., 40	
Cook, S. M., 47	Knöller, S., 173	
Crisco, J. J., 114	Kwon, B. K., 217	
D		L
Dawson, J. M., 68, 92		
DiAngelo, D. J., 155	Lai, S. M., 47	
Dunbar, W. L., 209	Lebwohl, N. H., 3	
Dvorak, M. F., 217	Lemons, J. E., 40	
Dzioba, R., 3	Linke, B., 101, 173	
F		M
Fisher, C. G., 217		
Foley, K. T., 155	Macenski, M. M., 68	
Friis, E. A., 143	Meyer, G., 173	
G	Montoya, J. A., 143	
Graber, C. D., 143	Morlock, M. M., 101	
Gray, E., 55		O
	Oxland, T. R., 217	

P

Paiva, J. A., 114
Pavlovic, J., 86
Pence, C. D., 143

R

Rand, N., 68

S

Samarasekera, D., 217
Schneider, E., 173
Selvitelli, D. M., 17
Serhan, H., 17, 34, 209

Shinbrot, A., 86
Slivka, M. A., 17, 34
Spenciner, D. B., 114
Springer, S. S., 55, 86

T

Tan, J. S., 217
Theiss, S. M., 81
Torres, K., 17

V

Venugopalan, R., 40

Subject Index

A

Allograft, 92
 Anchor-connector-rod assembly, 3
 Anterior cervical plate, 155
 Anterior column spinal units, 101
 ASTM standards (See also Standards)
 F 1692-96, 68
 F 1717-01, 24, 191
 F 1717-96, 17
 F 1717-97, 209
 F 1798-97, 3, 55, 63, 191
 Axial
 compression, 114, 217
 compressive load, 155
 compressive strength, 92
 gripping characteristics, 47, 191
 load cycles, 101
 rigidity, 143
 rotation, 24, 114

B

Bending
 fatigue, 3
 flexion, 63
 lateral, 3, 143
 moment distribution, 155
 Biaxial mechanical test system, 143
 Bilateral construct, 209
 Bilevel spinal implant constructs, 24
 Biomechanical testing
 model, 17
 parameters, 191
 protocol, 155
 Biomechanics, 114, 155
 Body-disc-body units, 101
 Bone mineral density, 217
 Bone screws, 68

C

Cage expulsion, 86
 Calf spine, 143
 Cervical spine, 155
 Clinical objectives, 191
 Compression bending, 17, 34, 209
 Compression-flexion-extension loading, 127
 Compression loads, 127, 155
 Compressive shear, 114
 Compressive strength, 92
 Connectors, 3
 transverse, 47, 191
 transverse rod, 34
 Corpectomy, 17, 34, 155, 173, 209
 Corrosion
 crevice, 40
 transverse connection site, 47

D

Discs
 artificial, 114
 prosthetic, 127
 Drop Entry Transverse Rod Connector (DETC), 47
 Durability test, 127
 Dynamic compression bending, 17, 34, 209
 Dynamic model, 101

E

Excessive resection, 81
 Extrusion, 81

F

Fatigue
 flexion tests, 3, 63

- four-point bend fatigue tests, 3
 - performance, 34
 - strength, 17, 34, 63
 - testing, 24
 - Femoral rings, 92
 - Finite element analysis, 24, 191
 - Fixation plates, 127
 - Fixation strength, 68
 - Fixed-fixed end assembly, 63
 - Fixed-free end assembly, 63
 - Flexibility testing, 173
 - Force sensing strut-graft (fssg), 155
 - Four-point bend fatigue test, 3
 - Freebody diagram analysis, 63
 - Freeze-dried allograft, 92
 - Frozen-thawed allograft, 92
 - Functional spinal units, 114
 - Fusion, clinical, 34
 - Fusion devices, 81, 86
- G**
- Gimbal-gimbal fixture, 24, 191
 - Gimbal-pushrod fixture, 191
 - Graft/cages, 3
 - Graft-plate load-sharing mechanics, 155
 - Gripping capacity, 47
- H**
- Hand held loaded models, 24
 - H construct, 3, 191
 - Human functional spinal unit (FSU), 114
 - Hysteresis area, 101
- I**
- Implant failure, correlation with fatigue test results, 3
 - Implant loosening, 217
 - Inferior test block mobility, 17
 - Insertion loading, 92
 - Instrumented strut-graft mechanics, 155
 - Instrumented-to-native (I/N)
 - comparison, 173
 - Interbody cage, 3, 86
 - Interbody fusion, 81, 86
 - Interbody structural allografts, 92
 - Interconnection mechanisms, 55, 63
 - International Organization for Standardization (ISO) standards, 217
 - Intervertebral disc, 101, 114, 127
 - space, 92
 - In vitro fatigue, 3
 - In vitro testing, 101, 191
 - Isola™ Drop Entry Transverse Rod Connector (DETC), 47
 - Isola™ Stainless Steel Spinal System, 209
 - Isola™ Threaded Transverse Rod Connector (TRC), 47
 - Isola™ -VSP, 3
- K**
- Kaplan-Meier
 - probability of reoperation, 47
 - survivorship analysis, 47
- L**
- Late operative site pain (LOSP), 47
 - Lateral bending
 - characteristics, 191
 - profile, 3, 143
 - Lateral translation, 24
 - Linkage analysis, 191
 - Load cycles, 101
 - Load-displacement behavior, 143, 173

Loading, 24, 127, 173
 insertion, 92
 interconnection, 63
 Lordotically contoured rods, 63
 Lumbar, 81, 209
 Lumbar spine, 114, 143, 173

M

Mechanical
 analogue model, 143
 properties, 114
 testing, 217
 Models and modeling
 biomechanical testing, 17
 dynamic, 101
 finite element, 24
 corpectomy, 17
 pull-out strength, 68
 push-out testing, 86
 spine, 143
 transfer function, 101

N

Neutral zone, 101

O

Occipito-cervical-thoracic corpectomy
 constructs, 17
 Orthopaedic medical devices, 68, 92

P

PA axis rotation, 24
 Peak to peak, 101
 Pedicle screws, 34
 angle, 209
 common complications, 55
 kinematics, 217
 mechanical behavior, 217
 pull-out, 68

PLIF, 81
 Posterior cervical, 17
 Preload, 173
 Prosthetic intervertebral disc (PID), 127
 Prosthetic nucleus (PN), 127
 Pull-out strength, 68, 86
 Push-out, 86
 Pushrod-gimbal fixtures, 24

R

Residual tensile stress, 63
 Retrieval analysis, 40
 Retropulsion, 86
 Rods, 3, 34, 55, 63

S

Scoliosis, 47
 Screw-rod interconnection, 55, 63
 Screws, 191
 bone, 68
 pedicle, 55, 68, 209, 217
 Segmental vertebral motion, 155
 Six degrees of freedom, 173, 191
 Spinal corpectomy
 (See also Corpectomy)
 Spinal fixation, 40
 Spinal fusion construct, 40, 92
 Spinal instrumentation, 155
 Spine model, 143
 Spine testing, 143
 Stainless steel, 40
 Standards (See also ASTM
 Standards), 40, 86
 ISO, 217
 Static compression bending, 209
 Static push-out test, 86
 Stiffness, 114, 155, 173, 209
 torsional, 17
 strength test, interconnector, 55

Stress relaxation, 101
Strut-graft load, 155
Surface finishes, 40
SynEx, 173

T

Test blocks, 209
 mobility, 17
Threaded transverse rod
 connector (TRC), 47
Three degrees of freedom, 24
Titanium, 40
Torsion, 17, 24, 47, 143
Torsional
 gripping characteristics, 47, 191
 stiffness, 34
Transfixed thoracolumbar constructs, 191
Transverse rod connectors, 34, 47, 191
Tutoplast® processed bone allograft, 92

U

UHMWPE, 217
Unconstrained finite element models, 24
Unilateral construct flexion fatigue test, 3

V

VentroFix, 173
Vertebrae motion, 24

Y

Yield load, 17
Yield strength, 209